DEVELOPMENT OF A SMALL ANIMAL MODEL FOR INTEGRATED ASSESSMENT OF CARDIAC CONTRACTILITY AND CALCIUM/CALMODULIN-DEPENDENT PROTEIN KINASE II

A thesis presented by

Laura Mooney

in fulfilment of the requirements for the degree of Doctor of Philosophy

Strathclyde Institute of Pharmacy & Biomedical Science
University of Strathclyde
161 Cathedral Street, Glasgow, G4 0RE, UK

October 2012

This thesis is the result of the author's original research, except where indicated in the text. It has been composed by the author and has not been previously submitted for examination which has led to the award of a degree.

Signed:

Date:

ACKNOWLEDGMENTS

Firstly, my thanks are offered to my University supervisors, Dr Susan Currie and Dr Susan Coker, for their encouragement, support and patience during my studies. I thank “The Susans” also for their guidance and constructive criticism – even if it has made me somewhat (more) of a pedant!

Secondly, I am grateful to AstraZeneca and the Medical Research Council for funding for my PhD studies. I offer further thanks to AstraZeneca for allowing me the opportunity to gain valuable experience in their Safety Pharmacology Department. My thanks are extended to several individuals within the Department who helped me during my time there, and beyond. Specifically, I thank my supervisor at AstraZeneca, Dr Matthew Skinner, for his advice and support throughout.

I have encountered many kinds of people along the way and I thank them for making things all the more interesting. In particular, I thank those closest to me who have provided welcome distractions at the right times - and probably also the wrong times - over the years.

Above all else, I am hugely indebted to my family. My sister, my friend, I could not ask for more - always caring, always encouraging, always fun. My parents go far beyond any expectation that a daughter could ever have. I hope they realise just how much this means to me. Without such a super family the things I have done and the things I will do would be far more difficult. No matter where I go, my home will always be my home. Mum, Dad and Jen, I thank you for your continued support and love.

CONTENTS

PUBLICATIONS

Full papers:

Mooney L, Marks L, Philp KL, Skinner M, Coker SJ, Currie S (2012). Optimising conditions for studying the acute effects of drugs on indices of cardiac contractility and on haemodynamics in anaesthetized guinea pigs. *Journal of Pharmacological and Toxicological Methods* **66** (1), 43‑51.

Abstracts:

Mooney L, Currie S, Coker SJ, Skinner M (2012). Effects of changes in blood pressure and heart rate on indices of cardiac contractility. *Proceedings of the Physiological Society* **27**, PC202.

Mooney L, Coker SJ, Skinner M, Currie S (2012). Integrated assessment of cardiac contractility and CaMKII delta expression and activity following sunitinib administration. *Journal of Molecular and Cellular Cardiology* **53** (2), S8.

Mooney L, Coker SJ, Skinner M, Currie S (2011). Integrated assessment of cardiac contractility and CaMKII delta expression and activity following acute and chronic isoprenaline administration. *Proceedings of the Physiological Society* **23**, C77.

COMMUNICATIONS

The Physiological Society, Edinburgh, UK (2012)

Poster: Effects of changes in blood pressure and heart rate on indices of cardiac contractility. *L Mooney, S Currie, SJ Coker, M Skinner.*

International Society for Heart Research (North American Section), Banff, AB, Canada (2012)

Poster: Integrated assessment of cardiac contractility and CaMKII delta expression and activity following sunitinib administration. *L Mooney, SJ Coker, M Skinner, S Currie.*

AstraZeneca Safety Science Showcase, Alderley Park, Macclesfield, UK (2012)

Poster and oral: Effects of changes in blood pressure and heart rate on $LVdP/dt_{max}$ and the QA interval. *L Mooney, S Currie, SJ Coker, M Skinner.*

The Physiological Society, University of Oxford, UK (2011)

Oral: Integrated assessment of cardiac contractility and CaMKII expression and activity following acute and chronic isoprenaline administration. *L Mooney, SJ Coker, M Skinner, S Currie.*

AstraZeneca Local Science Day, Alderley Park, Macclesfield, UK (2011)

Oral: Integrated assessment of cardiac contractility and CaMKII activity: Effects on haemodynamics *in vivo*. *L Mooney, S Currie, M Skinner, SJ Coker.*

AstraZeneca Local Science Day, Alderley Park, Macclesfield, UK (2011)

Poster: Integrated assessment of cardiac contractility and CaMKII delta: Effects on CaMKII delta expression and activity. *L Mooney, SJ Coker, M Skinner, S Currie.*

Mammalian Myocardium, University of Manchester, UK (2010)

Poster: Correlation of cardiac contractility with CaMKII activity following acute drug administration in anaesthetised guinea pigs. *L Mooney, SJ Coker, M Skinner, S Currie.*

Integrative Mammalian Biology, University of Glasgow, UK (2010); AstraZeneca Local Science Day, Alderley Park, Macclesfield, UK (2010); Scottish Cardiovascular Forum, University of Glasgow, UK (2010)

Poster: Development of a small animal model for assessment of cardiac contractility and haemodynamics. *L Mooney, S Currie, M Skinner, SJ Coker.*

ABSTRACT

Several drugs in development or on the market have adverse effects on cardiac contractility. Calcium/calmodulin-dependent protein kinase IIδ (CaMKIIδ) is an important regulator of cardiac contractility with a particularly prominent role in pathophysiological conditions where contractile dysfunction occurs. Therefore, CaMKIIδ may be an intracellular target for drugs that alter cardiac performance. The aim of the work presented in this thesis was to develop a small animal model for the integrated assessment of cardiac contractility and CaMKII.

An anaesthetised guinea pig model was developed to assess haemodynamics and cardiac contractility via two indices – left ventricular (LV) dP/dt_{max} and the QA interval. Acute administration of isoprenaline and ouabain increased contractility whilst verapamil, imatinib and sunitinib decreased contractility. There was a strong inverse correlation between $LVdP/dt_{max}$ and the QA interval. CaMKIIδ expression and CaMKII activity were not significantly altered by any acute drug treatment.

Both $LVdP/dt_{max}$ and the QA interval were influenced by changes in blood pressure. Additionally, $LVdP/dt_{max}$ was influenced by changes in heart rate. Measurement of contractility via LV pressure-volume loops was also assessed. Surgical approaches and recordings were optimised and isoprenaline and verapamil had positive and negative inotropic actions, respectively. Several issues were identified which require further attention.

Chronic administration of isoprenaline and verapamil decreased cardiac contractility and increased CaMKIIδ expression and CaMKII activity. Chronic imatinib and sunitinib treatments did not alter cardiac contractility significantly. However, both CaMKIIδ expression and CaMKII activity were increased.

The work presented in this thesis indicates that the guinea pig is suitable for the integrated assessment of cardiac contractility and CaMKII. Alterations in CaMKIIδ expression and CaMKII activity following chronic drug treatments could be an indication of cellular cardiotoxicity associated with contractile dysfunction at the whole animal level. The circumstances under which increased CaMKII expression and activity translate to compromised contractile performance require more detailed investigation.

ABBREVIATIONS

ABL	Abelson proto-oncogene
AC	Adenylyl cyclase
AIP	Autocamtide-2 related inhibitory peptide
ANOVA	Analysis of variance
ATP	Adenosine-5'-trisphosphate
AV	Atrioventricular
β-ARK	β-adrenoceptor kinase
BCR-ABL	Breakpoint cluster region-Abelson gene fusion
bcr-abl	Breakpoint cluster region-Abelson protein kinase fusion
BCRP	Breast cancer related protein
BP	Blood pressure
BSA	Bovine serum albumin
Ca^{2+}	Calcium ions
Ca^{2+}/CaM	Calcium bound calmodulin
$CaCl_2$	Calcium chloride
CaM	Calmodulin
CaMKII	Calcium/calmodulin-dependent protein kinase II
cAMP	Cyclic adenosine monophosphate
CICR	Calcium-induced calcium-release
c-Kit	Mast/stem cell growth factor receptor or CD117
CO_2	Carbon dioxide
CSF	Colony stimulating factor

$[Ca^{2+}]_i$	Intracellular calcium concentration
DBP	Diastolic blood pressure
DMSO	Dimethyl sulfoxide
DTT	Dithiothreitol
EC	Excitation-contraction
ECG	Electrocardiogram
ECL	Enhanced chemiluminescence
EDTA	Ethylene diamine tetraacetic acid
EGTA	Ethylene glycol tetraacetic acid
eNOS	Endothelial nitric oxide synthase
Epac	Exchange protein directly activated by cAMP
Erk	Extracellular-signal-regulated kinase
ESPVR	End-systolic pressure-volume relationship
FCS	Fetal calf serum
flt3	fms-like tyrosine kinase receptor-3
FS	Fractional shortening
GAPDH	Glyceraldehyde-3 phosphate dehydrogenase
GPCR	G-protein coupled receptor
GRK	G-protein receptor kinase
HCl	Hydrochloride
HEPES	4-(2-hydroxyethyl)-1-piperazineethanesulfonic acid
HPLC-MS/MS	High pressure liquid chromatography with Tandem mass spectroscopy
HPLC-UV	High pressure liquid chromatography with Ultraviolet detector

ICH	International Conference on Harmonisation
i.p.	Intraperitoneal
i.v.	Intravenous
IVC	Inferior vena cava
IVCO	Inferior vena cava occlusion
K^+	Potassium ions
KCl	Potassium chloride
KIT	gene encoding c-KIT
LA	Left atrial/atrium
LTCC	L-type calcium channel
LV	Left ventricular/ventricle
LVdP/dt	First derivative of left ventricular pressure
$LVdP/dt_{max}$	Maximum rate of rise of left ventricular pressure
LVEDD	Left ventricular end-diastolic diameter
LVEDP	Left ventricular end-diastolic pressure
LVEDV	Left ventricular end-diastolic volume
LVESD	Left ventricular end-systolic diameter
LV-mag	Left ventricular magnitude
LVP	Left ventricular pressure
LVSP	Left ventricular systolic pressure
LVSV	Left ventricular systolic volume
LVV	Left ventricular volume
MABP	Mean arterial blood pressure

MAP	Monophasic action potential
Met	Methionine
MLCK	Myosin light chain kinase
MTD	Maximum tolerated dose
Mg^{2+}	Magnesium ions
$MgCl_2$	Magnesium chloride
MOPS	3-(N-morpholino)propanesulfonic acid
MW	Molecular weight
Na^+	Sodium ions
NaCl	Sodium chloride
NaH_2PO_4	Sodium phosphate
Na^+/K^+ ATPase	Sodium/potassium ATPase transporter
NCX	Sodium/calcium exchanger
NO	Nitric oxide
PCO_2	Carbon dioxide partial pressure
PDGF	Platelet-derived growth factor
PDGFR	Platelet-derived growth factor receptor
PE	Phenylephrine
PI3-K	Phosphoinositide-3 kinase
PKA	Protein kinase A
PKC	Protein kinase C
PKI	Protein kinase A inhibitor
PLB	Phospholamban

PM	Pressure-magnitude
PO_2	Oxygen partial pressure
PP1	Protein phosphatase 1
PP2A	Protein phosphatase 2A
PPB	Plasma protein binding
PRSW	Preload recruitable stroke work
pSer2815-RyR	Ryanodine receptor phosphorylated at Serine2815
pThr286-CaMKII	Calcium/calmodulin-dependent protein kinase II phosphorylated at Threonine286
PV	Pressure-volume
QC	Quality control
RA	Right atrial/atrium
RET	Rearranged during transfection
ROCK	Rho-dependent kinase
ROS	Reactive oxygen species
RV	Right ventricular/ventricle
RyR	Ryanodine receptor
SA	Sino-atrial
SBP	Systolic blood pressure
SDS-PAGE	Sodium dodecyl sulphate-polyacrylamide gel electrophoresis
SEM	Standard error of mean
Ser	Serine
SERCA	Sarco-endoplasmic reticulum calcium ATPase
s.c.	subcutaneous

SNP	Sodium nitroprusside
SR	Sarcoplasmic reticulum
S.R.	Specific radioactivity
TBS	Tris buffered saline
Thr	Threonine
Thr/Ser	Threonine/Serine
Tris	Tris(hydroxymethyl)aminomethane
T-tubules	Transverse tubules
Ved	Volume at end-diastole
VEGF	Vascular endothelial growth factor
VEGFR	Vascular endothelial growth factor receptor

CHAPTER 1 INTRODUCTION

1.1 Basic cardiac function

The primary role of the heart is to pump blood to all parts of the body. Blood flows through a network of blood vessels that extend between the heart and the peripheral tissues. The blood vessels are divided into the pulmonary circulation, which carries blood to and from the gas exchange surfaces of the lung, and the systemic circulation which transports blood to and from the rest of the body. Each circuit begins and ends at the heart and blood travels through these circuits in sequence. Arteries carry blood away from the heart whilst veins return it. Capillaries connect the smallest arteries and smallest veins, and permit exchange of nutrients, dissolved gases and waste products between the blood and the surrounding tissue.

The heart is located near the anterior chest wall, directly posterior to the sternum and is contained within the pericardial sac which provides protection and lubrication for the heart. The mammalian heart consists of four muscular chambers: two upper chambers called atria, and two lower chambers, called ventricles. The right atrium (RA) receives deoxygenated blood from the systemic circuit through the two great veins: the superior and inferior vena cava. Blood then passes from the RA to the right ventricle (RV) through the right atrioventricular (AV or tricuspid) valve. From the RV the blood enters the pulmonary circulation. Blood flows via the pulmonary artery to the lungs where the pulmonary artery branches repeatedly to the capillaries where gas exchange occurs. These small vessels then reunite to form the pulmonary vein which carries the oxygenated blood back to the left atrium (LA) of the heart. Via the left AV (or bicuspid) valve blood then enters the left ventricle (LV). From here blood is ejected via the aortic (or semilunar) valve into the ascending aorta, through the aortic arch and into the descending aorta. The large systemic circuit then carries the blood throughout the entire body including the coronary circulation which supplies the heart with the blood necessary for normal function (Martini, 2004).

The sequential flow of blood described above is maintained by the coordinated contraction and relaxation of the atria and the ventricles. In a single heartbeat the entire heart contracts in series: the atria contract and then the ventricles contract. Two types of cardiac cells are involved in the normal heartbeat: i) specialised cells of the conducting system, which control and coordinate the heartbeat; and ii)

contractile cells (cardiomyocytes), which produce the powerful contractions that propel blood.

1.1.1 Electrical activity of the heart

Each heartbeat begins with an action potential generated at the sino-atrial (SA) node (the pacemaker) embedded in the wall of the right atrium. The conducting system (Figure 1.1) then propagates and distributes the electrical impulse ensuring that the atria and ventricles contract in series and blood is moved in the right direction at the right time. From the SA node the electrical impulse spreads across the atrial surface to the AV node located between the atria and the ventricles. This causes the atria to contract. After a short delay to ensure that atrial contraction is complete, the impulse travels within the AV bundle through the intraventricular septum (IVS) and down the left and right bundle branches. The branches extend towards the apex of the heart, turn and fan out conducting the impulse to the Purkinje fibres. The Purkinje fibres rapidly distribute the stimulus to the ventricular myocardium initiating the contraction of the ventricles (Martini, 2004).

1.1.2 Mechanical events of the heart

The period between the end of one heartbeat and the beginning of the next is a single cardiac cycle. The cardiac cycle is divided into two phases: systole and diastole. Respectively, these phases refer to contraction - when blood is ejected from one heart chamber into the next or into an arterial trunk, and relaxation – when the chambers fill with blood. Throughout the cardiac cycle the pressure within each chamber rises during systole and falls during diastole. Thus blood moves from an area of high pressure to an area of low pressure. The pressure relationships are dependent on the timing of cardiac contractions.

During atrial systole the atria contract increasing atrial pressure and pushing blood through the AV valve into the ventricles. During this period, blood cannot flow into the atria because the atrial pressure exceeds venous pressure and so the volume of blood in the atria decreases. The pressure in the atria also falls and when lower than that in the ventricles, the AV valve closes and the atria enter atrial diastole which continues until the start of the next cardiac cycle. At the same time the ventricles, now filled with blood, enter ventricular systole. The volume of blood in the ventricles remains constant and the pressure rises until the pressure in the ventricle exceeds that of the pulmonary or aortic trunk. The aortic valve then opens

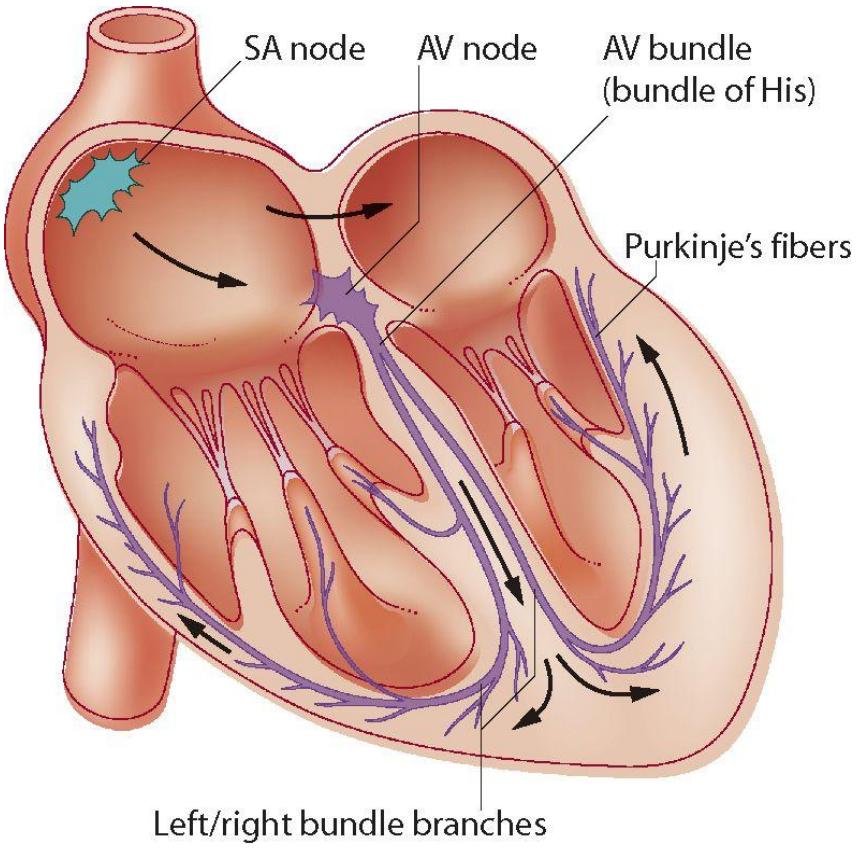

Figure 1.1 The conducting system of the heart. An action potential is generated at the sino-atrial (SA) node embedded in the wall of the right atrium. The electrical impulse is then propagated to the atrioventricular (AV) node causing the atria to contract. After a short delay, the impulse is then propagated further to the AV bundle through the intraventricular septum, down the left and right bundle branches and eventually reaching the Purkinje fibres which initiate contraction of the ventricles. The conducting system of the heart therefore regulates the stimulation of the contractile cells of the heart (cardiomyocytes) ensuring that the atria and ventricles contract in series and blood is moved in the right direction at the right time. Taken from Cunningham (2002).

and blood is ejected into the systemic and pulmonary circulations. During ventricular ejection both the volume and pressure in the ventricles decrease. At the end of ventricular systole the aortic valve closes and the ventricles enter diastole. When ventricular pressures fall below those in the atria, the AV valve reopens. Both the atria and ventricles are in diastole allowing blood to passively flow from the vena cava, into the atria and into the ventricles. Once the atria and ventricles have recovered the next cardiac cycle begins with atrial systole and the events are repeated (Levick, 2003). The pressure and volume changes throughout the cardiac cycle are shown in Figure 1.2.

1.1.3 Assessing cardiac function *in vivo*

The electrical events occurring in the heart can be detected by electrodes on, or just underneath, the surface of the body. A recording of these events is an electrocardiogram (ECG) shown in Figure 1.3. The ECG is directly related to the performance of specific nodal, conducting and contractile components of the heart. Thus the ECG allows normal, and abnormal, patterns of impulse to be monitored.

A typical ECG recording consists of a P wave, a QRS complex and a T wave. The small P wave represents the depolarisation of the atria, and atrial contraction follows shortly after the start of the P wave. The QRS complex appears as the ventricles depolarise. This is a strong signal with a much larger amplitude than the P wave because the ventricles have a much larger muscle mass than the atria. The ventricles begin contracting shortly after the peak of the R wave. The smaller T wave indicates ventricular repolarisation. Atrial repolarisation occurs whilst the ventricles are depolarising and the electrical event corresponding to this is masked by the QRS complex.

To analyse the ECG the voltage changes are measured and the durations and temporal relationships of the various components are determined. These parameters can then be used to identify any abnormal heart rates and/or rhythms. For example, an excessive increase in the size of the QRS complex may indicate that the heart has become enlarged. In contrast, a decrease in electrical signals may indicate a decrease in cardiac muscle mass. The size and shape of the T wave may also be affected by any condition that slows ventricular repolarisation such as coronary ischemia which may decrease the size of the T wave. The time intervals between waves are also measured and reported as segments or intervals. For

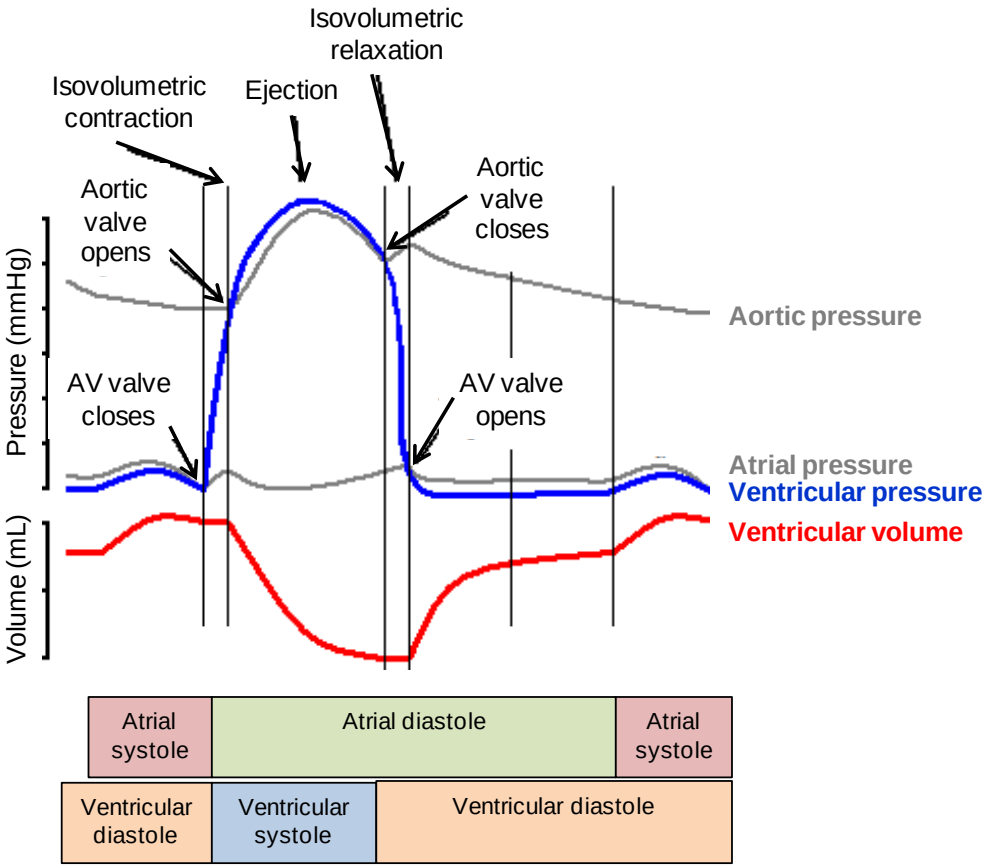

Figure 1.2 Pressure and volume changes throughout the cardiac cycle. AV, atrioventricular. Adapted from Martini (2004).

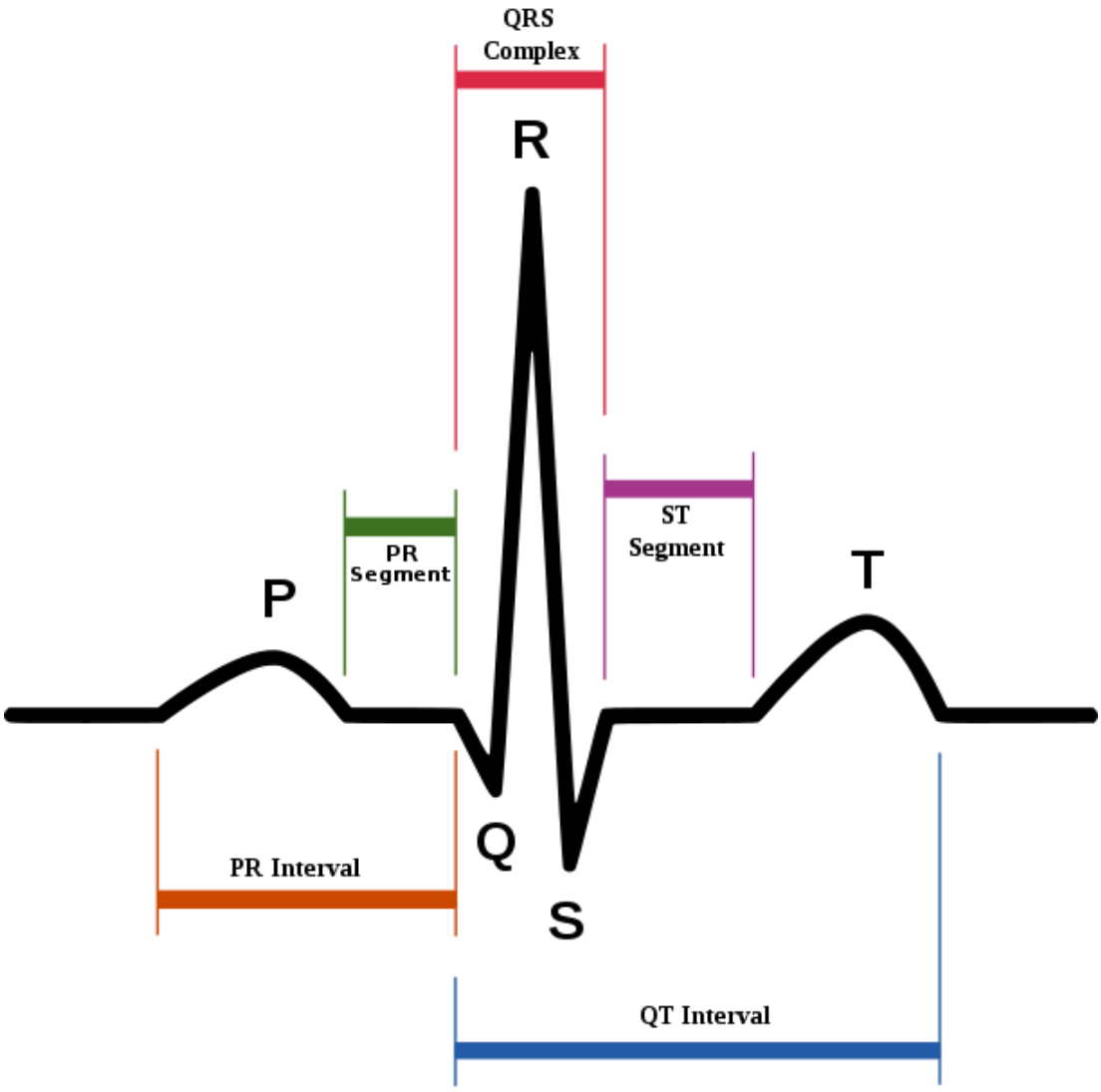

Figure 1.3 The Electrocardiogram (ECG). Taken from Wikipedia.org (http://en.wikipedia.org/wiki/File:SinusRhythmLabels.svg)

example, the QT interval indicates the time required for both ventricular depolarisation and repolarisation to occur. The QT interval can be prolonged by conduction problems, coronary ischemia or myocardial damage (Martini, 2004).

The contractile activity of the heart can also be monitored by various methods. Measurement of the LV pressure (LVP) and/or volume (LVV) throughout the cardiac cycle allows several indices of cardiac contractility to be calculated. Such measurements are made by inserting a catheter into the lumen of the LV to measure LVP and/or LVV. LVdP/dt is the first derivative of LVP, which is computed by software algorithms using calculus. Its peak value, $LVdP/dt_{max}$, is a well-established and commonly used indicator of changes in cardiac contractility (Beek, 1982; Hayes, 1982; Salyers *et al.*, 1988). $LVdP/dt_{max}$ is explained in more detail in Section 2.1. By combining LVP measurements with LVV measurements, LV pressure-volume (PV) loops can be constructed (Burkhoff *et al.*, 2005; Pacher *et al.*, 2008; Clark *et al.*, 2009). This method is considered the "gold standard" in assessing cardiac contractility and is described in detail in Section 4.1. A less invasive approach to assessing cardiac contractility is by measuring the QA interval. This is the time interval from the onset of the Q wave of the ECG to the beginning of the upstroke of the following arterial blood pressure wave. This approach is also described in more detail in Section 2.1.

A further technique to assess cardiac function is by echocardiography. Echocardiography uses ultrasound technology to create moving images of the heart. These images can provide a wealth of information on heart size, shape and function (St John Sutton *et al.*, 2009). By measuring the size of the LV during systole and diastole several indices of contractility, such as fractional shortening, can be calculated. Echocardiography is described in more detail in Section 5.1.

1.1.4 Cardiac dysfunction

It is well known that cardiac dysfunction is a consequence of many pathophysiological disease states, such as hypertrophy, hypertension, myocardial infarction, coronary artery disease, ischemia and arrhythmias (Martini, 2004). However, cardiac dysfunction is also a major safety concern associated with the development of new chemical entities for use as therapeutic drug molecules. Safety issues in general are a major cause of drug attrition during preclinical and clinical development and post-approval withdrawal of medicines. Cardiovascular safety

liabilities, in particular, are a leading cause of drug attrition rates (Laverty *et al.*, 2011).

Safety pharmacology is a distinct discipline which aims to integrate the best practices of pharmacology, physiology and toxicology (Ewart *et al.*, 2012). Pharmacological safety studies are designed to investigate adverse effects of new drug candidates particularly with respect to effects on the vital organ systems (cardiovascular, respiratory and nervous systems). Safety pharmacology is governed by regulatory guidelines from the International Conference on Harmonisation (ICH) which state that assessment of cardiac function *in vivo* is part of the core battery of tests required for pharmacological safety studies.

The cardiovascular effects of new drug candidates are often evaluated in telemetry studies in large animals (Hammond *et al.*, 2001). In these studies, animals are surgically implanted, or externally mounted, with devices that detect, measure and transmit cardiovascular parameters (such as ECG and blood pressure) via electromagnetic radio waves from a conscious, freely moving animal to an externally located receiver. Once the signal is received, it is transferred to a data acquisition system for processing. In addition, haemodynamic effects can be assessed in small animals in early preclinical tests which, in line with regulatory requirements, are primarily designed to assess effects on the ECG.

ICH guidelines specifically highlight the assessment of drug-induced effects on blood pressure, heart rate and the ECG (ICH, 2000) with a particular emphasis on drug-induced effects on the QT interval (ICH, 2005). The QT interval receives special attention as prolongation of this interval can result in the potentially fatal ventricular tachyarrhythmia known as *torsades de pointes*. This is due mainly to blockade of a voltage-gated potassium channel known as the rapidly activated delayed rectifier channel (I_{Kr}) which is encoded by the human Ether-a-go-go Related Gene (hERG) (Yap & Camm, 2003). In the heart I_{Kr} is involved in cardiac repolarisation. The major example of drugs that prolong the QT interval is the class III antiarrhythmics (e.g. amiodarone). These drugs, commonly used for the treatment of atrial fibrillation, are in fact *designed* to block cardiac potassium channels. However, a number of non-cardiac drugs have also been reported to non-specifically block I_{Kr}, prolong the QT interval and induce *torsades de pointes* (e.g. citalopram, ketoconazole, terfenadine and cisapride) (Haverkamp *et al.*, 2000). Such drugs pose a great arrhythmogenic risk and have been withdrawn from or

restricted in clinical use. In drug development, extensive *in vitro* and *in vivo* preclinical screens have been designed to assess such risks resulting in withdrawal of compounds from further pharmaceutical development if necessary (Champeroux *et al.*, 2000).

More recently, there has been increasing awareness that drugs can also have serious adverse effects on cardiac contractile function (Force & Kerkelä, 2008). Furthermore, a higher incidence of effects on contractility has been noted during phase 1 clinical trials compared to effects on QT intervals (Moors *et al.*, 2007). Adverse drug reactions concerning cardiac contractility have previously received little attention and often such effects are not routinely assessed in pharmacological safety studies. However, there is a clear need to assess these risks early in the drug development process. Measurement of functional parameters relating to cardiac contractility should be integrated with existing tests of cardiac function to provide a fuller and more comprehensive assessment of the cardiovascular system. However, in order to assess these risks and therefore contribute to decreasing the attrition rates of drug candidates due to cardiotoxicity, the mechanisms governing cardiac contractility in normal physiological states must first be understood. With this knowledge potential mechanisms underlying cardiotoxicity can be identified.

1.2 Cardiac contractility

Cardiac contraction refers to the shortening of cardiac muscle to generate force to propel blood out of the heart and around the body. It is important that cardiac contraction is coordinated for normal regulation of blood pressure and blood flow.

1.2.1 Excitation-contraction coupling

Calcium (Ca^{2+}) signalling plays a central role in the regulation of cardiac contractility and changes in the intracellular Ca^{2+} concentration ($[Ca^{2+}]_i$) affect cardiac function. The Ca^{2+} transients which accompany each cardiac cycle trigger cardiac muscle contraction in a process known as excitation-contraction (EC) coupling.

In the heart, EC-coupling specifically refers to the sequence of events that commences with electrical excitation of the myocyte by an action potential, and concludes with contraction of the cell (and ultimately the entire heart). With the arrival of the action potential the myocyte is depolarised activating voltage-

dependent L-type Ca^{2+} channels (LTCC) on the transverse tubules (T-tubules) of the sarcolemmal membrane. The resultant influx of Ca^{2+} is itself insufficient to initiate contraction, but triggers the opening of functionally coupled ryanodine receptors (RyRs) located on the sarcoplasmic reticulum (SR) membrane (Currie, 2009).

Upon opening of RyRs, Ca^{2+} is released from the SR. This process is known as 'Ca^{2+}-induced Ca^{2+}-release' (CICR; Fabiato, 1983), raising $[Ca^{2+}]_i$ approximately 10-fold from 100nM to 1 µM (Maier & Bers, 2002). This increase in $[Ca^{2+}]_i$ is sufficient to allow Ca^{2+} to bind to and activate the myofilaments.

The myofilaments contain thick filaments consisting of the protein myosin and thin filaments consisting of the protein actin which are organised in subunits called sarcomeres. Troponin, attached to tropomyosin, lies in between actin filaments and consists of a complex of troponin T, I and C. Binding of Ca^{2+} to troponin C causes troponin and the associated tropomyosin to undergo a conformational change. This exposes the myosin binding sites on actin allowing actin and myosin to form a link (cross bridge). Myosin then pulls the actin filaments towards each other causing sarcomere shortening and cardiomyocyte contraction during systole (Martini, 2004).

Following systole, $[Ca^{2+}]_i$ declines breaking the link between actin and myosin. Troponin and tropomyosin revert back to their original conformation and the myosin binding sites on actin are blocked. Sarcomere length increases and diastole occurs. The decrease in $[Ca^{2+}]_i$ is achieved by: i) RyR inactivation; and ii) transport of Ca^{2+} out of the cytosol (Bers, 2002). A major contributor to Ca^{2+} removal is the sarco-endoplasmic reticulum Ca^{2+} ATPase (SERCA), which is responsible for the reuptake of Ca^{2+} into the SR and is regulated by the accessory protein, phospholamban (PLB). The Na^+/Ca^{2+} exchanger (NCX) also contributes to Ca^{2+} removal by extruding one Ca^{2+} ion across the plasma membrane in exchange for three sodium ions (Na^+). Quantitatively, the importance of these mechanisms varies between species with SERCA and NCX contributing ~70% and ~28% respectively in rabbit, guinea pig and human, and ~90% and ~7% respectively in rat and mouse (Bers, 2002). The remainder of cytosolic Ca^{2+} is removed by the sarcolemmal Ca^{2+} ATPase and the mitochondrial Ca^{2+} uniporter (Bers, 2002).

The processes described above are illustrated in Figure 1.4. The inset shows the time course of an action potential, Ca^{2+} transient and contraction (measured in a rabbit ventricular myocyte at 37ºC). Contraction lags behind the action potential

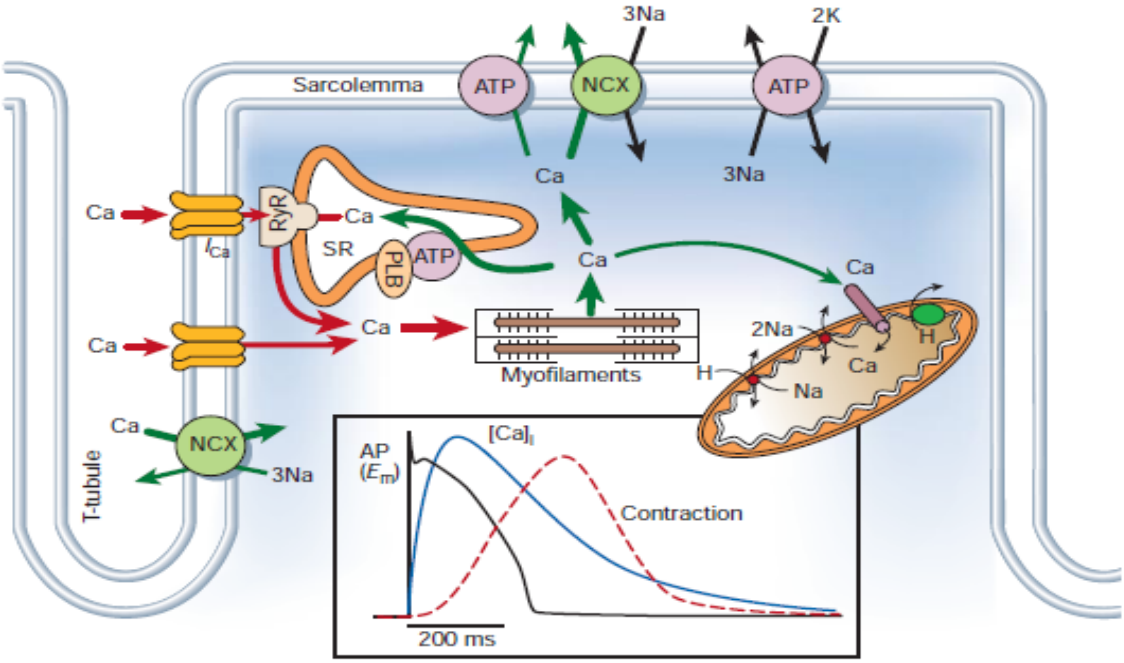

Figure 1.4 Ca^{2+} transport in ventricular myocytes. Inset shows the time course of an action potential, intracellular Ca^{2+} transient and contraction measured in a rabbit ventricular myocyte at 37ºC. AP, action potential; ATP, ATPase; Ca, calcium ions; Ica, calcium current; H, hydrogen ions; K, potassium ions; Na, sodium ions; NCX, Na^{+}/Ca^{2+} exchanger; PLB, phospholamban; RyR, ryanodine receptor; SR, sarcoplasmic reticulum; T-tubule, transverse tubule (Taken from Bers, 2002).

(passage of the electrical impulse), with the delay representing the time taken for Ca^{2+} to enter the cell, increase $[Ca^{2+}]_i$ and activate the contraction process.

1.2.2 Regulation of cardiac contractility

For normal cardiac contractile activity the mechanisms involved in cardiac Ca^{2+} handling must be tightly regulated. The most prominent regulator of cardiac contractility is the β_1-adrenoceptor system which is endogenously activated by the sympathetic nervous system transmitters, noradrenaline and adrenaline. Ligand binding activates the G_s-coupled β_1-adrenoceptor which increases the catalytic activity of adenylyl cyclase (AC) thus raising cyclic adenosine monophosphate (cAMP) synthesis within the cell (Brodde & Michel, 1999) and positively influencing contractility. Opposing this pathway is the parasympathetic muscarinic M_2 receptor pathway which is activated by acetylcholine. The M_2 receptor is G_i-coupled thus inhibiting AC and reducing cAMP formation (Brodde & Michel, 1999) and consequently contractility.

Many cellular functions are regulated by intracellular second messengers such as cAMP, through the activation of protein kinases. Cardiac Ca^{2+} handling can be included in this category (Sugden & Bogoyevitch, 1995). Calcium/calmodulin-dependent protein kinase II (CaMKII), cAMP-dependent protein kinase A (PKA), protein kinase C (PKC), mitogen-activated protein kinases (MAPKs), and tyrosine kinases have all been shown to play critical roles in the regulation of the proteins involved in cardiac Ca^{2+} handling (Schaub *et al.*, 2006; Grueter *et al.*, 2007; Ikeda *et al.*, 2008).

1.2.2.1 Protein kinases

Protein kinases are enzymes that modify other proteins by covalently attaching phosphate groups (phosphorylation) from adenosine trisphosphate (ATP) to specific amino acids with a free hydroxyl group (Berg *et al.*, 2002). Kinases can act on residues of serine and threonine (serine/threonine kinases), tyrosine (tyrosine kinases), serine, threonine and tyrosine (dual-specificity kinases), or histidine (histidine kinases). Phosphorylation usually induces a functional change in the protein substrate by altering the activity, cellular location or association with other proteins. Protein kinases are thus critical mediators of cell signalling which regulate diverse cellular processes including cell cycle progression, metabolism, transcription, and apoptosis (Cohen, 2001).

The activity of protein kinases is also subject to regulation by phosphorylation. This can be by the kinase itself (autophosphorylation) or by the binding of activator or inhibitor proteins. Furthermore, phosphorylation is reversible and the action of protein kinases is counterbalanced by protein phosphatases which dephosphorylate serine, threonine, tyrosine and/or histidine residues. The phosphorylation and dephosphorylation of proteins by protein kinases and protein phosphatases are shown in Figure 1.5.

1.2.3 Pharmacological modulation of cardiac contractility

Knowledge of the processes responsible for contraction of the heart has allowed the development of pharmacological agents which can be used to modulate cardiac contractility. Such agents are termed 'inotropes' of which both positive and negative are recognised.

Positive inotropes act to increase the force of contraction and can be used therapeutically in conditions where contractility is negatively impaired (e.g. acute heart failure). Negative inotropes decrease cardiac contractility which may be desirable in some medical conditions, such as hypertension. Alterations in contractility can be achieved by targeting various levels of signal transduction, e.g. upstream at the receptor level or downstream at the signalling molecules or effector proteins.

Agonists at the β_1-adrenoceptor, such as isoprenaline and dobutamine (sympathomimetics) increase the force of contraction (Rang *et al.*, 2003). Possessing similar positive inotropic effects are the phosphodiesterase inhibitors (e.g. milrinone) which prevent cAMP degradation by phosphodiesterases (Boswell-Smith *et al.*, 2006). Conversely, antagonists at the β_1-adrenoceptor (e.g. oxprenolol and atenolol) - the so-called 'β-blockers', which have been hugely successful therapeutic agents - prevent β_1-adrenoceptor signalling resulting in negative inotropy (Sproat & Lopez, 1991). Muscarinic M_2 receptor agonists mimic the parasympathetic influence on the heart thereby also being negatively inotropic (Brodde & Michel, 1999).

Drugs can also alter $[Ca^{2+}]_i$ by interacting directly with LTCCs. For example, Bay K 8644 is used experimentally to increase the opening of LTCCs and has positive inotropic activity in the heart (Schramm *et al.*, 1985; Thomas *et al.*, 1985). The LTCC can also be targeted by Ca^{2+} channel blockers (e.g. verapamil) that decrease

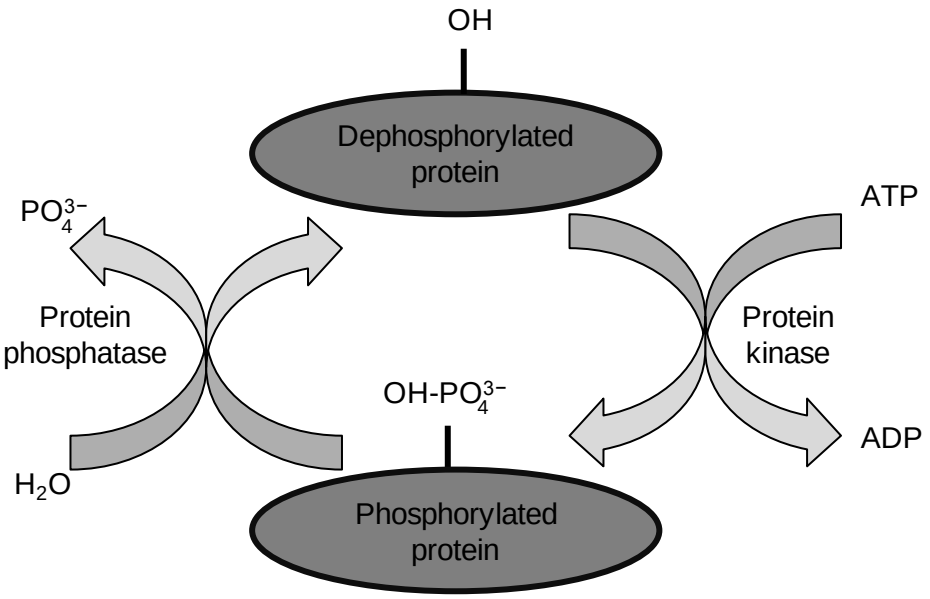

Figure 1.5 Phosphorylation and dephosphorylation of proteins by protein kinases and protein phosphatases. Protein kinases covalently attach phosphate groups (PO^{3-}_4) from adenosine trisphosphate (ATP) to specific amino acids with a free hydroxyl group (OH) (phosphorylation). Protein phosphatases remove phosphate groups by hydrolysis (dephosphorylation). ADP, adenosine diphosphate; H_2O, water.

Ca^{2+} influx through LTCC resulting in decreased force of contraction (Elliott & Ram, 2011). At the subcellular level, cardiac glycosides (e.g. digitalis, ouabain) inhibit membrane Na^+/K^+ pumps which pump Na^+ out of the cell in exchange for K^+. Inhibition results in increased cytosolic Na^+, which consequently slows the extrusion of Ca^{2+} by NCX. The increased $[Ca^{2+}]_i$ then allows greater contractile force to be generated (Page, 1964). Phosphorylation of RyR can be altered, for example by caffeine, which increases RyR phosphorylation thus triggering Ca^{2+} release from the SR and increasing contraction (Fill & Copello, 2002).

Recently, therapeutic targeting of protein kinases to treat certain cardiovascular conditions has been highlighted. This is due to the recognition that dysfunction of protein kinases - specifically significant increases in expression and activity - underlies several cardiovascular disorders (Force *et al.*, 2004; Kumar *et al.*, 2007). For example, mounting evidence exists that CaMKII expression and activity are increased in heart failure suggesting this kinase plays a key role in this condition (Hoch *et al.*, 1999; Kirchhefer *et al.*, 1999). In addition, Rho-dependent kinases (ROCKs) have been indicated to contribute to the development of hypertension and coronary and vascular vasospasm (Brown *et al.*, 2006; Noma *et al.*, 2006) through their phosphorylation of myosin, and possibly endothelial dysfunction and atherogenesis through interactions with phosphoinositide-3 kinase (PI3-K), endothelial nitric oxide synthase (eNOS) and plasminogen activator inhibitor-1 (Kumar *et al.*, 2007). G-protein-coupled receptor kinases (GRKs), in particular β-adrenoceptor kinase 1 (β-ARK1) which regulates β-adrenoceptors in the heart, have been linked to heart failure due to the findings that β-ARK1 expression and activity are increased in heart failure (Iaccarino *et al.*, 2005; Hata *et al.*, 2006; Pandalai *et al.*, 2006).

Inhibition of the above examples, has been found to be beneficial to cardiac function providing further evidence that these kinases could be targeted in disease treatment (Khoo *et al.*, 2004; Williams *et al.*, 2004). However, kinase signalling pathways are intimately linked with regulation of Ca^{2+} homeostasis and thus cardiac contractility. Therefore, it is likely that *complete* kinase inhibition would have detrimental or even lethal consequences. An important aim of kinase targeted therapies should therefore be to *normalise* overactive/overexpressed kinases rather than completely abolish their activity.

1.3 Calcium/calmodulin-dependent protein kinase II

Calcium/calmodulin-dependent protein kinase (CaMK) is a multifunctional serine/threonine protein kinase which is found in many cells, including cardiac myocytes. CaMK exists as 3 types - Type I, II and IV - of which the most abundant in the heart is Type II (Colbran, 2004). CaMKII is encoded by four genes, α, β, γ and δ, each of which can exist as a variety of splice variants. In the mammalian heart CaMKII δ, γ and β are expressed although CaMKIIδ predominates (Tobimatsu & Fujisawa, 1989; Hagemann *et al.*, 1999). CaMKIIδ is further subdivided with the δ_B isoform mainly residing in the nucleus, and the δ_C isoform mainly in the cytoplasm (Srinivasan *et al.*, 1994; Hagemann *et al.*, 1999).

1.3.1 Structure and activation of CaMKII

CaMKII is a holoenzyme consisting of 8-12 subunits arranged in a circular-shaped structure. Each subunit contains an N terminus catalytic domain which performs the kinase function of the enzyme, and a C terminus association domain which directs multimeric assembly. These domains flank a regulatory domain which controls enzyme activation (Colbran, 2004).

CaMKII is activated by Ca^{2+}-bound calmodulin (Ca^{2+}/CaM). CaM is a ubiquitous, bilobed, intracellular protein with two Ca^{2+} binding motifs on each N and C terminal lobe. In the absence of Ca^{2+}, parts of the regulatory domain bind to the catalytic domain, preventing substrate binding. However, when the regulatory domain binds Ca^{2+}/CaM, a conformational change occurs releasing the catalytic domain from this autoinhibiton and allowing the transfer of the γ phosphate from ATP to serine/threonine residues within the substrate (Colbran, 2004).

As well as phosphorylating protein substrates, CaMKII has the ability to autophosphorylate thus regulating its own activity (Anderson, 2005). CaMKIIδ autophosphorylation occurs within the autoregulatory domain at threonine (Thr) 286 of adjacent CaMKII monomers. Autophosphorylation greatly increases the affinity of Ca^{2+}/CaM for CaMKII (from nM to pM), but also confers 20-80% Ca^{2+}/CaM-independent activity after Ca^{2+}/CaM dissociates (Maier & Bers, 2002). This Ca^{2+}/CaM-independent activity occurs by preventing reassociation of the catalytic domain with the autoinhibitory region of the regulatory domain (Hudmon & Schulman, 2002). Autophosphorylation thus allows CaMKII to maintain its

regulatory role for extended periods of time. Inactivation of CaMKII occurs following dephosphorylation by protein phosphatases PP1 and PP2A (Anderson, 2007).

Recently, it has been shown that increased levels of reactive oxygen species (ROS) cause oxidative modification of the methionine (Met) 281/282 pair within the regulatory domain of CaMKII (Erickson *et al.*, 2008). This blocks reassociation of the regulatory domain with the catalytic domain and preserves kinase activity via a similar but parallel mechanism to Thr286 autophosphorylation.

The structure of CaMKII is shown in Figure 1.6 where autophosphorylation and oxidation sites are indicated. The initial activation of CaMKII by Ca^{2+}/CaM and subsequent autophosphorylation or oxidation are also shown in Figure 1.6.

Initial activation of CaMKII by Ca^{2+}/CaM means that the kinase is responsive to changes in $[Ca^{2+}]_i$ rather than being linked to a specific receptor-activated signalling pathway. However, many receptor-activated cell signalling pathways mobilise intracellular Ca^{2+} which then activates CaMKII (Ginsburg & Bers, 2004). An example of such, is the β_1-adrenoceptor system. As described earlier, ligand binding activates G_s-protein-coupled-receptors, which in turn activates AC, increasing cAMP production and ultimately activating PKA. PKA then targets several Ca^{2+} handling proteins leading to enhanced Ca^{2+} mobilisation. Recent studies suggest that CaMKII is also activated by β-adrenoceptor signalling (Zhu *et al.*, 2003; Wang *et al.*, 2004; Grueter *et al.*, 2007).

1.3.2 Regulation of Ca^{2+} handling by CaMKII

CaMKIIδ colocalises with and phosphorylates many key proteins involved in cardiac Ca^{2+} handling including LTCC (Dzhura *et al.*, 2000), SERCA (Narayanan & Xu, 1997), PLB (Wegener *et al.*, 1989) and RyR (Currie *et al.*, 2004). Figure 1.7 illustrates the Ca^{2+} handling proteins that are known or putative targets for phosphorylation by CaMKIIδ.

1.3.2.1 RyR

RyR is a large transmembrane protein consisting of four identical subunits forming a Ca^{2+} release channel on the SR. Mammalian tissues express three isoforms of the RyR, known as RyR_1, RyR_2 and RyR_3, with RyR_2 being the predominant cardiac isoform (Nakai *et al.*, 1990). RyR_2 exists as a multiprotein complex associated with

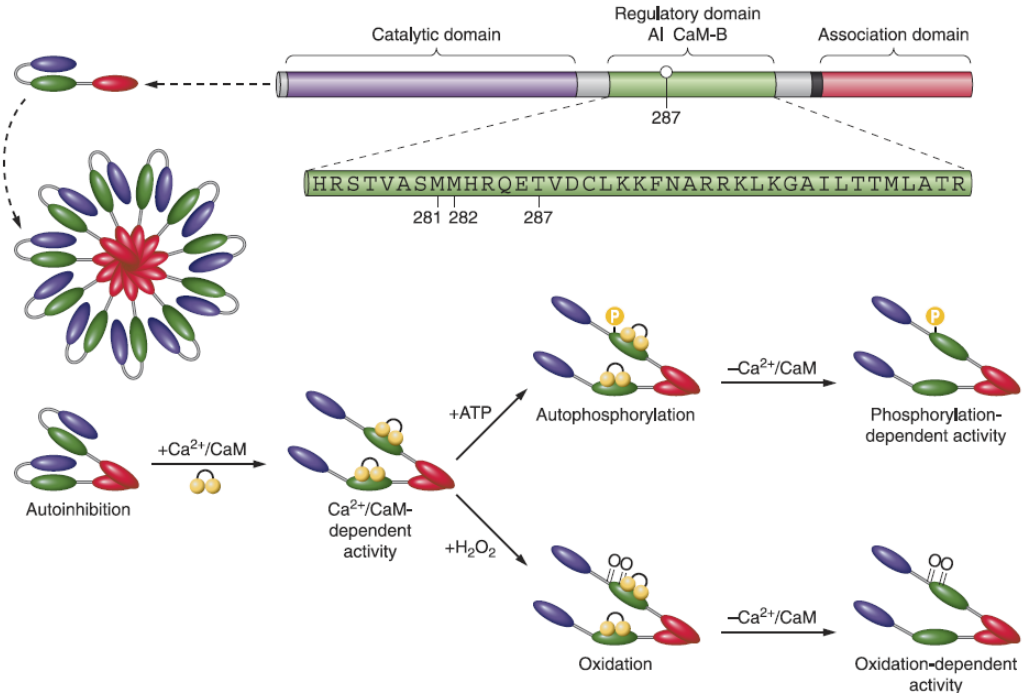

Figure 1.6 CaMKII structure and activation by Ca^{2+}/CaM and autophosphorylation or oxidation. (Taken from Erickson *et al.*, 2011).

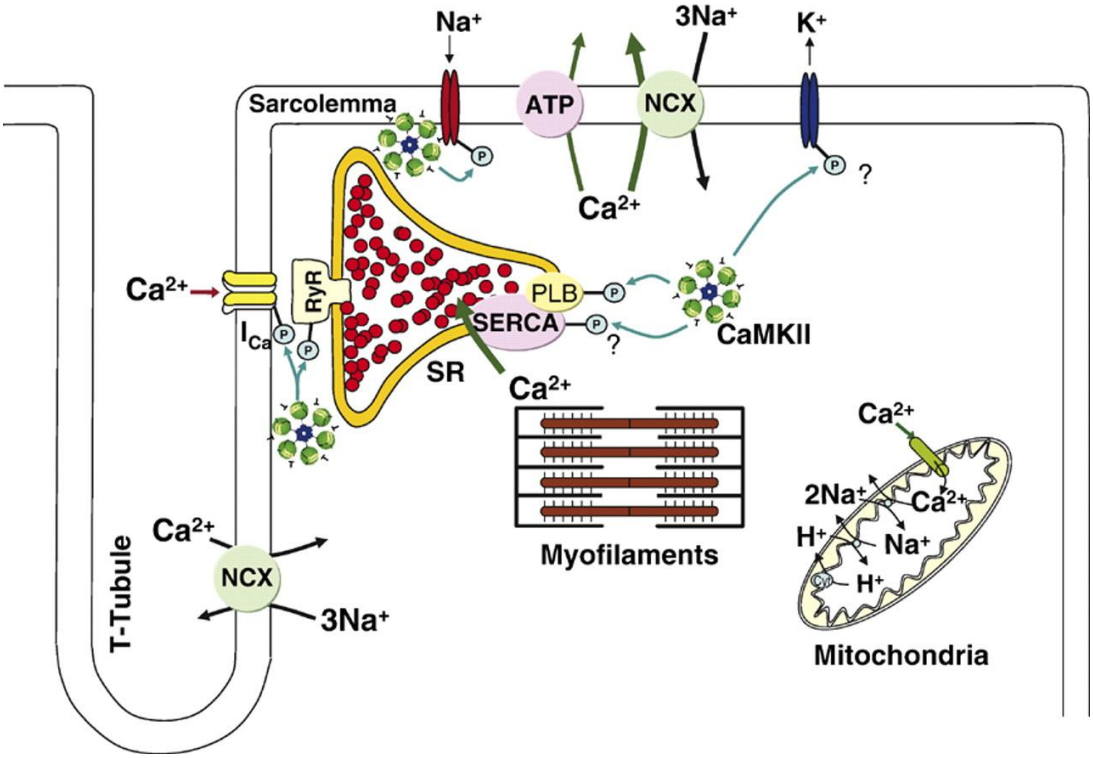

Figure 1.7 CaMKIIδ colocalises with and phosphorylates many key proteins involved in cardiac Ca^{2+} handling including LTCC, SERCA, PLB and RyR. In addition, Na^{+} channels and K^{+} channels may also be targeted by CaMKIIδ (Taken from Maier & Bers, 2007).

other RyR_2s, small molecules, and proteins such as enzymes, scaffolding proteins and Ca^{2+} binding proteins. Included in this complex is CaMKII (Wehrens *et al.*, 2004) which has been shown to affect Ca^{2+} released via RyR_2 both positively and negatively depending on the experimental conditions (Witcher *et al.*, 1991; Passier *et al.*, 2000; Wu *et al.*, 2001). The majority of studies have reported that CaMKII phosphorylation leads to increased RyR_2 activity but inhibitory consequences have also been reported (Yamaguchi & Meissner, 2007).

The specific site(s) of CaMKII phosphorylation of RyR_2 is still under investigation. Direct phosphorylation was initially suggested at Ser2809 (Otsu *et al.*, 1990; Witcher *et al.*, 1991), which was later shown to also be phosphorylated by PKA (Rodriguez *et al.*, 2003). Further work has suggested Ser2815 to be a phosphorylation site exclusive to CaMKII (Wehrens *et al.*, 2004). It is also possible that CaMKII could regulate RyR_2 indirectly by phosphorylating one or more of the multiple proteins in the RyR_2 complex. The Ca^{2+} binding protein, sorcin, which has inhibitory effects on RyR_2, has been investigated in such a context (Anthony *et al.*, 2007) and PP2A and triadin have also been highlighted as potential candidates (Currie, 2009).

1.3.3 Role of CaMKII in cardiac dysfunction

CaMKII activity and expression can be altered in many conditions of cardiac dysfunction. Although patient studies are limited, increased CaMKII activity has been associated with the progression of heart failure (Hoch *et al.*, 1999; Kirchhefer *et al.*, 1999). The majority of evidence, however, comes from animal models. In models of genetic (Wu *et al.*, 2002) and surgical (Colomer, 2002) structural heart disease, CaMKII activity and expression were increased. Zhang *et al.* (2002, 2003) reported that overexpression of CaMKIIδ_B and δ_C in mice resulted in cardiac hypertrophy. Maier *et al.* (2003) further reported cardiac chamber enlargement, myocardial dysfunction and dysregulation of intracellular Ca^{2+} homeostasis following CaMKIIδ_C overexpression. Conversely, inhibition of CaMKII in mice has been shown to reduce LV dilation and improve myocardial function after surgically-induced myocardial infarction (Khoo *et al.*, 2004). Similarly, overexpression of the CaMKII inhibitory peptide, AC3I, was found to prevent LV dysfunction following myocardial infarction induced by chronic β_1-adrenoceptor activation (Grueter *et al.*, 2007).

CaMKII has also been suggested to be involved in apoptosis in the heart (Fladmark *et al.*, 2002). Zhu *et al.* (2003) concluded that *in vitro* apoptosis, as a result of chronic isoprenaline treatment activating β_1-adrenoceptors, occurs through activation of CaMKII. Furthermore, Yang *et al.* (2006) reported that inhibition of CaMKII *in vivo* protected against apoptosis during myocardial infarction or chronic β_1-adrenoceptor stimulation with isoprenaline. Together, these findings point to proapoptotic actions of CaMKII.

CaMKII has also been recognised as having a role in cardiac arrhythmias (Erickson & Anderson, 2008). Again, inhibition of CaMKII has been shown to be beneficial as in a mouse model of cardiac hypertrophy a CaMKII inhibitory peptide was shown to eliminate early after depolarisations (Wu *et al.*, 2002).

1.4 Cardiotoxicity

Recently several drugs in development or on the market have been found to cause cardiotoxicity. Although cardiotoxicity describes a broad range of drug-induced adverse effects on heart function many agents have been found to affect the myocardium causing left ventricular dysfunction, heart failure and in some cases death (Kerkelä *et al.*, 2006; Chu *et al.*, 2007). Such effects may emerge throughout the drug discovery and development process, however, often this is not the case and cardiotoxic effects are revealed in clinical testing, or even after the drug has been licensed for human use. In addition, the mechanisms leading to cardiotoxicity are largely unknown despite several investigative studies and reports (Kerkelä *et al.*, 2006; Chu *et al.*, 2007; Chen *et al.*, 2008; Force & Kerkelä, 2008; Mellor *et al.*, 2011). Understanding, identifying and combating these risks are clearly of high importance in the development of new drug therapies.

1.4.1 Mechanisms of cardiotoxicity

Preclinical detection of drug effects on cardiac contractility is a necessity, however, understanding what causes these effects and why they occur is also important. The mechanisms underlying drug-induced cardiotoxicity are largely unknown. It is known, however, that cardiotoxicity is often associated with agents targeting specific protein kinases (Force & Kerkelä, 2008).

1.4.1.1 Protein kinases as drug targets

Dysfunction of protein kinases is increasingly recognised as underlying several diseases including inflammatory diseases, cardiovascular diseases, metabolic diseases, neurodegenerative diseases and cancer (Cohen, 2001). These kinases are therefore putative targets for drug development and indeed kinases have become the second most important group of drug targets after G-protein coupled receptors (GPCRs) (Cohen, 2002) and have accounted for 25 to 30% of all targets screened in the pharmaceutical industry (Netterwald, 2007).

Small molecule kinase inhibitors targeting intracellular kinases involved in signal transduction are divided into three types: Type I compete with ATP for access to the ATP binding pocket; Type II also bind to the ATP pocket plus an additional adjacent region only accessible when the kinase is inactive, thus locking the kinase in an inactive state; Type III act at sites other than the ATP pocket, such as the substrate recognition site. Type I inhibitors are by far the most prevalent as these agents can be designed with relative ease attributable to the fact that the structure of the ATP binding pocket has been well-studied and is highly conserved across the kinome (Verkhivker, 2007).

The vast majority of kinase inhibitors have been developed in the field of oncology. Protein kinases, in particular tyrosine kinases, have been shown to play an important role in the pathogenesis of cancer (Krause & Van Etten, 2005). Aberrant activation of kinases resulting from acquired or inherited genetic mutations make such kinases key therapeutic targets in oncology drug discovery.

Imatinib (Gleevec®, Novartis) was the first of this class of drugs to be developed and gained FDA approval in 2001 after positive results on patient survival (Sherbenou & Druker, 2007). Imatinib is used therapeutically in the treatment of chronic myeloid leukaemia, where it inhibits the aberrant activity of the bcr-abl (breakpoint cluster region - Abelson proto-oncogene) fusion kinase. In addition, imatinib also inhibits c-Kit kinase activity and platelet-derived growth factor receptors (PDGFRs) α and β allowing its application in the treatment of gastrointestinal stromal tumours.

Following the success of imatinib, and as the role of kinases in cancer (and other diseases) has been further understood, interest in kinase inhibition has grown rapidly. There are over 500 members of the kinome, providing enormous scope for

future drug development (Manning *et al.*, 2002). In 2009, Zhang *et al.* reported approximately 80 small-molecule kinase inhibitors in clinical trials. However, concerns have been raised regarding the selectivity and safety of kinase inhibitors (Sebolt-Leopold & English, 2006; Force & Kerkelä, 2008).

1.4.1.2 Concerns related to kinase inhibition

Generally, kinase inhibitors tend to be fairly non-selective and inhibit several kinases. Of the kinase inhibitors Type I are the least selective due to a high degree of conservation in the protein sequence of the ATP binding site throughout the kinome. By targeting additional or alternative regions, Type II and Type III inhibitors aim to improve selectivity but because they exploit novel structural aspects of individual kinases they are more difficult to design.

Kinases are ubiquitously expressed and inhibition of aberrant kinase activity in pathological tissue could well inhibit beneficial or normal activity of the kinase in other tissues (e.g. the heart and/or vasculature). This has been termed an "on-target" effect as the specific kinase affected is the one which the drug was intended to hit. "Off-target" effects may also be an issue where unintended inhibition of multiple kinases beyond the intended target kinase (or kinases) occurs. Although these off-target kinases may or may not have a role in tumour progression, they may be essential to the function of the heart.

The growing trend towards 'multi-targeted' agents, which are by design nonselective and intended to inhibit multiple kinases with one drug, is also a concern. The aim of targeting multiple kinases is to increase drug efficacy and applicability. Theoretically, inhibition of growth factors or their receptors involved in angiogenesis (e.g. vascular endothelial growth factor receptors (VEGFRs) and PDGFRs), as well as inhibition of kinases involved in tumour cell proliferation, could broaden anticancer activity arising from this dual pharmacological effect (Faivre *et al.*, 2007). However, in the case of VEGFR inhibition it has become increasingly apparent that this induces significant hypertension (Bhargava, 2009) which can lead to substantial stress on the heart.

Sunitinib (Sutent®, Pfizer) is one such multi-targeted kinase inhibitor that gained FDA approval in 2006 for the treatment of renal cell carcinoma and imatinib-resistant gastrointestinal stromal tumours. Targets of sunitinib include all PDGFRs, VEGFRs, and c-Kit. In addition it is also stated as inhibiting RET (rearranged during

transfection), CSF (colony stimulating factor)-1R and flt3 (fms-like tyrosine kinase receptor-3) kinases (Pfizer, 2006).

Inhibition of non-kinase targets is a further concern as any enzyme that requires ATP to perform its various functions could be inhibited by small molecule kinase inhibitors. Indeed this has been reported for the oxidoreductase NQO2 and the transmembrane transporter, breast cancer related protein (BCRP) in the case of imatinib (Houghton *et al.*, 2004; Burger *et al.*, 2004). The toxicological consequences of inhibiting non-kinase targets are unclear, but may significantly increase the potential for side effects.

1.4.1.3 Kinase inhibition and cardiotoxicity

Kinase inhibitors have had a major impact on cancer patient survival and generally the majority of approved agents have appeared to be well tolerated from a cardiac safety perspective (Cheng & Force, 2010). However, several of these agents have been reported to adversely affect cardiac function in a subset of treated individuals and the true extent of these risks is relatively unknown (Force & Kolaja, 2011). Cardiotoxicity relating to two kinase inhibitors widely used as anti-cancer agents, imatinib and sunitinib, is discussed below.

Imatinib was the first of these kinase inhibitors to gain FDA approval and cardiotoxicity was not predicted by preclinical studies although hepatic, renal, immunological, and teratogenic effects were highlighted as safety issues relevant to humans (FDA, 2001). No abnormal pathological changes were observed in rat hearts in a 26 week repeat dose study and no cardiac pathological changes were reported in a 13 week dog study or a 39 week study in monkeys. A dose-dependent, short-lasting decrease in arterial blood pressure was observed immediately following a single intravenous (i.v.) dose in rats but there were no effects on the ECG. There were also no effects on the rate of beating or force of contraction in isolated guinea pig atria, and a single oral dose had no effect on blood pressure, heart rate or ECG in dogs.

Following approval, a report was published associating imatinib with the development of severe heart failure (Kerkelä *et al.*, 2006). This alarmed oncologists and resulted in a revision of the imatinib prescribing information to describe possible heart failure and LV dysfunction. In this publication (Kerkelä *et al.*, 2006) ten patients developed heart failure associated with mild LV dilation and a decline in the

mean LV ejection fraction whilst being treated with imatinib. Mice treated with imatinib experienced a decline in LV function along with a loss of myocardial mass consistent with cell loss. These effects were suggested to be mediated by inhibition of ABL and induction of the endoplasmic stress response. A further study describing a structurally reengineered form of imatinib that inhibited KIT but not ABL and showed less cardiotoxicity supported this suggestion (Fernández *et al.*, 2007) whilst another study suggested that imatinib may affect cardiac Akt and Erk1/2 phosphorylation predisposing to cardiac failure under conditions of stress (Trent *et al.*, 2010).

Retrospective evaluations of the incidence of heart failure in patients receiving imatinib on clinical trials showed that imatinib treatment resulted in only very low rates of heart failure or LV dysfunction, compared to those expected in the general population (Verweij *et al.*, 2007; Dematteo *et al.*, 2009; Trent *et al.*, 2010). Furthermore, it was suggested that heart failure in patients with underlying cardiovascular disease could have been exacerbated by fluid retention, a known common side effect of imatinib (Verweij *et al.*, 2007; Atallah *et al.*, 2007*a*; Hochhaus *et al.*, 2008). It was also noted that the majority of the affected patients in the Kerkelä *et al.* (2006) study and other studies (Hatfield *et al.*, 2007; Atallah *et al.*, 2007*a*) had pre-existing conditions predisposing to heart failure (e.g. hypertension, coronary artery disease or diabetes) and many had previous exposure to one or more cardiotoxic drugs. However, these studies were retrospective analyses of cardiac endpoints which were not previously defined. In addition, the known overlap of heart failure symptoms and side effects of imatinib (e.g. dyspnoea, fatigue, and oedema) make clinical assessment difficult, possibly leading to underestimated reports of imatinib-induced heart failure (Thanopoulou & Judson, 2012).

Recently it was found that cytotoxic concentrations of imatinib were required to trigger markers of apoptosis and stress responses in neonatal rat ventricular myocytes and fibroblasts, implying that at clinically relevant concentrations imatinib is not cardiotoxic (Wolf *et al.*, 2010). A study evaluating imatinib-treated patients for cardiotoxicity (via cardiac imaging) reported no evidence of myocardial deterioration over 12 months of imatinib treatment (Estabragh *et al.*, 2011), whilst in another study substantial increases in serum levels of brain natriuretic peptide, indicative of possible heart failure, were observed in 4% of patients after 3 months (Perik *et al.*, 2007).

Taken together, the reports discussed above demonstrate that imatinib-induced cardiotoxicity is clearly controversial. The reports are, however, significant enough to warrant caution in prescribing imatinib and to consider imatinib-treated patients at risk of heart failure, but without structural heart disease or symptoms (Trent *et al.*, 2010). The mechanisms leading to cardiotoxicity in some patients are also debatable and remain to be fully elucidated.

Unlike imatinib, sunitinib is a kinase inhibitor that is clearly associated with clinical cardiotoxicity. Preclinical evaluation of sunitinib revealed several adverse cardiovascular effects. The action potential duration was increased in canine Purkinje fibres and the hERG channel was potently blocked. In primates the QT interval was prolonged and heart rate decreased whilst echocardiography showed reductions in the ratio of left atrial to aortic diameter, LV ejection time and LV area. In addition, histological assessments identified capillary proliferation, myocardial vacuolization, and pericardial inflammation (FDA, 2006).

In the clinic, QT interval prolongation was also found (Bello *et al.*, 2009) as well as decreases in LV ejection fraction (Pfizer, 2006; Motzer *et al.*, 2007). Retrospective studies found that 15% of sunitinib-treated patients developed symptomatic grade 3/4 LV dysfunction (Telli *et al.*, 2008). Further studies showed a gradual decline in LV ejection fraction over 24 weeks of treatment and 8% of patients developed heart failure following 33.6 weeks median treatment duration (Chu *et al.*, 2007). Similar to imatinib, previous heart failure and/or coronary artery disease or anthracycline therapy were significant risk factors for LV dysfunction with sunitinib treatment (Telli *et al.*, 2008).

1.4.1.4 Kinase inhibition and cardiac contractility

A major concern with kinase inhibitor therapies, in development or on the market, is inhibition (on or off target) of signalling pathways regulating cardiomyocyte function - especially under cardiac stress. There is significant overlap in many of the pathways involved in cancer cell survival and cardiomyocyte homeostasis. Inhibition of the kinases in these pathways may well be beneficial in cancer, but not for maintaining cardiac contractile function. How such therapies may perturb the signalling pathways regulating cardiac contractility requires further investigation.

1.4.2 Potential role of CaMKII in cardiotoxicity

As detailed earlier, contractile dysfunction with resultant heart failure is one of the most common cardiotoxic effects of agents targeting protein kinase pathways. Several reports have implied that this cardiotoxicity results from effects of these agents on kinases with central roles in maintaining cardiac function (Cheng & Force, 2010; Force & Kolaja, 2011; Mellor *et al.*, 2011) and some have even specifically highlighted CaMKII (Stummann *et al.*, 2009; Force & Kolaja, 2011). Somewhat surprising, therefore, is that CaMKII, as a key regulator of normal and abnormal cardiac Ca^{2+} handling, has not been investigated in the context of cardiotoxicity associated with these kinase inhibitors.

Furthermore, CaMKII has previously been linked to cardiotoxicity associated with another anti-cancer agent, doxorubicin (Sag *et al.*, 2011). Doxorubicin belongs to the anthracycline class of drugs and works by intercalating DNA. It is one of the most effective anti-cancer agents, but cardiotoxicity limits its use. In isolated cardiomyocytes doxorubicin treatment increased CaMKII phosphorylation and induced CaMKII-dependent SR Ca^{2+} leak contributing to impaired Ca^{2+} homoeostasis. This suggests CaMKII inhibition may reduce doxorubicin-induced cardiotoxicity.

Taken together, these reports suggest that CaMKII may be an intracellular target for drugs that alter cardiac contractility. If drug-induced changes in cardiac contractility can be linked to changes in CaMKII, CaMKII could be identified as an *in vitro* marker of *in vivo* changes in contractility offering great potential as a marker of cardiac safety in drug development. Firstly, however, a potential link needs to be investigated and the nature of any such link characterised.

1.5 Hypotheses and aims

To test the hypothesis that CaMKIIδ may be an intracellular target for drugs that alter cardiac contractility, and as such may be a useful marker of cardiac safety, the overall aim of this thesis was to develop a small animal model for integrated assessment of cardiac contractility and CaMKIIδ.

Specific aims of individual Chapters were:

- Chapter 2

    (i) To establish and characterise a small animal model measuring haemodynamics and cardiac contractility.

    (ii) To investigate the effects of selected drugs following acute *in vivo* administration.

- Chapter 3

    (i) To optimise methods to assess CaMKIIδ expression and CaMKII activity in LV tissue from guinea pig.

    (ii) To use these methods to determine if corresponding changes in CaMKIIδ expression and/or CaMKII activity can be detected following acute *in vivo* drug administration.

- Chapter 4

    (i) To investigate factors that may influence indices of cardiac contractility.

- Chapter 5

    (i) To investigate the effects of selected drugs following chronic *in vivo* administration.

    (ii) To determine if corresponding changes in CaMKIIδ expression and/or CaMKII activity can be detected following chronic *in vivo* drug administration.

CHAPTER 2 *IN VIVO* MEASUREMENT OF CARDIAC CONTRACTILITY AND HAEMODYNAMICS

2.1 Introduction

$LVdP/dt_{max}$ is a commonly used index of cardiac contractility (Beek, 1982; Hayes, 1982; Salyers *et al.*, 1988). In order to obtain $LVdP/dt_{max}$, LVP must first be measured and then the mathematical derivative 'dP/dt_{max}' calculated (Figure 2.1a). $LVdP/dt_{max}$ represents the maximum rate of rise of LVP - an increase in which would signify an increase in contractility. However, if a drug alters the preload or afterload on the heart it can be difficult to separate such effects from a direct action on myocardial contractility.

An alternative parameter that has been suggested to be less sensitive to changes in cardiac loading is the QA interval. The QA interval is the time interval from the onset of the Q wave of the ECG to the beginning of the upstroke of the following arterial blood pressure wave (Figure 2.1b). The QA interval was initially proposed quite some time ago (Cambridge & Whiting, 1986) and more recently there has been a revival of interest in the potential of this parameter. If the QA interval proved equally or more useful than $LVdP/dt_{max}$ in assessing cardiac contractility it may be preferred as it offers a less invasive and simpler method that would be quicker and easier to perform. Comparisons of the QA interval and $LVdP/dt_{max}$ as indices of cardiac contractility in the dog (Norton *et al.*, 2009) and the rat (Adeyemi *et al.*, 2009) have been published but no studies have been performed in guinea pigs.

LVP can be measured, similar to arterial blood pressure, via a fluid filled cannula inserted into the lumen of the LV. Alternatively, a catheter consisting of an ultraminiature pressure sensor at the distal end of the catheter with an electrical connector at the proximal end can be used. The pressure sensor produces an electrical signal which varies in direct proportion to the magnitude of sensed pressure. Electrical signals can then be recorded using an amplifier and appropriate software (see Section 2.2.4) and $LVdP/dt_{max}$ can be calculated.

Preliminary experiments in rats developed the surgical techniques required to measure LVP, with simultaneous measurement of the QA interval achieved via ECG recording and arterial blood pressure measurement (via a femoral artery). The feasibility of measuring LVP via each of the above methods was explored. This work in rats also allowed drug doses to be explored and experimental protocols to be established.

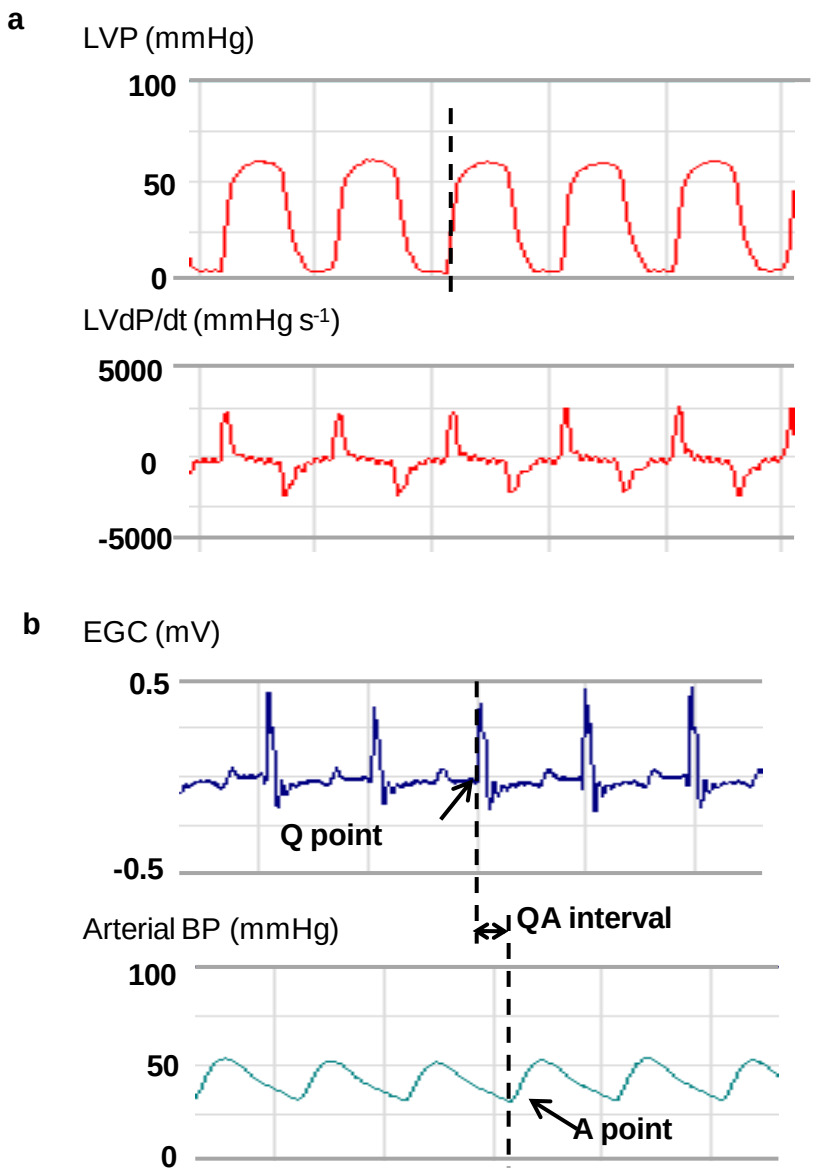

Figure 2.1 *In vivo* indices of cardiac contractility. **a)** Left ventricular (LV)dP/dt_{max}, representing the maximum rate of rise of left ventricular pressure (LVP) and derived from the LVP signal, and **b)** the QA interval, the time from the onset of the Q wave of the electrocardiogram (ECG) to the beginning of the upstroke of the arterial blood pressure (BP) wave.

Following this initial work in rats, the guinea pig became the small animal of choice for several reasons:

- Anaesthetised guinea pigs have been used to assess drug effects on cardiac electrophysiology, contractility and haemodynamics (Hauser *et al.*, 2005) and guinea pig models have already been established for routine assessment of drug-induced QT prolongation (Batey *et al.*, 1997; Minematsu *et al.*, 1999*b*, 1999*a*; Hamlin *et al.*, 2003; Drouin *et al*., 2004; Fossa *et al.*, 2004; Testai *et al.*, 2004).

- Compared to the rat, the guinea pig is more similar to man electrophysiologically. In the rat heart, repolarisation is mainly dependent on the transient outward potassium current (I_{to}) rather that the rapidly activating delayed rectifier potassium current (I_{Kr}) (Busch *et al.*, 1994). The rat ventricle also poorly mimics human cellular Ca^{2+} fluxes due to differences in Ca^{2+} handling proteins (Bers, 2002).

- In relation to cardiac contractility, the guinea pig responds normally to cardiac glycosides whereas the rat is relatively insensitive (Repke *et al.*, 1965; Akera *et al.*, 1979; Koomen *et al.*, 1984; Weinhouse *et al.*, 1989; Koga *et al.*, 1989).

In the guinea pig, however, arterial access is limited as the femoral arteries are too small and fragile to be cannulated routinely. Therefore, in order to measure LVP and arterial blood pressure simultaneously, thus allowing $LVdP/dt_{max}$ and the QA interval to be obtained in the same animal, both carotid arteries need to be cannulated. Such bilateral carotid artery occlusion eliminates any input from the baroreceptors situated in the walls of the carotid sinuses located near the base of the internal carotid arteries and may compromise the blood supply to the brain. This could substantially impair reflexes and affect responses to drugs that alter arterial blood pressure. As drugs that have inotropic activity may also affect arterial pressure, it is important to determine whether or not bilateral carotid occlusion alters the effects of drugs on heart rate and arterial blood pressure in guinea pigs. This is particularly important when planning to use $LVdP/dt_{max}$ as an index of cardiac contractility because this parameter can be altered by changes in heart rate, preload or afterload (Wallace *et al.*, 1963).

Another important consideration is the anaesthetic regime which must be suitable for the nature and duration of the experiments. Previously, sodium pentobarbital has been used in cardiovascular studies in anaesthetised rats (Coker & Ellis, 1987; Barnes & Coker, 1995; Philp *et al.*, 2006). Recently, however, inhalation anaesthetics have grown in popularity due to the advantages in terms of speed of induction and rapid responses to altering the dose during procedures to maintain steady anaesthesia. In guinea pigs, although some studies comparing different anaesthetics have been published (Brown *et al.*, 1989; Buchanan *et al.*, 1998; Schwenke & Cragg, 2004) none of these has measured cardiac contractility. Previous ECG studies in guinea pigs employed a variety of anaesthetic regimes: pentobarbital (Batey *et al.*, 1997; Fossa *et al.*, 2004; Testai *et al.*, 2004), ketamine/xylazine (Hamlin *et al.*, 2003), urethane/α-chloralose (Minematsu *et al.*, 1999*b*) thiobutabarbital/urethane (Yao *et al.*, 2008) and urethane (Hauser *et al.*, 2005). It is therefore not clear which anaesthetic may be best for these types of experiments.

As this model is intended to assess drug-induced changes in haemodynamics and cardiac contractility, standard drugs with known responses must be tested. Drugs tested included the positive inotropes, isoprenaline and ouabain, and the negative inotrope, verapamil. To assess adverse effects, identified cardiotoxic agents, imatinib and sunitinib, were also tested.

2.1.1 Aims

To test the hypothesis that the anaesthetised guinea pig is a suitable model for detection of changes in cardiac contractility and haemodynamics, the aims of the work presented in this Chapter were:

(i) To perform preliminary experiments in rat to gain experience of surgical techniques, establish an experimental protocol, and optimise recording of LVP.

(ii) To choose an anaesthetic regime suitable for the nature and duration of future experiments in guinea pigs.

(iii) To determine if bilateral carotid occlusion (by insertion of cannulae) compromises the effects of drugs on heart rate and blood pressure.

(iv) To investigate the effects of known and potential inotropic agents on cardiac contractility and haemodynamics following acute *in vivo* drug administration.

(v) To compare the usefulness of the QA interval and $LVdP/dt_{max}$ as indices of cardiac contractility.

2.2 Methods

Suppliers of equipment and materials are detailed in Appendix A. Suppliers of drugs and reagents and their storage information are detailed in Appendix B.

2.2.1 Animals

All animal experiments were performed in accordance with the UK Animals (Scientific Procedures) Act 1986, approved by institutional ethical review committees and conducted under the authority of Project Licences held at the University of Strathclyde or at AstraZeneca.

Six male Sprague Dawley rats weighing 390 – 430 g were bred in-house and were housed in small groups on gold flakes bedding. Rooms were held at a temperature of 21°C, with 45 to 65% relative humidity and a 12 hour light/dark cycle. Food (Special Diet Services CRM (p) rat diet) and water were available ad libitum.

A total of fifty-seven male Dunkin Hartley guinea pigs weighing 425 – 720 g were allowed a minimum of one week acclimatisation following arrival and were housed in small groups, on aspen chip bedding and sizzle nest, or hay. Rooms were held at temperatures between 16 and 23°C, with 40 to 70% relative humidity and a 12 hour light/dark cycle. Food (Special Diet Services FD1 guinea pig diet or Teklad global higher fibre guinea pig diet 2041, plus fresh fruit and vegetables) and water were available ad libitum.

2.2.2 Anaesthesia

2.2.2.1 Rats

In rats anaesthesia was induced by inhalation of isoflurane (5% in 100% O_2 at a rate of 1L min^{-1}) in an anaesthetic chamber. Initially anaesthesia was maintained with isoflurane (~1.5-3% in 100% O_2 at a rate of 0.5L min^{-1}) delivered via a nose cone (n = 3). In later animals, whilst recording ECG and arterial blood pressure, several i.v.

bolus doses of sodium pentobarbital were given using an infusion pump (n = 3). The isoflurane and oxygen were discontinued after the first dose of pentobarbital had been given. Normally, 6 to 8 x 3 mg doses of pentobarbital (~ 45 to 60 mg kg^{-1}) were required to replace the isoflurane. Sodium pentobarbital (12 mg mL^{-1}) was infused at 500 µL min^{-1} for 30 s for bolus doses and then continuously at 6 mg kg^{-1} hr^{-1}. If throughout experiments the continual infusion of sodium pentobarbital was not sufficient, bolus doses were administered as necessary by increasing the infusion pump rate.

2.2.2.2 Guinea pigs

In nineteen guinea pigs weighing 490 – 720 g, preliminary experiments focused on determining suitable anaesthetic regimes and were performed in collaboration with AstraZeneca. The anaesthetics tested were isoflurane (n = 3), a combination of Hypnorm® and Hypnovel® (n = 4), and sodium pentobarbital either given alone (n = 4) or after premedication with fentanyl (n = 4). Experiments with Hypnorm/Hypnovel and pentobarbital alone were performed by Louise Marks at AstraZeneca whereas those with isoflurane and fentanyl/pentobarbital were performed concurrently at the University of Strathclyde. Subsequently, a different isoflurane protocol was assessed by Karen Philp at AstraZeneca (n = 4). Animals anaesthetised with isoflurane were breathing 100% oxygen, the first 3 breathing spontaneously, the latter 4 artificially ventilated. All others were artificially ventilated with room air. Details of the doses and routes of administration for the induction and maintenance of anaesthesia with all agents are given in Table 2.1. All subsequent experiments at the University of Strathclyde were performed in guinea pigs anaesthetised with the fentanyl/pentobarbital combination. Body temperature was measured via a rectal thermometer and maintained at ~37°C with a heating lamp.

2.2.3 Surgical preparation

2.2.3.1 Rats

Immediately after induction of an adequate level of anaesthesia, as determined by the absence of corneal and/or pedal withdrawal reflexes, subcutaneous needle electrodes were inserted to record limb lead ECGs. Both femoral veins were dissected free from surrounding tissue and cannulated, one for infusion of maintenance anaesthetic and the other for test drugs. A femoral artery was dissected free from surrounding tissue and cannulated, to allow measurement of

Table 2.1 Doses and routes of administration of agents used for the induction and maintenance of anaesthesia in guinea pigs.

Anaesthetic	**Induction**		**Maintenance**	
	Dose	***Route***	***Dose***	***Route***
Isoflurane[a]	5%	Inhalation	2.0 – 2.5%	Inhalation
Isoflurane[a]	2 – 4%	Inhalation	1.5 – 2.5%	Inhalation
Hypnorm/Hypnovel[b]	8 mL kg^{-1}	i.p.	1.25 mL kg^{-1} hr^{-1}	i.v.
Sodium Pentobarbital[c]	60 mg kg^{-1}	i.p.	6 mg kg^{-1} hr^{-1}	i.v.
Fentanyl[d] *plus*	50 µg kg^{-1}	s.c.		
Sodium Pentobarbital[c]	50 – 60 mg kg^{-1}	i.p.	6 mg kg^{-1} hr^{-1}	i.v.

[a]Isoflurane was given by inhalation via a nose cone in 100% oxygen delivered at 1 L min^{-1} for induction and at 0.5 L min^{-1} for maintenance of anaesthesia. [b]A solution containing 1 part Hypnorm (a solution containing fentanyl citrate 0.315 mg mL^{-1} and fluanisone 10 mg mL^{-1}); 1 part Hypnovel (midazolam HCl 5 mg mL^{-1}) and 2 parts water made up freshly each day. [c]Sodium pentobarbital was dissolved at 60 mg mL^{-1} in distilled water daily for induction of anaesthesia and diluted to 6 or 12 mg mL^{-1} in normal saline (0.9% w/v NaCl in water) for maintenance, just before the start of each experiment. [d]Fentanyl (Sublimaze®) was supplied as a solution of 50 µg mL^{-1} and was given 5 min before sodium pentobarbital. i.p., intraperitoneal; s.c., subcutaneous.

arterial blood pressure. All cannulae were filled with heparin treated saline (0.9% w/v NaCl containing 5 - 10 units heparin mL^{-1}) and secured in position by a ligature. The trachea was isolated and prepared for later cannulation in animals transferred to pentobarbital anaesthesia. In these animals, following transfer the trachea was cannulated to ensure a clear passage for respiration throughout experiments and to permit artificial ventilation, if required, by means of a ventilation pump at a rate of 64 strokes min^{-1} and a stroke volume of 10 – 12 mL kg^{-1} body weight.

In some animals, the right carotid artery was isolated and either a fluid filled cannula or a 2F Millar Mikro-tip® catheter pressure transducer was advanced through the artery so that its tip lay in the lumen of the LV. This catheter was used to measure LVP and its position was indicated by the change of the amplitude and contour of the pressure pulse wave, and by the rise in $LVdP/dt_{max}$.

Body temperature was monitored throughout experiments via a thermometer placed in the rectum of the animal and maintained at ~37ºC with a heating lamp. All animals were allowed to stabilise for at least 20 min before experiments were begun.

2.2.3.2 Guinea pigs

Immediately after induction of an adequate level of anaesthesia, determined as in rats, the neck area was shaved to allow isolation of the trachea which was cannulated to ensure a clear passage for respiration throughout experiments and to permit artificial ventilation with room air by means of a ventilation pump. At the University of Strathclyde a Bioscience pump was used, set at a rate of 60 breaths min^{-1} and a stroke volume of 7 – 8 mL kg^{-1}. Oxygen saturation and expired CO_2 were measured continuously using a Medair Lifesense™ Vet pulse oximeter / capnograph. If necessary, during the preparation and stabilisation phases, the stroke volume of the pump was adjusted to keep the expired CO_2 value between 35 and 45 mmHg and oxygen saturation above 95%. At AstraZeneca a TOPO™ dual mode ventilator was used with the rate set at 20 – 40 breaths per minute, and the peak inspiration pressure set to 19.5 cm H_2O. If necessary these ranges were adjusted to achieve arterial blood gas values within a set range: PO_2 >70 and <110 mmHg, PCO_2 >25 and <45 mmHg. Oxygen saturation was also assessed continuously using a pulse oximeter where a desirable reading was >90%.

Needle electrodes were inserted subcutaneously to record limb lead ECGs. Both jugular veins were dissected free from surrounding tissue and cannulated, one for infusion of maintenance doses of anaesthetic and the other for test drugs. Anaesthetic test drugs were delivered by an infusion pump. A fluid filled cannula was placed in the right carotid artery for measurement of arterial blood pressure and/or blood sampling. As before, all cannulae were filled with heparin treated saline and secured in position by a ligature. The left carotid artery was isolated and a 2F or 3F Millar Mikro-tip® catheter pressure transducer or 1.6F Scisense pressure catheter was advanced through the artery so that its tip lay in the lumen of the LV. This catheter was used to measure LVP and its position was indicated as before. A stabilisation period of at least 20 min was allowed following completion of the surgical preparation.

2.2.4 Data acquisition and analysis

At the University of Strathclyde the ECG electrodes were connected to Gould 6615-65 ECG or 6615-58 bioelectric amplifiers and Leads I, II, and III of the ECG were recorded simultaneously. The fluid filled cannula for arterial blood pressure measurement was connected via a Bell and Howell Type 4-442 transducer to a Gould 6615-30 DC bridge amplifier and calibrated daily using a mercury manometer. The Millar catheter was connected via a Millar TC-510 control box to another bridge amplifier and calibrated daily via electrical signals. All data were recorded continuously using Ponemah P3 Plus software. In rat experiments the amplified blood pressure signal was recorded at a sampling rate of 250 Hz whilst the ECG and LVP were recorded at 1000 Hz. In guinea pig experiments all signals from the amplifiers were recorded at 1000 Hz. At AstraZeneca cardiovascular data were recorded using a PharmLab system or Notocord HEM system. The lead II ECG and the pressure signals were recorded at rates of 500 and 250 Hz, respectively, with the PharmLab system and 1000Hz and 500 Hz, respectively, with the Notocord system.

Heart rate was derived from the arterial blood pressure signal and recorded along with systolic, diastolic and mean arterial pressure. LV systolic and end-diastolic pressures were recorded along with $LVdP/dt_{max}$ as an index of cardiac contractility. The QA interval was also recorded in guinea pig experiments. At time points of interest, data were averaged over a 5 s interval. In some experiments QA intervals were measured manually by taking the average of 5 consecutive beats.

2.2.5 Experimental protocols

2.2.5.1 Rats

In rat experiments isoprenaline was administered in cumulative doses (0.1, 0.3, 1.0, 3.0 nmol kg^{-1} min^{-1}) as a continuous i.v. infusion for 10 min per dose. Prior to administration of the first dose of isoprenaline a 'priming' dose was given to ensure the cannula was filled with isoprenaline. A period of 20 min was then given to allow responses to return to pre-prime levels. Following administration of the highest dose of isoprenaline a 10 min period was allowed to observe drug effects reversing. In some animals following recovery from isoprenaline either a fluid filled cannula or a 2F Millar catheter was inserted into the lumen of the LV to record LVP. Animals were then euthanised by i.v. overdose of sodium pentobarbital (500 mg kg^{-1}).

2.2.5.2 Guinea pigs

In eight guinea pigs weighing 425 – 625 g the first group of experiments was designed to compare responses to drugs with either one or both carotid arteries occluded by cannulation. Before the LV catheter was inserted but after a 20 min stabilisation period, either isoprenaline (0.1, 0.3 and 1.0 nmol kg^{-1} min^{-1}) or angiotensin II (0.03, 0.1 and 0.3 nmol kg^{-1} min^{-1}) was administered as a continuous i.v. infusion for 10 min per dose (n = 4 per group). A recovery period of 10 min was allowed and then the LV catheter was inserted followed by a further 20 min stabilisation period. After this the infusions of either isoprenaline or angiotensin II were repeated.

A second group of experiments, using a total of thirty guinea pigs weighing 455 – 690 g, focused on comparing the effects of drugs on cardiac contractility. After completing the full surgical preparation and allowing a 20 min stabilisation period, drug delivery cannulae were primed with the appropriate drug. Following recovery from the prime, guinea pigs were given either isoprenaline (0.1, 0.3 and 1.0 nmol kg^{-1} min^{-1}), ouabain (1, 3 and 10 nmol kg^{-1} min^{-1}), verapamil (14, 42 and 140 nmol kg^{-1} min^{-1}), imatinib (3, 10 and 30 µmol kg^{-1} min^{-1}), sunitinib (0.3, 1.0 and 3 µmol kg^{-1} min^{-1}) or vehicle (equal volumes of normal saline; 20, 60, 200 µl kg^{-1} min^{-1}) as continuous i.v. infusions with each dose being infused for 15 min. The experiments with isoprenaline, ouabain, verapamil, imatinib and vehicle were performed at the University of Strathclyde with animals assigned randomly to drug groups. The experiments with sunitinib were carried out at a later date at AstraZeneca. For

direct comparisons of $LVdP/dt_{max}$ and the QA interval, LVP measurements were required in n = 4 guinea pigs per group. In some groups up to n = 6 experiments were required to achieve this. Immediately following the end of the final drug dose in every experiment, the chest was opened and the heart was removed as described in Section 3.2.2 for subsequent analysis of CaMKII expression and activity. Blood was then collected from the open chest for analysis of plasma drug concentrations.

2.2.6 Plasma drug concentrations

Blood samples were collected in 1.3 mL lithium heparin tubes from the open-chest at the end of the dosing period and immediately after removal of the heart. Plasma was prepared by centrifugation at 3000 rpm for 10 min, aliquoted and stored at -80°C until analysis.

Analysis was performed by Clare Hammond at AstraZeneca. 1 mg mL^{-1} stock solutions of each drug (solubilised in DMSO) were serially diluted in DMSO to generate calibration/quality control (QC) samples. Control guinea pig plasma was spiked with 5% calibration/QC solutions to generate an 11-point calibration curve (range 0.5 to 5000 ng mL^{-1}) and a set of QC samples (5, 50, 500 ng mL^{-1}) in a total volume of 25 µL. At least one 25 µL sample of control guinea pig plasma was also included to ensure no background contaminants were present.

Compounds were extracted by protein precipitation with 75 µL acetonitrile containing an appropriate internal standard. Resultant extracts and all calibration/QC samples were then aliquoted into a 1 mL 96-well plate and mixed by gentle shaking of the plate followed by centrifugation. 50 µL of supernatant was transferred to a 2 mL 96-well plate and 300 µL of water was added. Samples were then analysed for the total plasma concentrations using High pressure liquid chromatography with Tandem mass spectroscopy detection (HPLC-MS/MS). The response for each sample was calculated using the ratio of the peak area of the analyte and internal standard. The parameters for each calibration curve were used to obtain concentrations for extracted samples by interpolation.

To calculate free plasma concentrations, total concentrations were corrected for plasma protein binding (PPB) in the guinea pig. PPB data was determined by Ian Morrison at AstraZeneca. The first apparent binding constant of each drug was determined in 10% control guinea pig plasma (diluted in buffer isotonic with plasma) by equilibrium dialysis in a high throughput dialysis plate (Kariv *et al.*, 2001). Total

drug concentrations of 20μM were used at a temperature of 37 ± 2°C. The compounds were dialysed overnight and the resulting samples were analysed by HPLC-Ultraviolet (HPLC-UV) coupled with Mass spectral peak identification.

2.2.7 Statistical analysis

Data are presented as mean ± S.E.M. Paired *t* tests were used to compare values at two time points within groups. The effects of increasing doses of individual drugs with time were assessed using a one-way ANOVA followed by Dunnett's test. For comparison of the effects of a drug under conditions of unilateral versus bilateral carotid occlusion the areas under the dose/time-response curves were calculated and compared using paired *t* tests. One-way ANOVA followed by Tukey's tests, or Kruskal-Wallis tests (for data that were not distributed normally), were used for comparisons among groups. Correlations were calculated using SigmaPlot software and all statistical analyses were performed using StatsDirect software.

2.2.8 Drugs

Isoflurane, Hypnorm®, Hypnovel®, sodium pentobarbital and fentanyl were prepared as detailed in Table 2.1. Angiotensin II acetate (AT receptor agonist), isoprenaline HCl (β-adrenoceptor agonist), ouabain (Na^+/K^+ pump inhibitor), verapamil HCl (Ca^{2+} channel blocker), imatinib mesylate and sunitinib malate (both kinase inhibitors) were all dissolved in 0.9% w/v NaCl.

2.3 Results

2.3.1 The effects of isoprenaline in isoflurane and pentobarbital anaesthetised rats

Isoprenaline caused a dose-dependent decrease in systolic, diastolic and mean arterial blood pressure, and a dose-dependent increase in heart rate. Figure 2.2 shows a typical recording observed during isoprenaline administration in a pentobarbital anaesthetised rat. The effects of isoprenaline on arterial blood pressure were not clear until higher doses were administered (1.0 and 3.0 nmol kg^{-1} min^{-1}) whilst heart rate clearly increased from the lowest dose. Upon cessation of isoprenaline administration arterial blood pressure recovered within about 3 min showing a rebound increase in blood pressure compared to pre-drug values. Heart

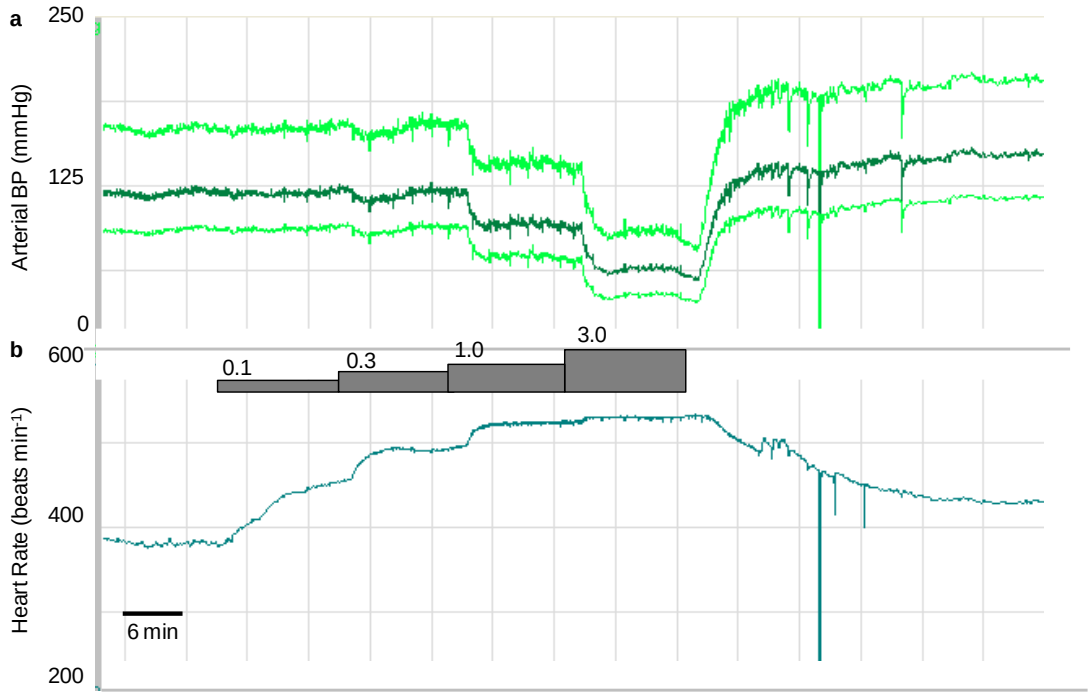

Figure 2.2 The effects of isoprenaline on **a)** arterial blood pressure (BP) and **b)** heart rate in a pentobarbital anaesthetised rat. The arterial BP panel (a), shows systolic BP (top line, light green), followed by mean arterial BP (dark green) and diastolic BP (light green). The grey bars indicate the dose of isoprenaline in nmol kg^{-1} min^{-1}.

rate did not fully recover to pre-drug values but did plateau slightly higher than pre-drug after a period of about 20 min.

The effects of cumulative doses of isoprenaline on systolic and diastolic blood pressure in rats anaesthetised with isoflurane (n = 3) and pentobarbital (n = 3) are shown in Figure 2.3a and b, respectively. In pentobarbital anaesthetised rats initial systolic and diastolic blood pressure were higher. This difference was maintained with doses of isoprenaline up to 1.0 nmol kg^{-1} min^{-1}. However, with the highest dose of isoprenaline systolic and diastolic blood pressure in the pentobarbital and isoflurane groups reached similar levels. Similarly, baseline heart rate in the pentobarbital group was higher than the isoflurane group (Figure 2.3c). In contrast, however, this difference was maintained throughout administration of all doses of isoprenaline. Additionally, in both pentobarbital and isoflurane groups, with each dose of isoprenaline arterial blood pressure responses showed complete or partial reversal with lower and higher doses, respectively, whilst heart rate responses were sustained.

LVP was initially recorded in rats via a fluid filled cannula, which was later replaced by a 2F Millar catheter. LVP signals obtained via a fluid filled cannula were damped compared to signals obtained via the Millar catheter (Figure 2.4). Importantly, $LVdP/dt_{max}$ derived from the damped LVP signal was approximately 50% of the $LVdP/dt_{max}$ value derived from the Millar catheter.

2.3.2 Comparison of anaesthetics in guinea pigs

Pentobarbital, either given alone or after fentanyl, provided stable anaesthesia whereas the anaesthesia obtained with Hypnorm/Hypnovel tended to be less stable over time and isoflurane was unsuitable. Induction of anaesthesia with 5% isoflurane resulted in profuse salivation and in the first animal tested, regurgitation of food. In the two following animals food was withdrawn the night before the experiments but there was still marked salivation, spontaneous respiration was rather erratic and the concentration of isoflurane had to be adjusted frequently to try to maintain a stable heart rate within normal limits. In the subsequent batch of guinea pigs given isoflurane, induction with 2 - 4% caused less salivation but the necessity for frequent adjustments of the concentration of isoflurane remained. In addition, mean arterial blood pressure and heart rate were significantly lower (Figure 2.5).

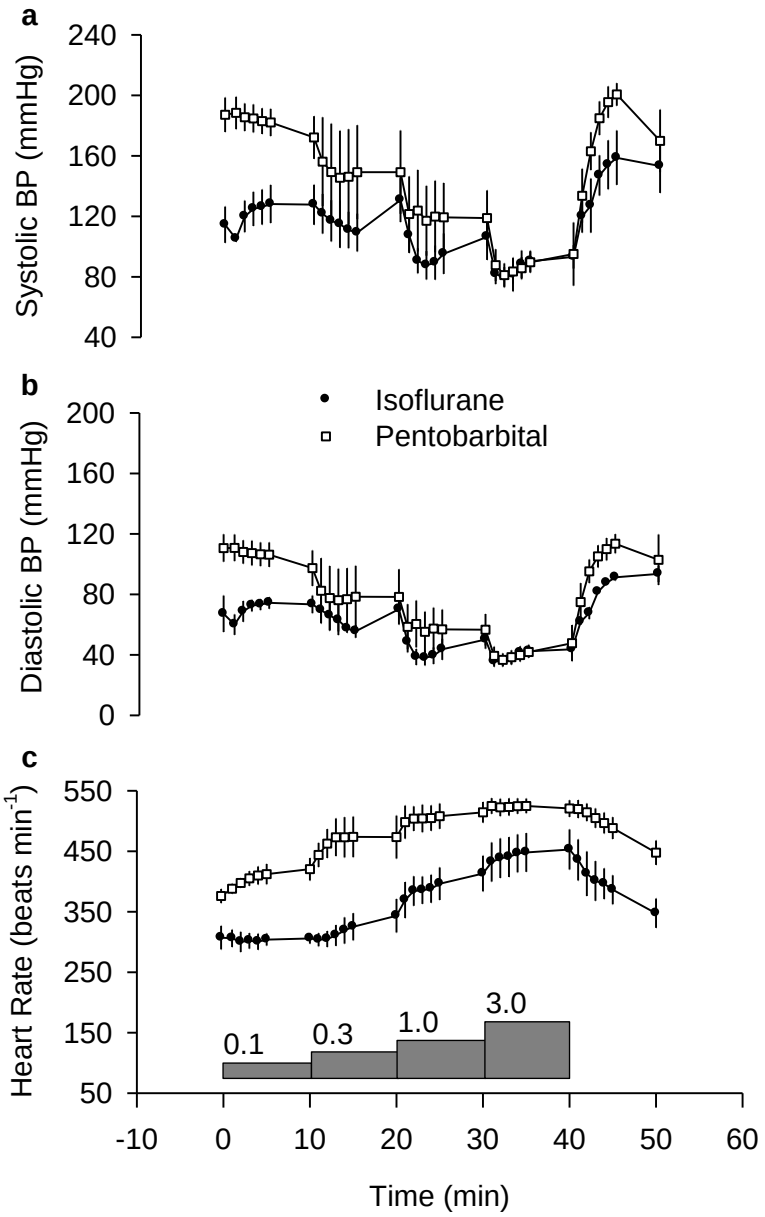

Figure 2.3 The effects of isoprenaline on **a)** systolic blood pressure (BP), **b)** diastolic BP and **c)** heart rate in isoflurane vs pentobarbital anaesthetised rats. The grey bars indicate the dose of isoprenaline in nmol kg^{-1} min^{-1}. Mean ± S.E.M, n = 3.

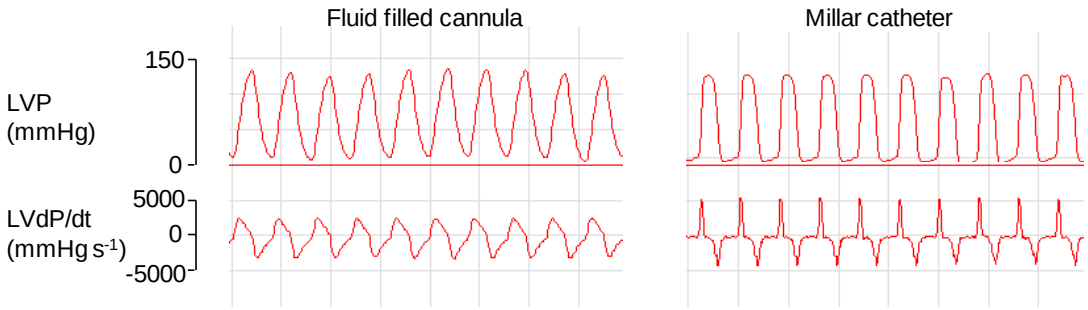

Figure 2.4 Examples of left ventricular pressure (LVP) and LVdP/dt signals recorded from two different pentobarbital anaesthetised rats. The left hand panel shows a damped LVP signal recorded using a fluid filled cannula whereas the right hand panel shows the signals obtained using a 2F Millar catheter. Note that the maximum positive value for LVdP/dt ($LVdP/dt_{max}$) is approximately twice as high with the Millar catheter.

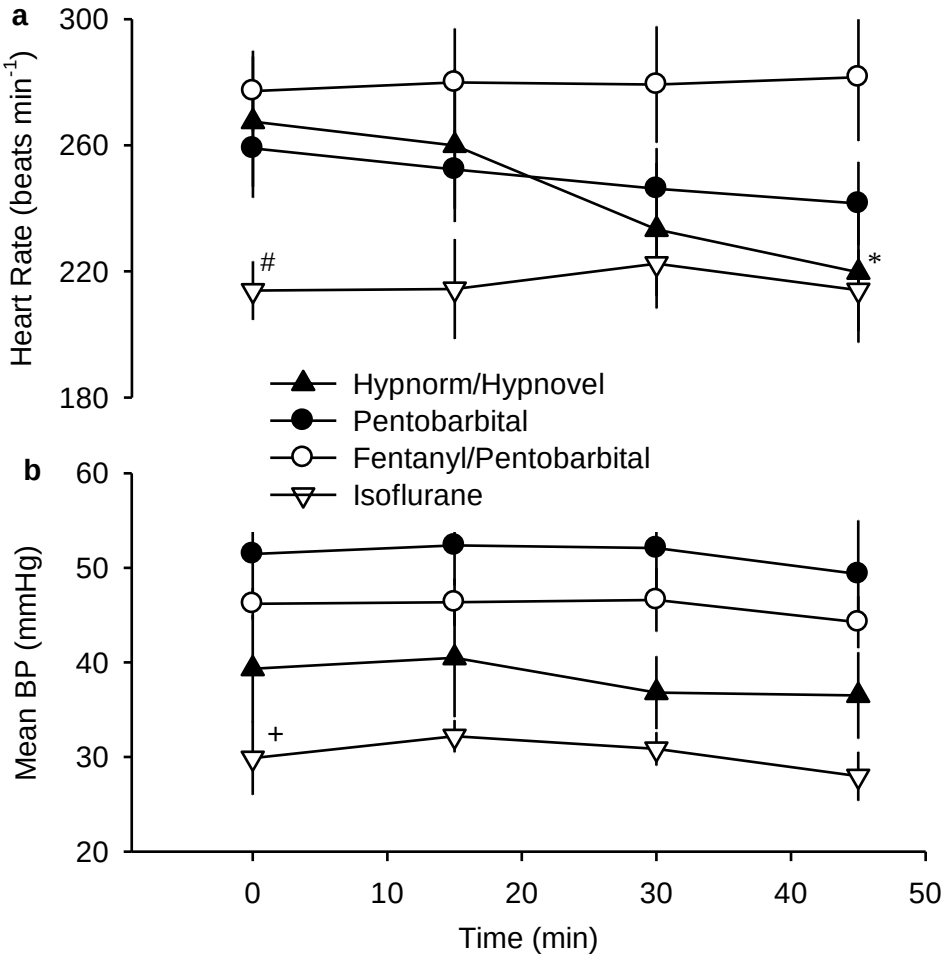

Figure 2.5 a) Heart rate and **b)** mean arterial blood pressure (BP) with time in groups of animals anaesthetised with either Hypnorm/Hypnovel, isoflurane, pentobarbital alone or given after pre-medication with fentanyl. All data were recorded after completion of a minimum 20 min stabilisation period. The experiments with Hypnorm/Hypnovel, isoflurane and pentobarbital were performed at AstraZeneca whereas those with fentanyl/pentobarbital were carried out at the University of Strathclyde. Data are shown as mean ± S.E.M, n = 4 per group. * indicates $P<0.05$ compared with time 0 min within group, paired t test. # indicates $P<0.05$ compared with fentanyl/pentobarbital group at that time, + indicates $P<0.05$ compared with pentobarbital group at that time, one way ANOVA with Tukey's test.

The time taken to reach surgical anaesthesia with Hypnorm/Hypnovel was 12 ± 1 min (individual data: 9, 11, 13, 15 min), with pentobarbital alone was 18 ± 9 min (individual data: 6, 7, 15, 43 min) and with pentobarbital given 5 min after fentanyl was 6 ± 1 min* (individual data: 5, 5, 5, 7 min); * indicates $P<0.05$ compared to other groups, Kruskal-Wallis test. After completion of the surgical preparation and a 20 min stabilisation period, baseline values for heart rate were similar with these three anaesthetic regimes (Figure 2.5a) but there was more variation in the baseline mean arterial blood pressures (Figure 2.5b). With Hypnorm/Hypnovel mean arterial blood pressure tended to be lower and the heart rate had declined significantly by the end of the recording period (Figure 2.5a). In contrast, there were no significant differences between the initial and final values for heart rate or mean arterial blood pressure in either pentobarbital group (Figure 2.5).

2.3.3 Responses during unilateral and bilateral carotid artery occlusion in guinea pigs

Occlusion of the second carotid artery did not alter baseline values for heart rate, systolic or diastolic arterial blood pressure (Figure 2.6). Isoprenaline increased heart rate in a dose-dependent manner but had limited effects on systolic and diastolic arterial blood pressure (Figure 2.6a-c). In contrast, angiotensin II caused significant dose-dependent increases in systolic and diastolic pressure but had very little effect on heart rate (Figure 2.6d-f). When the data obtained during unilateral and bilateral carotid artery occlusion are compared visually it can be seen that the patterns of responses are virtually identical (Figure 2.6). Statistical analysis of the areas under the curve of the dose/time-response relationships of the data expressed as percentage change from baseline (Figure 2.7) indicated that there were no significant differences in the heart rate or blood pressure responses to either isoprenaline or angiotensin II during bilateral compared to unilateral carotid occlusion.

2.3.4 Haemodynamic and contractility responses following acute *in vivo* drug administration in guinea pigs

Isoprenaline caused heart rate to rise in a dose-dependent manner (Figure 2.8b) while ouabain increased heart rate more slowly reaching significance at 45 min (Figure 2.8c). Verapamil (Figure 2.8d) and imatinib (Figure 2.8e) both decreased

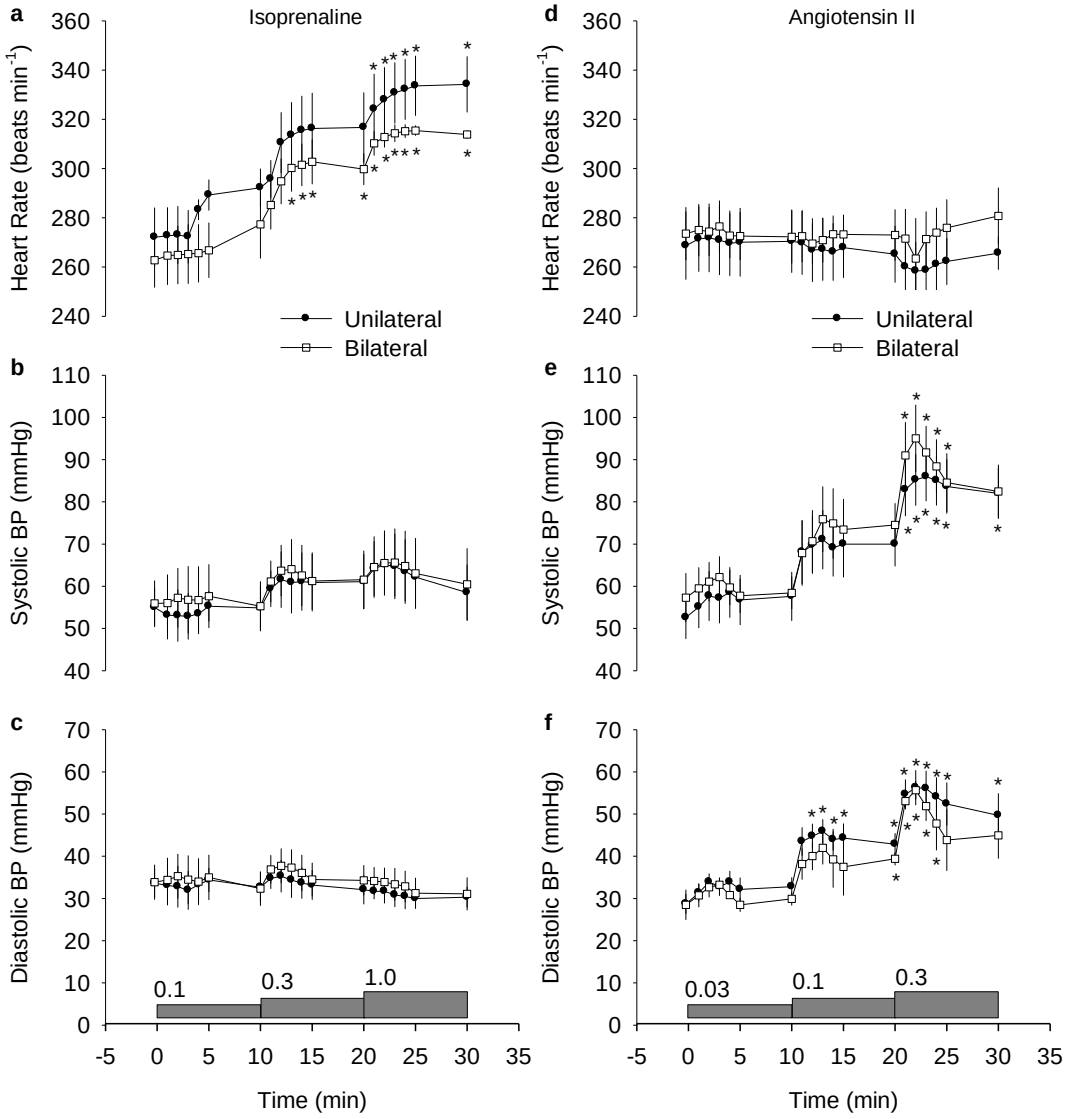

Figure 2.6 The effects of isoprenaline on **a)** heart rate, **b)** systolic arterial blood pressure (BP), **c)** diastolic BP, and of angiotensin II on **d)** heart rate, **e)** systolic BP, **f)** diastolic BP during unilateral and bilateral carotid artery occlusion. The grey bars indicate the dose of the drugs in nmol kg^{-1} min^{-1}. Mean ± S.E.M, n = 4. * indicates $P<0.05$ compared to value within group at time 0 min, one way ANOVA with Dunnett's test.

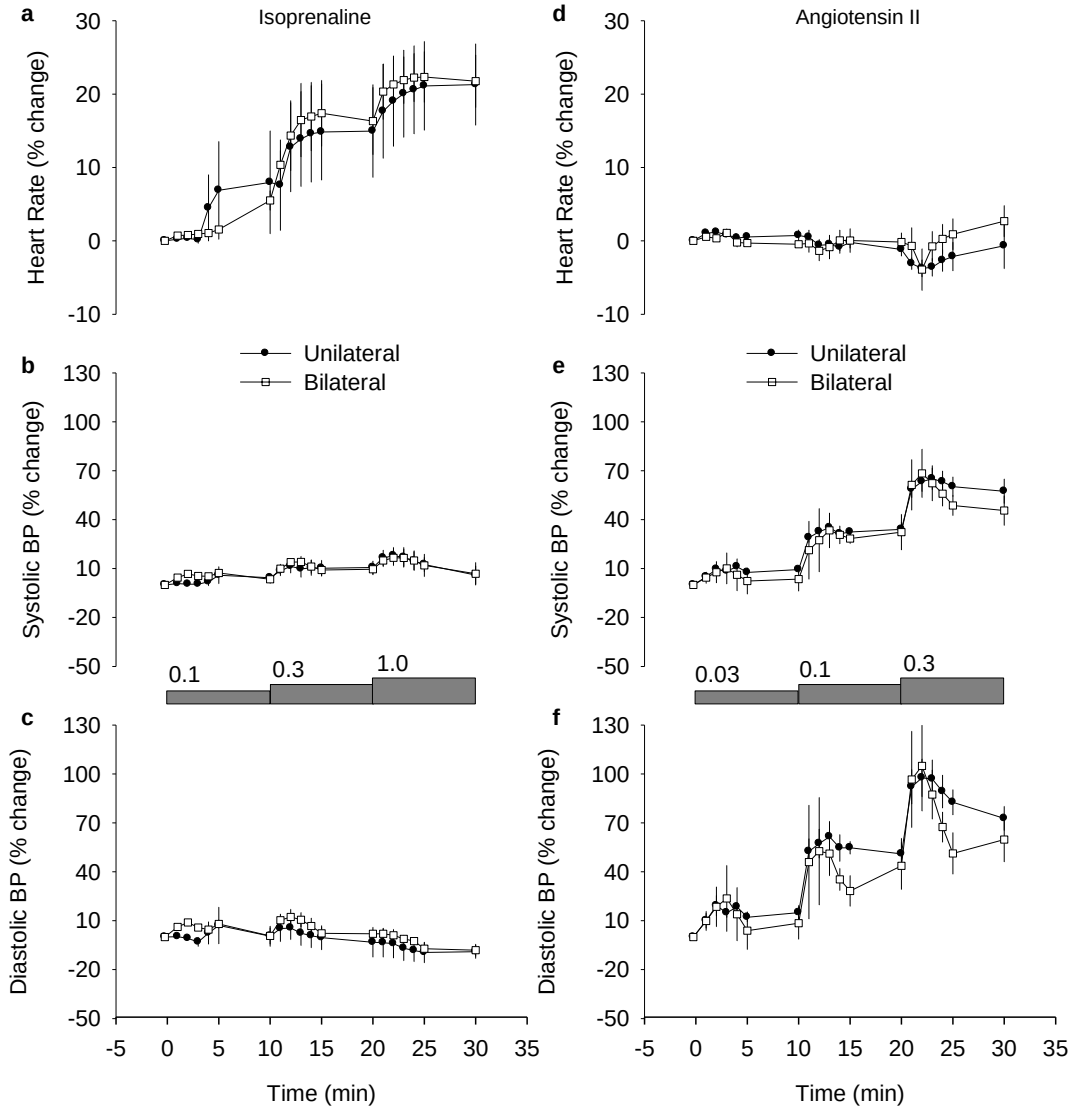

Figure 2.7 The % change effects of isoprenaline on **a)** heart rate, **b)** systolic arterial blood pressure (BP), **c)** diastolic BP and of angiotensin II on **d)** heart rate, **e)** systolic BP, **f)** diastolic BP during unilateral and bilateral carotid artery occlusion. The grey bars indicate the dose of the drugs in nmol kg^{-1} min^{-1}. Mean ± S.E.M, n = 4.

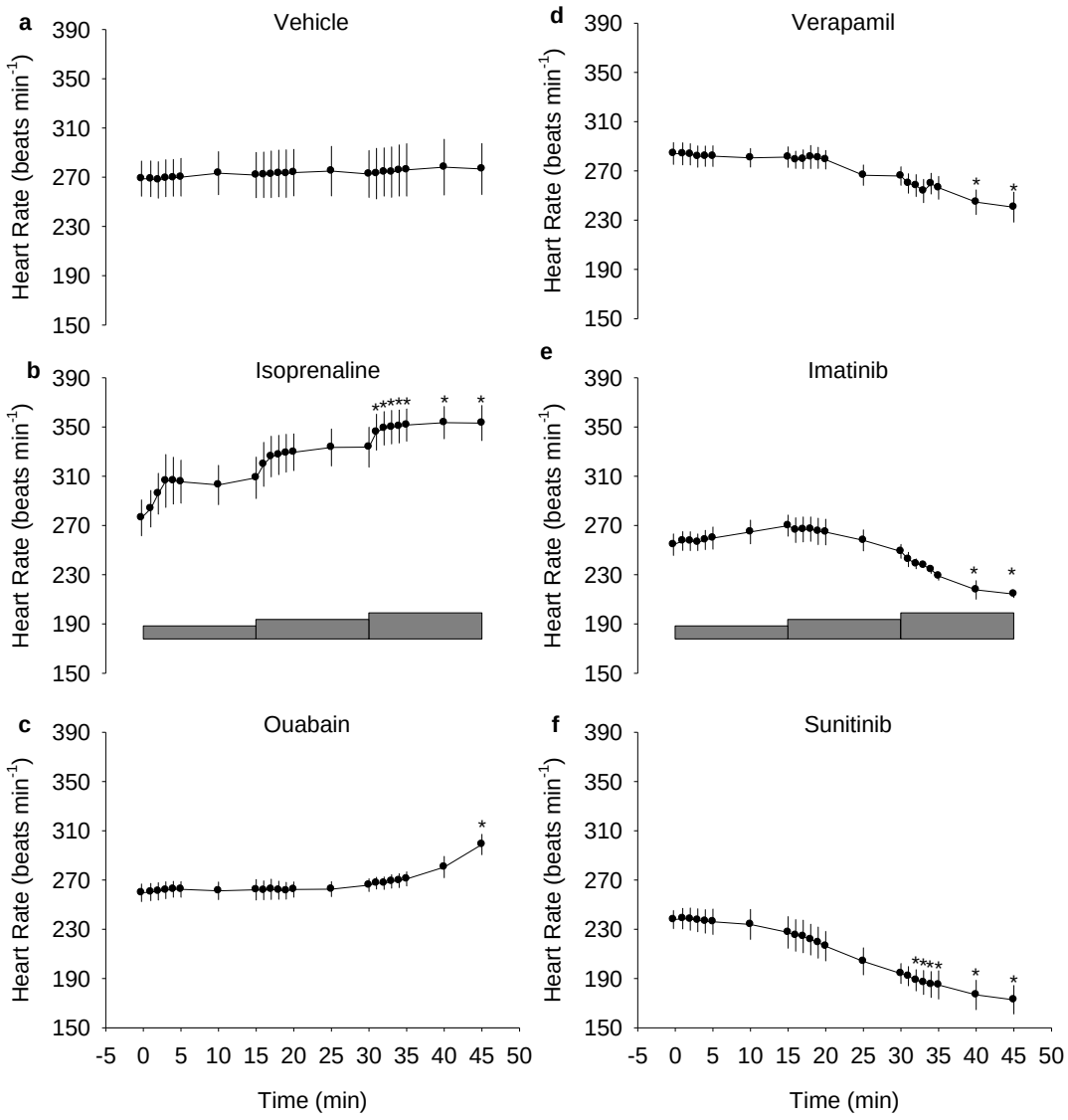

Figure 2.8 Heart rate responses to administration of **a)** vehicle, **b)** isoprenaline, **c)** ouabain, **d)** verapamil, **e)** imatinib, **f)** sunitinib. The grey bars indicate increasing drug doses: isoprenaline 0.1, 0.3 and 1.0 nmol kg^{-1} min^{-1}; ouabain 1, 3 and 10 nmol kg^{-1} min^{-1}; verapamil 14, 42 and 140 nmol kg^{-1} min^{-1}; imatinib 3, 10 and 30 µmol kg^{-1} min^{-1}; sunitinib 0.3, 1.0 and 3 µmol kg^{-1} min^{-1}; vehicle 20, 60, 200 µL kg^{-1} min^{-1}. Mean ± S.E.M, n = 4. * indicates $P<0.05$ compared to value within group at time 0 min, one way ANOVA with Dunnett's test.

heart rate at 40 and 45 min while sunitinib (Figure 2.8f) increased heart rate throughout administration of the highest dose.

Isoprenaline had no significant effect on systolic, diastolic or mean blood pressure (Figure 2.9b). Ouabain appeared to gradually increase systolic, diastolic and mean blood pressure (Figure 2.9c) but this was not significant. Diastolic blood pressure was not altered significantly by verapamil administration, however, systolic and mean blood pressure were both decreased at points during the final dose (Figure 2.9d). With imatinib (Figure 2.9e), mean and systolic blood pressure were decreased after 40 and 45 min administration, respectively, and whilst diastolic blood pressure looked to follow this decrease this did not reach statistical significance ($P = 0.133$). Systolic, diastolic and mean blood pressure gradually declined with administration of sunitinib, becoming statistically significant with the highest dose (Figure 2.9f).

Left ventricular systolic pressure (LVSP) was not changed by isoprenaline (Figure 2.10b). Ouabain (Figure 2.10c), similar to its effects on arterial blood pressure, tended to increase LVSP although again this was not significant. Throughout the infusion of verapamil LVSP gradually fell showing a significant decrease at 35 min, however, this effect was not sustained at 40 and 45 min (Figure 2.10d). Both imatinib and sunitinib decreased LVSP at the highest dose with the effects of imatinib appearing a little later than sunitinib (Figure 2.10e and f). Left ventricular end-diastolic pressure (LVEDP) was not altered by any of the drug treatments (Figure 2.10a-f).

Isoprenaline caused a rapid dose-dependent rise in $LVdP/dt_{max}$ while ouabain again showed a slower and more gradual effect, increasing $LVdP/dt_{max}$ towards the end of the highest dose (Figure 2.11b and c respectively). Verapamil tended to reduce $LVdP/dt_{max}$ although this did not quite reach significance ($P = 0.051$) (Figure 2.11d). In the case of imatinib (Figure 2.11e) $LVdP/dt_{max}$ initially appeared to increase slightly until around 20 to 25 min when a noticeable fall was observed although overall no significant change was found ($P = 0.141$). Sunitinib gradually decreased $LVdP/dt_{max}$ having significant effects from 25 min onwards (Figure 2.11f).

As the pre-drug value for $LVdP/dt_{max}$ was significantly lower in the sunitinib group than in each other group, $LVdP/dt_{max}$ data were also plotted as percentage change from pre-drug value (Figure 2.12). When plotted in this way the overall profile of

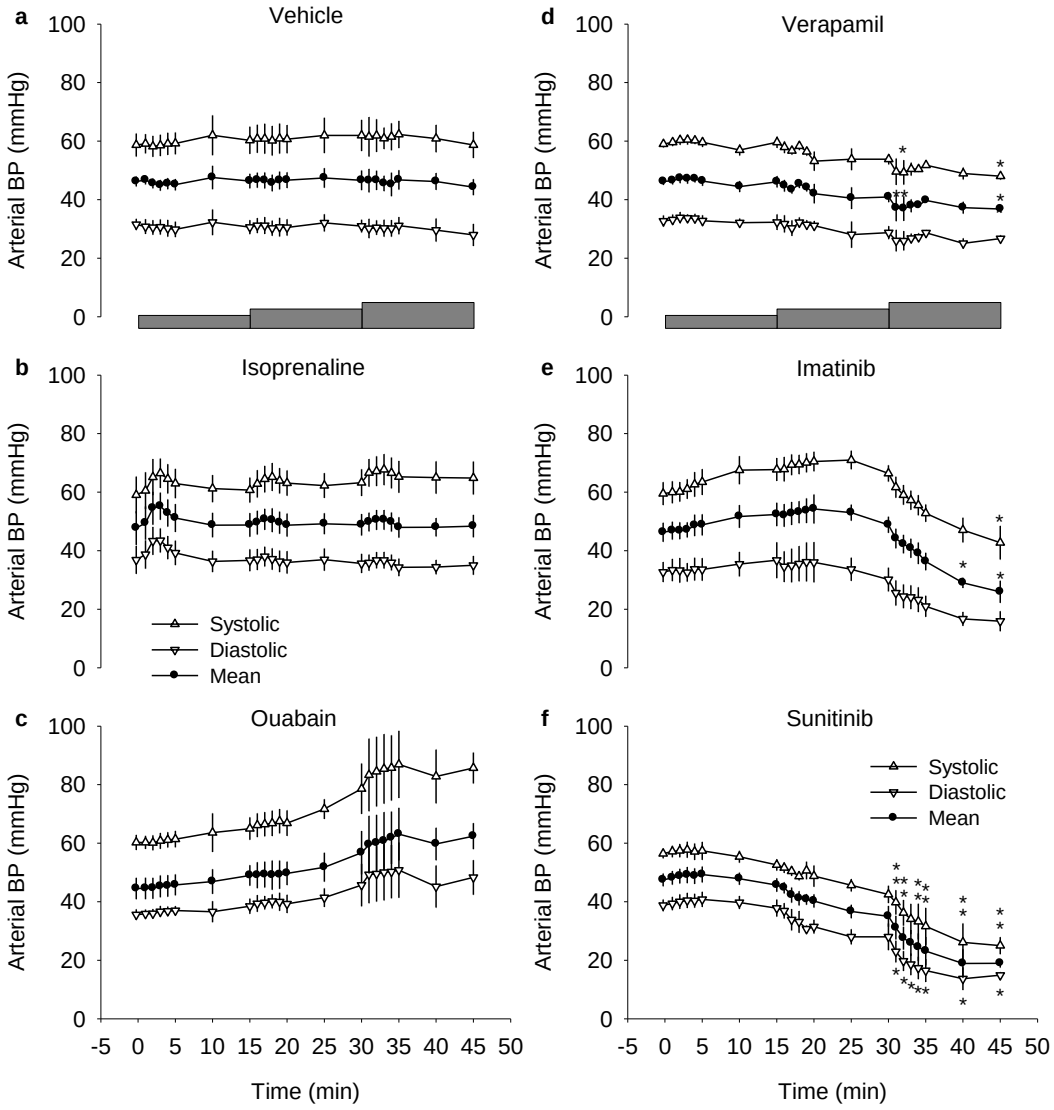

Figure 2.9 Systolic, diastolic and mean arterial blood pressure (BP) responses to administration of **a)** vehicle, **b)** isoprenaline, **c)** ouabain, **d)** verapamil, **e)** imatinib, **f)** sunitinib. The grey bars indicate increasing drug doses: isoprenaline 0.1, 0.3 and 1.0 nmol kg^{-1} min^{-1}; ouabain 1, 3 and 10 nmol kg^{-1} min^{-1}; verapamil 14, 42 and 140 nmol kg^{-1} min^{-1}; imatinib 3, 10 and 30 µmol kg^{-1} min^{-1}; sunitinib 0.3, 1.0 and 3 µmol kg^{-1} min^{-1}; vehicle 20, 60, 200 µL kg^{-1} min^{-1}. Mean ± S.E.M, n = 4. * indicates $P<0.05$ compared to value within group at time 0 min, one way ANOVA with Dunnett's test.

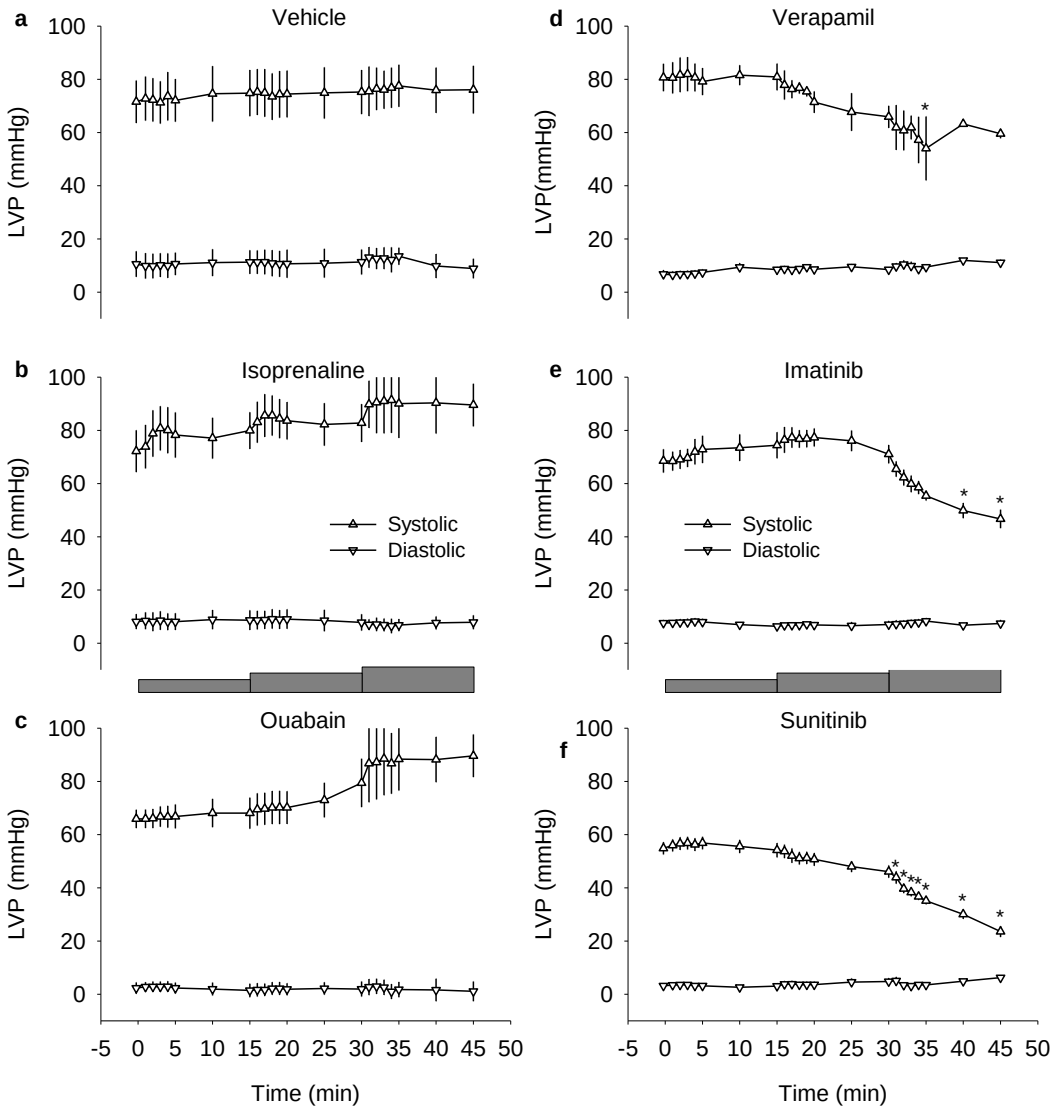

Figure 2.10 Left ventricular systolic pressure (LVSP) and end-diastolic pressure (LVEDP) responses to administration of **a)** vehicle, **b)** isoprenaline, **c)** ouabain, **d)** verapamil, **e)** imatinib, **f)** sunitinib. The grey bars indicate increasing drug doses: isoprenaline 0.1, 0.3 and 1.0 nmol kg^{-1} min^{-1}; ouabain 1, 3 and 10 nmol kg^{-1} min^{-1}; verapamil 14, 42 and 140 nmol kg^{-1} min^{-1}; imatinib 3, 10 and 30 µmol kg^{-1} min^{-1}; sunitinib 0.3, 1.0 and 3 µmol kg^{-1} min^{-1}; vehicle 20, 60, 200 µL kg^{-1} min^{-1}. Mean ± S.E.M, n = 4. * indicates $P<0.05$ compared to value within group at time 0 min, one way ANOVA with Dunnett's test.

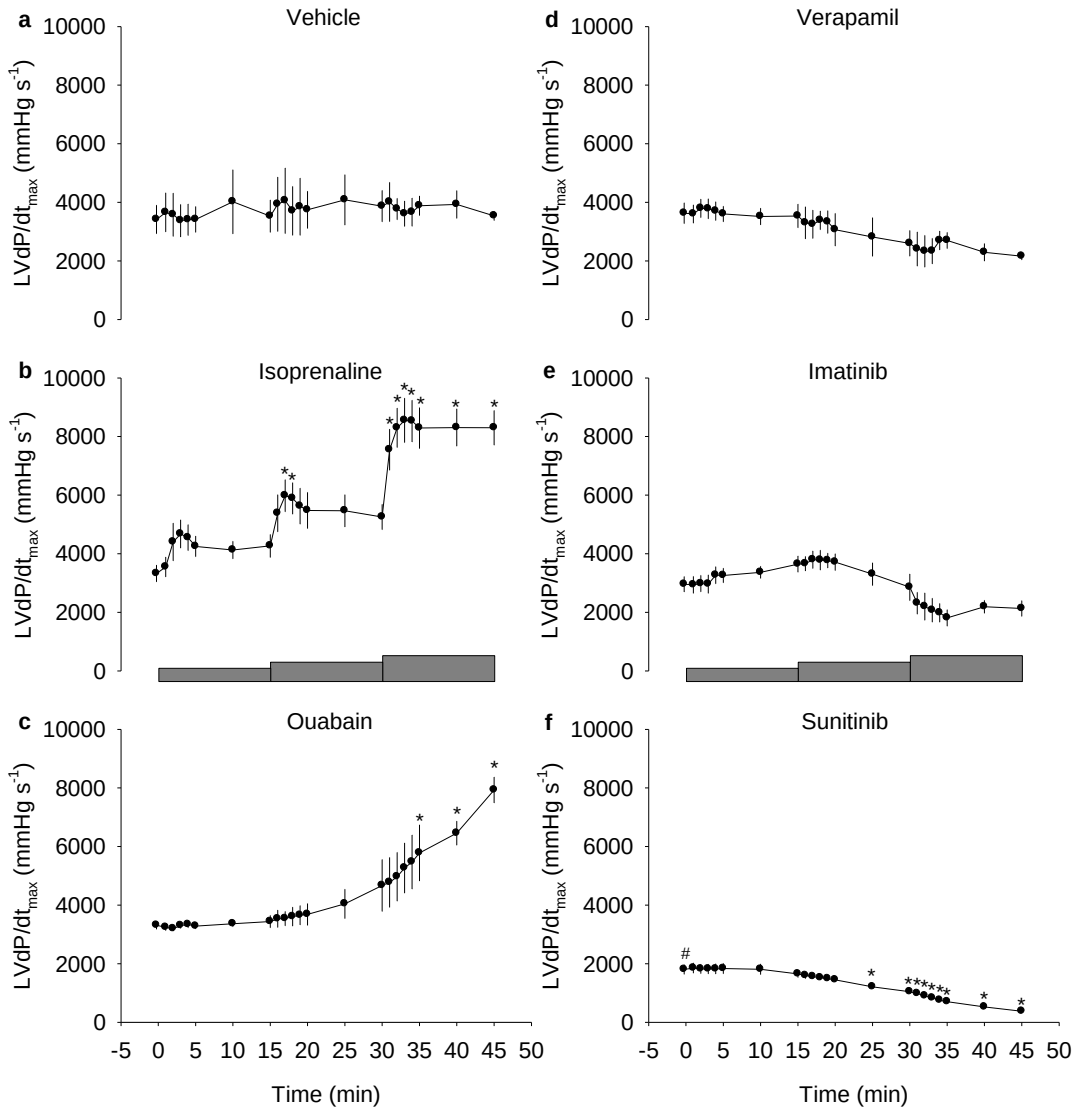

Figure 2.11 Left ventricular (LV) dP/dt_{max} responses to administration of **a)** vehicle, **b)** isoprenaline, **c)** ouabain, **d)** verapamil, **e)** imatinib, **f)** sunitinib. The grey bars indicate increasing drug doses: isoprenaline 0.1, 0.3 and 1.0 nmol kg^{-1} min^{-1}; ouabain 1, 3 and 10 nmol kg^{-1} min^{-1}; verapamil 14, 42 and 140 nmol kg^{-1} min^{-1}; imatinib 3, 10 and 30 µmol kg^{-1} min^{-1}; sunitinib 0.3, 1.0 and 3 µmol kg^{-1} min^{-1}; vehicle 20, 60, 200 µL kg^{-1} min^{-1}. Mean ± S.E.M, n = 4. * indicates $P<0.05$ compared to value within group at time 0 min, one way ANOVA with Dunnett's test. $^{\#}P<0.05$ compared to pre-drug values in each other group, one way ANOVA with Tukey's test.

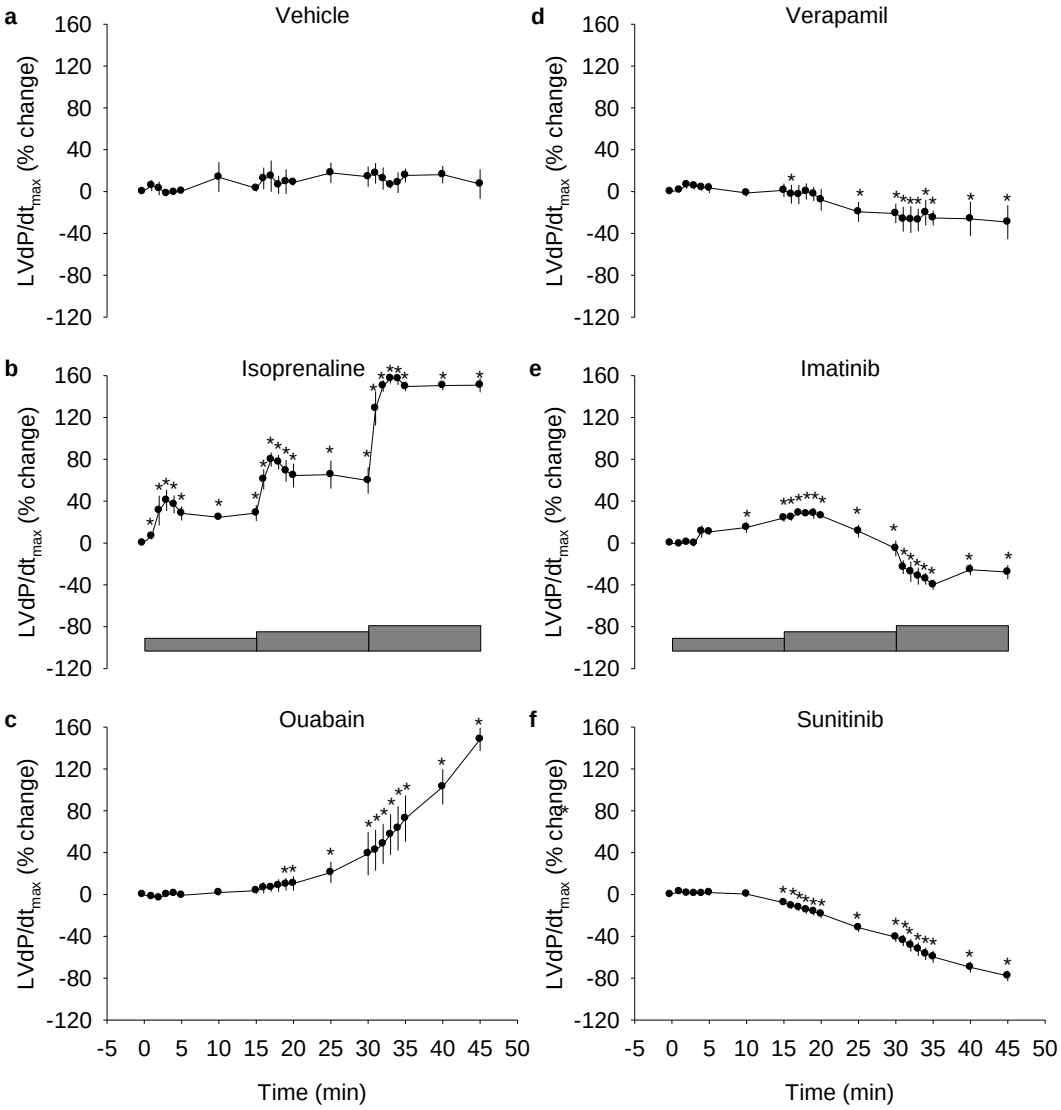

Figure 2.12 Left ventricular (LV) dP/dt_{max} % change responses to administration of **a)** vehicle, **b)** isoprenaline, **c)** ouabain, **d)** verapamil, **e)** imatinib, **f)** sunitinib. The grey bars indicate increasing drug doses: isoprenaline 0.1, 0.3 and 1.0 nmol kg^{-1} min^{-1}; ouabain 1, 3 and 10 nmol kg^{-1} min^{-1}; verapamil 14, 42 and 140 nmol kg^{-1} min^{-1}; imatinib 3, 10 and 30 µmol kg^{-1} min^{-1}; sunitinib 0.3, 1.0 and 3 µmol kg^{-1} min^{-1}; vehicle 20, 60, 200 µL kg^{-1} min^{-1}. Mean ± S.E.M, n = 4. * indicates $P<0.05$ compared to value within group at time 0 min, Kruskal-Wallis test.

drug effects were as described above. However, the drugs that had significantly altered LVdP/dt_{max} (isoprenaline, ouabain and sunitinib) now had significant effects at lower doses whilst the drugs with apparent effects that had not reached significance (verapamil and imatinib) now caused significant changes in LVdP/dt_{max}.

Isoprenaline caused the QA interval to fall and this effect was sustained during continuous infusion of the drug (Figure 2.13b). The effects of ouabain on the QA interval mirrored its effects on LVdP/dt_{max} with the reduction in the QA interval also reaching statistical significance during infusion of the highest dose (Figure 2.13c). Verapamil caused the QA interval to increase with significant changes detected at several time points during administration of the final dose (Figure 2.13d). Imatinib and sunitinib administration did not alter the QA interval (Figure 2.13e and f).

All parameters were also assessed during infusion of the same volumes of vehicle. Vehicle administration did not alter any of the parameters assessed (Figure 2.8a to Figure 2.13a).

2.3.5 Plasma drug levels

For each drug, except isoprenaline, total plasma concentrations were measured. PPB data was then determined allowing free drug concentrations to be calculated (Table 2.2). The total concentration of imatinib was much higher than the other drugs. This was then followed by sunitinib, verapamil and ouabain. Whilst PPB was fairly similar for ouabain, verapamil and sunitinib, imatinib was much more highly bound. This meant free concentrations of all drugs were more similar than total concentrations although imatinib was still the highest, again followed by sunitinib, verapamil then ouabain.

2.3.6 Relationship between LVP/dt_{max} and the QA interval

The observation that the graphs of LVdP/dt_{max} and QA interval data seem to be mirror images of each other suggests that there may be inverse correlations between these two indices of contractility. To examine this further, Figure 2.14 shows the relationships between LVdP/dt_{max} and QA interval following administration of the standard inotropes (isoprenaline, ouabain and verapamil). Plotting the QA interval against LVdP/dt_{max} revealed a curvilinear relationship (Figure 2.14a) which could be converted to a linear correlation by plotting the $\log_{10}$ values for each of these parameters (Figure 2.14b).

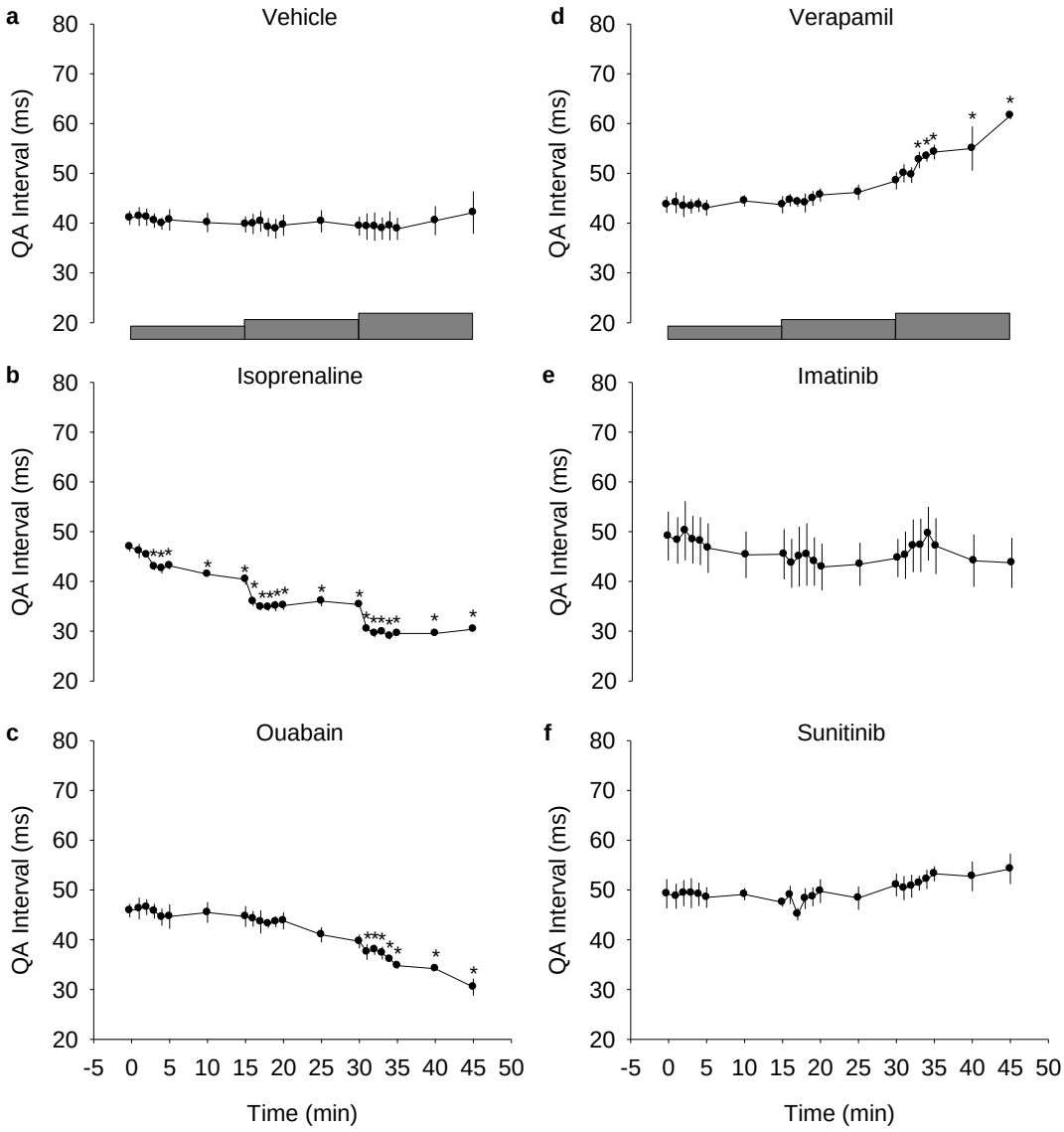

Figure 2.13 QA interval responses to administration of **a)** vehicle, **b)** isoprenaline, **c)** ouabain, **d)** verapamil, **e)** imatinib, **f)** sunitinib. The grey bars indicate increasing drug doses: isoprenaline 0.1, 0.3 and 1.0 nmol kg^{-1} min^{-1}; ouabain 1, 3 and 10 nmol kg^{-1} min^{-1}; verapamil 14, 42 and 140 nmol kg^{-1} min^{-1}; imatinib 3, 10 and 30 µmol kg^{-1} min^{-1}; sunitinib 0.3, 1.0 and 3 µmol kg^{-1} min^{-1}; vehicle 20, 60, 200 µL kg^{-1} min^{-1}. Mean ± S.E.M, n = 4. * indicates $P<0.05$ compared to value within group at time 0 min, one way ANOVA with Dunnett's test.

Table 2.2 Drug concentrations measured in blood plasma following acute *in vivo* drug administration

Drug	Total dose given (μmol kg^{-1})	Total plasma concentration (μM)	PPB (% free)	Calculated free concentration (μM)
Ouabain	0.21	2.99 ± 0.32	> 14.75	> 0.44 ± 0.05
Verapamil	2.94	7.82 ± 2.85	19.44	1.52 ± 0.55
Imatinib	645	1122.36 ± 220.52	0.37	4.15 ± 0.94
Sunitinib	64.5	25.39 ± 8.34	13.40	3.40 ± 1.29

PPB, plasma protein binding. Data are presented as mean ± S.E.M. Ouabain and verapamil n = 6, imatinib and sunitinib n = 4.

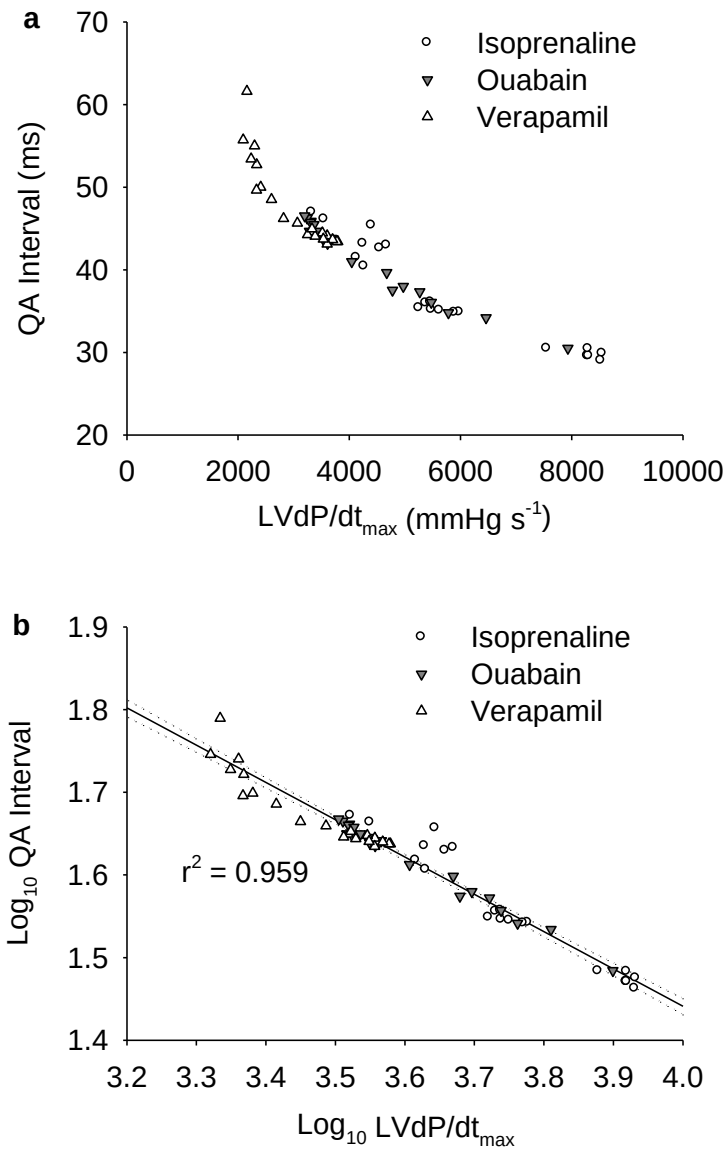

Figure 2.14 Correlations between **a)** $LVdP/dt_{max}$ and the QA interval and **b)** $\log_{10}$ $LVdP/dt_{max}$ and $\log_{10}$ QA interval in guinea pigs which received isoprenaline, ouabain or verapamil. Dotted lines indicate the 95% confidence limits.

2.4 Discussion

2.4.1 Main findings

This work demonstrates the detection of drug-induced changes in haemodynamics and cardiac contractility (via $LVdP/dt_{max}$ and the QA interval) measured in anaesthetised guinea pigs using known and potential inotropic drugs. In addition, fentanyl plus sodium pentobarbital offered the best anaesthesia and the results prove that cannulation of both carotid arteries in this species does not have any detrimental effects on responses to drugs, thus validating this approach.

2.4.1.1 Effects of isoprenaline in isoflurane and pentobarbital anaesthetised rats

Isoprenaline was chosen as a well-known positive inotrope and activator of CaMKII (Ginsburg & Bers, 2004; Yoo *et al.*, 2009), therefore, being a useful tool to investigate a possible link between changes in contractility and CaMKII expression and activity. Isoprenaline is a non-selective β-adrenoceptor agonist and so therefore acts on both β_1- and β_2- adrenoceptor subtypes. β_1-adrenoceptors are located on pacemaker cells and cardiac myocytes and signal through the G_s-coupled pathway. Activation of this pathway increases the catalytic activity of AC thus raising cAMP synthesis within the cell. This results in a positive chronotropic effect (i.e. increased heart rate) and a positive inotropic effect (i.e. increased force of cardiac contraction). β_2-adrenoceptors are found on vascular smooth muscle also signalling through a G_s-coupled pathway increasing cAMP synthesis via AC. This then activates PKA which phosphorylates and inactivates myosin light chain kinase (MLCK) causing vasodilation and thus decreasing arterial blood pressure (Robertson, 2004).

In rats, generally, arterial blood pressure responses had a greater tendency to reverse after a few minutes of drug administration whilst heart rate responses were sustained (Figure 2.2 and Figure 2.3). Heart rate also showed greater responses to the lower doses of isoprenaline. This may suggest that β_1-adrenoceptors (mediating the heart rate response) are more sensitive to isoprenaline than β_2-adrenoceptors (mediating the arterial blood pressure response). Alternatively, it is possible that at lower isoprenaline doses an indirect effect of β_1-adrenoceptor stimulation increased arterial blood pressure (as a consequence of increased heart rate and contractility) thus masking the β_2-mediated decrease in arterial blood pressure.

In rats, isoflurane offered rapid and smooth induction of anaesthesia. Maintenance of anaesthesia using isoflurane was adequate, however, isoflurane (and other inhalation anaesthetics) have some disadvantages in this respect: i) In procedures of longer duration there is often a need to keep adjusting the dose to maintain steady anaesthesia and the subsequent alterations in heart rate, blood pressure, etc. could interfere with interpretation of the effects of drugs being studied; ii) If there is any obstruction of the airways, e.g. due to a build up of mucous, then it is difficult to continue adequate delivery of an inhalational anaesthetic and therefore there is a risk that the animal's welfare may suffer as a result of inadequate anaesthesia; iii) using 100% oxygen to deliver isoflurane results in a non-physiological high PO_2; iv) isoflurane is much more expensive to use – not only the cost of the anaesthetic itself, but oxygen for delivery and maintenance of equipment. For these reasons, the feasibility of transferring to a continuous pentobarbital infusion following induction with isoflurane was assessed. Pentobarbital is used widely and can provide stable anaesthesia over long periods of time, with no rapid fluctuations in heart rate and blood pressure provided that an adequate level of anaesthesia is maintained.

In comparison of isoflurane and pentobarbital anaesthetised rats, overall, arterial blood pressure and heart rate were higher in the pentobarbital group than the isoflurane group (Figure 2.3c). In the case of arterial blood pressure, but not heart rate, higher doses of isoprenaline appeared to abolish this difference (Figure 2.3a and b). It should be noted, however, that one rat in the pentobarbital group had much more profound decreases in arterial blood pressure than the others in the group and so this may account for this observation. The sustained differences in heart rate between isoflurane and pentobarbital rats could be due to the level of anaesthesia in that isoflurane rats were more deeply anaesthetised than the pentobarbital rats despite neither group responding to the corneal or pedal reflex tests. Interestingly, a similar difference in baseline heart rate in pentobarbital and isoflurane anaesthetised rats has been observed in other experiments (Coker & Kane, 2009). Alternatively, this difference could be due to a depressive effect of isoflurane on heart rate potentially related to the delivery of isoflurane in 100% oxygen.

In rats the surgical skills necessary to measure LVP were developed. Initial attempts at measuring LVP in rat were made by passage of a heparinised saline

filled cannula, attached to a pressure transducer, via the right carotid artery. However, this sometimes resulted in a damped signal which substantially underestimated $LVdP/dt_{max}$ (Figure 2.4). To help overcome this problem a Millar Mikro-tip® catheter pressure transducer was employed. This resulted in high quality LVP signals which allowed $LVdP/dt_{max}$ to be derived more accurately. Interestingly, when later applying this technique in guinea pigs, access to the LV was found to be much easier via the left rather than the right carotid artery. Thus it would seem that to measure LVP in rats a catheter should be advanced into the LV via the right carotid artery, and indeed this has been stated by others (Hughes, 1997), whilst in guinea pig the left carotid artery should be used.

2.4.1.2 Guinea pig anaesthesia

As the main aim of the work in this Chapter was to optimise conditions for studying the effects of drugs on haemodynamics and cardiac contractility in anaesthetised guinea pigs, it was important first of all to reconsider the suitability of sodium pentobarbital as the anaesthetic of choice (Batey *et al.*, 1997; Michael *et al.*, 2008). Previous studies on ECG intervals in guinea pigs have employed a variety of anaesthetics. Although Hamlin *et al.* (2003) used ketamine/xylazine, their experiments used non-invasive methods for assessing the ECG and others have reported that this anaesthetic regime was not sufficient for surgical interventions in guinea pigs (Buchanan *et al.*, 1998). Hauser *et al.* (2005) used urethane but as this is carcinogenic (Field & Lang, 1988), for the sake of operator safety, this was also excluded from the list of possible anaesthetics for the present study.

As explained previously, inhalational anaesthetics can be advantageous particularly in terms of speed of induction of anaesthesia. In rats, isoflurane provided smooth induction of anaesthesia and a protocol to transfer to pentobarbital for maintenance anaesthesia was established. Unfortunately, however, guinea pigs tended to hold their breath for some time upon smelling the isoflurane, which meant that induction was not as smooth as in rats. Guinea pigs also salivated profusely and once placed on their backs on the operating table this excess fluid could potentially impede respiration. To maintain intact baroreceptor reflexes in this model antimuscarinic premedication to reduce the secretion of saliva was not desired. Using a lower concentration of isoflurane for induction of anaesthesia in the second batch of experiments did reduce salivation but heart rate and mean arterial blood pressure

were lower than with other anaesthetics and there were still difficulties in maintaining stable haemodynamics. Thus experiments with this anaesthetic were discontinued.

In previous experience (SJ Coker, personal observation), rats anaesthetised with pentobarbital or Hypnorm/Hypnovel normally breathe spontaneously whereas artificial respiration is almost always necessary in pentobarbital anaesthetised guinea pigs. At the doses used in the present study artificial ventilation was required in Hypnorm/Hypnovel anaesthetised guinea pigs thus offering no advantage over pentobarbital in this respect. It was also found that heart rate declined significantly in the Hypnorm/Hypnovel group but not in those given pentobarbital indicating that the latter was more suitable for the purpose of experiments in this study (Figure 2.5).

Although pentobarbital is used commonly for terminal anaesthesia of laboratory animals, veterinary surgeons prefer to use anaesthetics, such as Hypnorm/Hypnovel, that also have analgesic properties. For this reason it was investigated whether premedication with fentanyl prior to pentobarbital had any advantages or disadvantages. The dose of fentanyl used here (50 μg kg^{-1} s.c.) seemed to relax the guinea pigs and this may have contributed to the faster induction time after the subsequent administration of pentobarbital. However, as fentanyl was given 5 min before pentobarbital, the overall time from first injection to surgical anaesthesia was very similar. During induction of anaesthesia with pentobarbital, animals can go through a hyperalgesic phase (Ewen *et al.*, 1995) and there is evidence of increased nociception after i.p. administration of pentobarbital (Svendsen *et al.*, 2007). Premedication with an analgesic such as fentanyl will offset these actions of pentobarbital, thus improving animal welfare. Fentanyl had no adverse effects on haemodynamics or the ECG (for ECG intervals see Mooney *et al.*, 2012).

2.4.1.3 Bilateral carotid artery occlusion

In general, guinea pigs are considered to be more difficult to work with than other similarly sized species such as the rat. As well as being more difficult to anaesthetise (Buchanan *et al.*, 1998) the blood vessels of the guinea pig are much smaller (Librizzi *et al.*, 1999) and very fragile. As a consequence it can be technically challenging to successfully isolate and cannulate femoral arteries (or veins) in the guinea pig. Previously, it was noticed that when both carotid arteries

were cannulated in the anaesthetised rat, the heart rate and blood pressure responses to drugs such as isoprenaline and angiotensin II were unusual because they lacked the normal reflex components (SJ Coker, personal observation). The data presented above demonstrate that this does not apply in the guinea pig, as the responses to isoprenaline and angiotensin II were virtually identical when either one or both carotid arteries were cannulated (Figure 2.6 and Figure 2.7). This suggests that the baroreceptors in the aortic arch are much more important than those in the carotid sinuses in guinea pigs. Unlike the rat, two thirds of the blood supply to the brain in the guinea pig is delivered through the vertebrobasilar arterial system (Majewska-Michalska, 1998; Librizzi *et al.*, 1999). Thus bilateral occlusion of the carotid arteries is unlikely to seriously compromise blood flow to the brain in the guinea pig.

2.4.1.4 Assessment of cardiac contractility and haemodynamics

To assess the ability of the anaesthetised guinea pig to detect drug-induced changes in haemodynamics and cardiac contractility standard positive and negative inotropes were studied alongside identified cardiotoxic agents.

Isoprenaline

The mechanism of action of isoprenaline is described in 2.4.1.1. Similar to rats, isoprenaline caused a dose-dependent increase in heart rate in guinea pigs, but unlike the rat, there were no significant changes in arterial blood pressure (Figure 2.8b and Figure 2.9b). The predominant increases in heart rate and contractility (via $LVdP/dt_{max}$ and the QA interval) in guinea pig may suggest that β_1-adrenoceptors are more sensitive to isoprenaline than β_2-adrenoceptors. However, it may be that at the doses of isoprenaline used the indirect effect of β_1-adrenoceptors to increase arterial blood pressure (as a consequence of increased heart rate and contractility) masked the β_2-mediated decrease in arterial blood pressure in guinea pigs.

Lower doses of isoprenaline were selected than those used by Hauser *et al.* (2005). Initially in rats equivalent doses to those used by Hauser *et al.* (2005) were tried, however, the second dose (12 nmol kg^{-1} min^{-1}) caused severe and lethal depressions of arterial blood pressure. Furthermore, the lowest dose used by Hauser *et al.* (2005) had the maximal effect and the preliminary data with isoprenaline in pentobarbital anaesthetised rats shown here suggested that lower doses would be sufficient.

In this study, plasma concentrations of isoprenaline were not determined. It was advised that there were difficulties establishing a suitable method as isoprenaline did not interact favourably with any of the available HPLC columns. With organic columns isoprenaline did not bind whereas with inorganic columns isoprenaline tended to be retained and not eluted. This was also the case in an independent study which attempted to measure isoprenaline concentrations following acute *in vivo* drug administration (L Marks, personal communication). One alternative method was also assessed – laser diode thermal desorption (Beattie *et al.*, 2012). This method omits the HPLC step, however, this was also unsuccessful.

Ouabain

Ouabain exerted similar effects to isoprenaline showing positive inotropic effects although these were more gradual and slower in onset than the positive inotropic effects of isoprenaline (Figure 2.11c and Figure 2.13c). Ouabain is a cardiac glycoside inhibiting Na^+/K^+ pumps in the sarcolemmal membrane which pump Na^+ out of the cell in exchange for K^+. Inhibition results in increased cytosolic Na^+, which consequently slows the extrusion of Ca^{2+} by the NCX. The increased $[Ca^{2+}]_i$ then allows more Ca^{2+} to be stored in the SR, thus increasing the amount of Ca^{2+} released by each action potential hence increasing the force of contraction (Rang *et al.*, 2003). Cardiac glycosides have also been shown to have a cardiac slowing effect and reduced rate of conduction through the AV node by increasing vagal activity via an action on the central nervous system (Toda & West, 1969). However, at higher doses cardiac glycosides can increase sympathetic nerve activity (Brunton *et al.*, 2011) and this may account for the increase in heart rate in the latter stages of the final dose shown here (Figure 2.8c).

This increase in heart rate combined with increased contractility may account for the apparent increases in arterial blood pressure and LVSP (Figure 2.9c and Figure 2.10c). Hauser *et al.* (2005) observed increases in arterial blood pressure and LVSP with the later infusions of ouabain. The increase in arterial blood pressure occurred at a dose equivalent to the top dose used in the present study whilst the increase in LVSP occurred with an additional 3-fold higher dose of ouabain. No significant effects on arterial blood pressure or LVSP were reached in the present study. Inspection of individual animal data showed that throughout the middle and final dose of ouabain one animal had far greater pressure responses than the others in the group increasing the error associated with the mean. When this animal was

excluded (see below) the error decreased, however, significance was still not achieved perhaps due to the low group number.

The doses of ouabain used in this study were selected from within the ranges used by Hauser *et al.* (2005), however, the highest dose was omitted. This was due to the occurrence of lethal arrhythmias at this dose in our pilot studies and Hauser *et al.* (2005) noted this as a toxic dose. The highest dose used by us caused arrhythmias in the latter stages of infusion in one animal and for this reason at 40 and 45 min, data for this animal were excluded from analysis. Hauser *et al.* (2005) reported an intense rise in the number of extrasystoles at this dose.

Accurate PPB data for ouabain could not be determined as the area of the spectral peak for ouabain fell below the limit of quantification. As a definitive value could not be determined the free concentrations were reported as a minimum value (Table 2.2).

Verapamil

Verapamil had modest effects on heart rate, arterial blood pressure, LVP, $LVdP/dt_{max}$ (when expressed as % change) and the QA interval (Figure 2.8d, Figure 2.9d, Figure 2.10d, Figure 2.12d and Figure 2.13d). Verapamil prevents Ca^{2+} entry triggered by depolarisation of cardiac myocytes thereby having a negative inotropic effect (Rang *et al.*, 2003). This may be indicated by the decrease in percentage change in $LVdP/dt_{max}$ and contrasting increase in the QA interval observed here. Verapamil also blocks Ca^{2+} channels on smooth muscle cells of the vasculature which would account for the reductions in arterial blood pressure.

In one experiment in the verapamil group there was no response to verapamil at all; the heart rate, arterial blood pressure, LVP, $LVdP/dt_{max}$ and QA interval values remained steady throughout the whole experiment just like those in a vehicle experiment. In all the other individual animals given verapamil (or isoprenaline or ouabain) the effects of the drug can be seen clearly. Analysis of the plasma concentrations of verapamil for this particular experiment revealed that both the total and free concentrations of verapamil (0.57 and 0.11 μM, respectively) were less than 10% of the mean of those in the other animals in the verapamil group (7.06 ± 2.34 and 1.37 ± 0.45 μM). This suggests that the “non-responder” received lower doses (maybe 10 fold less), probably because a mistake was made when preparing the drug solution for that experiment. As it cannot be verified that this animal

received the correct doses of verapamil the decision was made to exclude it and include data from a replacement experiment. The total and free serum verapamil concentrations in this replacement animal were 8.63 and 1.68 µM respectively. Unfortunately in this replacement experiment it was not possible to insert the catheter into the LV meaning LVP and LVdP/dt_{max} data from this animal were not available. Therefore, for these parameters the verapamil group size is n = 3 animals which may account for the lack of significant effects on the absolute values of LVdP/dt_{max}.

Verapamil doses were also selected from within the ranges used by Hauser *et al.* (2005), but again the highest dose was omitted following advice from our AstraZeneca collaborators based on their experience with verapamil in the monophasic action potential (MAP) model previously used for safety pharmacology testing. In this open-chest anaesthetised guinea pig model a higher dose of verapamil was found to be lethal. Hauser *et al.* (2005) found their top dose caused AV block in two cases and death in another. Adverse effects were noted in one animal in these experiments which had extremely pronounced reductions in arterial blood pressure such that pressure data (and as a consequence LVdP/dt_{max} and QA interval data) could not be obtained at 40 and 45 min in this experiment.

Therapeutic plasma concentrations of verapamil are reported to be in the range of 0.18 to 0.88 µM (Opie & Gersh, 2009). Mean total (7.82 ± 2.84 µM) and free (1.52 ± 0.55 µM) concentrations measured here are higher than this range, however, individual experimental data is quite variable and free concentrations close to these clinically relevant values were achieved in some experiments (Table 2.2).

Cardiotoxic drugs (imatinib and sunitinib)

Imatinib and sunitinib, as identified cardiotoxic agents causing LV contractile dysfunction (Kerkelä *et al.*, 2006; Chu *et al.*, 2007), were included to assess the ability of the anaesthetised guinea pig to detect adverse effects associated with these agents. Both imatinib and sunitinib were found to decrease all parameters assessed, except the QA interval (Figure 2.8 to Figure 2.13d and e, respectively). Overall, sunitinib effects appeared earlier than imatinib effects, being present throughout infusion of the highest dose, whereas imatinib effects only appeared towards the end of the highest dose. Sunitinib also resulted in greater percentage reductions in LVdP/dt_{max} (Figure 2.12). In general, imatinib is regarded as having much lower cardiovascular risks than sunitinib (Distler & Distler, 2007; Chen *et al.*,

2008; Ribeiro *et al.*, 2008) and has been shown to have less pronounced effects on cardiac Ca^{2+} handling dynamics and contraction rate (Qian & Guo, 2010). These findings are consistent with the differing extent of effects seen here.

For imatinib and sunitinib, there are few studies examining acute effects on the heart, and guinea pig studies are particularly scarce. Doses were therefore used at the highest possible without causing mortality. This decision was based on advice from colleagues at AstraZeneca who use doses a few fold below the maximum tolerated dose (MTD) when looking at novel compounds in investigative toxicology studies.

Clinical concentrations of imatinib have been reported as 5 µM (Wolf *et al.*, 2010). Clearly the total plasma concentrations (1122.36 ± 220.52 µM) measured here are well above the clinical concentration, however, free levels (4.15 ± 0.94 µM) are very similar. Sunitinib plasma concentrations have been reported as 0.03 µM (Minkin *et al.*, 2009) – much lower than the total (25.39 ± 8.34 µM) and free (3.40 ± 1.29 µM) levels measured here. It should also be noted that in these experiments imatinib and sunitinib are being given acutely for only 15 min each dose and clinical signs of LV decline are reported in patients following weeks/months of treatment (7.2 ± 5.4 months of imatinib treatment (Kerkelä *et al.*, 2006) and 33.6 weeks of sunitinib treatment (Chu *et al.*, 2007)).

As alluded to earlier, in the sunitinib group, the pre-drug values of $LVdP/dt_{max}$ were significantly lower than those in each other group (Figure 2.11). This particular group of experiments was performed at AstraZeneca where $LVdP/dt_{max}$ values are consistently lower than those measured at the University of Strathclyde. Anaesthetic and experimental protocols were identical at AstraZeneca and the University of Strathclyde, however, hardware and software differences did exist (see Section 2.2.4). The anomaly may, therefore, be due to a difference in calibration of the hardware to the software. Although the precise reason remains unclear, pre-drug $LVdP/dt_{max}$ values recorded at the University of Strathclyde are similar to those previously reported in the anaesthetised guinea pig (Hauser *et al.*, 2005).

2.4.1.5 Relationship between $LVdP/dt_{max}$ and the QA interval

For many years $LVdP/dt_{max}$ has been used as an index of cardiac contractility despite the limitation that it can be influenced by changes in heart rate, preload and afterload (Wallace *et al.*, 1963). For safety pharmacology purposes this is not

necessarily a disadvantage as any undesired effect on heart rate or blood pressure would also be of concern. The QA interval could be an even simpler method of assessing cardiac contractility as it does not require insertion of a catheter into the lumen of the LV. However, since it was first described as an index of cardiac contractility (Cambridge & Whiting, 1986) only about a dozen other full papers using the QA interval have been published. Just two of these papers have looked at relationships between the QA interval and $LVdP/dt_{max}$ (Adeyemi *et al.*, 2009; Norton *et al.*, 2009).

In conscious rats, Adeyemi *et al.* (2009) found an inverse linear correlation between $\log_{10}$ $LVdP/dt_{max}$ and $\log_{10}$ QA interval whereas in conscious dogs, Norton *et al*. (2009) reported inverse linear correlations between drug-induced changes in the absolute values of these parameters. In the latter report on the experiments in dogs the correlations found with a positive inotrope (pimobendan) and a negative inotrope (atenolol) were shown in separate graphs. Although reasonable linear correlations were found for each drug individually it is not possible to tell whether or not there would still be a linear relationship if the data had all been plotted on the same graph. Adeyemi *et al.* (2009) plotted separate straight lines (on the same graph) through the correlations between the absolute values of $LVdP/dt_{max}$ and the QA interval for each of the three drugs they had used (verapamil, milrinone and salmeterol). The slope of the line through their verapamil data is steeper than the slopes of the lines through the data obtained with the positive inotropes, milrinone and salmeterol, suggesting that when all of their data are considered together there is a curvilinear relationship between the absolute values of $LVdP/dt_{max}$ and the QA interval. The results detailed above (Figure 2.14) indicate that in the anaesthetised guinea pig there is also a curvilinear relationship between the absolute values for $LVdP/dt_{max}$ and the QA interval which becomes a linear correlation when the $\log_{10}$ values of both parameters are plotted. Thus these results in the anaesthetised guinea pig agree well with those found in conscious rats (Adeyemi *et al.*, 2009).

The use of only three standard drugs here is quite limiting and several reports in the literature outline additional factors that may influence either or both indices of contractility, such as heart rate and cardiac loading (Wallace *et al.*, 1963; Cambridge & Whiting, 1986; Hamlin & Del Rio, 2010; Markert *et al.*, 2012; Marks *et al.*, 2012). Therefore, $LVdP/dt_{max}$ and the QA interval are explored and discussed in more detail in Chapter 4.

2.4.2 Limitations

Small group sizes have been used in these studies for two reasons. First, UK legislation on the use of animals for scientific procedures requires Licence holders to reduce the number of animals used wherever possible. Thus if significant differences can be obtained with n = 4 it is difficult to justify using more animals per group. Second, the model is intended for use in safety pharmacology studies where time and costs are important factors. However, if certain test compounds have effects of lower magnitude or there is wider variation between the responses in individual animals within a group, increased numbers may be required to see statistically significant effects.

In vivo experiments therefore required LVP measurements to be achieved in four animals per group. In some groups this was achieved in the first four animals used (i.e. imatinib and sunitinib), however, in other groups up to six animals were required to achieve a complete LVP data set. Placement of a catheter in the LV can be difficult and in some animals it was just not possible to insert the catheter and collect LVP data. LV tissue was obtained from all drug-treated animals and used in subsequent analysis of CaMKII expression and activity.

2.4.3 Conclusions

The results presented above indicate that pentobarbital, either given alone or after fentanyl, provides anaesthesia suitable for the nature and duration of these experiments in the guinea pig. Occlusion of both carotid arteries (by cannulation) did not alter drug-induced changes in heart rate or blood pressure thus indicating that this approach is valid in the guinea pig and both $LVdP/dt_{max}$ and the QA interval can be measured in the same animal. Typical responses to known positive and negative inotropes were seen and adverse cardiovascular effects were detected with cardiotoxic agents. Strong correlations between $LVdP/dt_{max}$ and the QA interval were found although further work is required to explore this potential relationship in more detail.

Taken together these results indicate that the anaesthetised guinea pig has great potential as an early pre-clinical model in safety pharmacology for the simultaneous detection of drug-induced changes in haemodynamics and cardiac contractility.

CHAPTER 3 ASSESSMENT OF CAMKII EXPRESSION AND ACTIVITY FOLLOWING ACUTE *IN VIVO* DRUG ADMINISTRATION

3.1 Introduction

CaMKIIδ is a pivotal regulator of cardiac contractility acting via phosphorylation of key Ca^{2+} handling proteins in cardiac myocytes (Witcher *et al.*, 1991; Bassani *et al.*, 1995; Hain *et al.*, 1995; Karczewski *et al.*, 1997; Maier & Bers, 2007). Importantly, it is also a recognised molecular switch triggering abnormal Ca^{2+} handling and contractile dysfunction in cardiomyopathy (Hoch *et al.*, 1999; Currie & Smith, 1999; Boknık *et al.*, 2001; Colomer, 2002; Mishra *et al.*, 2003; Zhang *et al.*, 2003; Erickson & Anderson, 2008). Therefore, CaMKIIδ may be an important intracellular target for drugs that alter cardiac performance.

A key example of drug-induced CaMKII activation is observed following isoprenaline treatment of cardiac preparations. Isoprenaline targets the β_1-adrenoceptor and alters cardiac function through positive chronotropic and inotropic effects. Several reports exist in the literature linking β_1-adrenoceptor stimulation to activation of CaMKII (see Grimm & Brown, 2010 for review).

As increased $[Ca^{2+}]_i$, along with calmodulin (CaM), is required for initial activation and phosphorylation of CaMKII (Hanson *et al.*, 1994; Braun & Schulman, 1995), drugs that alter Ca^{2+} balance and flux in cardiomyocytes have the potential to alter CaMKII activation. Therefore, drugs such as ouabain and verapamil which increase and decrease $[Ca^{2+}]_i$, respectively, may also alter CaMKII activity and/or expression. Increased CaMKII activity may be measured *in vitro* as increased phosphoThr286-CaMKII (pThr286-CaMKII) or increased phosphorylation of a CaMKII-specific peptide substrate, e.g. commercially available autocamtide-2.

Imatinib and sunitinib are anti-cancer agents designed as multiple kinase inhibitors. The ability of these drugs to target numerous kinases offers several advantages in fighting tumour progression, however, this promiscuity is thought to underlie the associated cardiac problems that many of these drugs, including imatinib and sunitinib, exhibit (Force & Kerkelä, 2008). A decline in cardiac contractility is a significant symptom of imatinib and sunitinib and both drugs have been shown to alter $[Ca^{2+}]_i$ dynamics in guinea pig ventricular cardiomyocytes (Qian & Guo, 2009, 2010). Taken together, these findings suggest the potential for an effect of imatinib and sunitinib on CaMKII, however, no studies have investigated the action of these drugs on cardiac contractility and CaMKII simultaneously.

If changes in cardiac contractility can be linked to concomitant changes in CaMKII, CaMKII could be identified as an *in vitro* marker of *in vivo* changes in contractility offering great potential as a marker of cardiac safety in drug development. Firstly, however, the possibility of a link needs to be investigated and the nature of any such link characterised.

As described in Chapter 2, the anaesthetised guinea pig has proved to be suitable for assessment of cardiac contractility, however, this is not a common species used to examine CaMKII and so there is a paucity of reports in the literature describing CaMKII expression and activity in the guinea pig. Guinea pig is also not a species used previously in our laboratory so characterisation of CaMKII expression and activity and the methods employed to measure changes in CaMKII is important.

3.1.1 Aims

To test the hypothesis that drugs altering cardiac contractility may do so via actions on CaMKII the aims of the work described in this Chapter were:

(i) To optimise methods to detect and quantify CaMKIIδ and pThr286-CaMKII expression in guinea pig LV homogenates via immunoblotting.

(ii) To optimise a previously established radioactive assay to measure CaMKII activity in guinea pig LV homogenates.

(iii) To use these methods to assess changes in CaMKIIδ expression and/or CaMKII activity following acute *in vivo* drug administration.

3.2 Methods

Suppliers of equipment and materials are detailed in Appendix A. Suppliers of drugs and reagents and their storage information are detailed in Appendix B.

3.2.1 Buffer compositions

The compositions of buffers mentioned throughout the Methods Section are detailed below:

Krebs buffer: 120 mM NaCl; 20 mM 4-(2-hydroxyethyl)-1-piperazineethanesulfonic acid (HEPES); 5.4 mM KCl; 0.52 mM NaH_2PO_4; 3.5 mM $MgCl_2$; 20 mM taurine; 10 mM creatine, pH 7.4

Homogenisation buffer 1: 20 mM Tris (Tris(hydroxymethyl)aminomethane)-HCl, pH 7.2; 1 mM dithiothreitol (DTT); 1x protease inhibitor cocktail

Phosphatase inhibitor cocktail: 0.02 mM calyculin A, 80 mM Na orthovanadate

Homogenisation buffer 2: 20 mM Tris-HCl, 1 mM DTT, 1x protease inhibitor cocktail, 1x phosphatase inhibitor cocktail, pH 7.2

Transfer buffer: 25 mM Trizma® base; 0.2 M glycine; 20% methanol, pH 8.5

Blocking buffer 1: 3% bovine serum albumin (BSA) in antibody incubation buffer

Tris Buffered Saline (TBS) 10x: 0.2 M Trizma® base, 1.4 M NaCl; pH 7.6

Blocking buffer 2: 1X TBS; 0.1% Tween-20; 5% w/v non-fat dry milk

Antibody incubation buffer 1: 1% Tween-20; 1% Triton® X-100; 100 mM $MgCl_2$; 100 mM Trizma® base; 1% BSA; 5% fetal calf serum (FCS); 1% Thimerosol, pH 7.5

Antibody incubation buffer 2: 1X TBS, 0.1% Tween-20 with 5% BSA

Wash buffer 1: Rinse buffer, 142 mM NaCl; 1% Triton® X-100; 1 mM ethylene diamine tetraacetic acid (EDTA), pH 7.5; 1 mM Tris-HCl and High salt rinse buffer, 595 mM NaCl; 1% Triton® X-100; 1 mM EDTA; 1 mM Tris-HCl, pH 7.5

Wash buffer 2: 1X TBS; 0.1% Tween-20

ECL: Reagent 1, 25 µM luminol; 1.125 mM coumaric acid; 0.1 M Tris-HCl pH 8.5, Reagent 2, 64 µL hydrogen peroxide, 0.1 M Tris- HCl pH 8.5

CaMKII substrate cocktail: 500 µM autocamtide-2; 2.4 mM calmodulin

PKA/PKC inhibitor cocktail: 2 µM PKA inhibitor peptide; 2 µM PKC inhibitor peptide

Assay dilution buffer I: 20 mM 3-(N-morpholino)propanesulfonic acid (MOPS), pH 7.2, 25 mM β-glycerol phosphate; 5 mM ethylene glycol tetraacetic acid (EGTA); 1 mM Na orthovanadate, 1 mM DTT

Assay dilution buffer II: 20 mM MOPS, pH 7.2, 25 mM β-glycerol phosphate; 1 mM Na orthovanadate, 1 mM DTT, 1 mM $CaCl_2$

Mg^{2+}/ATP cocktail: 75 mM $MgCl_2$; 500 µM adenosine-5'-trisphosphate (ATP)

3.2.2 Tissue preparation

To obtain untreated tissue, animals (guinea pig, mouse, rabbit) were euthanised by overdose with i.p. sodium pentobarbital. The heart was swiftly removed and placed in ice cold Krebs solution. The LV was dissected free whilst the heart was in Krebs solution, immediately weighed and cut into small pieces in homogenisation buffer 1 at five volumes per wet tissue weight. Tissue was homogenised using an Ultra Turrax®.

Untreated dog tissue was obtained from AstraZeneca sent as snap frozen LV chunks. Upon thawing, chunks were immediately weighed and cut into small pieces in homogenisation buffer 1 at five volumes per wet tissue weight. Tissue was homogenised as before using an Ultra Turrax®.

Drug-treated tissue was obtained from acute *in vivo* drug-treated guinea pigs in Chapter 2. Immediately following the final *in vivo* drug infusion, the heart was removed and the LV was dissected free and cut into chunks. LV chunks were then snap-frozen in liquid nitrogen and stored at -80°C until required. To prepare LV homogenates snap frozen tissue was quickly weighed then pulverised in liquid nitrogen using a mortar and pestle. Tissue was then thawed in the presence of homogenisation buffer 2 at five volumes per tissue weight.

All homogenised tissue was aliquoted and stored at -80ºC until use.

3.2.3 Determination of protein content

Total protein content of LV homogenates was determined using the Coomassie Plus Protein Assay with BSA standards (0.1-1.0 mg mL^{-1}) to generate a standard curve. Samples were appropriately diluted to fall within the linear range of the standard curve. In a 96-well plate, 10 µL of each standard and 10 µL of each diluted sample was loaded in triplicate, and a row of distilled water served as a blank background. 200 µL of Coomassie Plus Reagent was then added into each well. The plate was read using a microplate reader at a wavelength of 595 nm. Standards were plotted using a sigmoidal fit and only samples with absorbance readings falling in the linear region of the curve were quantified.

3.2.4 Electrophoresis and immunoblotting

Sodium dodecyl sulphate-polyacrylamide gel electrophoresis (SDS-PAGE) was performed as previously described (Anthony *et al.*, 2007) using the NuPAGE®

system with 10% Bis-Tris gels and MOPS running buffer for detection of CaMKIIδ and pThr286-CaMKII. Samples (1mg mL^{-1}), prepared in sample loading buffer containing 75mM DTT, were denatured by heating at 70ºC for 10 min. Gels were subjected to electrophoresis at a constant voltage of 200 V for 1 h for both CaMKIIδ and pThr286-CaMKII. Proteins were transferred to nitrocellulose membranes at 25 V for 1 h then, depending on the primary antibody used (Table 3.1), two different protocols were followed for membrane blocking of non-specific binding sites and antibody incubations (solutions are described previously for each). Membranes were blocked in either blocking buffer 1 or blocking buffer 2 for 1 h at room temperature. Blots were incubated overnight at 4ºC with the relevant primary antibody. Membranes were washed for either 3 x 15 min (wash buffer 1) or 5 x 5 min (wash buffer 2), depending on the protocol adhered to, and then incubated for 2 h at room temperature with the appropriate secondary antibody (Table 3.1). Primary and secondary antibodies were diluted to the required concentration in antibody incubation buffer 1 or 2, depending on the protocol followed. Membranes were then washed as previously, before being treated with enhanced chemiluminescence (ECL) reagent and exposed onto film. Films were scanned using a densitometer and quantified using Quantity One software.

To ensure that total protein loaded on to gels was consistent between wells, glyceraldehyde-3 phosphate dehydrogenase (GAPDH) was used as an internal standard. This was used for normalisation within a single gel. CaMKII:GAPDH and pThr286-CaMKII:GAPDH ratios were calculated for each sample and these were then normalised to an untreated sample included in every gel to allow normalisation between different gels. The latter normalisation was performed due to the number of samples, which were required to be run across several different gels. This normalisation ensured that there were no discrepancies between different gels.

Molecular weight (MW) markers were used to identify proteins of interest (CaMKIIδ and pThr286-CaMKII MW = 56 kDa, GAPDH MW = 37 kDa). See Table 3.1 for specific details.

Table 3.1 Primary and secondary antibodies

Protein	Primary antibody	Secondary antibody	Protocol
CaMKIIδ	"Abgent CaMKIIδ" Rabbit, polyclonal 1:500	"Anti-rabbit" Goat anti-rabbit IgG (whole molecule)-peroxidase conjugated 1: 10,000	Blocking buffer 1 Wash buffer 1 (x 3) Antibody incubation buffer 1
	"R&D CaMKIIδ" Mouse, monoclonal 1:500	"Anti-mouse 1" Sheep anti-mouse IgG-horseradish peroxidise linked species-specific whole antibody 1:10,000	Blocking buffer 1 Wash buffer 1 (x 3) Antibody incubation buffer 1
	"Abgent CaMKIIδ-like" Rabbit, polyclonal 1:500	"Anti-rabbit" Goat anti-rabbit IgG (whole molecule)-peroxidase conjugated 1: 10,000	Blocking buffer 1 Wash buffer 1 (x 3) Antibody incubation buffer 1
	"Bers CaMKIIδ" Rabbit, polyclonal 1:5000	"Anti-rabbit" Goat anti-rabbit IgG (whole molecule)-peroxidase conjugated 1:5000	Blocking buffer 1 Wash buffer 1 (x 3) Antibody incubation buffer 1
	"Custom CaMKIIδ" Rabbit, polyclonal 1:1000	"Anti-rabbit" Goat anti-rabbit IgG (whole molecule)-peroxidase conjugated 1:5000	Blocking buffer 2 Wash buffer 2 (x 5) Antibody incubation buffer 2
GAPDH	GAPDH antibody Mouse, monoclonal 1:60,000	"Anti-mouse 2" Donkey anti-mouse IgG-peroxidase conjugated 1:80,000	Blocking buffer 2 Wash buffer 2 (x 5) Antibody incubation buffer 2
pThr286-CaMKII	pThr286-CaMKII antibody Mouse, monoclonal 1:500	"Anti-mouse 2" Donkey anti-mouse IgG-peroxidase conjugated 1:5000	Blocking buffer 2 Wash buffer 2 (x 5) Antibody incubation buffer 2

3.2.5 CaMKII activity assay

The CaMKII activity assay was adapted from a commercial kit from Upstate Biotechnology (Lake Placid, NY, USA) and measured the phosphotransferase activity of CaMKII. The assay was based on phosphorylation of a specific substrate peptide (autocamtide-2) by the transfer of γ-phosphate of adenosine-5'-[^{32}P]triphosphate ([γ-^{32}P]ATP) by CaMKII.

Assay components were mixed on ice. Sample solutions were prepared to a total volume of 40 µL containing 10 µL CaMKII substrate cocktail, 10 µL PKA/PKC inhibitor cocktail and the source of CaMKII (recombinant protein or LV homogenate) diluted to the desired concentration using assay dilution buffer II. In Ca^{2+} free controls, assay dilution buffer II was substituted for assay dilution buffer I.

Reactions were initiated by addition of 10 µL [γ-^{32}P]ATP diluted to 1 µCi µL^{-1} with Mg^{2+}/ATP cocktail. Each sample was run in triplicate and incubated for 10 min at 30°C with constant agitation. Following incubation, the reaction was terminated by spotting 25 µL of each solution on to individual squares of P81 phosphocellulose paper. Squares were then washed with 0.75% phosphoric acid (3 x 2 min) to remove residual radioactivity, followed by acetone (1 x 30 s) to aid drying. When dry, squares were immersed in a scintillation vial containing 4 mL scintillation fluid and read by a scintillation counter to quantify the bound phosphorylated substrate.

The specific radioactivity (S.R.) of the Mg^{2+}/cold ATP-hot ATP mixture was determined by transferring 5 µL of the mixture directly into the scintillation fluid. Background counts (due to non-specific binding of [γ-^{32}P]ATP and its breakdown products) were determined from samples in which the CaMKII source was absent. CaMKII activity in each sample was then calculated according to the equation: Sample counts – background counts / S.R. x incubation time. Individual activity values were then converted to pmol of phosphate incorporated min^{-1} µg protein^{-1} and normalised to the calculated activity of an untreated sample included in every assay. This normalisation was performed to be consistent with immunoblotting analyses.

3.2.6 Statistical analysis

Data are presented as mean ± S.E.M mean. In Figure 3.7 to Figure 3.10 no statistical analysis was performed as each bar represents only one sample. In

Figure 3.11 to Figure 3.13 Kruskal-Wallis tests were used for comparisons among groups because some of the data were not distributed normally.

3.3 Results

3.3.1 Characterisation of CaMKII expression and activity in guinea pig

A key objective of this Chapter was to determine whether concomitant alterations in CaMKIIδ expression and CaMKII activity occurred following acute *in vivo* drug treatments (specified in Chapter 2). Therefore it was essential that: i) western blot analysis be performed to determine whether CaMKIIδ (expression) and pThr286-CaMKII (activity) could be detected in LV homogenates from guinea pig. Optimisation of these protocols would then allow accurate quantitative immunoblotting for untreated and drug-treated samples; ii) Optimisation of a radioactive activity assay be performed to allow a second method of measuring CaMKII activity in untreated and drug-treated samples.

As commercially available CaMKIIδ specific antibodies are limited and antibody specificity, as well as CaMKIIδ expression, varies between species, a selected series of antibodies (Table 3.1) was used to assess CaMKIIδ expression in LV homogenates from guinea pig. Due to species differences in CaMKIIδ expression, LV homogenates from dog, rat, mouse and rabbit were tested alongside guinea pig for comparison. As rabbit and mouse LV homogenates have been tested previously in our lab using some of these antibodies (Currie *et al.*, 2005; Anthony & Currie, unpublished observations) these samples served as positive controls. Alternatively, in some experiments human recombinant CaMKIIδ protein served as a positive control.

The first antibody tested was the “Abgent CaMKIIδ” antibody (Figure 3.1) and guinea pig, dog, rat and rabbit LV homogenates were assessed at increasing loads of total protein. In guinea pig, dog and rat no signals were detected up to 30 µg total protein (Lanes 1 to 9). A band of increasing intensity with increasing total protein load, corresponding to CaMKIIδ, was detected in rabbit (Lanes 10-13) and a strong band corresponding to recombinant CaMKIIδ was evident (Lane 14).

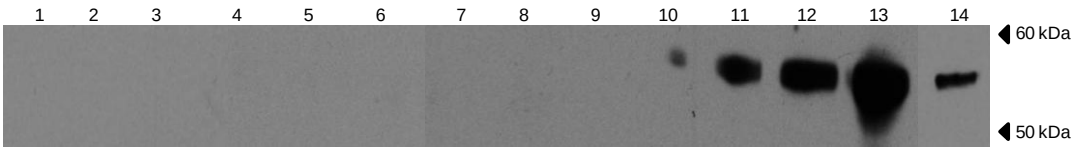

Figure 3.1 Detection of CaMKIIδ in LV homogenates using the "Abgent CaMKIIδ" antibody (1:500). Lanes 1-3, guinea pig 10, 20, 30 µg total protein loads; Lanes 4-6, dog 10, 20, 30 µg total protein loads; Lanes 7-9, rat 10, 20, 30 µg total protein loads; Lanes 10-13, rabbit 10, 20, 30, 40 µg total protein loads; Lane 14, recombinant CaMKIIδ 100 ng total protein load. Molecular weight markers are indicated.

The second antibody tested was the “R&D CaMKIIδ” antibody (Figure 3.2). CaMKIIδ expression in rat and guinea pig LV homogenates was assessed using increasing amounts of total protein as before. Faint bands corresponding to CaMKIIδ were detected with higher total protein loads from guinea pig and rat (Lanes 1 to 8). A faint band was also detected corresponding to recombinant CaMKIIδ (Lane 9).

The third antibody tested was the “Abgent CaMKIIδ-like” antibody (Figure 3.3). Faint bands of slightly increasing intensity were detected with increasing total protein loads in guinea pig (Lanes 1 to 3). In dog, a clear band of increasing intensity with increasing amounts of total protein was detected corresponding to CaMKIIδ (Lanes 4 to 6). Similarly, in rat a band of increasing intensity with increasing amounts of total protein was detected corresponding to CaMKIIδ (lanes 7 to 9). Additionally, strong bands were also detected in rabbit (Lane 10) and recombinant CaMKIIδ (lane 11).

As none of the commercial antibodies tested gave a clear signal in guinea pig, a custom-made antibody kindly gifted to us from the Bers Laboratory (University of California) (“Bers CaMKIIδ”) was tested (Figure 3.4). In guinea pig (Lanes 1 and 2), rat (Lanes 5 and 6) and mouse (Lanes 7 and 8) a very faint band was detected which was more prominent with a greater total protein load, however in dog no band was evident (Lanes 3 and 4).

The “Bers CaMKIIδ” antibody provided a promising signal in guinea pig at a higher protein load (30 µg), therefore, a custom-made antibody against the C terminus of CaMKIIδ similar to that obtained from the Bers Laboratory was prepared by Eurogentech. This was tested in guinea pig, dog and mouse LV homogenates (Figure 3.5). In all species strong bands corresponding to CaMKIIδ were detected and these increased in intensity with increasing total protein loads in guinea pig (Lanes 1 to 4) and mouse (Lanes 6 to 9).

As the “custom CaMKIIδ” antibody proved best for detecting CaMKIIδ expression in guinea pig LV homogenates, this antibody was selected for use in further experiments. To determine the optimal amount of total protein for this antibody a broad range of total protein loads was assessed for CaMKIIδ expression alongside GAPDH (Figure 3.6a and b). In Figure 3.6a protein loads from 2 to 40 µg were used. Below 4 µg total protein CaMKIIδ was not detected and GAPDH showed a

Figure 3.2 Detection of CaMKIIδ in LV homogenates using the "R&D CaMKIIδ" antibody (1:500). Lanes 1-4, guinea pig 10, 20, 30, 40 µg total protein loads; Lanes 5-8, rat 10, 20, 30, 40 µg total protein loads; Lane 9, recombinant CaMKIIδ 100 ng. Molecular weight markers are indicated.

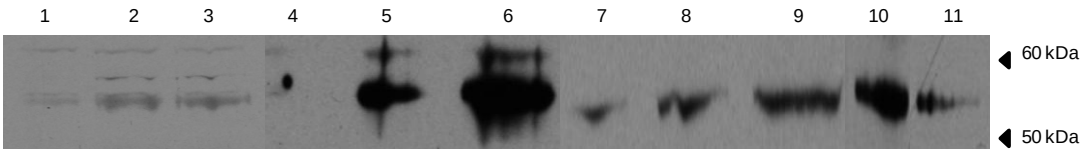

Figure 3.3 Detection of CaMKIIδ in LV homogenates using the "Abgent CaMKIIδ-like" antibody (1:500). Lanes 1-3, guinea pig 10, 20, 30 µg total protein loads; Lanes 4-6, dog 10, 20, 30 µg total protein loads; Lanes 7-9, rat 10, 20, 30 µg total protein loads; Lane 10, rabbit 10 µg; Lane 11, recombinant CaMKIIδ 100 ng total protein load.

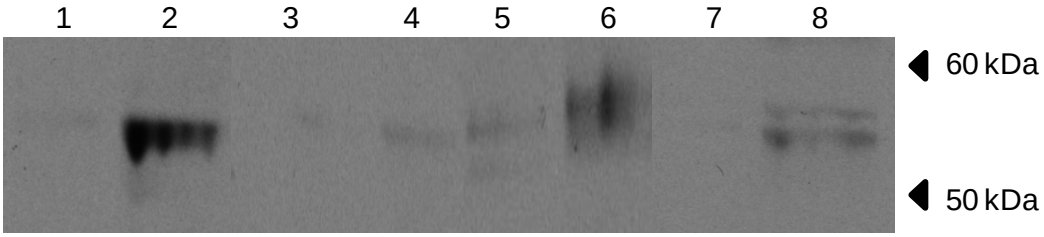

Figure 3.4 Detection of CaMKIIδ in LV homogenates using the "Bers CaMKIIδ" antibody (1:5000). Lanes 1-2, guinea pig 10, 30 µg total protein loads; Lanes 3-4, dog 10, 30 µg total protein loads; Lanes 5-6, rat 10, 30 µg total protein loads; Lanes 7-8 mouse 10, 30 µg total protein loads. Molecular weight markers are indicated.

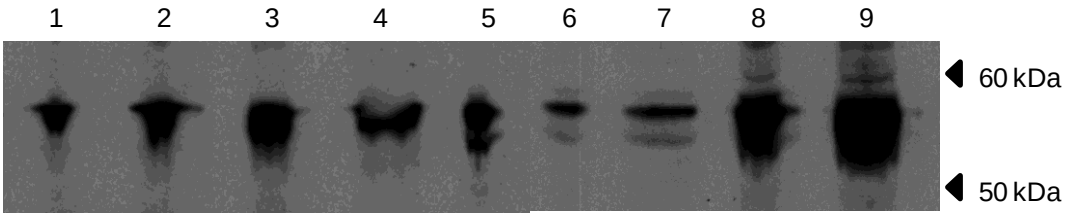

Figure 3.5 Detection of CaMKIIδ in LV homogenates with the "custom CaMKIIδ" antibody (1:1000). Lanes 1-4, guinea pig 10, 20, 30, 40 µg total protein loads; Lane 5, dog 20 µg total protein; Lane 6-9, mouse 10, 20, 30, 40 µg. Molecular weight markers are indicated.

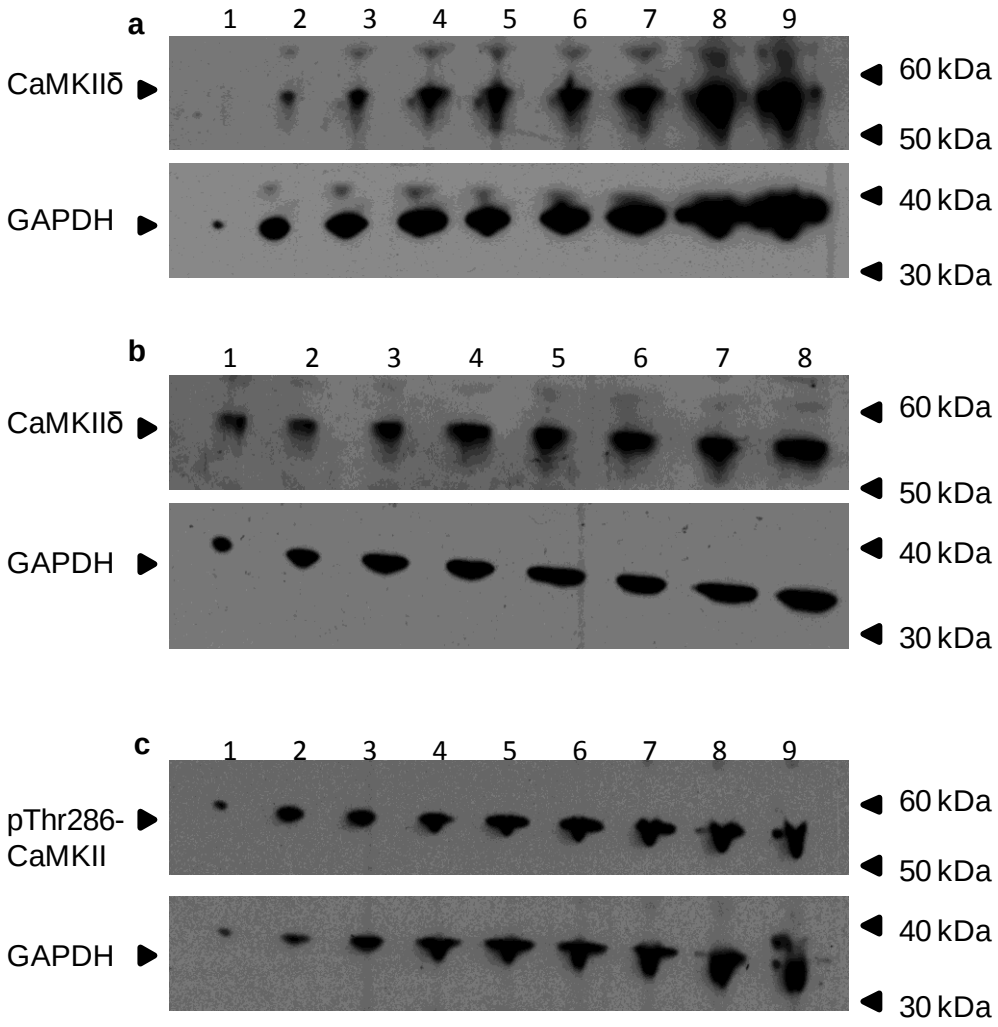

Figure 3.6 Determination of optimal protein loads for (**a** and **b**) CaMKIIδ and (**c**) pThr286-CaMKII with GAPDH. Total protein loads were in **a)** Lanes 1-9: 2, 4, 6, 10, 12, 15, 20, 30, 40 µg, **b)** Lanes 1-8: 4, 6, 7, 8, 9, 10, 12, 15 µg, **c)** Lanes 1-9: 2, 4, 6, 10, 12, 15, 20, 30, 40 µg.

very weak signal. Above 4 µg bands of increasing intensity with increasing total protein loads were evident for both CaMKIIδ and GAPDH with overexposed signals appearing at the higher loads. Figure 3.6b concentrated on a smaller range of protein loads between 4 and 15 µg. Again strong bands of increasing intensity were evident throughout this range of loads. From these experiments 6 µg was chosen as the optimal amount of total protein for simultaneous detection of CaMKIIδ and GAPDH. This was based upon the signal strength and the linear range for quantification using a calibrated densitometer.

One method of measuring CaMKII activity involves quantifying expression of the autophosphorylated and active form of CaMKII (pThr286-CaMKII). This can be detected using an antibody raised against the autophosphorylation site of CaMKII at Thr286. To assess the expression of pThr286-CaMKII in guinea pig LV homogenates a range of total protein loads from untreated hearts was also tested using the pThr286-CaMKII antibody (Figure 3.6c). At 2 µg a weak band was evident for both pThr286-CaMKII and GAPDH. As total protein loads gradually increased to 40 µg the intensity of these bands also gradually increased. From this experiment the optimal total protein load for simultaneous detection of pThr286-CaMKII and GAPDH was determined as 10 µg again based on the signal strength and linear limitations of the densitometer.

A second method to measure CaMKII activity uses a radioactive assay measuring the incorporation of radiolabelled phosphate (^{32}P) into a CaMKII peptide substrate, autocamtide-2. To optimise this assay for measuring CaMKII activity in guinea pig LV homogenates, recombinant CaMKII protein and untreated guinea pig LV homogenates were tested alongside a series of negative control samples.

Firstly, recombinant CaMKII protein was tested. [^{32}P] counts were determined at two amounts of total protein, 10 and 30 ng (Figure 3.7a). With the greater amount of total protein [^{32}P] counts increased by almost 3 fold. Both 10 and 30 ng of recombinant protein were then tested in control experiments excluding either the substrate, Ca^{2+} or CaMKII. All controls showed greatly decreased and very low [^{32}P] counts, however, controls without Ca^{2+} tended to have slightly higher counts than the other controls. Measured radioactivity was then converted to CaMKII activity and expressed per µg total protein (Figure 3.7b). Both 10 and 30 ng total protein samples showed similar CaMKII activity as results are expressed per µg total

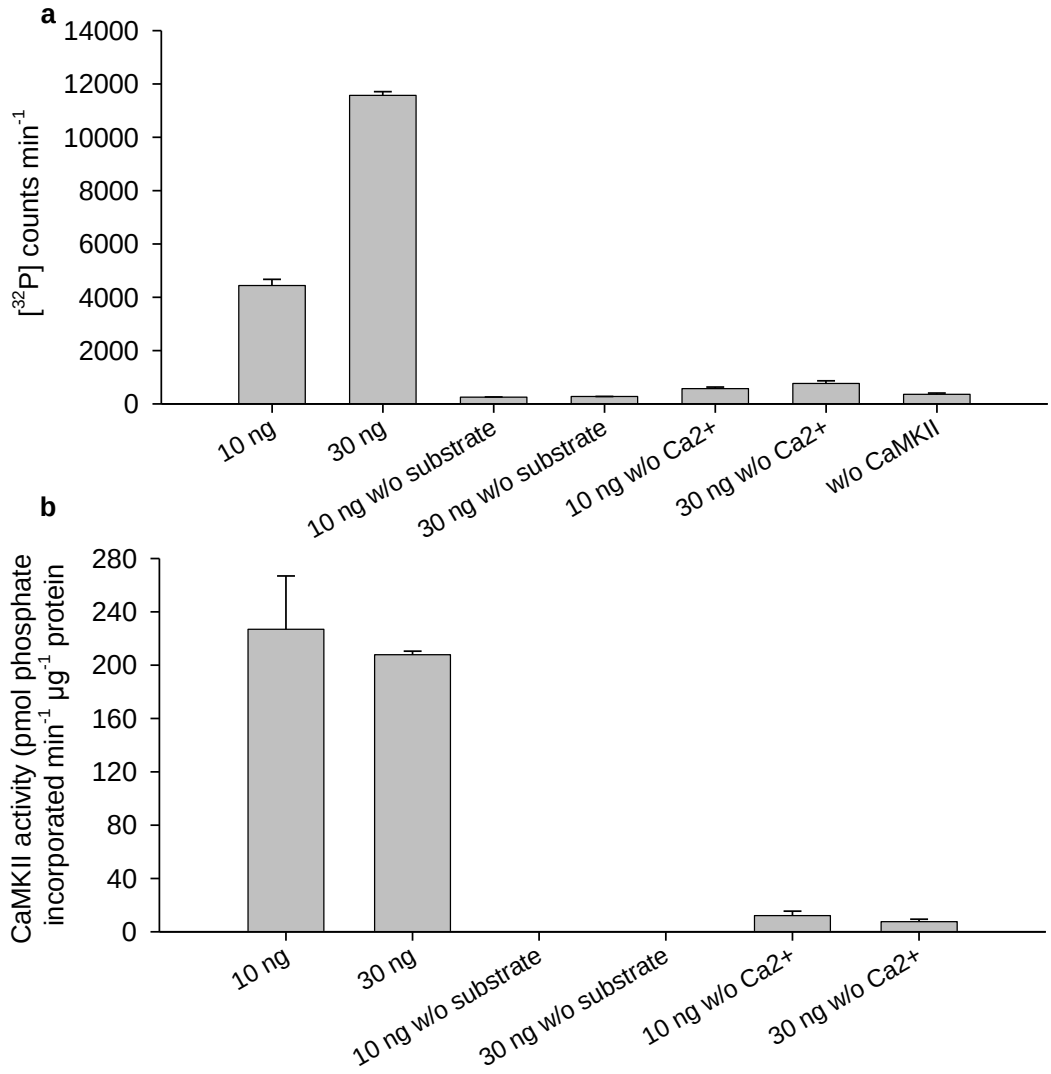

Figure 3.7 Recombinant CaMKII protein **a)** [^{32}P] counts for 10 and 30 ng total protein and controls without (w/o) substrate, Ca^{2+} or CaMKII, and **b)** calculated CaMKII activities for 10 and 30 ng total protein and controls without (w/o) substrate or Ca^{2+}. Data are presented as mean ± S.E.M value for one sample determined in triplicate. No statistical analysis was performed.

protein. In control samples CaMKII activity was greatly decreased and, similar to [^{32}P] counts, Ca^{2+} controls tended to have slightly higher activity.

Guinea pig LV homogenates were then tested in a similar manner as the recombinant CaMKII protein. [^{32}P] counts were determined at 10 and 20 µg total protein (Figure 3.8a) and again counts increased (approximately 1.5 fold) with the greater amount of total protein. Since sufficient activity was achieved with 10µg total protein and since this amount has been used previously by our group with mouse and rabbit homogenates (Anthony *et al.*, 2007), 10 µg total protein was then tested in initial experiments. As with recombinant CaMKII, all control samples showed greatly decreased and very low [^{32}P] counts and again controls without Ca^{2+} tended to have slightly higher counts than the other controls. When measured radioactivity was then converted to CaMKII activity and expressed per µg total protein (Figure 3.8b) both 10 and 20 µg samples showed similar CaMKII activity. In control samples CaMKII activity was greatly decreased and, similar to [^{32}P] counts, Ca^{2+} controls tended to have slightly higher activity. Recombinant CaMKII protein (30 ng) was included in this experiment for direct comparison with the native CaMKII protein in guinea pig LV homogenates. [^{32}P] counts were higher than in both amounts of guinea pig LV homogenate and when converted to CaMKII activity per µg total protein, CaMKII activity was much greater (approximately 650 fold) than CaMKII activity of the guinea pig homogenates.

To assess the ability of the CaMKII activity assay to detect decreases in CaMKII activity, guinea pig LV homogenate was pre-treated with the CaMKII peptide inhibitor AIP at three increasing concentrations (Figure 3.9). At 1 µM AIP, CaMKII activity was similar to untreated guinea pig LV homogenate, however, activity was inhibited by 48% at 3 µM and further decreased to 30% of the untreated guinea pig LV homogenate at 10 µM.

For comparison with other species CaMKII activities for mouse and dog LV homogenates were determined alongside guinea pig LV homogenates (Figure 3.10). At the same amounts of total protein (10 µg) guinea pig tended to show a higher CaMKII activity than mouse and just slightly higher than dog.

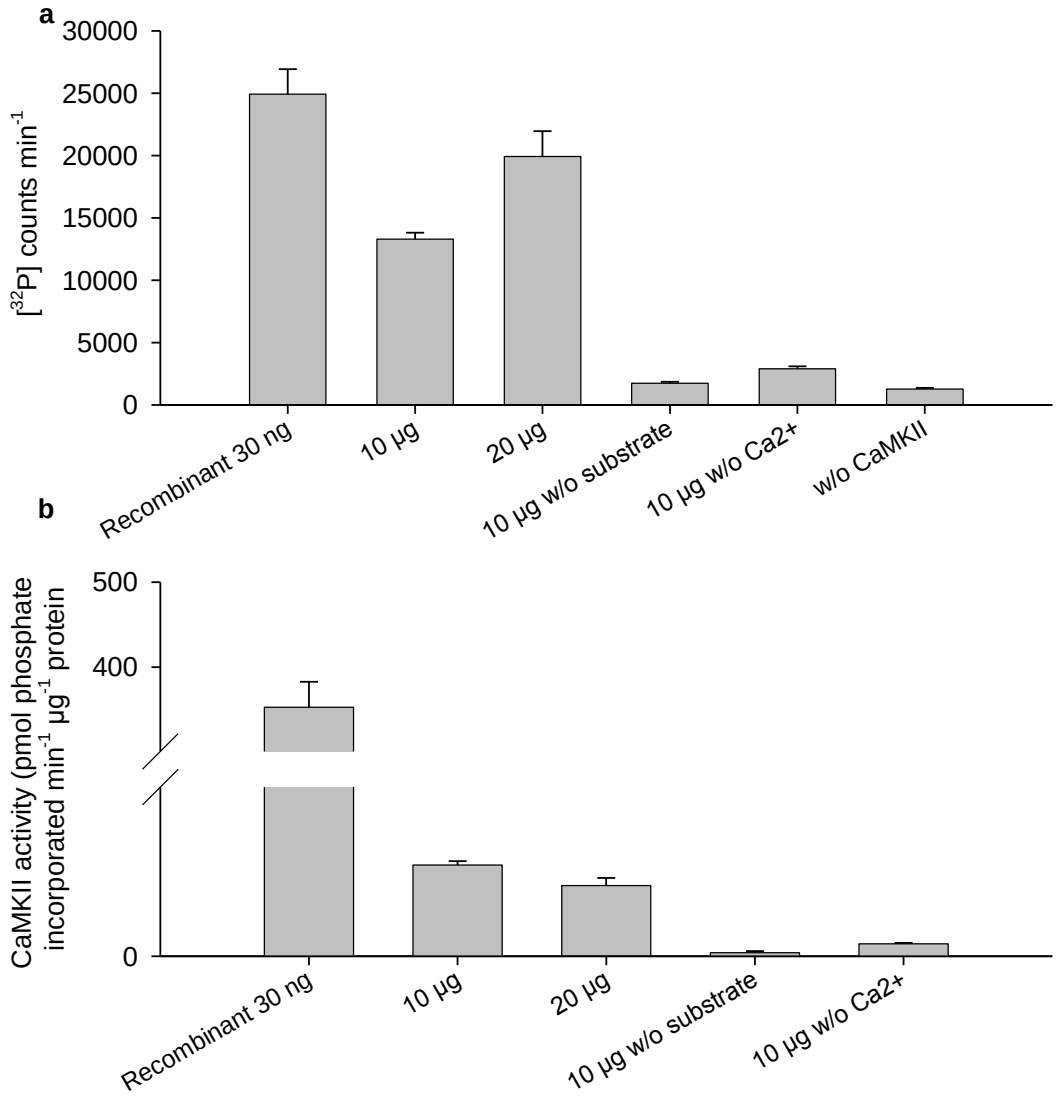

Figure 3.8 Guinea pig left ventricular (LV) homogenate **a)** [^{32}P] counts for 10 and 20 µg total protein and 10 µg controls without (w/o) substrate, Ca^{2+} or CaMKII, and **b)** calculated CaMKII activities for 10 and 20 µg total protein and 10 µg controls without (w/o) substrate and w/o Ca^{2+}. Recombinant CaMKII protein (30 ng) was included for direct comparison. Data are presented as mean ± S.E.M value for one sample determined in triplicate. No statistical analysis was performed.

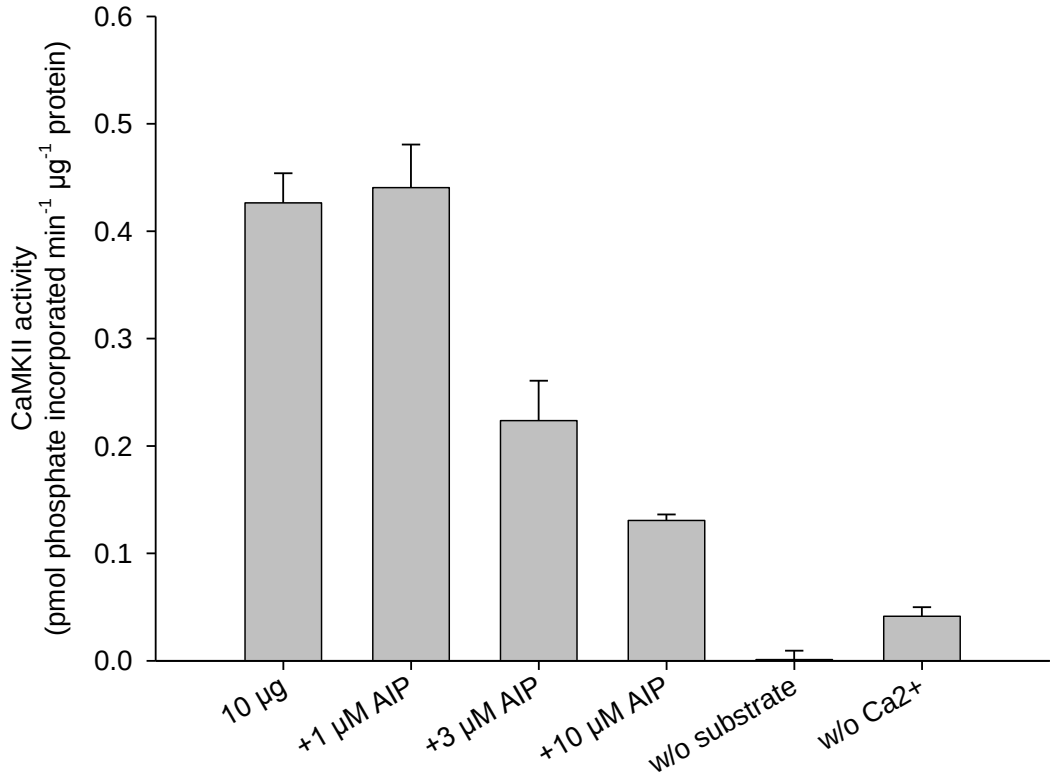

Figure 3.9 Calculated CaMKII activity in guinea pig left ventricular (LV) homogenate (10 µg), and guinea pig LV homogenate pre-treated with 1, 3 and 10 µM autocamtide-2 related inhibitory peptide (AIP). Data are presented as mean ± S.E.M value for one sample determined in triplicate. No statistical analysis was performed.

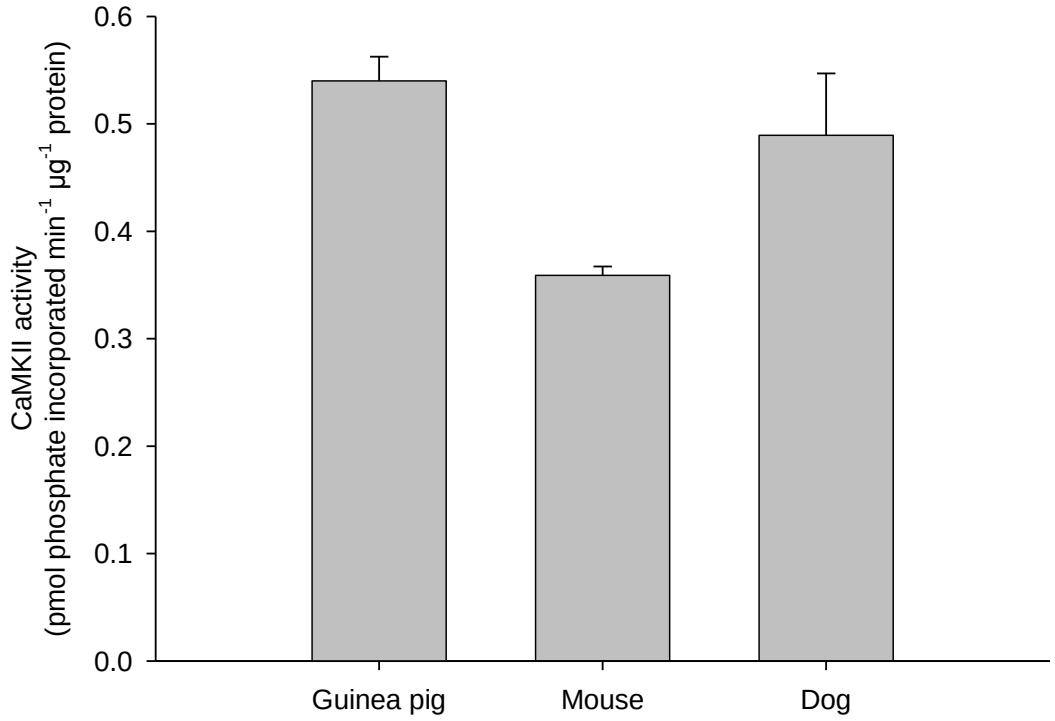

Figure 3.10 Calculated CaMKII activity in LV homogenate from guinea pig, mouse and dog all tested at 10 µg total protein. Data are presented as mean ± S.E.M value for one sample determined in triplicate. No statistical analysis was performed.

3.3.2 Effects of acute *in vivo* drug administration on CaMKII expression and activity

Following *in vivo* administration of isoprenaline, ouabain, verapamil, imatinib, sunitinib, or vehicle (as outlined in Chapter 2), LV homogenates were prepared and CaMKII expression and activity were assessed.

Across treatment groups CaMKIIδ expression was similar and not significantly altered compared to vehicle group (Figure 3.11). Similarly, pThr286-CaMKII expression was not significantly different in any treatment group compared to vehicle (Figure 3.12), however, both verapamil and sunitinib groups came close to significant decreases. Assessment of CaMKII activity by the radioactive assay showed similar results to the expression of pThr286-CaMKII (Figure 3.13). Overall there were no significant changes in CaMKII activity, however, there was a close to significant decrease in CaMKII activity in the sunitinib group and the decrease in CaMKII activity in the verapamil group was very close to significance.

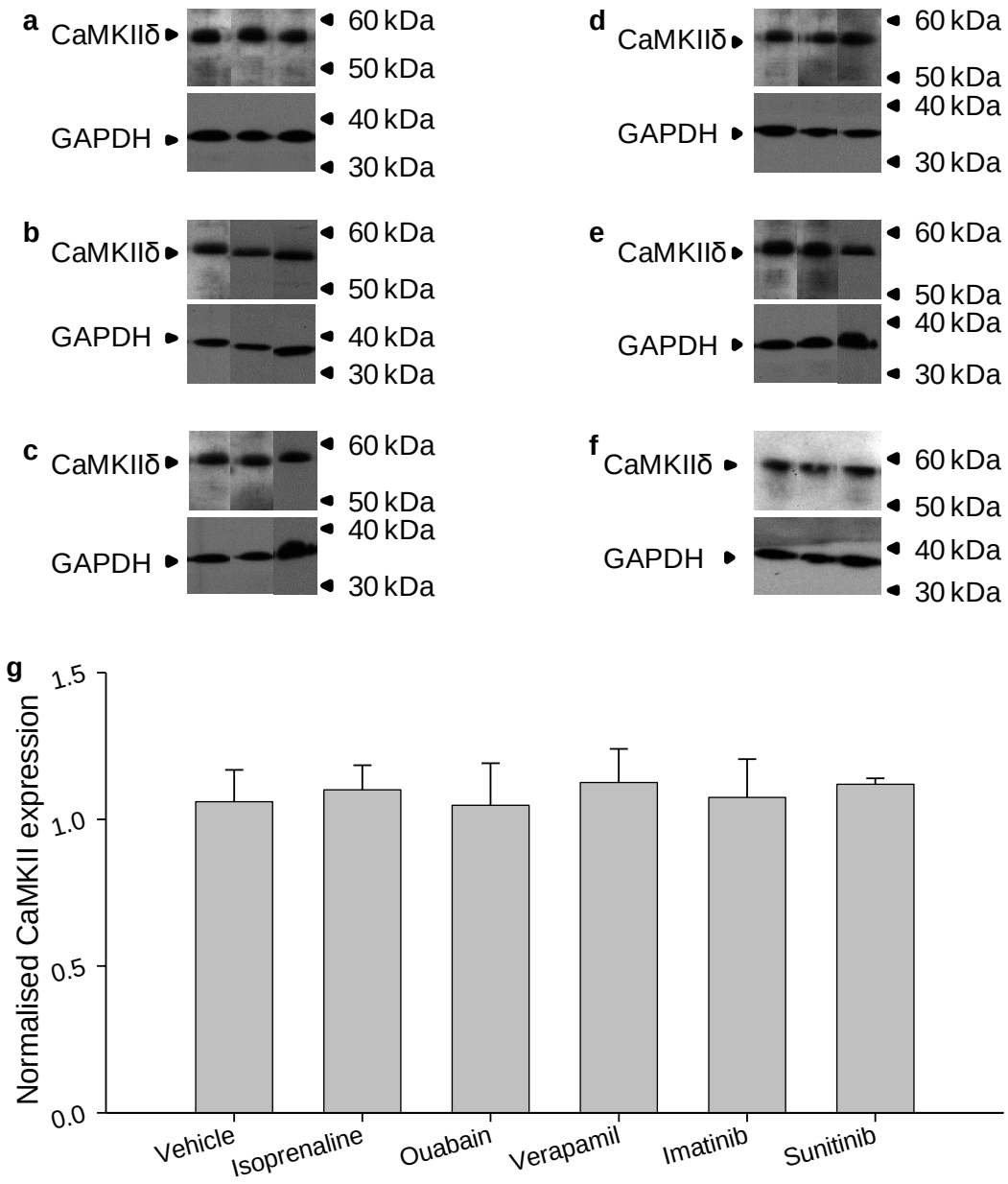

Figure 3.11 CaMKIIδ expression following acute *in vivo* drug administration. Representative blots in triplicate following administration of **a)** vehicle, **b)** isoprenaline, **c)** ouabain, **d)** verapamil, **e)** imatinib, **f)** sunitinib. Pooled data for each treatment are shown in **g)**. Data are presented as mean ± S.E.M values. Vehicle n = 6, isoprenaline n = 5, ouabain n = 6, verapamil n = 5, imatinib n = 4, sunitinib n = 4. There were no significant differences in any treatment group compared to vehicle, Kruskal-Wallis test.

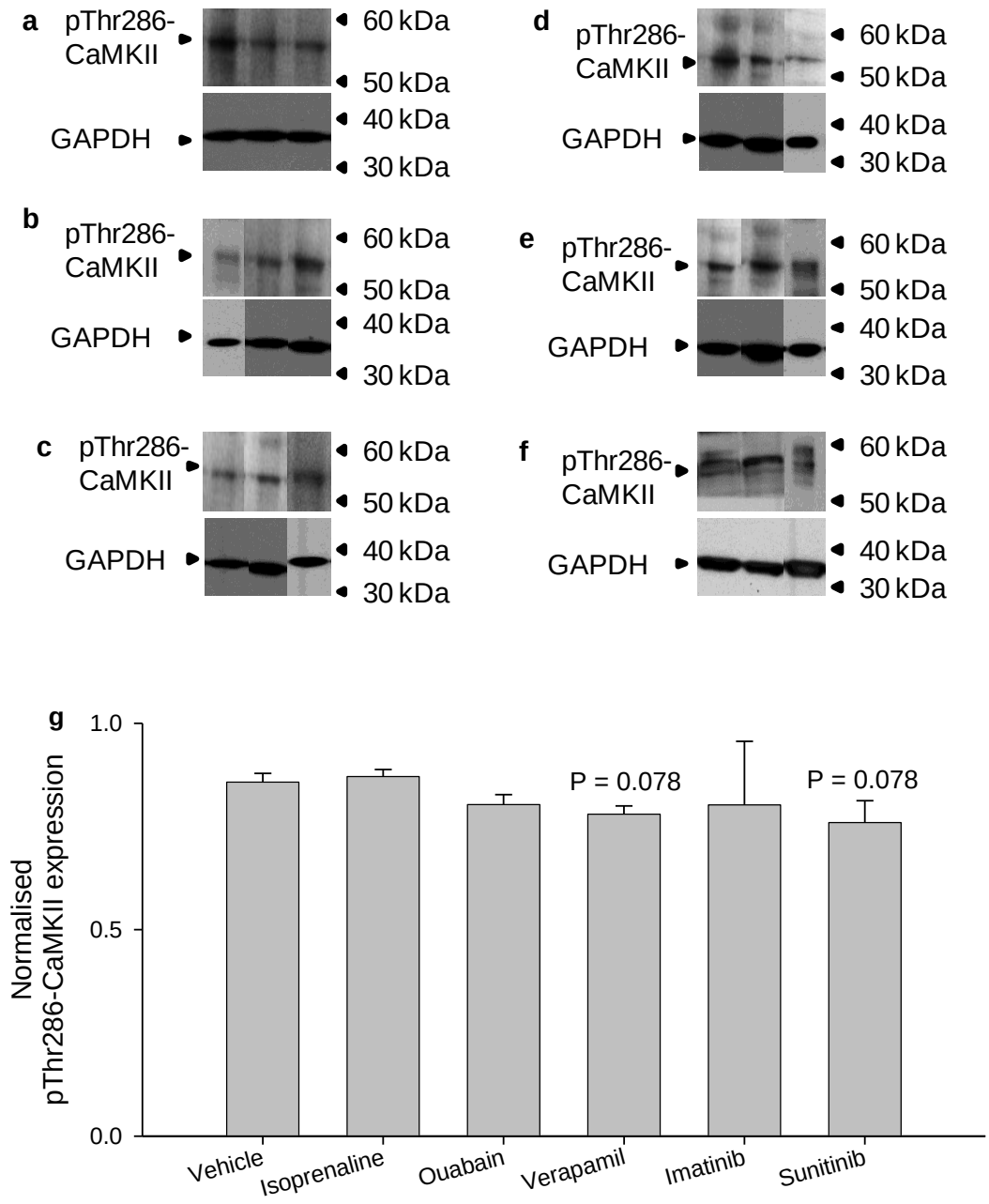

Figure 3.12 CaMKII activity assessed via pThr286-CaMKII expression following acute *in vivo* drug administration. Representative blots in triplicate following administration of **a)** vehicle, **b)** isoprenaline, **c)** ouabain, **d)** verapamil, **e)** imatinib, **f)** sunitinib. Pooled data for each treatment are shown in **g)**. Data are presented as mean ± S.E.M values. Vehicle n = 6, isoprenaline n = 5, ouabain n = 6, verapamil n = 5, imatinib n = 4, sunitinib n = 4. There were no significant differences in any treatment group compared to vehicle, Kruskal-Wallis test.

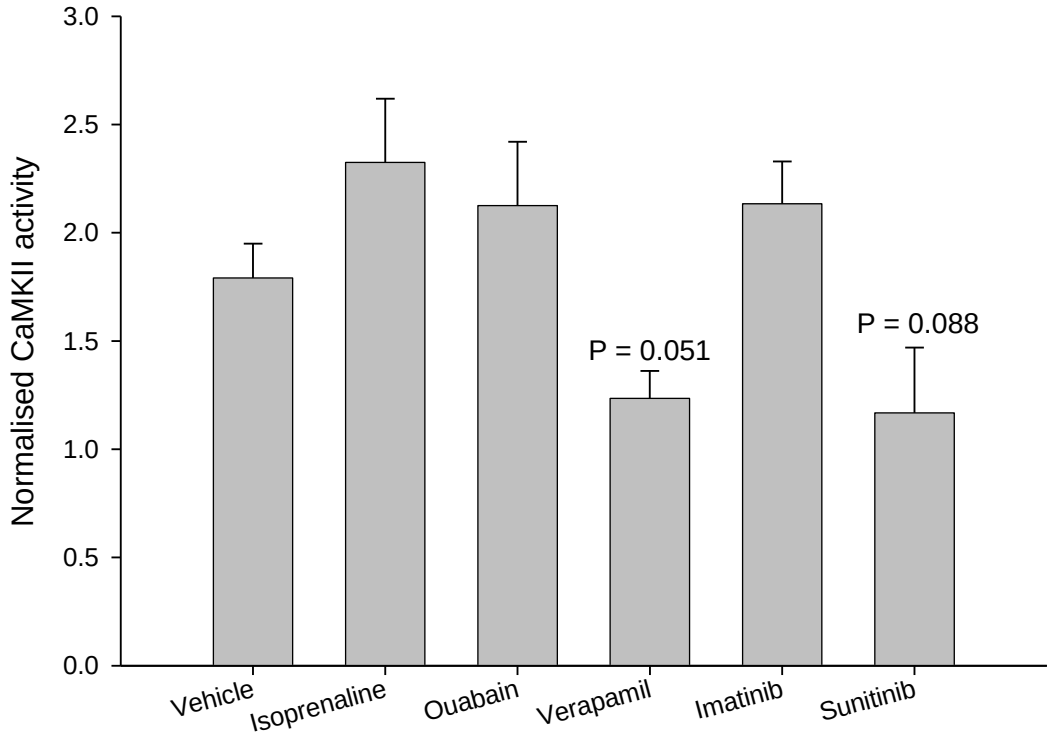

Figure 3.13 CaMKII activity assessed via the radioactive assay following acute *in vivo* drug administration. Data are presented as mean ± S.E.M values. Vehicle n = 6, isoprenaline n = 5, ouabain n = 6, verapamil n = 5, imatinib n = 4, sunitinib n = 4. There were no significant differences in any treatment group compared to vehicle, Kruskal-Wallis test.

3.4 Discussion

3.4.1 Main findings

This work demonstrates that the “custom CaMKIIδ” antibody provided the best detection of CaMKIIδ in guinea pig LV homogenates following a screen of several commercially available CaMKIIδ antibodies and one other custom-made CaMKIIδ antibody from the Bers Laboratory. Suitable total protein loads for quantification were determined as 6 µg and 10 µg for CaMKIIδ and pThr286-CaMKII detection, respectively. The CaMKII activity assay showed significant detection of CaMKII activity in guinea pig LV homogenates and the assay was sensitive to both increases and decreases in CaMKII activity.

Using these methods CaMKII activity and expression were assessed in LV homogenates from guinea pigs following acute *in vivo* drug administration. Compared to vehicle treatment, CaMKII expression was not altered by acute administration of isoprenaline, ouabain, verapamil, imatinib, or sunitinib. CaMKII activity, assessed by both pThr286-CaMKII immunoblotting and the CaMKII activity assay, was also not significantly altered by any drug treatment although both approaches indicated that acute verapamil and sunitinib treatments tended to decrease CaMKII activity.

3.4.1.1 Characterisation of CaMKII expression and activity in guinea pig

For detection of CaMKIIδ expression in guinea pig LV homogenates the “custom CaMKIIδ” antibody was the antibody of choice. The "Abgent CaMKIIδ” antibody (Figure 3.1) failed to detect CaMKIIδ in rat, guinea pig and dog tissue. When rabbit protein was included as a positive control, CaMKIIδ expression increased dependent upon the amount of total protein. This highlights the selectivity of this antibody for rabbit CaMKIIδ. Recombinant CaMKIIδ protein was also detected by this antibody. The “R&D CaMKIIδ” antibody (Figure 3.2) failed to convincingly detect CaMKIIδ in guinea pig and rat LV homogenates. Although recombinant CaMKIIδ protein was included as a positive control in this experiment it also was not detected well. The “Abgent CaMKIIδ-like” antibody (Figure 3.3) showed faint CaMKIIδ expression in guinea pig LV homogenates, reasonable detection in rat and recombinant CaMKIIδ, and strong detection in dog and rabbit LV homogenates. In all species, again CaMKIIδ expression increased with increasing amounts of total protein.

Commercial antibodies are usually tested by the company for species reactivity. For CaMKIIδ antibodies it would seem that human, mouse and rat are commonly tested, rabbit and dog less commonly and guinea pig very rarely, if at all. For the antibodies used here, guinea pig was not listed as a tested species so there was no indication as to whether CaMKIIδ detection should be expected. CaMKIIδ expression is also not commonly examined in guinea pigs and so reports of this species in the literature are sparse. There is, however, 99% homology between human, rat, rabbit and mouse CaMKIIδ so guinea pig may also be expected to show high homology although such information could not be located perhaps suggesting that this has not been investigated.

Before purchasing our own custom-made CaMKIIδ antibody directed against the C-terminus of the protein, a similar custom-made CaMKIIδ antibody (directed against the same sequence) from the Bers Laboratory was tested. This had been used previously in mouse (Huke *et al.*, 2011). Unfortunately only a very faint signal in dog and a very slightly stronger signal in mouse were detected. In guinea pig and rat, however, higher total protein loads gave fairly clear signals (Figure 3.4). The difference in signal quality between our laboratory and the Bers Laboratory may be due to slight differences in protocol/equipment (NuPAGE® vs BioRad systems), mouse strain (C57BL/6 vs Black Swiss), or tissue preparation (cardiomyocytes lysates vs LV homogenates). It may also be due to the sensitivity of the antibody depending on rabbit responses to the antigen or possible freeze/thawing of the antibody during transit.

As well as antibody suitability for the particular species and tissue preparation, protein detection by antibodies can be affected by blotting conditions (e.g. buffers) and so it is possible that by modifying certain aspects of our protocol we may have achieved better detection using the commercial or Bers Laboratory antibodies. However, the protocols used here have been used in our laboratory and by others across a range of immunoblotting experiments assessing a range of proteins expressed in the heart. Furthermore, signals that may have been able to be manipulated to improve the intensity (i.e. by adjusting experimental conditions) already required high amounts of total protein loads (>20 µg) suggesting that the sensitivity of the antibody in guinea LV homogenate was low.

As previously mentioned, our custom-made antibody was designed to target an amino acid sequence at the C terminus of CaMKIIδ (unique to the δ isoform) and

using this antibody strong and clear detection of CaMKIIδ in guinea pig, dog and mouse LV homogenates was achieved (Figure 3.5). In assessing a range of total protein loads sufficient signals from 6 µg total protein were obtained allowing smaller amounts of total protein to be used (Figure 3.6). In testing this antibody the protocol was changed to use a TBS based protocol following recommendations from a nearby laboratory. These buffers are commonly used throughout various laboratories and are quicker and easier to prepare than the buffers used by us previously. Together with the "custom CaMKIIδ" antibody this approach provided by far the best detection of CaMKIIδ.

From this work it appears that CaMKIIδ expression levels in guinea pig are similar to those in rat and possibly dog and rabbit. However, as we did not simultaneously assess the expression of GAPDH (a 'housekeeping' protein which is often stably and constitutively expressed at high levels) in these experiments, apparent differences/similarities between species cannot be verified as there is not a 'loading control' to ensure that total protein loads were equal for each sample.

In choosing a protein for normalisation within gels (e.g. GAPDH) it is important that this is stably expressed throughout all samples, i.e. it is not affected by experimental interventions. Although drug-induced changes in GAPDH expression were not formally assessed here, it is not believed that GAPDH expression would be altered under these conditions as it has been reported to remain stable when examined in a model of coronary artery ligation induced LV dysfunction (Currie *et al.*, 2005). Furthermore, GAPDH is widely used for normalisation in studies of CaMKIIδ expression (e.g. Hoch *et al.*, 1999; Passier *et al.*, 2000; Colomer, 2002; Zhang *et al.*, 2003; Kohlhaas *et al.*, 2006).

The CaMKII activity assay showed concentration dependent increases in [^{32}P] counts for both recombinant CaMKII protein and LV guinea pig homogenates (Figure 3.7 to Figure 3.8). The fold differences seemed to be close to the fold difference in protein concentration suggesting some degree of linearity between the amount of total protein and the measured radioactivity. Using both recombinant CaMKII protein and guinea pig LV homogenates, control samples excluding either substrate, Ca^{2+} or CaMKII resulted in greatly decreased [^{32}P] counts and therefore CaMKII activity. Note that CaMKII activity is not able to be calculated in samples where CaMKII protein was excluded. Across all experiments including controls, the control excluding Ca^{2+} (using Assay dilution buffer 1, Section 3.2.1) seemed to have

higher counts/activity than the other controls. It is possible that this is due to a level of autophosphorylation allowing a low level of CaMKII activation in the absence of Ca^{2+}.

To ensure that the CaMKII assay was sensitive to decreases as well as increases in CaMKII activity, guinea pig LV homogenate samples were pre-treated with AIP (Figure 3.9). AIP is a non-phosphorylatable analog of the CaMKII peptide substrate, autocamtide-2, which specifically and potently inhibits CaMKII by competing with autocamide-2. Increasing concentrations of AIP caused corresponding reductions in CaMKII activity indicating that the assay is suitable for detection of decreases in CaMKII activity. The assay also indicated that CaMKII activity levels in untreated LV homogenates from guinea pig are similar to dog, but higher than mouse (Figure 3.10).

3.4.1.2 Effects of acute in vivo drug administration on CaMKII expression and activity

CaMKIIδ plays a central role in normal cardiac Ca^{2+} handling and contractility. Importantly, it is also a recognised molecular switch triggering abnormal Ca^{2+} handling and contractile dysfunction in cardiomyopathy. CaMKIIδ may therefore be an important intracellular target for drugs that alter cardiac performance. In order to investigate this, tissue from drug-treated guinea pigs in Chapter 2 was assessed for corresponding changes in CaMKII expression and/or activity using the methods established above.

Isoprenaline

Isoprenaline, by stimulation of the β_1-adrenoceptor, has been shown in several reports to increase CaMKII expression and activity (see Grimm & Brown, 2010 for review). Activation of CaMKII following β_1-adrenoceptor stimulation resulted from PKA-dependent increases in $[Ca^{2+}]_i$ (Kuschel *et al.*, 1999; Said *et al.*, 2002; Ferrero *et al.*, 2007). PKA-independent mechanisms of activation have also been proposed via a guanine nucleotide exchange protein directly activated by cAMP (Epac) (Oestreich *et al.*, 2007, 2009; Pereira *et al.*, 2007; Métrich *et al.*, 2008).

In the current study no changes in CaMKII expression were found (Figure 3.11) which is not surprising as such an acute level of stimulation (3 cumulative doses infused i.v. for 15 min each dose) is unlikely to induce changes in expression of any protein as the events leading to this (transcription and translation) occur over a

longer period of time. There were also no significant changes in CaMKII activity (Figure 3.12 to Figure 3.13). Again this might be due to the time scale of the acute drug administration. Wang *et al.* (2004) chronically stimulated β_1-adrenoceptor of adult cardiomyocytes for 24 h and demonstrated that contraction amplitude was enhanced to the same extent as acute β_1-adrenoceptor stimulation. The major difference was, however, that acute effects were mediated via PKA whereas chronic effects were mediated by via CaMKII. Therefore, the duration of β_1-adrenoceptor stimulation in the experiments presented here may not have been sufficient to activate CaMKII leaving PKA largely responsible for the induced increases in contractility.

Ouabain

Ouabain as described in Section 2.4.1.4 leads to an overall increase in $[Ca^{2+}]_i$ (Rang *et al.*, 2003) which may, as suggested in Section 3.1, lead to activation of CaMKII. In the current experiments CaMKIIδ expression was not altered (Figure 3.11) and there was no evidence of increased CaMKII activity (Figure 3.12 to Figure 3.13) following acute *in vivo* administration of ouabain. Recent studies investigating ouabain-induced apoptosis (Sapia *et al.*, 2010) and arrhythmias (Gonano *et al.*, 2011) have both implicated a role for CaMKII in these effects suggesting that ouabain increases CaMKII activation. However, the former study chronically stimulated cardiomyocytes and so again it may be that the acute stimulation in the present study was not sufficient to activate CaMKII. Additionally, the latter study used a concentration of ouabain that caused arrhythmogenic activity in cardiomyocytes. As definitive plasma concentrations of ouabain were not obtainable in the study here and the Gonano *et al*. (2011) study used rat cardiomyocytes, which show greatly reduced sensitivity to cardiac glycosides (Repke *et al.*, 1965; Akera *et al.*, 1979; Koomen *et al.*, 1984; Weinhouse *et al.*, 1989; Koga *et al.*, 1989), direct comparison of dose/concentration and response is difficult. However, such adverse effects were avoided in the present study by limiting the dose of ouabain so perhaps the dosing protocol was not sufficient for CaMKII activation.

Verapamil

In contrast to the effects of ouabain, verapamil results in an overall decrease in $[Ca^{2+}]_i$ (Rang *et al.*, 2003). As Ca^{2+} entry through the L-type Ca^{2+} channel activates

CaMKII (Bodi *et al.*, 2005), blockade of this route of Ca^{2+} entry would be expected to decrease CaMKII.

In this study verapamil treatment did not alter CaMKIIδ expression (Figure 3.11). No significant effects were found on CaMKII activity assessed by both immunoblotting for pThr286-CaMKII (Figure 3.12) and by the radioactive assay (Figure 3.13). Both methods, however, suggested small reductions in CaMKII activity which came close to significance. Verapamil and nifedipine (also a Ca^{2+} channel blocker) have both been shown to decrease CaMKII activity assessed via the CaMKII phosphorylation site (Thr17) of phospholamban (Kuschel *et al.*, 1999). The concentration of verapamil used in this study (1 μmol L^{-1}) was similar to the free plasma concentration determined in the current study (1.52 ± 0.55 μM, Table 2.2) suggesting that the dose used here would be sufficient to achieve similar effects.

Cardiotoxic drugs (imatinib and sunitinib)

As alluded to earlier, alteration of CaMKII expression and/or activity may be related to the cardiotoxic effects of imatinib and sunitinib. In this study CaMKIIδ expression was not altered following imatinib or sunitinib administration *in vivo* (Figure 3.11). With imatinib treatment CaMKII activity was also not altered, however, sunitinib treatment, although not reaching significance, tended to decrease CaMKII activity (Figure 3.12 to Figure 3.13).

In Chapter 2, imatinib did not produce significant effects on cardiac contractility whereas sunitinib had more pronounced effects significantly decreasing contractility (via $LVdP/dt_{max}$). Therefore, the findings here may suggest that the differing effects on contractility are due to differing actions on CaMKII.

In an evaluation of kinase selectivity using a panel of 242 kinases, sunitinib was shown to potently inhibit CaMKIIδ (IC_{50} = 20 nM) supporting the results indicated in our study (Kumar *et al.*, 2009). Imatinib was not tested in this study, however, another study (Si & Collins, 2008) reporting CaMKIIγ as a critical regulator of signalling networks regulating proliferation of myeloid leukaemia cells implies that imatinib inhibition of the BCR-ABL oncogene leads to inhibition of CaMKIIγ. The concentration of imatinib used in this study (5 μM) was similar to the determined free plasma concentration in the present study (4.15 ± 0.94 μM, Table 2.2), however, it cannot be assumed that a similar consequence would occur for the δ isoform of CaMKII. Furthermore, if, as Si & Collins (2008) seem to imply, CaMKII inhibition is

via BCR-ABL rather than a direct action of imatinib on CaMKII, the oncogene must be expressed in the heart before any action on CaMKII could occur.

Again the point must be raised here, as before, that acute drug treatment methods may not bear relevance to the clinical situation where imatinib and sunitinib are given over much longer periods of time. Therefore any observed consequence - action, inaction or otherwise - for CaMKII may be quite different on largely extended timescales.

3.4.1.3 Correlation of changes in cardiac contractility and CaMKII activity and/or expression

Due to the lack of (significant) effects on CaMKII it is difficult to assess whether changes in cardiac contractility following acute *in vivo* drug treatment can be related to the level of CaMKII expression and/or activity. It may be that CaMKII is either not involved in the effects of these drugs or CaMKII involvement occurs over a longer period of time of drug treatment.

Apparent changes in CaMKII activity appeared more pronounced using the CaMKII activity assay compared to pThr286-CaMKII immunoblotting suggesting that this method may be more sensitive for detecting changes in CaMKII activity in guinea pig LV homogenates. Looking at the results of the CaMKII activity assay alone, although no significant effects were reached, mean CaMKII activities for the positive inotropes (isoprenaline and ouabain) tend to be slightly higher than the mean CaMKII activity in the vehicle group, whereas the negative inotropes (verapamil and sunitinib) tend to show reduced CaMKII activities than the vehicle group suggesting that with further investigation a correlation may exist.

3.4.2 Limitations

The lack of significant effects in this study may be related to the low n numbers. As LV tissue was taken from *in vivo* drug-treated animals the number of samples available for CaMKII assessment was limited by the number of animals used in the *in vivo* phase of the study (Chapter 2). As explained in Section 2.4.2 animal numbers were kept as low as possible to abide by UK legislation. Drugs were administered to all guinea pigs whether or not it was possible to insert a catheter into the LV to measure LVP, and this “extra” tissue was used in CaMKII analysis.

As outlined throughout, another reason why expected significant effects were not found may be related to the duration of treatment. Although reasonable plasma concentrations of drugs were achieved, this was over a relatively short period of time (45 min). Chronic drug administration may produce different results, either as a consequence of drug accumulation or because of adaptive responses to persistent drug action. For example, it is well known that chronic administration of β-adrenoceptor agonists causes receptor down-regulation and a change in the agonist induced-response (Harden, 1983).

3.4.3 Conclusions

The work presented in this Chapter has shown that immunoblotting techniques have been optimised to detect CaMKIIδ and pThr286-CaMKII expression in LV homogenates from guinea pig. Additionally, a radioactive assay has also been optimised to measure CaMKII activity. Using these techniques CaMKII expression and activity were assessed in guinea pig LV homogenates from acute *in vivo* drug-treated animals. CaMKIIδ protein expression was similar across treatment groups. CaMKII autophosphorylation was not shown to be altered in any treatment group when pThr286-CaMKII protein expression was assessed and CaMKII activity, assessed by a radioactive assay, was not significantly altered throughout groups although verapamil and sunitinib treatments tended to decrease CaMKII activity.

Following acute drug treatments, therefore, it was not possible to establish a correlation between *in vivo* drug effects on cardiac contractility and CaMKII activity and/or expression. It was therefore decided that these drugs would be assessed on a chronic treatment level to further assess whether drugs that exhibit effects on cardiac contractility *in vivo* may alter CaMKII activity and/or expression.

CHAPTER 4 FACTORS INFLUENCING INDICES OF CARDIAC CONTRACTILITY

4.1 Introduction

As shown in Chapter 2, $LVdP/dt_{max}$ (the maximum rate of rise of LVP) and the QA interval (the time interval from the onset of the Q wave of the ECG to the beginning of the upstroke of the following arterial blood pressure wave) are sensitive to changes in cardiac contractility and are therefore useful in assessing drug-induced effects on contractility. With changes in contractility $LVdP/dt_{max}$ and the QA interval should respond in opposite directions, i.e. with an increase in contractility $LVdP/dt_{max}$ increases whilst the QA interval decreases and *vice versa* with a decrease in contractility. Reports in the literature have indicated strong inverse correlations between $LVdP/dt_{max}$ and the QA interval (Adeyemi *et al.*, 2009; Norton *et al.*, 2009; Mooney *et al.*, 2012) supporting the work presented in Chapter 2 (Figure 2.14). However, these studies have tended to use only a few drugs with well established effects on contractility. In studies where larger numbers of drugs have been tested the relationship between $LVdP/dt_{max}$ and the QA interval has not always been consistent (Marks *et al.*, 2012; Johnson *et al.*, 2012).

In addition to studies advocating $LVdP/dt_{max}$ and the QA interval as indices of contractility there are several suggestions in the literature that, in addition to changes in inotropy, changes in cardiac loading and/or heart rate may also influence $LVdP/dt_{max}$ and/or the QA interval. Increases in preload (determined by LV end-diastolic volume; LVEDV) and afterload (determined by diastolic blood pressure) are well documented as increasing $LVdP/dt_{max}$ (Wallace *et al.*, 1963; Mahler *et al.*, 1975; Quinones *et al.*, 1976; Cambridge & Whiting, 1986). More recently a direct relationship between increases/decreases in heart rate and increases/decreases in $LVdP/dt_{max}$ have also been reported (Hamlin & Del Rio, 2012; Markert *et al.*, 2012). Importantly, none of these studies have been performed in guinea pig despite the suitability of this species for the assessment of cardiac contractility. Furthermore, no studies have directly investigated the influence of blood pressure and/or heart rate on the QA interval despite several additional factors that theoretically influence the QA interval being highlighted (Cambridge & Whiting, 1986; Hamlin & Del Rio, 2010).

According to Hamlin & Del Rio (2010) the QA interval depends upon:

- The time taken for Na^+ channels to open and Na^+ to enter the myocyte, and the speed of Ca^{2+} release from the SR and how rapidly it binds to troponin C. Slowing these processes would prolong the QA interval.

- Myocardial contractility - rate of cycling of heavy meromyosin heads. Greater contractility will shorten the isovolumetric time, thus shortening the QA interval.

- The pressure difference between LVEDP and the diastolic aortic pressure which determines the pressure that the LV must develop to open the aortic valve and begin ejecting blood into the aorta. The greater the pressure that the LV must develop, the greater the time will be, thus prolonging the QA interval.

- The distance of the arterial pressure sensor from the heart. The farther away from the LV the sensor is the longer the QA interval will be.

- The stiffness of the arterial tree (dependent on the degree of constriction of arterial smooth muscle) determines the velocity of propagation of the pulse wave down the arterial tree from the LV to the pressure sensor. The stiffer the arterial tree the shorter the QA interval.

- The systemic arterial pressure also determines the stiffness of the arterial tree. The higher the systemic arterial pressure, the stiffer the arterial tree thus shortening the QA interval as above.

To what extent changes in blood pressure and/or heart rate may affect $LVdP/dt_{max}$ and the QA interval in the anaesthetised guinea pig is currently unclear. Therefore it is plausible that instances where $LVdP/dt_{max}$ and QA interval are not well correlated and do not respond reciprocally, may be related to confounding effects of changes in blood pressure and/or heart rate. For greater understanding and interpretation of $LVdP/dt_{max}$ and the QA interval data in the anaesthetised guinea pig it is important to investigate these matters.

An alternative method, recognised as the 'gold standard' for assessing cardiac contractility is by measurement of pressure-volume (PV) loops. LV PV loops are obtained from the pressure and volume changes during each cardiac cycle and loops are generated by plotting LVP against LVV at multiple time points throughout a complete cardiac cycle (Figure 4.1a). The PV loop begins at point A when the mitral valve is open and blood enters the LV from the LA. This represents the filling phase of the PV loop when the volume of blood in the LV is increasing with little change in LVP and continues until point B. At point B the mitral valve closes and

this is the end-diastolic point. The ventricle then begins to contract isovolumetrically and LVP increases while the LVV remains constant. Once LVP exceeds the aortic diastolic pressure, the aortic valve opens (point C) and blood is expelled from the LV into the aorta. This is the ejection phase where LVV decreases as LVP increases to a peak value and then decreases as the ventricle begins to relax. The ejection phase ends at point D, the end-systolic point, with closure of the aortic valve and the ventricles relax isovolumetrically with a fall in LVP and a constant LVV. When the LVP falls below the LA pressure the mitral valve opens and the cycle is repeated.

In order to optimise the information gained from PV loops, a series of loops should be obtained at rest and as ventricular preload is reduced. Preload is reduced by transiently occluding the inferior vena cava (inferior vena caval occlusion, IVCO). The IVCO can be performed in animals by pulling on a suture placed around the vessel, by lifting the vessel with a small stick or compressing it with forceps. In some cases reasonable IVCOs can be obtained by compression of the vessel through the diaphragm. However, this requires considerable experience and may not be as reproducible as the other methods (Pacher *et al.*, 2008).

Once a series of PV loops is obtained there are several options to assess cardiac contractility. The end-systolic pressure-volume relationship (ESPVR) was originally proposed by Sagawa *et al.* (1977) and is constructed by fitting a line through the end-systolic points of several PV loops achieved during varying preload. The slope of this line is related to contractility - an increase in which would signify an increase in contractility. Sometime after this the preload recruitable stroke work (PRSW) defining the linear relationship between stroke work and the volume at end diastole (Ved) was reported (Glower *et al.*, 1985). Stroke work is defined as the work done by the ventricle to eject a volume of blood and is represented by the area of the PV loop. Again the slope of this relationship represents contractility with an increase in the slope signifying an increase in contractility and *vice versa*. $LVdP/dt_{max}$ can still be achieved from PV loop measurement and with the additional measurement of Ved, $LVdP/dt_{max}/Ved$ can be calculated which has also been shown to be sensitive to changes in contractility (Little, 1985).

To measure and construct PV loops, traditionally, conductance technologies have been used (Baan *et al.*, 1984; Georgakopoulos *et al.*, 1998; Feldman *et al.*, 2000; Yang *et al.*, 2001). Conductance technologies aim to measure the changing volume of blood in the LV during a cardiac cycle and display the value as a voltage signal.

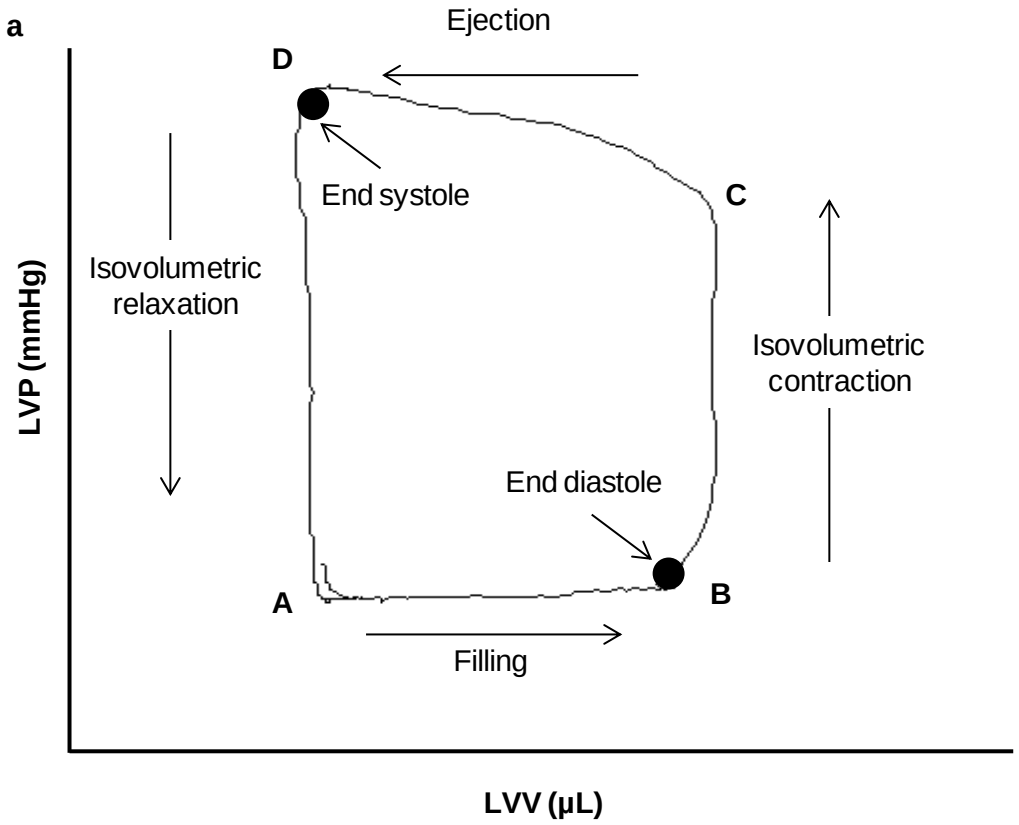

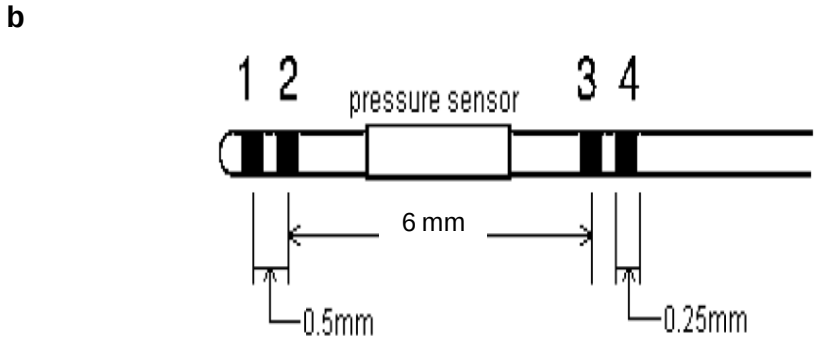

Figure 4.1 a) Example of a left ventricular (LV) pressure-volume loop, **b)** diagram of the tip of the PV catheter (adapted from Clark et al., 2009). The catheter has two pairs of rings that are spaced so that one set is located at the apex of the LV and the other set in located just inside the aortic valve. The outermost rings (1 and 4) supply the constant current (Iin) whilst the inner set of rings (2 and 3) measure the voltage across the LV (Vxb). The pressure sensor is located between the two sets of rings.

The technology is based on the basics of electrical relationships: Voltage (V) = Current (I) x Resistance (R). An electrical current is passed through the length of the LV long axis. Since blood has a resistive nature, the blood in the LV is modelled as a resistor spanning the length of the long axis. The volume of blood in the LV changes throughout each cardiac cycle and therefore the value of the blood resistance is represented as variable resistance (Rxb). The current flow through the blood (Iin) is kept constant. The changing volume of blood in the LV throughout each cardiac cycle is measured as a variable voltage (Vxb) which is sinusoidal and will have the same frequency as the heartbeat. The catheter supplies the electrical current and measures the resulting voltage. The catheter has two pairs of rings that are spaced so that one set is located at the apex of the LV and the other set in located just inside the aortic valve (Figure 4.1b). The outermost rings (distal and proximal ends of catheter) supply the constant current (Iin) whilst the inner set of rings measure the voltage across the LV (Vxb). The pressure sensor is located between the two sets of rings.

However, the methods above make some assumptions that must be corrected for:

The first assumption is that the resistive value of blood is linear with volume. This is based upon: i) the volume of blood is modelled as having a uniform diameter; ii) the electrical field generated by the current is uniform along the axis and volume of the LV. Since neither of these is actually true, the volume to voltage relationship is inaccurate. To correct for these assumptions “conductance” is used rather than “resistance”. Conductance is the inverse of resistance (1/resistance). The relationship between the conductance values and increasing blood volume is linear.

To convert conductance measurements to volume values the following equation proposed by Baan *et al.* (1984) is used: $LVV = 1/\alpha\ (\rho L^2)\ (G_{meas}-G_p)$

α = volume calibration factor, ρ = blood resistivity, L = distance between voltage sensing electrodes of catheter, G_{meas} = measured conductance, G_p = parallel conductance of muscle (see below).

The value α is a volume calibration factor known as the Field Correction Factor alpha. This compensates for the non-uniform diameter of the LV and the electrical field. It is a constant dependent on the stoke volume although Baan *et al.* (1984) assumed it to be 1.

The second assumption is that the electrical field generated by the catheter is contained within the LV and as such the voltage represents the volume of blood in the LV. However, this is not the case as the electrical field will enter both blood and tissue (cardiac muscle) in its path. The conductance signal measured by the catheter rings is, therefore, the sum of conductance values for the LV blood pool (Gb) and the surrounding muscle resulting in an overestimation of blood volume in the LV. The current flow through the muscle is termed "parallel conductance" (Gp) and needs to be subtracted from the conductance signal to obtain an accurate value of LV volume. To separate the blood conductance from the parallel conductance, the saline bolus dilution method is used (Baan *et al.*, 1984). This involves injecting a small bolus of 10% hypertonic saline solution into the bloodstream that washes into the LV without affecting LVP or LVV. The volume of the saline bolus should equate to the stroke volume of the heart which is dependent on animal size. Injecting this solution will change the resistive value of the blood (but not the muscle) which is seen as an offset in the volume signal. Commercially available software packages then solve a system of linear equations and correct for the parallel conductance leaving only the blood component.

The above method of correction calculates the parallel conductance as a constant. However, the parallel conductance is not constant and is time-dependent. This is because the muscle component varies throughout the cardiac cycle as the LV contracts and fills and because the distance from the catheter to the muscle changes. The method also models both blood and cardiac muscle as resistive components only and ignores the capacitive properties of cardiac muscle. Furthermore, the procedures necessary to determine the parallel conductance are extremely user-dependent and often increase the variability and introduce further errors in the measurements (Nielsen *et al.*, 2007).

The Scisense ADVantage™ system addresses these shortcomings. To address the inaccuracies associated with determining the parallel conductance, the ADVantage™ system uses "admittance" technology which measures both the conductive and capacitive properties of blood and cardiac muscle. The "magnitude" of admittance is equivalent to the traditional conductance measurement. However, the basis of measuring admittance instead of conductance is that at frequency ranges of about 20 kHz, blood is purely resistive and has no measurable capacitance, but muscle has both capacitance and resistance properties.

Therefore, the capacitive nature of cardiac muscle is used to identify its contribution to the combined conductance signal. This is based on the electrical principle that an AC signal in a circuit with capacitance will exhibit a phase shift at the output when compared to the original input signal (Figure 4.2). By tracking this "phase angle" in real-time and mathematically relating it to the resistance of the cardiac muscle, the ADVantage™ system allows continuous, non-invasive tracking of parallel conductance throughout the heartbeat. The magnitude and phase angle of the measured admittance are, therefore, used to determine PV loops inside the LV on a beat-to-beat basis (Raghavan *et al.*, 2004; Porterfield *et al.*, 2009).

The ADVantage™ system also employs an improved conductance-to-volume conversion equation (see Scisense, 2009 for detailed equations). Wei's equation replaces the Field Correction Factor alpha to correct for the non-uniform nature of the catheter electrical field distribution. Wei's equation assumes a non-linear relationship between conductance and volume thus improving the accuracy of volume calculation over a wider range (Porterfield *et al.*, 2009).

The ADVantage™ system has an onboard digital microprocessor that collates all of the above information to provide true ventricular blood volume. The approach of the system is said to offer substantial improvements in PV loop measurement (Raghavan *et al.*, 2004).

Whilst measurement of PV loops via conductance and admittance methods is well established and frequently used *in vivo* in mice (Georgakopoulos *et al.*, 1998; Feldman *et al.*, 2000; Yang *et al.*, 2001; Clark *et al.*, 2009), rat (Pacher *et al.*, 2008; Foote & Loughrey, 2010), and human (Baan *et al.*, 1984; Feneley *et al.*, 1992), this technique has rarely been explored *in vivo* in guinea pigs and there is a scarcity of published literature in this species.

On the version of the ADVantage™ system used in this study the primary recording method was the W method which relies on the principles outlined above. However, a second method of recording was also available, termed the D method. This method uses a novel calculation algorithm that does not depend on quantifying muscle incursion and then subtracting it, i.e. the phase signal is not required for volume calculation (for further description see Scisense, 2009 and Appendix C). Although the D mode has been tested extensively in-house by Scisense, studies with this method have not been published. In the current study the W method

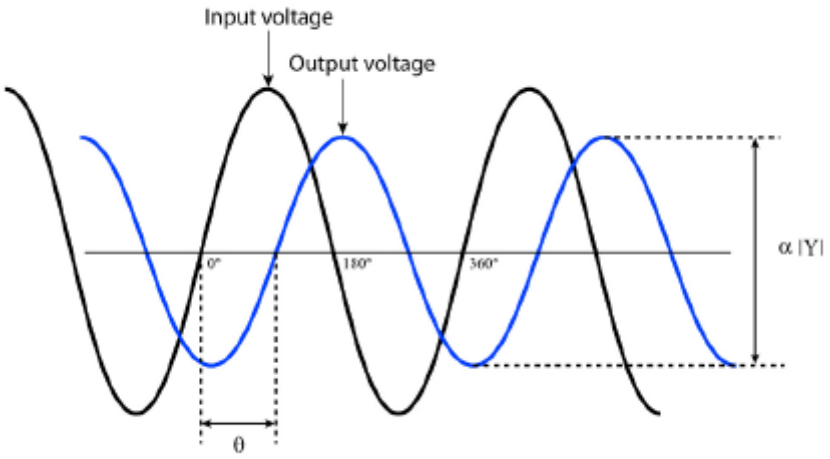

Figure 4.2 The Output voltage shows a “delay” compared to the Input voltage signal used to generate the electric field. The signal delay, caused by myocardial capacitance, is measured in terms of degrees and is referred to as “Phase angle”. Taken from Scisense, 2009.

was tried initially, however, the D method produced much better recordings and was subsequently the recording method of choice.

4.1.1 Aims

To test the hypothesis that $LVdP/dt_{max}$ and the QA interval may be influenced by changes in heart rate and/or blood pressure the aims of the work presented in this Chapter were:

(i) To analyse data from the AstraZeneca cardiovascular database to identify the response of $LVdP/dt_{max}$ and the QA interval following compound administration and to determine if significant changes in other haemodynamic parameters accompanied any inconsistent responses.

(ii) To assess the effects of blood pressure and heart rate on $LVdP/dt_{max}$ and the QA interval.

(iii) To assess the feasibility of PV loop measurement in the anesthetised guinea pig using the Scisense ADVantage™ system.

4.2 Methods

Suppliers of equipment and materials are detailed in Appendix A. Suppliers of drugs and reagents and their storage information are detailed in Appendix B.

4.2.1 AstraZeneca database analysis

Guinea pig cardiovascular data held in the AstraZeneca Safety Pharmacology database were analysed to identify the effects (increase, decrease or null) on LVdP/dt_{max} and the QA interval following administration of 45 compounds. Compounds were grouped according to the response of each index. Inconsistent responses were classed as those where LVdP/dt_{max} and the QA interval did not respond reciprocally – e.g. where one index was altered but the other was not or where the changes in both indices were in the same direction. The most commonly occurring inconsistencies were identified and the data for these compounds were analysed to identify effects on other parameters (heart rate, arterial blood pressure and LVP).

4.2.2 Animals

All animal experiments were performed in accordance with the UK Animals (Scientific Procedures) Act 1986, approved by institutional ethical review committees and conducted under the authority of Project Licences held at AstraZeneca. Eighteen male Dunkin Hartley guinea pigs weighing 510 – 650 g were allowed a minimum of one week acclimatisation following arrival and were housed in small groups, on aspen chip bedding and sizzle nest. Rooms were held at temperatures between 16 and 23°C, with 40 to 70% relative humidity and a 12 hour light/dark cycle. Food (Teklad global higher fibre guinea pig diet 2041, plus fresh fruit and vegetables) and water were available ad libitum.

4.2.3 Surgical preparation

In all experiments anaesthesia was induced using fentanyl and sodium pentobarbital as described in Section 2.2.2.2. Guinea pigs were ventilated as described in Section 2.2.3.2.

4.2.3.1 Blood pressure and heart rate experiments

In blood pressure experiments guinea pigs were surgically prepared as detailed in Section 2.2.3.2. In heart rate experiments an additional thoracotomy was performed. Guinea pigs were positioned on their left side and an incision made at

the level of the heart on the right side. Cutaneous and subcutaneous tissues were cleared until the ribs were visible below. A puncture was then made in the fourth intercostal space and widened to allow a retractor to be inserted to spread the ribs. Once the heart was visible the pericardium was cleared and a pacing clip was attached to the right atrial appendage. A section of gauze moistened with saline was then placed over the wound opening and guinea pigs were returned to the supine position. The right vagus nerve was isolated alongside the carotid artery and stimulating electrodes attached.

4.2.3.2 PV loop experiments

In PV loop experiments guinea pigs were surgically prepared as in Section 2.2.3.2 except that the left carotid artery was not cannulated and ECG leads were not inserted. In initial PV loop experiments the catheter was inserted into the LV via the left carotid artery thus maintaining a closed-chest approach. A laparotomy was performed to access the IVC in the abdomen for later occlusions. To open the abdomen an incision was made over the xyphoid process and the abdominal wall was cut laterally exposing the liver. Attempts were made to locate the IVC in the abdomen just above the liver and below the diaphragm. In later experiments the chest was opened for insertion of the PV catheter. To open the chest an incision was made over the xyphoid process and the abdominal wall was cut laterally as before. The diaphragm was then cut from beneath to expose the apex of the heart. Before inserting the catheter into the heart, the IVC was isolated just above the diaphragm and a suture placed around the vessel. The pericardium was then removed from the heart and using a 23 G needle, a stab wound was made near the apex of the heart into the LV. The needle was then removed and replaced with the catheter which was advanced until the proximal electrode was just inside the ventricular wall.

The position of the catheter in the LV was initially indicated by an appropriate LVP signal. Pressure versus magnitude loops were then observed and the catheter was manipulated to maximise the width of these loops. The phase angle was also used to position the catheter within the LV with a low mean phase signal indicating a better position (i.e. closer to the centre of the LV).

In all experiments body temperature was monitored throughout via a thermometer in the rectum of the animal and maintained at ~37ºC via a heat blanket. All animals

were allowed to stabilise for at least 20 min before experiments were begun. At the end of the experiments animals were euthanised by overdose with i.v. sodium pentobarbital.

4.2.4 Data acquisition and analysis

In blood pressure and heart rate experiments, data were recorded using a Notocord HEM system. The lead II ECG and the pressure signals were recorded at rates of 1000Hz and 500 Hz, respectively. Heart rate was derived from the arterial blood pressure signal and recorded along with systolic, diastolic and mean arterial pressure. LVSP and LVEDP were recorded along with $LVdP/dt_{max}$ as an index of cardiac contractility. The QA interval was also recorded. At time points of interest, data were averaged over a 5 s interval.

In PV loop experiments the PV catheter was connected via an ADVantage™ PV System Control Box to the Notocord HEM system used to record data. The arterial blood pressure signal was recorded at a rate of 500 Hz and all signals from the ADVantage™ system were recorded at 1000 Hz.

4.2.5 Experimental protocols

4.2.5.1 Blood pressure experiments

The first group of experiments was designed to investigate the effects of changes in blood pressure on $LVdP/dt_{max}$ and the QA interval. Following stabilisation after surgical preparation, guinea pigs were given phenylephrine (4 and 14 nmol kg^{-1} min^{-1}), immediately followed by sodium nitroprusside (34 and 68 nmol kg^{-1} min^{-1}), n = 6, as continuous i.v. infusions with each dose being infused for 5 min. A recovery period of 10 min was allowed and then both the left and right vagus nerves were sectioned and a bolus i.v. dose of atenolol (1 mg kg^{-1}) was given followed by a further 10 min stabilisation period. After this the infusions of phenylephrine and sodium nitroprusside were repeated.

4.2.5.2 Heart rate experiments

A second group of experiments investigated the effects of heart rate on $LVdP/dt_{max}$ and the QA interval. Following stabilisation after surgical preparation, the heart rate of guinea pigs was increased via a bipolar pacing electrode attached to the right atrial appendage or decreased by stimulation of the right vagus nerve. The diastolic threshold for stimulation was determined by increasing the amplitude of stimulation

until there was one pulse per heart beat. Guinea pigs were then stimulated at twice this value. The pulse width duration during atrial pacing was 1 ms and during vagus stimulation it was 0.1 ms. Depending on the sinus rate of individual guinea pigs atrial pacing or vagus nerve stimulation was employed to achieve heart rates of approximately 175, 205, 235, 265, 295 and 325 beats min^{-1}. Heart rate was altered by changing the frequency of stimulation. Increases in heart rate (i.e. atrial pacing) were performed first, followed by decreases in heart rate (i.e. vagus nerve stimulation).

4.2.5.3 PV loop experiments

For PV loop experiments, stroke volume (SV) was independently determined from echocardiography data presented in Chapter 5. SV was calculated by the LV end-diastolic diameter^3 – LV end-systolic diameter^3. See Section 5.2.4 and Figure 5.1 for description of LV end-diastolic diameter and LV end-systolic diameter measurements. The mean value of 220 µL was input to the ADVantage™ system prior to experiments.

The surgical techniques required to insert the PV catheter into the LV were established first. Both open- and closed-chest approaches were tried to insert the catheter and locate and isolate the IVC. Signal quality was then optimised via catheter positioning and using both the W method and D method of recording. Following optimisation of surgery and recording signals, experiments were performed to assess the ability of the ADVantage™ system to detect changes in cardiac contractility. Isoprenaline and verapamil were administered to increase and decrease cardiac contractility, respectively. The doses used in Chapter 2 were tried initially: isoprenaline (0.1, 0.3 and 1.0 nmol kg^{-1} min^{-1}) and verapamil (14, 42 and 140 nmol kg^{-1} min^{-1}) infused for i.v. for 15 min each dose. However, the doses used for the analysed data were 0.3 nmol kg^{-1} min^{-1} for isoprenaline and 42 nmol kg^{-1} min^{-1} for verapamil.

During a period of recording data to be analysed the ventilator was switched off. After switching off, loops were allowed 1-2 sec to stabilise and, if required, an IVCO was performed. The ventilator was then switched back on immediately.

The IVC was occluded by swiftly pulling the suture placed around the vessel directly upwards and holding up for approximately 3 sec (observe loops moving in left and downward direction) before releasing. At least three IVCOs were performed before

beginning drug infusions to ensure that these were reproducible and that the arterial blood pressure, heart rate and PV loop position recovered to pre-occlusion states. Isoprenaline or verapamil were then infused for 1 min and 10 min, respectively. Post-drug IVCOs were performed immediately following the end of drug infusions.

4.2.6 Statistical analysis

Data are presented as mean ± S.E.M. The effects of increasing doses of individual drugs with time were assessed using a two-way ANOVA (paired ANOVA) followed by Dunnett's test. Paired *t* tests were used to compare values pre- and post-drug administration in PV loop studies. Statistical tests were performed using StatsDirect software.

4.2.7 Drugs

Suppliers and storage information are detailed in Appendix B. Details for fentanyl, sodium pentobarbital, isoprenaline and verapamil are as in Chapter 2. Phenylephrine (α_1-adrenoceptor agonist) and sodium nitroprusside (nitric oxide donor) were dissolved in 0.9% w/v NaCl.

Doses for phenylephrine and sodium nitroprusside were chosen in accordance with previous studies in guinea pigs (Mooney *et al.*, 2012) whilst isoprenaline and verapamil doses were chosen based upon the acute drug studies performed in Chapter 2.

4.3 Results

4.3.1 Observations from AstraZeneca database

Guinea pig cardiovascular data held in the AstraZeneca Safety Pharmacology database were analysed to identify the response of LVdP/dt_{max} and the QA interval following administration of 45 compounds. 40% of the compounds did not show reciprocal responses of LVdP/dt_{max} and the QA interval (i.e. increase LVdP/dt_{max} and decrease QA interval, or *vice versa*). The nature and frequency of occurrence of the inconsistencies between LVdP/dt_{max} and the QA interval responses are detailed in Table 4.1 expressed as a percentage of the compounds where reciprocal responses did not occur. The most common inconsistencies were: 1) a decrease in LVdP/dt_{max}

Table 4.1 Nature and frequency of occurrence of inconsistencies between LVdP/dt_{max} and the QA interval responses

LVdP/dt_{max}	**QA interval**	**Occurrence (%)**
Decrease	Decrease	6
Increase	No change	6
No change	Increase	5
Decrease	No change	39
No change	Decrease	44

LVdP/dt_{max}, left ventricular $dP/dt_{max.}$ Note that data are expressed as a percentage of the non-concordant data and not of the original dataset from 45 compounds.

with no change in the QA interval; and 2) no change in LVdP/dt_{max} with a decrease in QA interval.

Data for these cases were further analysed to identify concurrent changes in haemodynamics. In case (1) 71% of compounds also decreased heart rate, 57% decreased arterial blood pressure, 57% altered LVSP and 29% decreased LVEDP. In case (2) 75% of compounds also altered heart rate, 88% decreased arterial blood pressure, 63% decreased LVSP and 29% decreased LVEDP.

4.3.2 Effects of changes in blood pressure and heart rate on LVdP/dt_{max} and the QA interval

Concurrent changes in blood pressure and heart rate were noted frequently where LVdP/dt_{max} and QA interval responses were not reciprocal. Therefore, the effects of changes in blood pressure and heart rate on LVdP/dt_{max} and the QA interval were investigated in anaesthetised guinea pigs.

4.3.2.1 Effects of changes in blood pressure on LVdP/dt_{max} and the QA interval

To assess the effects of changes in blood pressure on LVdP/dt_{max} and the QA interval two doses of phenylephrine were administered to increase blood pressure. This was immediately followed by two doses of sodium nitroprusside to decrease blood pressure.

The lower dose of phenylephrine (4 nmol kg^{-1} min^{-1}) did not significantly alter arterial blood pressure, heart rate, LVP, LVdP/dt_{max} or the QA interval (Figure 4.3a-e). However, the higher dose of phenylephrine (14 nmol kg^{-1} min^{-1}) increased systolic, diastolic and mean arterial blood pressure, LVSP, LVdP/dt_{max} and the QA interval (Figure 4.3a, c, d and e) whilst heart rate remained stable (Figure 4.3b). LVEDP was also stable until near the end of the higher dose of phenylephrine when it was significantly increased (Figure 4.3c).

With infusion of sodium nitroprusside, systolic, diastolic and mean arterial blood pressure and LVSP sharply decreased (Figure 4.3a and c) falling only slightly further with the higher dose (68 nmol kg^{-1} min^{-1}). Both LVdP/dt_{max} and the QA interval also decreased and these effects were sustained throughout both doses (Figure 4.3d and e). Heart rate began to rise gradually with the lower dose of sodium nitroprusside (36 nmol kg^{-1} min^{-1}) becoming significantly increased during the higher dose (Figure 4.3b). LVEDP was unchanged (Figure 4.3c).

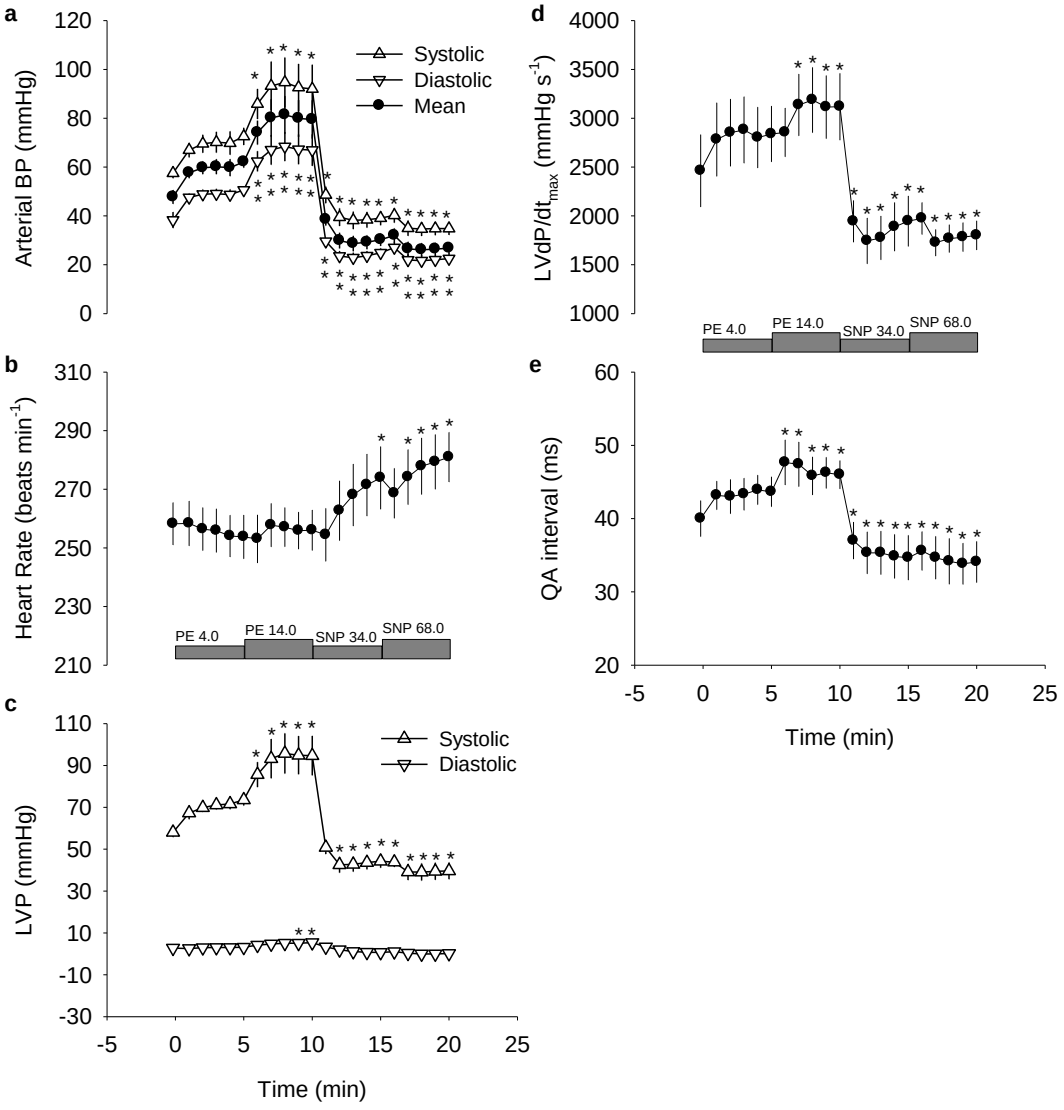

Figure 4.3 Effect of phenylephrine (PE) and sodium nitroprusside (SNP) on **a)** arterial blood pressure (BP), **b)** heart rate, **c)** left ventricular pressure (LVP), **d)** $LVdP/dt_{max}$ and, **e)** the QA interval. Experiments were performed with sympathetic and parasympathetic reflexes intact. The grey bars indicate drug infusions in nmol kg^{-1} min^{-1}. Mean ± S.E.M, n = 6. * indicates $P<0.05$ compared to value at time 0 min, two way ANOVA with Dunnett's test.

To eliminate any confounding heart rate effects resulting from activation of the baroreflex during alterations in blood pressure, these experiments were repeated with sympathetic and parasympathetic drives to the heart inhibited by sectioning the left and right vagus nerves and administering the β_1-adrenoceptor blocker atenolol. These interventions caused baseline heart rate to decrease significantly from 258 ± 7 to 206 ± 6 beats min^{-1} compared to the baseline heart rate in experiments with the vagus nerves intact and in the absence of atenolol ($P<0.05$, paired *t* test). $LVdP/dt_{max}$ also appeared slightly lower at 1961± 240 compared to 2462 ± 371 mmHg, whilst the QA interval appeared slightly higher at 45 ± 3 compared to 40 ± 2 ms, but neither of these apparent changes was statistically significant. Systolic, diastolic and mean arterial blood pressures and LVP were unchanged.

Sectioning the vagus nerves and administration of atenolol prevented the increase in heart rate during sodium nitroprusside infusions (Figure 4.4b). In general, effects on arterial blood pressure, LVP, $LVdP/dt_{max}$ and the QA interval followed similar profiles as experiments where reflex responses were intact (Figure 4.4a, c, d and e). However, increases in systolic, diastolic and mean blood pressure and LVSP reached statistical significance with the first dose of phenylephrine as did the increase in the QA interval. Additionally, the decrease in the QA interval with sodium nitroprusside was not sustained during the higher dose although values appeared to remain lower than the pre-drug value.

4.3.2.2 Effects of changes in heart rate on $LVdP/dt_{max}$ and the QA interval

To assess the effects of changes in heart rate on $LVdP/dt_{max}$ and the QA interval a combination of atrial pacing and vagus nerve stimulation was employed to increase and decrease heart rate, respectively, from sinus rate. This achieved a range of heart rates from 160 to 310 beats min^{-1} which were grouped into 30 beat min^{-1} intervals.

At heart rates <160 beats min^{-1} $LVdP/dt_{max}$ was lowest. This gradually increased as heart rate increased reaching a peak at heart rates between 220 and 249 beats min^{-1}. As heart rate further increased towards 310 beats min^{-1} $LVdP/dt_{max}$ began to fall gradually reaching a value similar to that at the lowest heart rates by >310 beats min^{-1} (Figure 4.5b). Systolic, diastolic and mean blood pressure and the QA interval fluctuated only slightly throughout the range of heart rates (Figure 4.5a and c).

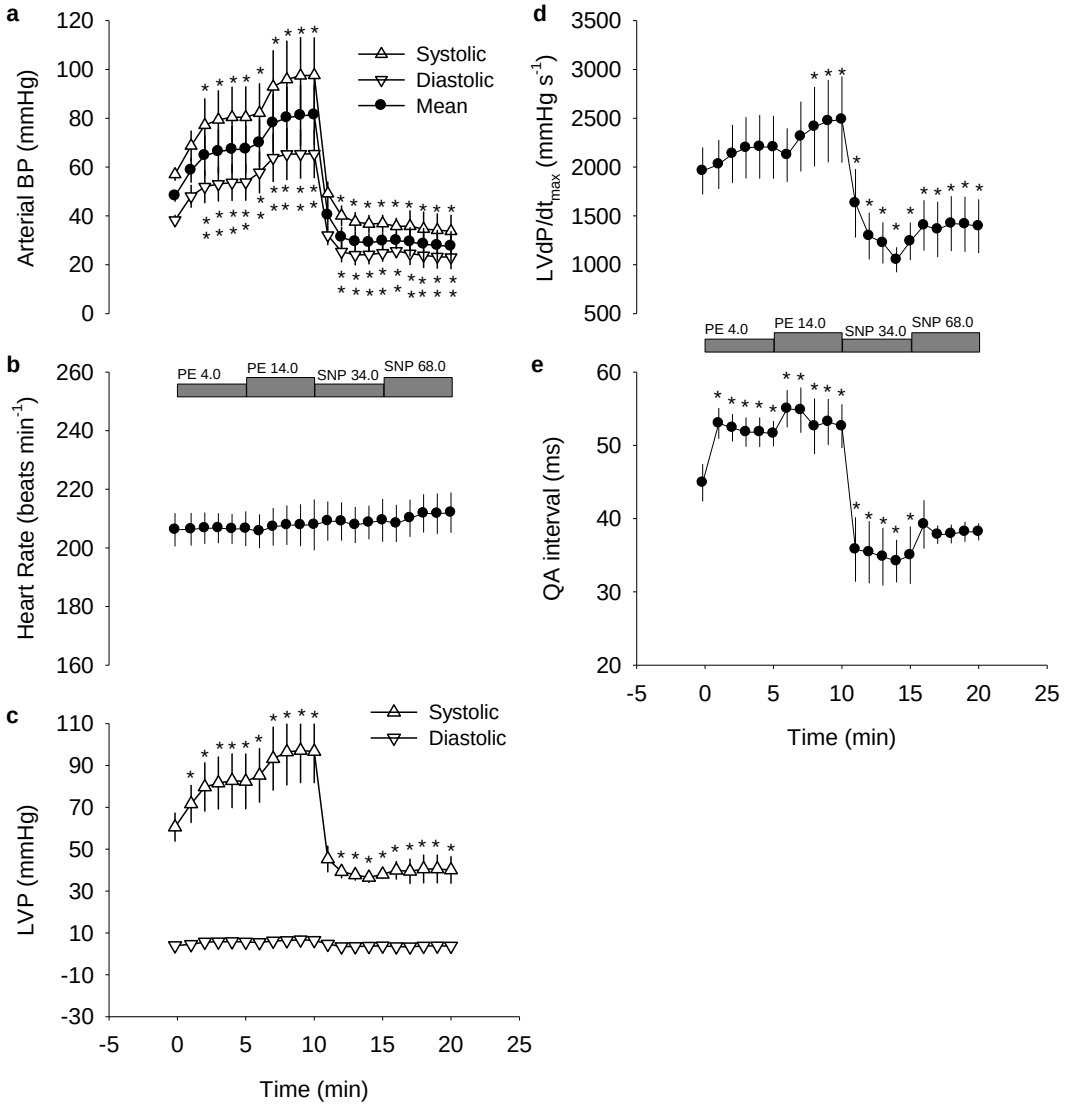

Figure 4.4 Effect of phenylephrine (PE) and sodium nitroprusside (SNP) on **a)** arterial blood pressure (BP), **b)** heart rate, **c)** left ventricular pressure (LVP), **d)** $LVdP/dt_{max}$ and, **e)** the QA interval. Experiments were performed with sympathetic and parasympathetic reflexes blocked by sectioning of the vagus nerves and administration of 1 mg kg^{-1} atenolol. The grey bars indicate drug infusions in nmol kg^{-1} min^{-1}. Mean ± S.E.M, n = 6. * indicates $P<0.05$ compared to value at time 0 min, two way ANOVA with Dunnett's test.

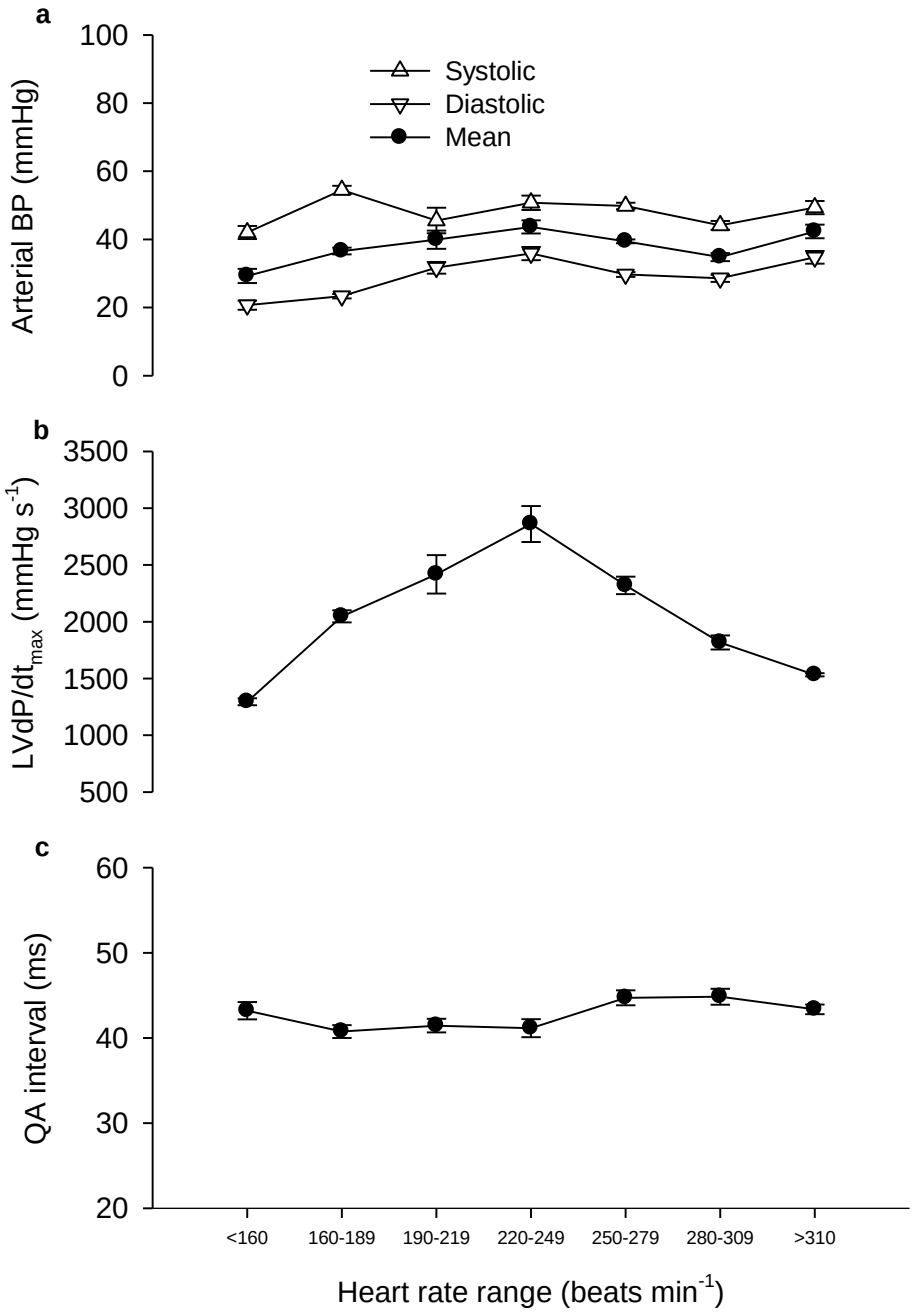

Figure 4.5 Effect of changes in heart rate on **a)** arterial blood pressure (BP), **b)** left ventricular (LV) dP/dt_{max} and, **c)** the QA interval. Mean ± S.E.M, n = 4. No statistical analysis was performed.

4.3.3 PV loop measurement in the anaesthetised guinea pig

An alternative approach to assessing cardiac contractility by measurement of LV PV loops using the Scisense ADVantage™ system was investigated. To measure PV loops a catheter must be inserted into the lumen of the LV. This can be done via a carotid artery thus maintaining a closed-chest setup or by opening the chest and performing an apical stab to insert the catheter through the apex of the heart (Pacher *et al.*, 2008).

Initial attempts at catheter insertion into the LV were made using the closed-chest approach, however, signals were generally of poor quality whereas these were greatly improved using the open-chest apical approach. Apical insertion offered additional advantages as the electrode rings could be visualised during insertion of the catheter ensuring that these were fully entered into the LV. Once inside the LV, the catheter could then be manipulated more easily into a position where optimal signals could be obtained. Opening the chest also allowed the IVC to be located easily above the diaphragm. Previous attempts to do this opening the abdomen only (i.e. without perforating the diaphragm) were unsuccessful.

As explained in detail in Section 4.1 the ADVantage™ system offers two methods to generate PV loops – the W method and the D method. As illustrated in Figure 4.6 the W method generated a poor quality volume signal which when combined with pressure to generate a PV loop resulted in non-physiological and variable loops. In anaesthetised guinea pigs the D method produced better quality volume (obtained from magnitude) signals and consequently much more consistent PV loops (see Figure 4.9 for examples). All subsequent results shown here were obtained using the D method.

Guinea pigs under pentobarbital anaesthesia usually need to be mechanically ventilated, however, in doing this respiratory artefacts were observed. This resulted in cyclical spikes at diastolic points and variation in systolic points on the magnitude trace (Figure 4.7a) which were reflected in the PV loop (Figure 4.7b). When the ventilator was turned off these artefacts disappeared (Figure 4.7a) and the PV loop regained its shape (Figure 4.7c).

To provide a full and comprehensive cardiovascular assessment in these experiments simultaneous ECG recording was desirable. However, attachment of subcutaneous ECG limb leads caused pronounced electrical interference on all

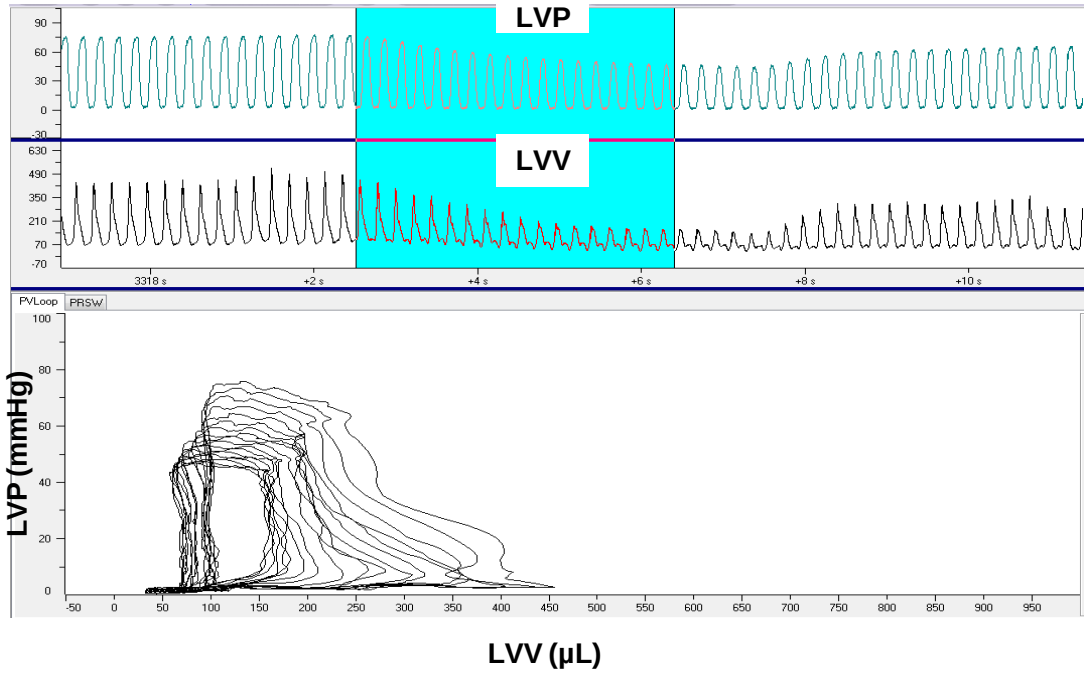

Figure 4.6 PV loop recording using the W method. Upper panel shows left ventricular pressure (LVP) and the LV volume (LVV) signal calculated using the W method. Lower panel shows the poor quality LVP vs LVV loop generated from these signals.

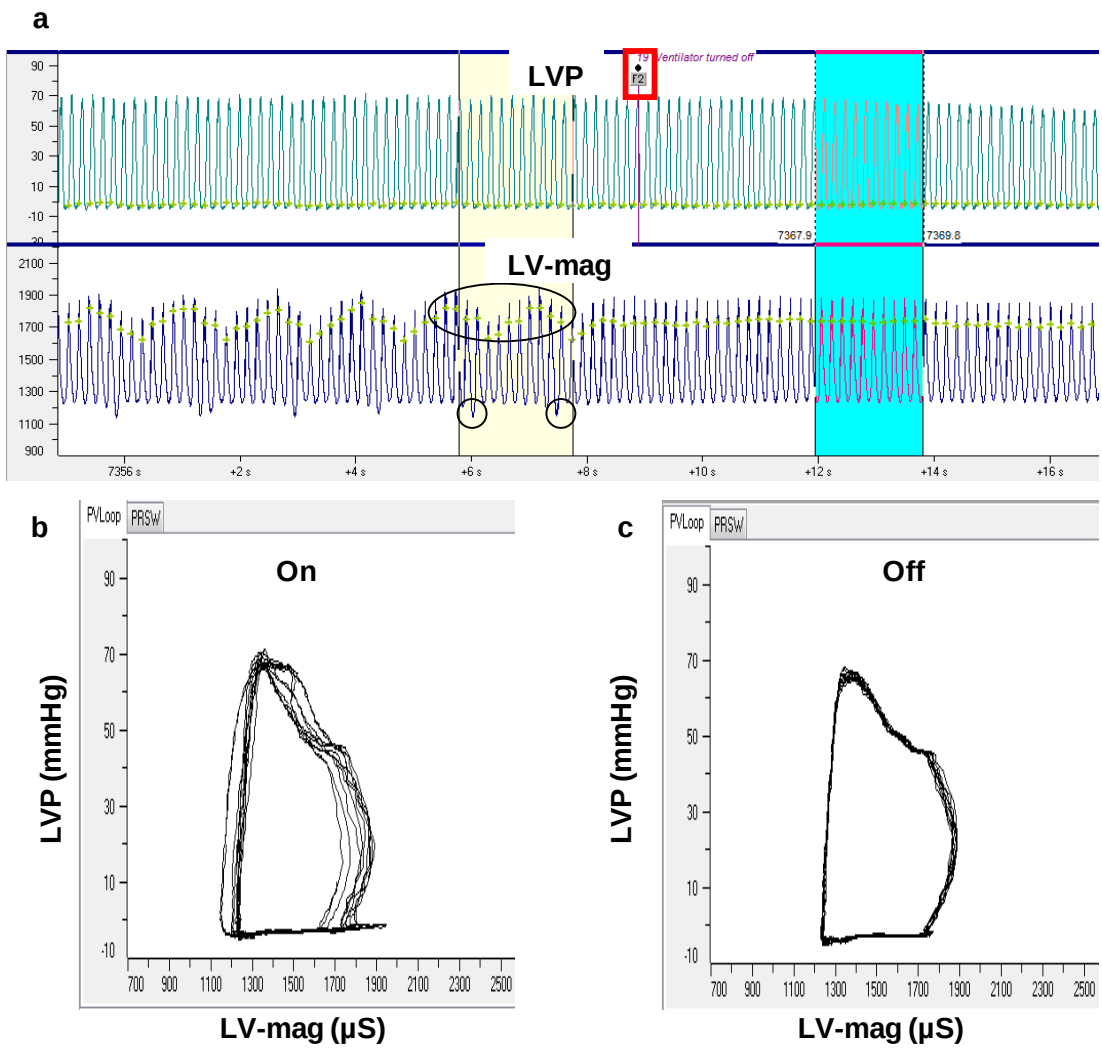

Figure 4.7 Respiratory artefacts observed during mechanical ventilation. **a)** Upper panel shows left ventricular pressure (LVP) trace, lower panel shows LV magnitude (LV-mag) trace. Cyclical artefacts at systolic and diastolic peaks whilst the ventilator was turned on are circled. F2 (boxed in red) marks where the ventilator was switched off. Note that artefacts disappear. **b)** Corresponding LVP vs LV-mag loops from left-hand shaded area in panel (a) showing loop variation when ventilator was switched on. **c)** Corresponding LVP vs LVV loops from right-hand shaded area in panel (a) showing little variation in loops when ventilator was switched off. Recordings were obtained using the D method.

recording channels associated with the ADVantage™ system (Figure 4.8). For this reason ECG recording was not possible alongside PV loop measurement.

Following optimisation of surgical techniques and experimental setup, high quality recordings of LVP, LVV and LV-mag were obtained using the D method (Figure 4.9a) producing high quality LVP vs LV-mag (PM) and PV loops (Figure 4.9b and c, respectively). Simultaneous measurement of arterial blood pressure was also possible via a fluid filled cannula in the right carotid artery. To obtain a series of PV loops to derive load-independent indices of systolic function the IVCO was performed by swiftly pulling a suture placed around the IVC directly upwards. Successful performance of this occlusion was vital in obtaining a good series of loops. In Figure 4.10a the shaded and boxed area, highlights where the occlusion was performed. This caused PM (Figure 4.10b) and PV (Figure 4.10c) loops to move in a left and downward direction.

4.3.3.1 Assessment of inotropic effects

As discussed earlier PV loop measurement offers numerous approaches to assess cardiac contractility. The ESPVR is a traditional and still commonly used index of contractility obtained from PV loops by connecting the end-systolic points at the top left-hand corner of each loop. Figure 4.11a illustrates a series of PV loops with the end-systolic points indicated and fitting a linear line to connect the points was straightforward. However, Figure 4.11b shows a different series of PV loops with the end-systolic points marked and here the determination of a linear ESPVR was more difficult as at least three potential fits for the linear line were apparent as indicated. These observations were important in calculating and using the ESPVR as an index of contractility as discussed in more detail in Section 4.4.1.4.

In order to assess the ability of the ADVantage™ system to detect changes in cardiac contractility, isoprenaline and verapamil were administered to increase and decrease cardiac contractility, respectively. In optimising the dosing protocol for isoprenaline and verapamil it was noted that the isoprenaline-induced increase and verapamil-induced decrease in LVP greatly affected the quality of signals (Figure 4.12a) compared to drug free examples (Figure 4.9). This resulted in distortion of the associated PV loops (Figure 4.12b). The implications of this in these experiments are discussed in Section 4.4.1.4.

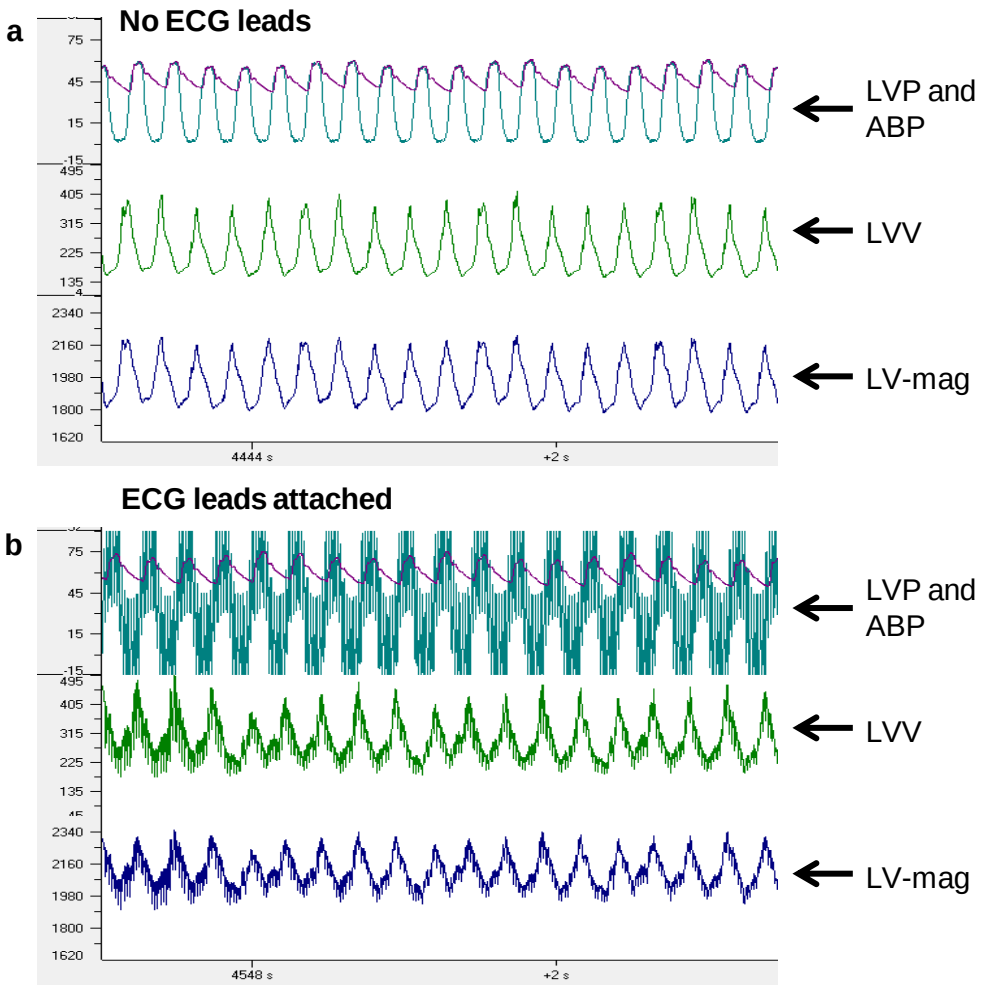

Figure 4.8 Electrical interference during simultaneous ECG recording. **a)** From upper to lower panel, left ventricular pressure (LVP) with arterial blood pressure (ABP) trace overlaid, LV volume (LVV) trace and LV magnitude (LV-mag) trace recorded without ECG leads attached, **b)** Continued recordings as above with subcutaneous ECG leads attached causing significant deterioration of all signals recorded via the Scisense ADVantage™ system (i.e. LVP, LVV and LV-mag).

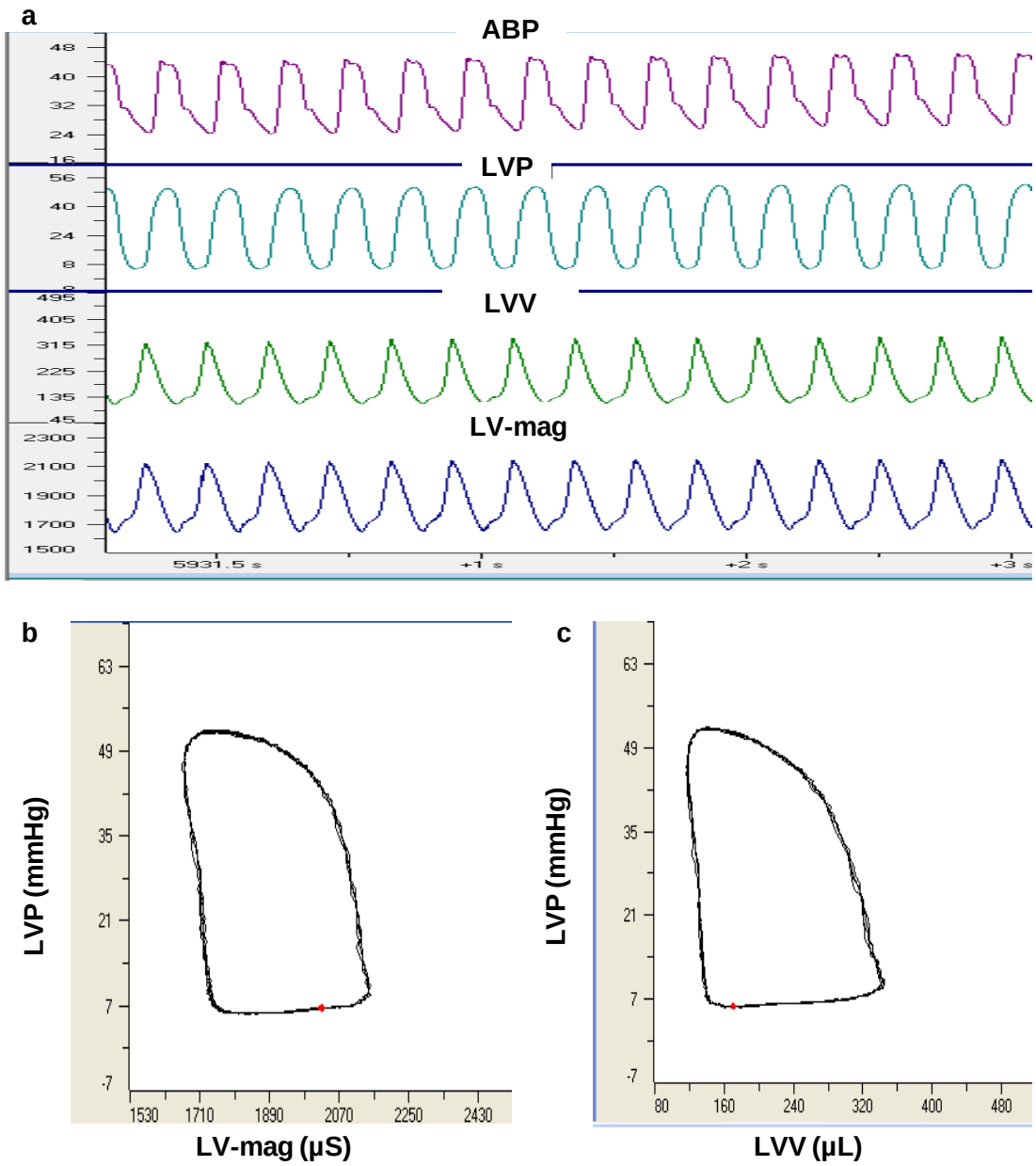

Figure 4.9 Baseline recordings of **a)** from upper to lower trace, arterial blood pressure (ABP), left ventricular pressure (LVP), LV volume (LVV) and LV magnitude (LV-mag), **b)** corresponding LVP vs LV-mag loops, and **c)** LVP vs LVV loops.

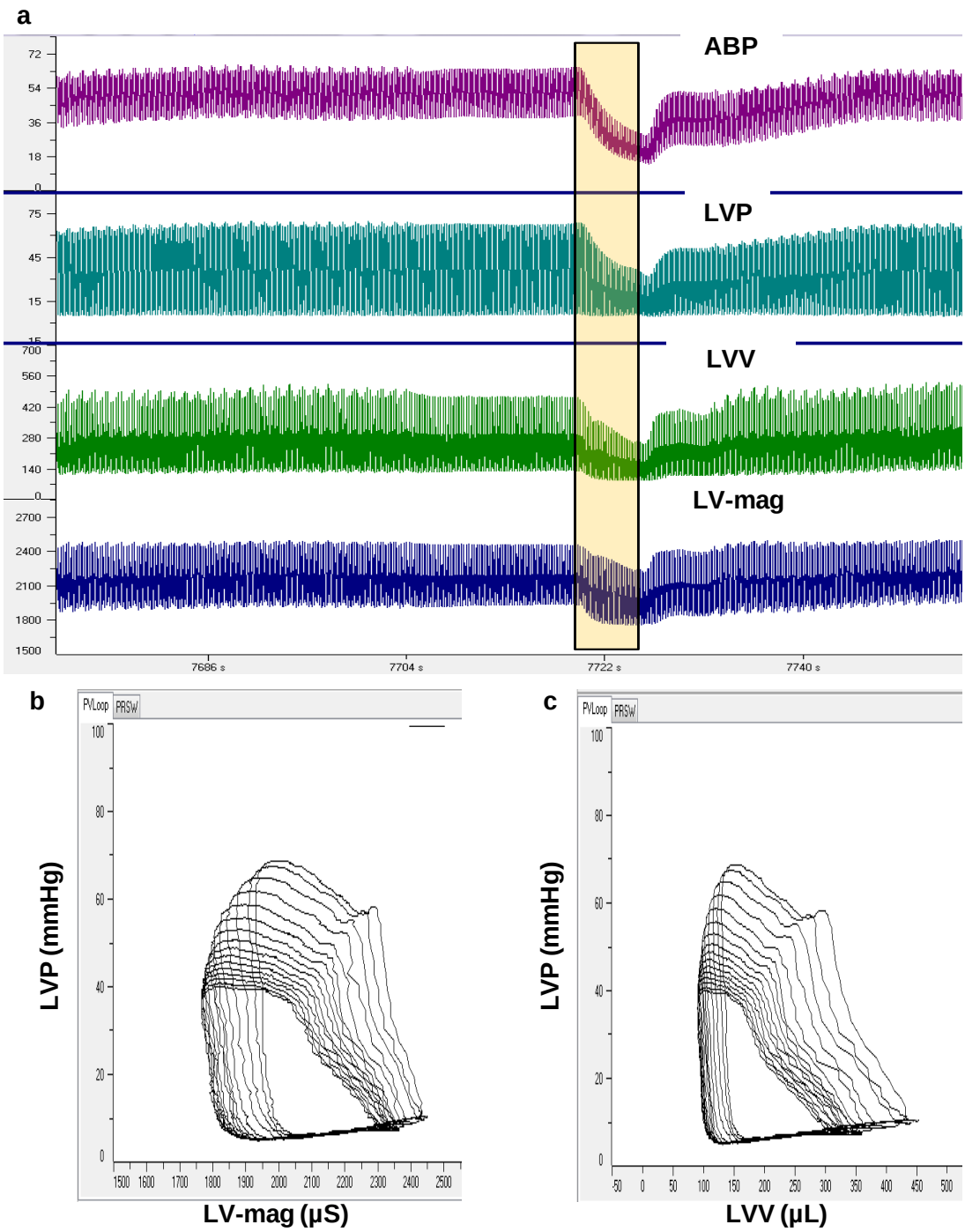

Figure 4.10 Inferior Vena Cava Occlusion (IVCO). **a)** From upper to lower panel, arterial blood pressure (ABP), left ventricular pressure (LVP), LV volume (LVV) and LV magnitude (LV-mag) traces. The boxed area indicates where the IVCO was performed, **b)** LVP vs LV-mag loops during IVCO, **c)** LVP vs LVV loops during IVCO.

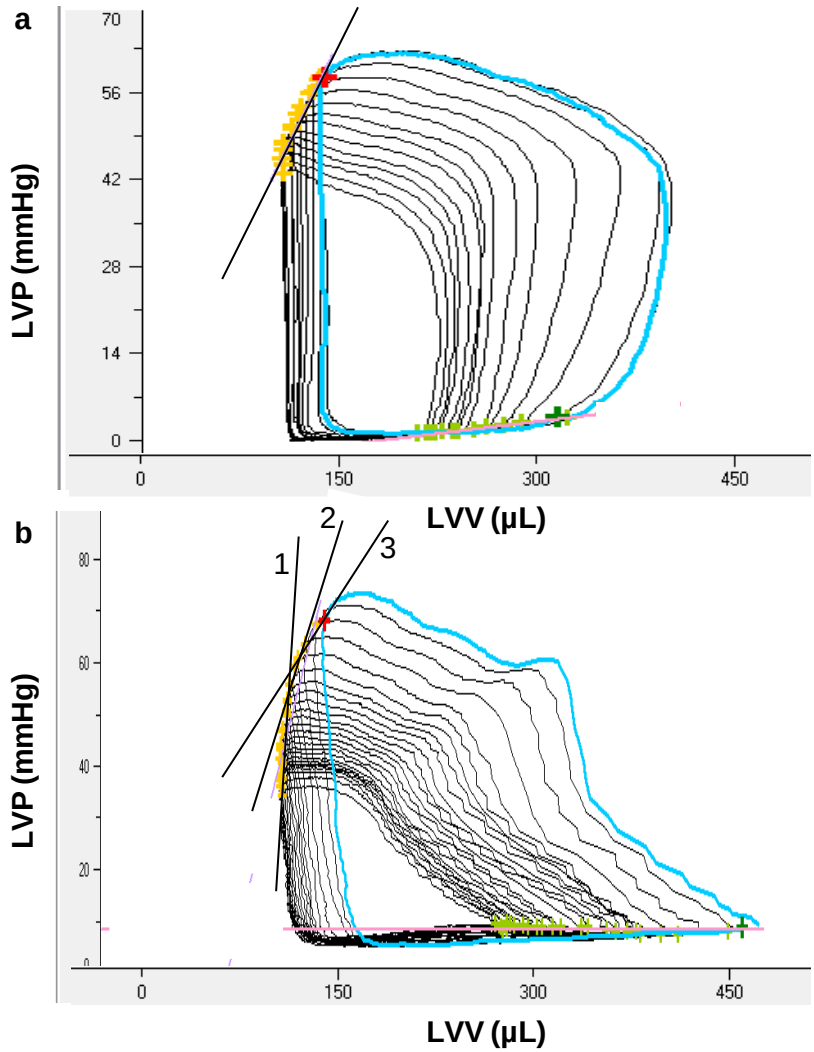

Figure 4.11 Example of pressure-volume loops displaying **a)** linear and **b)** non-linear end-systolic pressure-volume relationships (ESPVR).

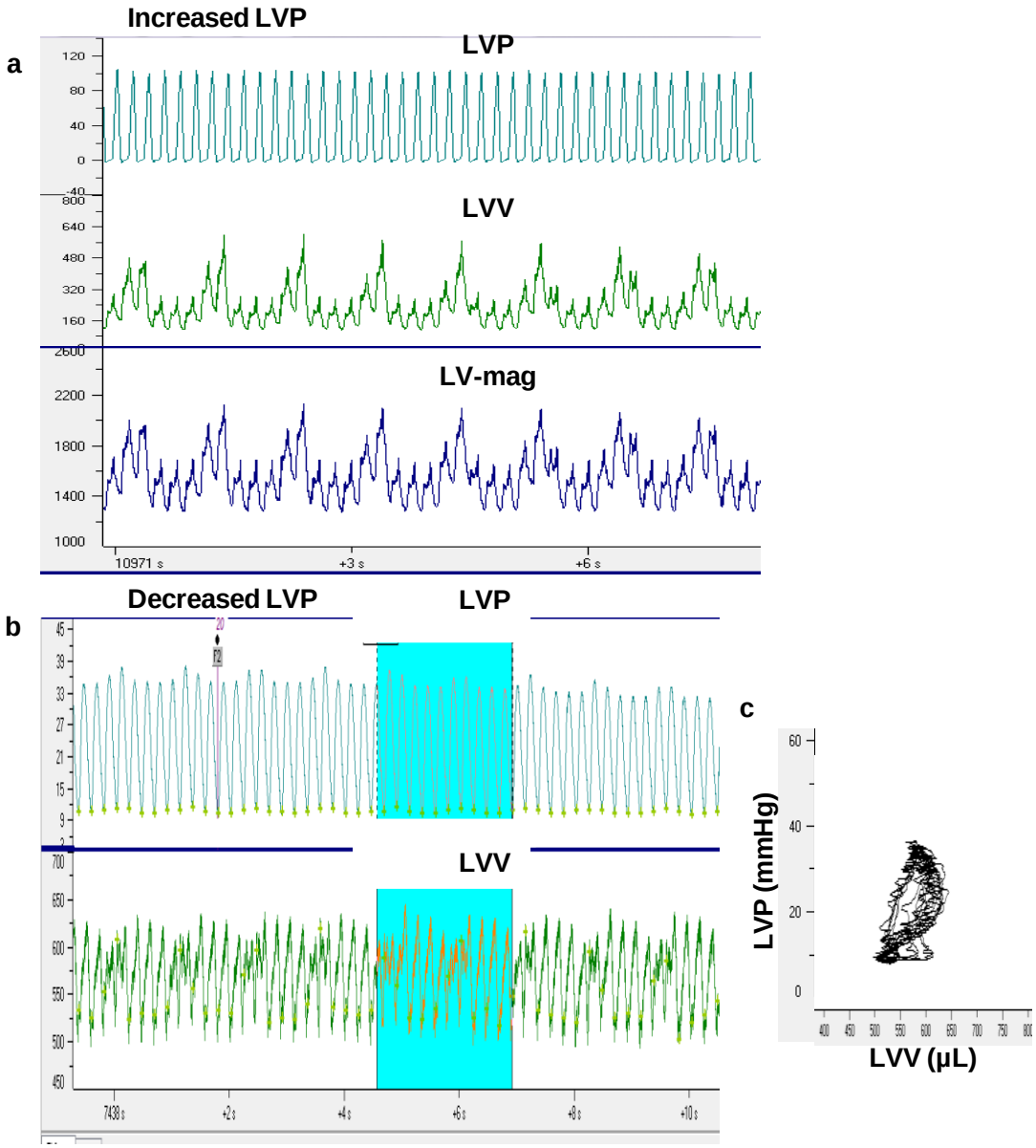

Figure 4.12 Signal and pressure-volume loop deterioration with drug-induced changes in left ventricular pressure (LVP). In the presence of, **a)** isoprenaline the increased LVP (upper panel) caused the quality of the LV volume (LVV, middle panel) and LV magnitude traces (LV-mag, lower panel) to greatly deteriorate, and **b)** verapamil the decreased LVP caused the LVV trace to greatly deteriorate and **c)** LVP vs LVV loop to distort.

PV loops measured before and after isoprenaline (Figure 4.13a and c, respectively) and verapamil (Figure 4.13b and d, respectively) administration are illustrated. Note that following isoprenaline administration loops were taller indicating an increase in LVP whereas following verapamil administration loops became wider indicating an increase in LVV.

The responses of four indices of contractility: ESPVR, PRSW, $LVdP/dt_{max}/Ved$ and $LVdP/dt_{max}$, were assessed (Table 4.2). Isoprenaline did not significantly alter ESPVR or $LVdP/dt_{max}/Ved$. $LVdP/dt_{max}$ was significantly increased and the increase in PRSW was very close to statistical significance (P=0.055). Verapamil significantly decreased ESPVR, PRSW and $LVdP/dt_{max}$ while the decrease in $LVdP/dt_{max}/Ved$ was very close to significance (P=0.056).

Effects on LVP and LVV were also measured by the ADVantage™ system and heart rate and arterial blood pressure were measured via the fluid filled cannulae in the right carotid artery (Table 4.3). Isoprenaline caused heart rate, systolic, diastolic and mean arterial blood pressure to increase, but LVSP, LVEDP, LVSV and LVEDV were not significantly altered. Verapamil had no significant effects on heart rate, systolic, diastolic or mean arterial blood pressure, LVSP, LVEDP or LVSV. LVEDV was, however, significantly increased.

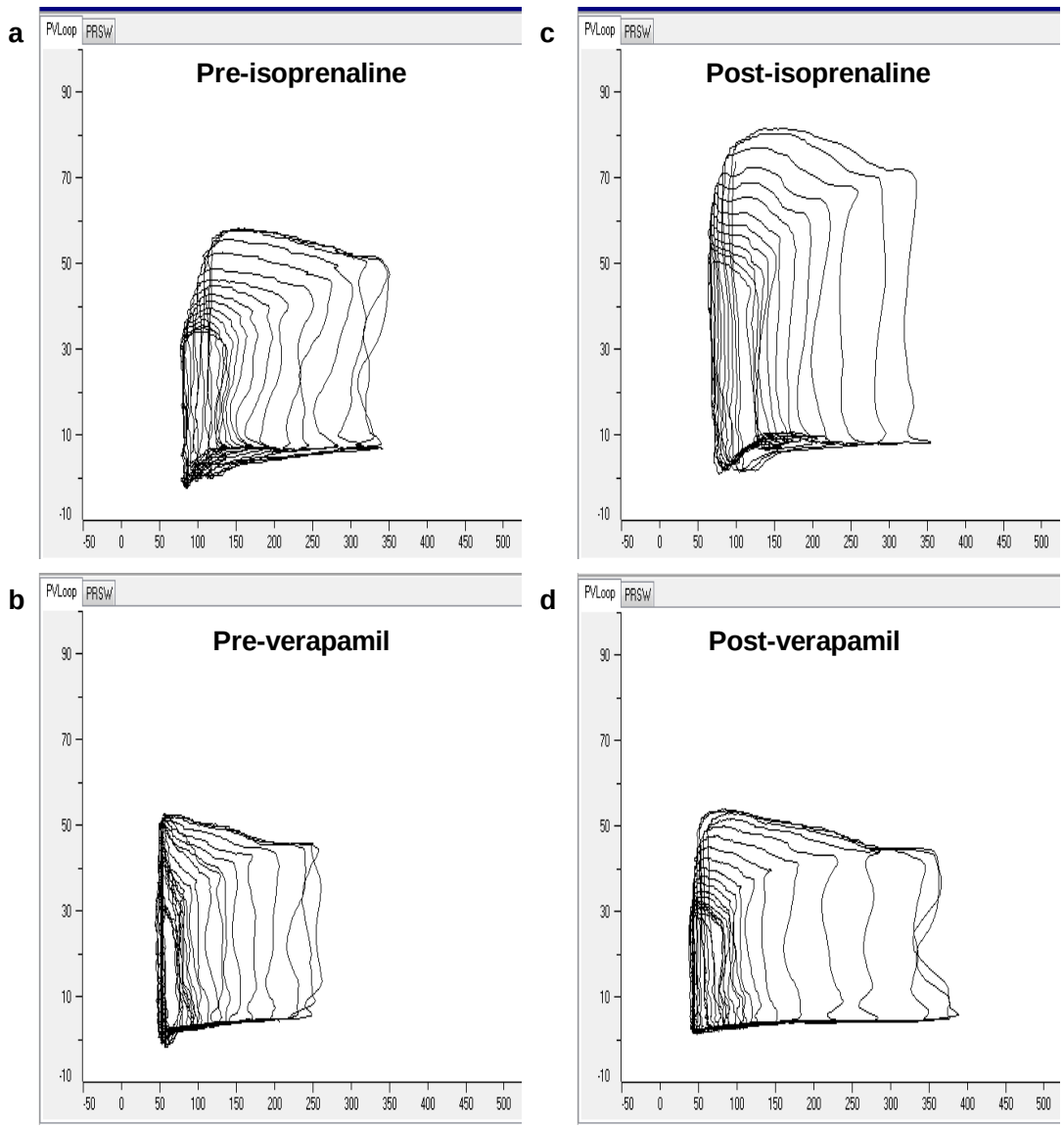

Figure 4.13 Examples of pressure-volume loops obtained in individual guinea pigs during IVCO and **a)** pre-isoprenaline, **b)** post-isoprenaline, **c)** pre-verapamil or **d)** post-verapamil administration.

Table 4.2 Effects of isoprenaline and verapamil on indices of cardiac contractility

	ESPVR (slope)	**PRSW (slope)**	**LVdP/dt$_{max}$/Ved (mmHg s^{-1} µL^{-1})**	**LVdP/dt$_{max}$ (mmHg s^{-1})**
Pre-isoprenaline	0.53 ± 0.04	55.58 ± 13.84	5.51 ± 0.9	2419 ± 222
Post- isoprenaline	1.05 ± 0.18	91.71 ± 11.30	11.60 ± 3.52	6179 ± 647*
Pre-verapamil	1.91 ± 0.35	70.70 ± 5.2	8.62 ± 1.34	2631 ± 365
Post-verapamil	0.94 ± 0.1$^{\#}$	57.13 ± 5.09$^{\#}$	5.59 ± 0.49	2335 ± 359$^{\#}$

ESPVR, End-systolic pressure-volume relationship; LVdP/dt$_{max}$, left ventricular dP/dt$_{max}$; LVdP/dt$_{max}$/Ved, left ventricular dP/dt$_{max}$/Volume at end diastole; PRSW, Preload recruitable stroke work. * indicates P<0.05 compared to pre-isoprenaline value, paired *t* test. $^{\#}$ indicates P<0.05 compared to pre-verapamil value, paired *t* test.

Table 4.3 Effects of isoprenaline and verapamil on haemodynamics

	Heart rate (beats min^{-1})	SBP (mmHg)	DBP (mmHg)	MABP (mmHg)	LVSP (mmHg)	LVEDP (mmHg)	LVSV (µL)	LVEDV (µL)
Pre-isoprenaline	256 ± 15	60 ± 4	38 ± 5	50 ± 4	67 ± 7	5 ± 2	293 ± 53	503 ± 74
Post- isoprenaline	315 ± 7*	75 ± 4*	54 ± 5*	56 ± 4*	112 ± 31	4 ± 1	196 ± 39	530 ± 97
Pre-verapamil	241 ± 7	52 ± 1	37 ± 1	46 ± 1	60 ± 3	4 ±1	98 ± 26	329 ± 61
Post-verapamil	233 ± 13	49 ± 2	37 ± 3	44 ± 2	58 ± 3	5 ± 1	102 ± 30	402 ± 63#

DBP, diastolic blood pressure; MABP, mean arterial blood pressure; LVEDP, left ventricular end-diastolic pressure; LVEDV, left ventricular end-diastolic volume; LVSP, left ventricular systolic pressure; LVSV, left ventricular systolic volume; SBP, systolic blood pressure. * indicates $P<0.05$ compared to pre-isoprenaline value, paired *t* test. # indicates $P<0.05$ compared to pre-verapamil value, paired *t* test.

4.4 Discussion

4.4.1 Main findings

This work demonstrates that although good correlations between LVdP/dt_{max} and the QA interval have been found, this relationship may differ for drugs that have additional effects on heart rate and/or blood pressure. By experimentally changing blood pressure or heart rate both LVdP/dt_{max} and the QA interval were found to be significantly altered. Additionally, measurement of LV PV loops was possible in the anaesthetised guinea pig, however, further optimisation and validation of this approach are required.

4.4.1.1 Observations from AstraZeneca database

Analysis of data from 45 compounds demonstrated that the responses of LVdP/dt_{max} and the QA interval were not reciprocal for several compounds. Further analysis of these data showed that there were often concurrent changes in blood pressure and/or heart rate when LVdP/dt_{max} and the QA interval were not reciprocal. These findings, along with suggestions in the literature that LVdP/dt_{max} and the QA interval can be influenced by cardiac loading and heart rate (Wallace *et al.*, 1963; Mahler *et al.*, 1975; Quinones *et al.*, 1976; Cambridge & Whiting, 1986; Hamlin & Del Rio, 2010; Markert *et al.*, 2012) then led to the hypothesis that LVdP/dt_{max} and the QA interval are sensitive to changes in blood pressure and/or heart rate.

4.4.1.2 Effects of changes in blood pressure on LVdP/dt_{max} and the QA interval

To test the hypothesis formed above, experiments were designed to increase (via phenylephrine) and decrease (via sodium nitroprusside) blood pressure whilst measuring LVdP/dt_{max} and the QA interval. Phenylephrine and sodium nitroprusside infusions were initially delivered with sympathetic and parasympathetic drives to the heart intact. Following a recovery period, infusions were then repeated in the presence of the β_1-adrenoceptor antagonist, atenolol, and with the vagus nerves sectioned thus inhibiting sympathetic and parasympathetic responses, respectively. During both reflex intact and reflex blocked drug infusions, LVdP/dt_{max} and the QA interval both increased with the increase in blood pressure caused by the higher dose of phenylephrine, and both decreased with the decrease in blood pressure caused by sodium nitroprusside (Figure 4.3 and Figure 4.4a).

During acute changes in blood pressure, baroreceptors may trigger reflex changes in heart rate and sympathetic outflow to the vasculature which serve to restore blood pressure to normal levels. Without sympathetic and parasympathetic blockade an increase in heart rate occurred as arterial blood pressure fell indicating that baroreceptors may have been activated (Figure 4.3b). It was assumed that this increase in heart rate was a reflex response to the decrease in arterial blood pressure. This was confirmed in the reflex blocked experiments as heart rate did not change as arterial blood pressure fell (Figure 4.4b). This, therefore, eliminates the possibility that this increase in heart rate may be responsible for the observed increase in $LVdP/dt_{max}$ and the QA interval.

With sympathetic and parasympathetic blockade the significant rise in arterial blood pressure previously occurring with only the higher dose of phenylephrine, was evident during the lower phenylephrine dose (Figure 4.4a). Similarly, the significant increase in the QA interval now appeared at the lower phenylephrine dose (Figure 4.4e). $LVdP/dt_{max}$ remained unaffected until higher arterial blood pressures were reached (Figure 4.4d) perhaps suggesting that a higher threshold is required before arterial blood pressure can affect this index. This would further suggest that $LVdP/dt_{max}$ is less sensitive than the QA interval to increases in arterial blood pressure.

A further difference in responses between drug infusions with reflexes intact and blocked was that in the reflex blocked situation the fall in the QA interval was not sustained throughout both sodium nitroprusside infusions. In the reflex intact situation a further slight decrease in arterial blood pressure occurred with the second dose of sodium nitroprusside. However, this was not apparent in the reflex blocked state and both $LVdP/dt_{max}$ and the QA interval responses reversed at this point. This may suggest that $LVdP/dt_{max}$ and the QA interval were perhaps recovering slightly without the influence of an additional, albeit small, decrease in blood pressure. Both indices appeared to plateau with $LVdP/dt_{max}$ remaining significantly decreased whilst the QA interval did not. This may suggest that in this case $LVdP/dt_{max}$ was more sensitive than the QA interval to decreases in arterial blood pressure.

It also appears that the lower dose of sodium nitroprusside may have caused near maximal responses. Even in experiments where reflexes were intact the effects of

the higher doses of sodium nitroprusside over the lower doses were minimal. With hindsight, a lower starting dose of sodium nitroprusside could have been tested. This may not have caused arterial blood pressure to significantly decrease, but may have provided more information on the threshold of decrease in arterial blood pressure which must be reached to cause $LVdP/dt_{max}$ and the QA interval to be affected.

The dependence of $LVdP/dt_{max}$ on preload and afterload is well documented (Wallace *et al.*, 1963; Mahler *et al.*, 1975; Quinones *et al.*, 1976; Cambridge & Whiting, 1986). Preload refers to the "load" imposed on the ventricle at the end of diastole. LVEDV is used as a measure of preload, however, in the absence of this data, LVEDP is used as a surrogate measure. Afterload refers to the mechanical "load" on the ventricle during ejection and, under normal physiological conditions, this is determined by the arterial system allowing diastolic blood pressure to be used as a measure of afterload. The finding in the current study that $LVdP/dt_{max}$ was altered with changes in blood pressure is therefore not surprising and is consistent with the studies cited above.

The primary effects of phenylephrine were on diastolic blood pressure rather than LVEDP (Figure 4.3c and Figure 4.4c) and so in these experiments effects on $LVdP/dt_{max}$ were largely attributable to afterload rather than preload. This is supported by Johnson *et al.*, (2012) who recently reported an increase in $LVdP/dt_{max}$ in the anaesthetised guinea pig following phenylephrine administration and also attributed this to increased afterload. Decreases in $LVdP/dt_{max}$ with sodium nitroprusside have been reported previously by Cambridge & Whiting (1986) who used sodium nitroprusside to reduce cardiac load and reported dose related reductions in $LVdP/dt_{max}$.

Although no studies have directly investigated the effects of cardiac loading on the QA interval, there are several factors that could theoretically influence the QA interval (Cambridge & Whiting, 1986; Hamlin & Del Rio, 2010). Relevant to the findings here is the pressure difference between that in the ventricle at end diastole and the diastolic aortic pressure which determines the pressure that the LV must develop to open the aortic valve and eject blood into the aorta. The more pressure the LV must develop to open the valve, the longer the QA interval (if all other factors are equal). Therefore, an increase in arterial blood pressure, requires greater

developed pressure by the LV and thus increases the QA interval and *vice versa*. Of note, is also the distance of the catheter from the heart as the farther this is, the longer the QA interval. However, this was always consistent within an individual animal and care was taken to minimise any possible differences between animals.

Another consideration in interpreting the findings here is the Anrep effect which describes an increase in ventricular inotropy following an abrupt increase in systolic pressure (von Anrep, 1912). Although the mechanism is not fully understood this effect is thought to be mediated via myocardial stretch receptors which activate a 'rapid' (occurring immediately, within a single heart beat) and secondary 'slow' (occurring over a few minutes) increase in the force of contraction. These increases in contractility have been shown to be related to enhanced myofilament Ca^{2+} sensitivity and increased intracellular Ca^{2+} transient, respectively (for review see Calaghan & White, 1999). Therefore, the effects of increased arterial blood pressure on $LVdP/dt_{max}$ may reflect changes in cardiac contractility but as a result of indirect effects on the myocardium.

Furthermore, there is the possibility that phenylephrine and/or sodium nitroprusside altered cardiac contractility independent of the changes in blood pressure. Phenylephrine, an α_1-adrenoceptor agonist, has been shown to increase contractility in several species including rabbit (Kronenberg *et al.*, 1989), dog (Endoh *et al.*, 1978) and guinea pig (McNeil & Verma, 1973). The positive inotropic effect mediated by α_1-adrenoceptors is reported to be less prominent in the guinea pig (Shibata *et al.*, 1980). However, at high doses phenylephrine has been reported to exert its positive inotropic effect via β-adrenoceptors rather than α_1-adrenoceptors in the guinea pig (Chess-Williams *et al.*, 1990). Nitric oxide (NO), produced by the breakdown of sodium nitroprusside, has been shown to have a positive inotropic effect at low concentrations and a negative inotropic effect at higher amounts (for review see Massion *et al.*, 2003). Phenylephrine and sodium nitroprusside were tested in a dog cardiomyocyte contractility assay at AstraZeneca (Harmer *et al.*, 2012). Phenylephrine caused modest increases in sarcomere shortening at 10 µM, but sodium nitroprusside had no effect up to 100 µM. As no blood samples were collected in these experiments plasma concentrations of phenylephrine and sodium nitroprusside are unknown. However, it is unlikely that the plasma concentrations would have exceeded the active concentrations in the contractility assay and so these doses were unlikely to have had any direct inotropic effects.

4.4.1.3 Effects of changes in heart rate on LVdP/dt$_{max}$ and the QA interval

To investigate the effect of changes in heart rate on LVdP/dt$_{max}$ and the QA interval a combination of right atrial pacing and vagus nerve stimulation was employed to achieve a range of heart rates whilst recording both indices. It should be stated that no formal statistical analysis was performed on these data following advice from a statistician who recommended that these data are best left as a purely visual interpretation of the evident trends.

Throughout the range of heart rates, arterial blood pressure and the QA interval changed very little (Figure 4.5a and c). A correlation between the QA interval and the RR interval has been shown for some drugs (Johnson *et al.*, 2012), suggesting that heart rate may have some influence on this index. In this study, however, there was no clear evidence of this.

At low heart rates, LVdP/dt$_{max}$ tended to be low and as heart rate increased LVdP/dt$_{max}$ also increased (Figure 4.5b). The relationship between contractility and heart rate is well-known. The Bowditch effect, Treppe (staircase) Phenomenon or chronotropic-inotropism describes an increase in myocardial contractility with an increase in heart rate (De Pauw *et al.*, 2004; Lakatta, 2004). This occurs in several species and is associated with an increase in the amount of Ca^{2+} entering cardiac myocytes with each beat thus enhancing EC-coupling (for review see Endoh, 2004). With this in mind it had been recommended that a factor that corrects LVdP/dt$_{max}$ for heart rate should be used (Hamlin & Del Rio, 2012; Markert *et al.*, 2012). In this study, however, the positive relationship between LVdP/dt$_{max}$ and heart rate was not apparent at heart rates above 250 beats min^{-1}. At this point LVdP/dt$_{max}$ decreased as heart rate increased. Such a negative force-frequency relationship may evidence signs of heart failure due to abnormalities in Ca^{2+} handling processes (Endoh, 2004). Alternatively, it may be a consequence of reduced LV filling times at higher heart rates. The reduction in preload could well reduce LVdP/dt$_{max}$ as explained earlier.

A point to raise is that vagal stimulation has been shown to cause negative inotropic effects on the LV (DeGeest *et al.*, 1965; Xenopoulos & Applegate, 1994) and by employing this method to decrease heart rate, contractility may also be decreased. However, immunohistochemical studies have shown a paucity of parasympathetic nerve fibres in the guinea pig LV myocardium implying that vagal efferent input has

little or no direct influence on ventricular contractile function in the guinea pig (Hoover *et al.*, 2004).

4.4.1.4 LV PV loop measurement in the anaesthetised guinea pig

The recognised "gold standard" method for estimating cardiac contractility is the PV loop. This technique is known to be challenging, however, given the inherent flaws of LVdP/dt_{max} and the QA interval in assessing cardiac contractility the feasibility of PV loop measurement in the anaesthetised guinea pig was assessed. This was done using recently developed admittance technology and was the first time that this particular system had been used in the anaesthetised guinea pig (Scisense, personal communication).

The catheter can be inserted into the LV via a carotid artery without opening the chest cavity (closed-chest approach) or via the apex of the heart after chest opening (open-chest approach) as described in mice and rats by Pacher *et al.* (2008). Initially, several attempts were made to enter the LV via the left carotid as ideally a closed-chest model was desired to be in line with the previously developed model. Although it was possible to get the catheter into the LV (indicated by the LVP trace), obtaining high quality signals across all PV system recordings (pressure, phase and magnitude) simultaneously was not possible. An open-chest approach was then tried and found to be much better not only in terms of signal quality, but for catheter placement and manipulation.

Irrespective of chest opening, it was necessary to open the abdomen in order to locate the inferior vena cava. In mice this vessel can be accessed easily below the diaphragm (K Foote, personal communication; Pacher *et al.*, 2008), however, due to mass and anatomical differences in the guinea pig this was very difficult, involving displacement of the liver and intestines. By cutting through the diaphragm it was much easier to locate the inferior vena cava in the lower part of the thoracic cavity and place a suture around it there.

Despite a general improvement in PV system signals with the open-chest approach, the phase signal in particular tended to be problematic due to electrical noise interference. The ADVantage™ PV system user manual acknowledges this fact stating:

"The phase channel is sensitive to other electrical devices and metal objects which act as antennae. Devices such as ECG leads, non-isolated rectal probes, heating pads or any other electrical instrument may contribute electrical noise during volume data collection."

Numerous attempts were made to remove this noise by systematically removing potential noise sources, changing the recording channel for the phase input, repositioning of the catheter tip within the LV, the guinea pig itself, the PV system equipment and other electrical equipment, but the issue persisted and appeared to increase with duration of use.

Communication from QTest labs (Ohio, USA) confirmed that they too experienced problems with noise on the phase signal and because of this they used the magnitude signal to generate PV loops in anaesthetised guinea pigs (Ueyama *et al.*, 2011). This is certainly a valid approach to determining changes in contractility although subtle changes may not be detected (Porterfield *et al.*, 2009). With this information and due to the continued problems, the decision was made to use the D method (which does not require the phase signal) for volume calculation rather than the W method.

Guinea pigs under pentobarbital anaesthesia generally need to be mechanically ventilated and opening of the chest cavity necessitated this. With ventilation, artefacts were observed which disappeared when the ventilator was switched off (Figure 4.7). Respiratory effects on PV signals with mechanical ventilation have also been observed in rats with waxing and waning of signals occurring (K Foote, personal communication). Therefore, during periods of recording which were to be analysed, the ventilator was switched off. This is the normal procedure for PV loop data collection allowing the acquisition of data without lung motion artefacts (Pacher *et al.*, 2008). In the current study the ventilator was switched off for approximately 10-15 seconds which did not detrimentally affect guinea pigs and pulse oximeter measurements indicated very little change in oxygen saturation. Mechanical ventilation has been also reported to cause a rightward shift in volume parameters (Foote & Loughrey, 2010) in rats. When the ventilator was switched off in the current study a slight repositioning of PV loops was observed in the first 1-2 seconds before loops stabilised. Therefore, after switching off the ventilator it was important to allow this to occur before analysis.

Ideally, to provide a full and comprehensive cardiovascular assessment, simultaneous ECG recording alongside PV loop measurement would be desirable. However, insertion of subcutaneous ECG leads in these experiments caused substantial electrical interference across all PV system signals, particularly LVP making this impossible (Figure 4.8).

To determine the ability of the PV system to detect changes in contractility the positive inotrope, isoprenaline, and negative inotrope, verapamil, were used. Contractility was assessed via the ESPVR, PRSW, $LVdP/dt_{max}$/Ved and $LVdP/dt_{max}$.

Initially an identical experimental protocol to previous acute experiments (Chapter 2) was tried, i.e. 3 cumulative doses of isoprenaline or verapamil infused for 15 minutes each dose. Experiments with isoprenaline were conducted first. About mid-way through the second dose of isoprenaline, however, signal quality deteriorated (Figure 4.12a) and PV loops were unrecognisable. It was concluded that this was due to the increased activity of the heart (rate and force of contraction) displacing the catheter thus skewing recordings. The experiment was then repeated with the catheter secured as much as possible, however, the same problem occurred. To overcome these issues it was decided that only the intermediate dose of isoprenaline would be used causing more subtle effects on the heart. Additionally a fast infusion of 1 minute was used to limit the recording time and hopefully maintain good signals. This worked well in terms of signal quality and stability. In the subsequent verapamil experiments it was assumed that a similar protocol could be used. However, the evoked decreases in pressure in this case also caused signals and PV loops to become skewed (Figure 4.12b and c). These problems were resolved by increasing the delivery time to 10 minutes via an infusion pump.

Once the dosing regimes were optimised, following isoprenaline administration the only parameter to increase significantly was $LVdP/dt_{max}$ although PRSW was very close to being significantly increased (Table 4.2). In contrast, following verapamil administration all parameters were significantly decreased except $LVdP/dt_{max}$/Ved which was very close to a significant decrease.

In general, r^2 values for the fit of the ESPVR line through end-systolic points in isoprenaline experiments were good (ranging from 0.91 to 0.96). However, in verapamil experiments r^2 values were very poor (ranging from 0.48 to 0.79) so

although a significant decrease in this parameter was found this cannot be assumed to be reliable.

Although the ESPVR was originally proposed as a linear relationship, more recently this has been shown not to be the case. As Burkhoff *et al.* (2005) explain the ESPVR is in general nonlinear and the precise shape varies with contractility. When data for constructing the ESPVR are obtained over a limited PV range the ESPVR may appear linear, however, when data are obtained over wider ranges the ESPVR is seen to be curvilinear (Burkhoff *et al.*, 1987; Kass *et al.*, 1989). In other words, at high and low pressures and volumes the ESPVR is nonlinear whereas at intermediate pressures and volumes it is. These points clearly have important implications for interpretation of PV data where the ESPVR is extrapolated linearly.

Deviations from linearity were often seen in the experiments presented here and would explain the poor r^2 values in the verapamil experiments where lower pressures were reached. In addition, as pressures in guinea pigs are lower than other species, nonlinearity of the ESPVR may be more common in this species. A further limitation to the use of the ESPVR in any species is evidence showing that the ESPVR is in fact not load-independent. Several investigators (e.g. Maughan *et al.*, 1984; Freeman *et al.*, 1986; Baan & van der Velde, 1988) have reported an upward and/or leftward shift, in the ESPVR with increased afterload.

In contrast, PRSW has been shown to be load-independent and linear over wide ranges of contractility and afterload (Glower *et al.*, 1985). In the experiments described in this Chapter PRSW decreased significantly following verapamil administration and was close to being increased significantly following isoprenaline administration. Group sizes in this study were small so this may account for the lack of significance in the isoprenaline group.

$LVdP/dt_{max}$/Ved has been reported to be less reproducible but more sensitive to changes in contractility than either the ESPVR or PRSW (Little *et al.*, 1989). In these experiments the apparent increase in $LVdP/dt_{max}$/Ved following isoprenaline was not statistically significant. The error associated with the mean was quite large indicating variability in this group suggesting that reproducibility was a problem. Following verapamil treatment the error associated with the mean was much smaller and the apparent decrease in this parameter was much closer to significance.

Again reproducibility issues with this parameter would be improved with larger group sizes.

$LVdP/dt_{max}$ was altered significantly following both isoprenaline and verapamil treatments. Whilst this may be reflective of the inotropic effects of these drugs, as explained previously this may additionally reflect the changes in heart rate, arterial blood pressure and/or LVEDV which also occurred (Table 4.3).

Overall, determination of the ESPVR has been shown to be difficult in guinea pigs. PRSW, $LVdP/dt_{max}$/Ved and $LVdP/dt_{max}$ are far more straightforward than the ESPVR with regards to analysis. However, $LVdP/dt_{max}$/Ved may be less reproducible than the PRSW and $LVdP/dt_{max}$ may be influenced by factors other than contractility. For these reasons the PRSW may offer the best assessment of contractility via PV loop measurement in anaesthetised guinea pigs.

4.4.2 Limitations

As in Chapter 2, group sizes were kept to a minimum in these studies to comply with UK legislation on animal use. In blood pressure and heart rate studies clear effects were achieved, however, in PV loop studies some apparent effects did not reach significance. This may be due to the number of guinea pigs in the study or alternatively due to the dose limitations as explained above.

In blood pressure and heart rate experiments no vehicle group was tested. However, infusions of greater volumes of saline had no effect in previous experiments (Figure 2.8 to Figure 2.13a) and statistical analysis used a paired test to determine drug effects within groups.

Opening the chest cavity tends to result in lower LVP and arterial BP and, therefore, these values are less physiological. However, in looking at drug effects the *change* in parameters is important rather than the absolute values which, under anaesthesia, may not be physiological anyway.

Clearly, measurements of PV loops in the anesthetised guinea pig using the ADVantage™ system needs further work. The system has been shown to be sensitive to drug-induced changes in contractility, however, stability of signals in the absence of drugs should be investigated as no formal assessment of this was made. Observations indicated that stability is an issue that needs to be improved for longer

studies. Furthermore, the limits of PV loop quality with regards to the magnitude of pressure change need to be investigated. The sensitivity of the system should also be validated using more drugs. However, an optimal dosing protocol needs to be established before doing this.

4.4.3 Conclusions

This work has shown that the relationship between $LVdP/dt_{max}$ and the QA interval can differ for different drugs and this may be due to changes in blood pressure and/or heart rate. Both $LVdP/dt_{max}$ and the QA interval were influenced by changes in blood pressure, and $LVdP/dt_{max}$ was additionally influenced by changes in heart rate. Measurement of LV PV loops may provide a more accurate assessment of true cardiac contractility, however, in the anaesthetised guinea pig this technique has been challenging and further optimisation and validation are required.

CHAPTER 5 CAMKII AS A MARKER OF CARDIAC CONTRACTILITY FOLLOWING CHRONIC *IN VIVO* DRUG ADMINISTRATION

5.1 Introduction

As highlighted in Chapter 3, CaMKIIδ plays a pivotal role in regulating cardiac contractility and is also a recognised molecular switch triggering abnormal Ca^{2+} handling and contractile dysfunction in cardiomyopathy. It is therefore also possible that CaMKIIδ may be an important intracellular target for drugs that alter cardiac performance and could serve as a useful *in vitro* marker of *in vivo* changes in cardiac contractility and cardiac safety in drug development.

In order to assess this possibility, in Chapters 2 and 3 inotropic agents (isoprenaline, ouabain and verapamil) along with anti-cancer agents (imatinib and sunitinib) were used to investigate a potential link between changes in cardiac contractility and concomitant changes in CaMKIIδ expression and/or CaMKII activity. However, following acute drug treatments although there were significant changes in cardiac contractility, there was a lack of significant effects on CaMKIIδ expression and CaMKII activity. Therefore, it was difficult to assess whether changes in cardiac contractility could be related to the level of CaMKIIδ expression and/or CaMKII activity.

CaMKII may not have been significantly affected in these experiments either because it is not involved in the effects of these drugs or because it is significantly affected only with longer durations of drug treatment. Since results from the CaMKII activity assay following acute drug treatments reflected higher activities for positive inotropes (isoprenaline and ouabain) and lower activities for negative inotropes (verapamil), this suggests that the former explanation is not the case and with greater/longer stimulation CaMKII may be significantly affected by these drugs.

Chronic drug administration may produce different results, either as a consequence of drug accumulation or because of adaptive responses to persistent drug action. Isoprenaline has been administered chronically in several studies in mice (e.g. Kudej *et al.*, 1997; Friddle *et al.*, 2000) and rat (e.g. Kitagawa *et al.*, 2007; Takeshita *et al.*, 2008), but less commonly in guinea pig (Maisel *et al.*, 1987). In all of these studies, chronic isoprenaline administration caused cardiac hypertrophy with some additional reports of decreased β-adrenoceptor density and receptor desensitisation (Maisel *et al.*, 1987; Kudej *et al.*, 1997; Takeshita *et al.*, 2008) or decreased SERCA and PLB expression (Takeshita *et al.*, 2008). CaMKII expression and activity are

known to be increased following chronic β-adrenoceptor stimulation and in hypertrophy and heart failure (Zhang *et al.*, 2003). Taken together these reports suggest that effects on both cardiac contractility and CaMKII expression and activity may be expected following chronic isoprenaline treatment.

Furthermore, chronic drug treatments are more relevant to the clinical situation where patients are treated for several weeks or months. The vast majority of *in vivo* studies administering imatinib and sunitinib have done so for periods of up to 6 weeks for imatinib (Kerkelä *et al.*, 2006; Wolf *et al.*, 2010) and up to 12 weeks for sunitinib (Chu *et al.*, 2007; Kerkelä *et al.*, 2009).

In this Chapter, the drugs tested in Chapters 2 and 3, with the exception of ouabain, were chronically administered to further assess whether drugs that exhibit effects on cardiac contractility *in vivo* may alter CaMKIIδ expression and/or CaMKII activity. In Chapter 2 drug effects on cardiac contractility were assessed via $LVdP/dt_{max}$ and the QA interval. However, as discussed in Chapter 4 these indices may be additionally influenced by factors such as heart rate and cardiac loading. For these reasons, in this Chapter echocardiography was incorporated as an additional assessment of cardiac contractility.

Ultrasound imaging is increasingly used to assess cardiovascular function (echocardiography). Echocardiography is based on the fact that sound is made up of several different frequency waves. The very high frequency range is inaudible to the human ear, i.e. ultrasound. The transducer beams ultrasound waves through the chest wall. When the beam encounters a boundary or interface between tissues of different acoustic impedance (due to a difference in density), part of the beam is reflected back to the transducer. The remaining ultrasound waves move through the tissue until they too are reflected back to the transducer. The transducer transmits ultrasound and constantly receives reflected waves. The reflected waves are collected and analysed by an ultrasound machine. By calculating the amount of time it takes for the beam to travel from and to the transducer, plus the consistency and changes in position of the different tissues that it passes through, the ultrasound machine can determine the shape, size, density and movement of all tissues that lie in the path of the ultrasound beams (Coatney, 2001).

Echocardiography allows quick and real-time imaging of the heart and provides structural, functional and haemodynamic information. With two-dimensional (2D)

and motion (M) mode imaging, the LV dimensions can be measured and using formulae established in human echocardiography, LV systolic function parameters, such as fractional shortening (FS), can be calculated (Coatney, 2001). FS refers to the percentage change in the diameter of the LV from diastole to systole and is calculated from the internal systolic and diastolic dimensions. FS is commonly used to assess cardiac contractility following surgical, drug or genetic interventions (Coatney, 2001).

5.1.1 Aims

To test the hypothesis that drugs altering cardiac contractility may do so via actions on CaMKII the aims of the work described in this Chapter were:

(i) To investigate the effects of known and potential inotropic agents on cardiac contractility and haemodynamics following chronic *in vivo* drug administration.

(ii) To assess concomitant changes in CaMKIIδ expression and/or CaMKII activity in LV tissue obtained from chronic *in vivo* drug-treated guinea pigs.

5.2 Methods

Suppliers of equipment and materials are detailed in Appendix A. Suppliers of drugs and reagents and their storage information are detailed in Appendix B.

5.2.1 Animals

All animal experiments were performed in accordance with the UK Animals (Scientific Procedures) Act 1986, approved by institutional ethical review committees and conducted under the authority of Project Licences held at the University of Strathclyde.

A total of thirty-six male Dunkin Hartley guinea pigs weighing 420 – 620 g at the start of procedures were allowed a minimum of one week acclimatisation following arrival and were housed in small groups on hay. Rooms were held at a temperature of 21°C, with 45 to 65% relative humidity and a 12 hour light/dark cycle. Food (Special Diet Services FD1 guinea pig diet) and water were available ad libitum.

5.2.2 Experimental protocol

On day 0 guinea pigs were anaesthetised and echocardiography was performed. An osmotic minipump was then implanted to deliver isoprenaline (0.372 mg kg^{-1} day^{-1}), verapamil (10 mg kg^{-1} day^{-1}), imatinib (100 mg kg^{-1} day^{-1}), sunitinib (20 mg kg^{-1} day^{-1}) or vehicle (0.1% acidified saline) over 6 days.

On day 6, guinea pigs were re-anaesthetised and echocardiography was repeated. Immediately following this guinea pigs were transferred for haemodynamic assessment. After allowing stabilisation of anaesthesia and recovery from surgical preparation, haemodynamic data were recorded.

Following completion of the haemodynamic assessment, the heart was immediately removed for subsequent biochemical and histological analysis and blood was collected for plasma preparation as described in Section 2.2.6. Plasma was then used for assessment of drug and cardiac troponin I levels.

5.2.3 Anaesthesia

Guinea pigs were anaesthetised with a combination of Hypnorm® and Hypnovel® (6 mL kg^{-1} i.p.) for echocardiography and minipump implantation. The anaesthesia was prepared as detailed in Table 2.1. At the dose given, guinea pigs breathed spontaneously and so artificial ventilation was not required.

Guinea pigs were transferred to sodium pentobarbital anaesthesia for final haemodynamic assessments. Before beginning surgical preparations, the level of anaesthesia was assessed by checking the corneal and pedal withdrawal reflexes. If required, guinea pigs were given a bolus dose of pentobarbital (3 mg i.p.). Most guinea pigs generally required between one and three bolus doses. Immediately following insertion of the jugular venous cannulae guinea pigs were given a continuous infusion of sodium pentobarbital to maintain anaesthesia as described in Table 2.1.

5.2.4 Echocardiography

Six guinea pigs were used to optimise the echocardiography procedure. In these guinea pigs the dose and suitability of anaesthesia was first assessed using the Hypnorm® and Hypnovel® mix used in Chapter 2. This was followed by assessing the effect of animal and transducer positioning on image quality. To determine the best positions the guinea pig was placed at different angles in the supine position.

The transducer was then positioned in various locations across the chest wall. Once positions were located that gave good quality 2D short-axis views of the LV along with good M-mode images, baseline measurements of LV diastolic diameter (LVDD), LV systolic diameter (LVSD) and FS were taken and compared to values reported in the literature.

Following optimisation of the echocardiography procedure, thirty guinea pigs were used to investigate drug effects on cardiac contractility, haemodynamics and CaMKII expression/activity. These animals were weighed and, once adequate anaesthesia was reached, guinea pigs were placed on a heat mat in the supine position with the head distal to the operator. Hair was removed from the chest by shaving followed by application of a depilatory cream. Guinea pigs were then rolled slightly onto their left side.

A layer of pre-warmed ultrasound gel was applied to the ultrasound transducer and transthoracic echocardiography was performed using an HDI® 3000CV ultrasound system. The transducer was positioned at 90º to the guinea pig body and placed in the intercostal spaces to the left of the sternum in the anterior axillary line at the level of the heart. The probe was rotated very slightly in both directions until a clear 2D short-axis image of the LV was achieved (see Figure 5.1a for example). M-mode images were then acquired.

During each echocardiography assessment three M-mode images were taken and LVDD and LVSD were measured at three different points within each image. These measurements were used to calculated individual FS values according to the equation FS = (LVDD-LVSD/LVDD) * 100. Data were then averaged to give one value for each guinea pig pre- and post-drug.

5.2.5 Surgical preparation for minipump implantation and final haemodynamic assessment

Immediately following echocardiography on day 0, guinea pigs were transferred to the prone position and an incision was made just below the neck between the shoulder blades. A subcutaneous pocket angled towards the flank was made and an osmotic minipump loaded with test drug was inserted. The wound was then closed using four to five 9 mm AutoClips per guinea pig. Guinea pigs were recovered overnight with each being singly housed in a cage with saw dust. Food

and water were provided and a heated mat was placed underneath the cage. The following morning guinea pigs were returned to group housing.

For haemodynamic measurements after 6 days of drug or vehicle treatment, guinea pigs were surgically prepared as detailed in Section 2.2.3.2. A stabilisation period of at least 20 min was allowed following completion of the surgical preparation.

Haemodynamic data were acquired at the University of Strathclyde as detailed in Section 2.2.4. The same parameters were analysed and data were averaged over a 15 min period.

5.2.6 Buffer compositions

Buffer compositions are detailed in Section 3.2.1.

5.2.7 Tissue preparation

Untreated and *in vivo* drug-treated tissues were prepared as detailed in Section 3.2.2. However, before the LV was cut into chunks the whole heart was quickly weighed. A transverse section through both the left and right ventricles was then taken and fixed in 10% formalin for subsequent histological analysis.

5.2.8 Determination of protein content

Total protein content of LV homogenates was determined as detailed in Section 3.2.3.

5.2.9 Electrophoresis and immunoblotting

CaMKIIδ and pThr286-CaMKII expression were determined as detailed in Section 3.2.4.

To measure CaMKII activity by an additional method, pSer2815-RyR (RyR phosphorylated at the CaMKII specific site, Ser2815) expression was assessed. The migration characteristics of RyR were first confirmed using a mouse anti-RyR monoclonal antibody (1:4000). For detection of pSer2815-RyR 7% Tris-acetate gels and Tris-acetate running buffer were used. Gels were subjected to electrophoresis as before for 50 min. Proteins were transferred as before and membranes were blocked in blocking buffer 2. Blots were incubated overnight at 4ºC with the pSer2815-RyR primary antibody. Membranes were washed and incubated for 2h at room temperature with the anti-rabbit secondary antibody used previously (Section

2.2.4). Primary (1:2000) and secondary (1:5000) antibodies were diluted to the required concentration in antibody incubation buffer 2. Blots were then washed before being treated with ECL reagent and exposed on to film and processed as before. Molecular weight (MW) markers were used to identify pSer2815-RyR (MW = 565 kDa).

Normalisation within gels was done as described previously (Section 3.2.4). pSer2815-RyR:GAPDH ratios were then normalised to the pSer2815-RyR:GAPDH ratio of a chronic isoprenaline treated sample included in every gel for normalisation between gels.

5.2.10 CaMKII activity assay

Assessment of activity via the radioactive assay was performed as detailed in Section 3.2.5.

5.2.11 Plasma drug levels

Concentrations of drugs in plasma samples were determined as detailed in Section 2.2.6.

5.2.12 Plasma cardiac troponin I levels

Blood samples were collected and plasma prepared as described in Section 2.2.6. Plasma samples were analysed by Sue Bickerton at AstraZeneca using the Siemens ADVIA Centaur® CP Immunosystem TnI-Ultra™ assay.

5.2.13 Histology

Histological assessments were performed by John Foster at AstraZeneca.

Transverse sections of the left and right ventricle were trimmed to approximately 2-3 mm thick slices in the transverse direction and placed into a graded series of ethanol dilutions (70%, 90%, 100%) followed by toluene, paraffin wax (60°C) and embedded in paraffin wax. Each stage was approximately 1h. Sections (4-5 µM) were then cut on a microtome, floated onto a water bath at 55°C and mounted onto charged glass slides and dried overnight at 40°C in an oven. The wax was removed from the slides by immersing in toluene and the slides were taken through a reverse alcohol gradation (100%, 90%, 70%) and into water. Slides were then stained with haematoxylin and eosin (H & E).

The stained sections were first examined by eye to assess any obvious changes in the volume of the chambers of the heart. The examination was done without knowledge of the groups. The sections were then examined under a light microscope beginning at the lowest magnification possible (2.5x) and progressing to higher magnifications if changes were observed at the lower magnifications. This examination was conducted with knowledge of the groups.

5.2.14 Statistical analysis

Data are presented as mean ± S.E.M. One-way ANOVA followed by Dunnett's tests or Tukey's test, or Kruskal-Wallis tests (for data that were not distributed normally), were used for comparisons among groups. Paired *t* tests were used to compare values pre- and post-drug administration. Statistical tests were performed using StatsDirect software.

5.2.15 Drugs

Details for isoprenaline, verapamil, imatinib and sunitinib are as described in Section 2.2.8. All drugs were dissolved in 0.1% ascorbic acid in 0.9% w/v NaCl, except imatinib which was dissolved in 0.9% w/v NaCl. Doses were chosen following a review of the literature cited in Section 5.1 and 5.4.

5.3 Results

5.3.1 Optimisation of echocardiography

In the first guinea pig tested the Hypnorm® and Hypnovel® mix was given at a dose of 8 mL kg^{-1}. Whilst anaesthetised, the guinea pig's spontaneous respiration was erratic and oxygen supplements were required frequently. This guinea pig also took several hours to recover from the anaesthesia. In subsequent guinea pigs, the dose of Hypnorm/Hypnovel was reduced to 6 mL kg^{-1}. These guinea pigs recovered more quickly (within a couple of hours) and spontaneous respiration was much improved.

For echocardiography to be performed guinea pigs were initially positioned with their head proximal to the operator. This position was, however, uncomfortable for the operator and restricted arm movement when manipulating the transducer. These issues were resolved by turning the guinea pig 180º so that the head was distal to the operator allowing more room for movement. Guinea pigs were initially laid flat

on their back and imaging was attempted at the level of the heart at several points from the right side of the chest across to the left. Imaging from the left side along the anterior axillary line gave the clearest images which were further improved when guinea pigs were rolled slightly onto their left side.

Baseline LV measurements were made for comparison to published values obtained by echocardiography in guinea pigs. LVDD was 6.00 ± 0.00 mm, LVSD was 2.26 ± 0.00 and FS was 64.16 ± 0.01%. Across seven papers (Ramírez-Gil *et al.*, 1998; Wang *et al.*, 1999; Ennis *et al.*, 2002; Bodi *et al.*, 2005; Cetin *et al.*, 2005; Micheletti *et al.*, 2007; Sharma *et al.*, 2007) the ranges of reported values were: LVDD, 6.1 ± 0.4 mm to 12.1 ± 0.6 mm; LVSD 2.8 ± 0.3 mm to 6.3 ± 0.18 mm; FS 28.0 ± 1.5 to 52.9 ± 6.6 mm.

5.3.2 Effects of chronic *in vivo* drug treatment on cardiac contractility and haemodynamics

Echocardiography was performed before and after drug treatments. LVDD and LVSD were measured and used to calculate FS. An example echocardiography recording is shown in Figure 5.1. LVDD was not altered following any drug treatments except with isoprenaline where LVDD increased by 23% (Figure 5.2). Following sunitinib treatment, however, LVDD came close to being significantly increased by 19%. LVSD also increased following isoprenaline administration (89%) and additionally, LVSD increased following verapamil administration (34%). No other significant changes in LVSD were found (Figure 5.3). FS significantly decreased in both isoprenaline and verapamil groups by 28% and 24%, respectively, and was unchanged by other treatments (Figure 5.4).

Haemodynamic parameters were assessed following drug administration (Table 5.1). Heart rate was not altered significantly in any treatment group compared to vehicle. Systolic, diastolic and mean arterial blood pressures were largely unchanged in all groups except with verapamil which decreased all arterial blood pressure parameters. Additionally, imatinib and sunitinib tended to decrease diastolic blood pressure although neither reached statistical significance (P = 0.068 and 0.101, respectively). LVP was unchanged by all treatments except isoprenaline which increased LVEDP. $LVdP/dt_{max}$ was unchanged in every group except with verapamil which decreased $LVdP/dt_{max}$. Finally, the QA interval was not changed significantly in any group although the apparent decrease in the QA interval

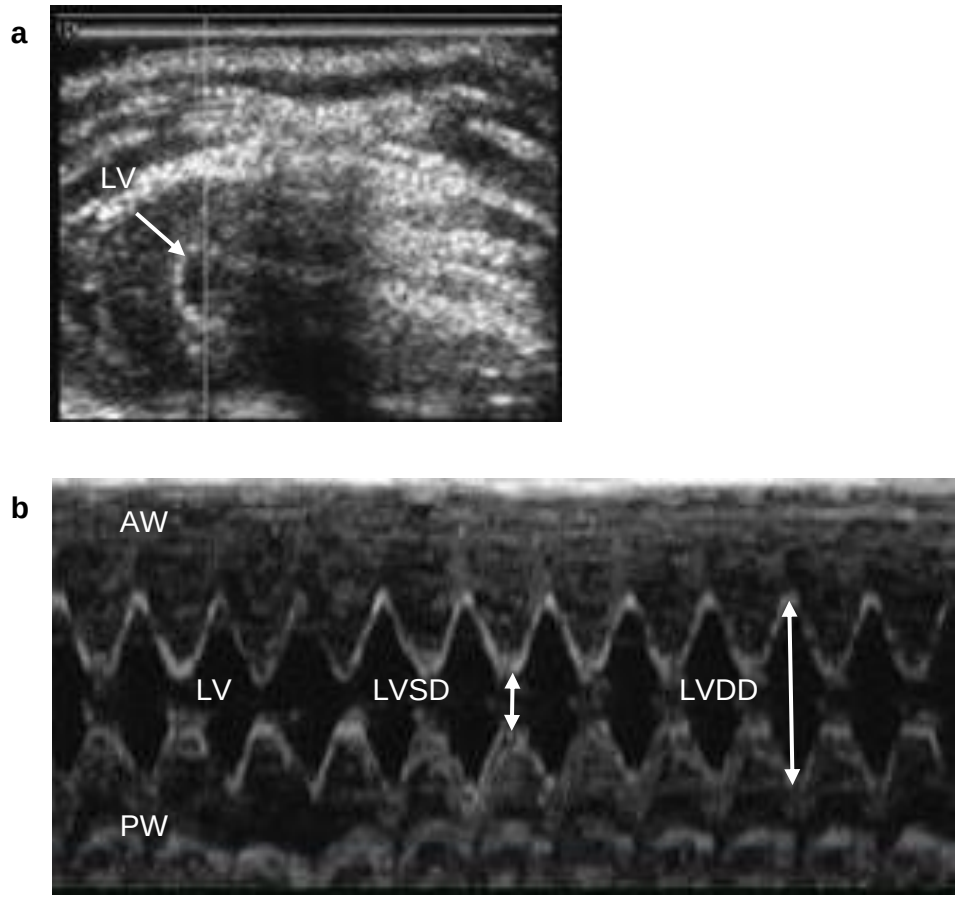

Figure 5.1 Example of echocardiography recordings pre-drug treatment. **a)** Two-dimensional short axis view of the left ventricle. **b)** M-mode recording indicating the lumen of the left ventricle (LV), anterior wall (AW), posterior wall (PW), LV systolic diameter (LVSD) and LV diastolic diameter (LVDD).

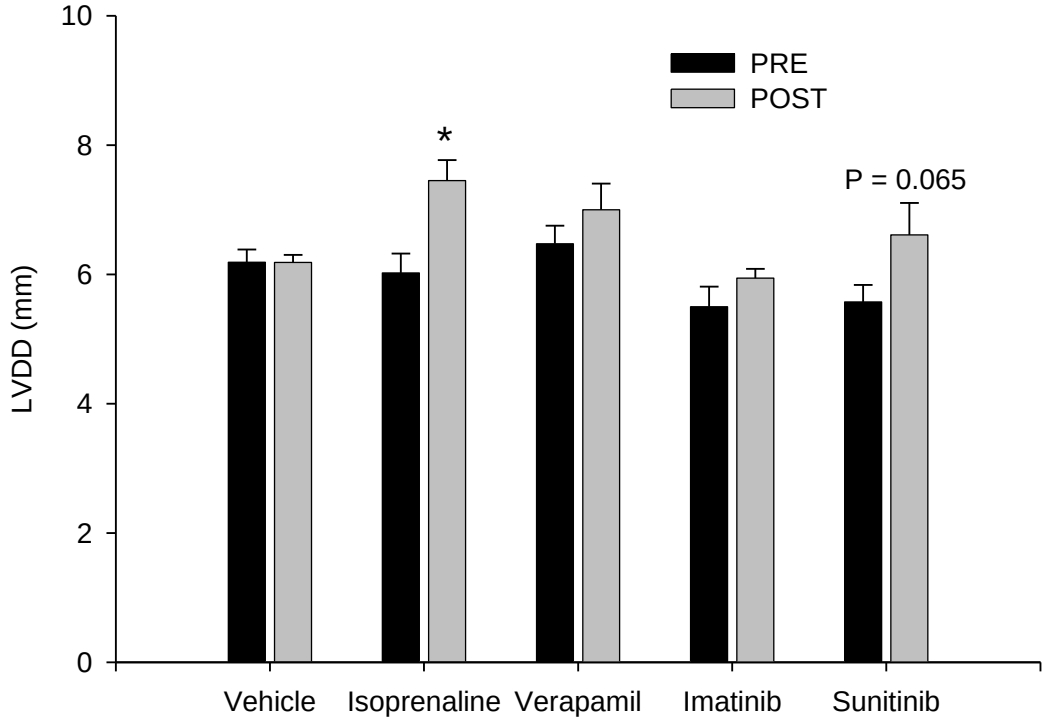

Figure 5.2 Left ventricular diastolic diameter (LVDD) pre and post chronic *in vivo* drug administration. Data are presented as mean ± S.E.M values. Vehicle, verapamil, and sunitinib n = 6, isoprenaline n = 7, imatinib n = 5. * indicates P<0.05 compared to pre-drug value group, paired *t* test.

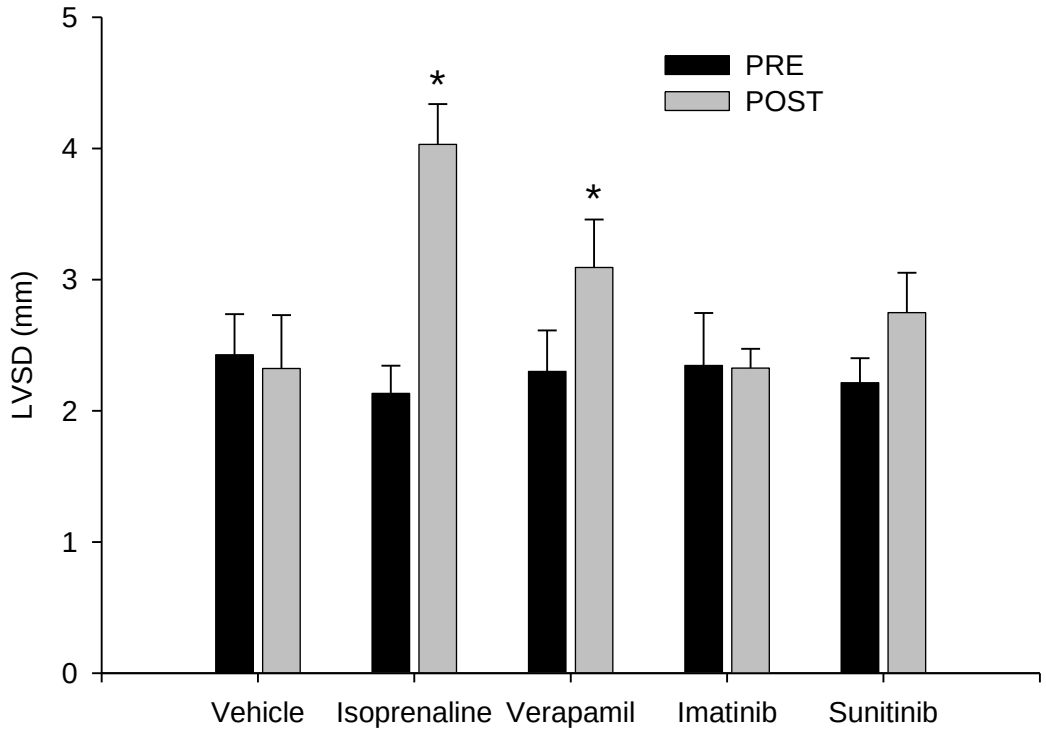

Figure 5.3 Left ventricular systolic diameter (LVSD) pre and post chronic *in vivo* drug administration. Data are presented as mean ± S.E.M values. Vehicle, verapamil, and sunitinib n = 6, isoprenaline n = 7, imatinib n = 5. * indicates $P<0.05$ compared to pre-drug value group, paired *t* test.

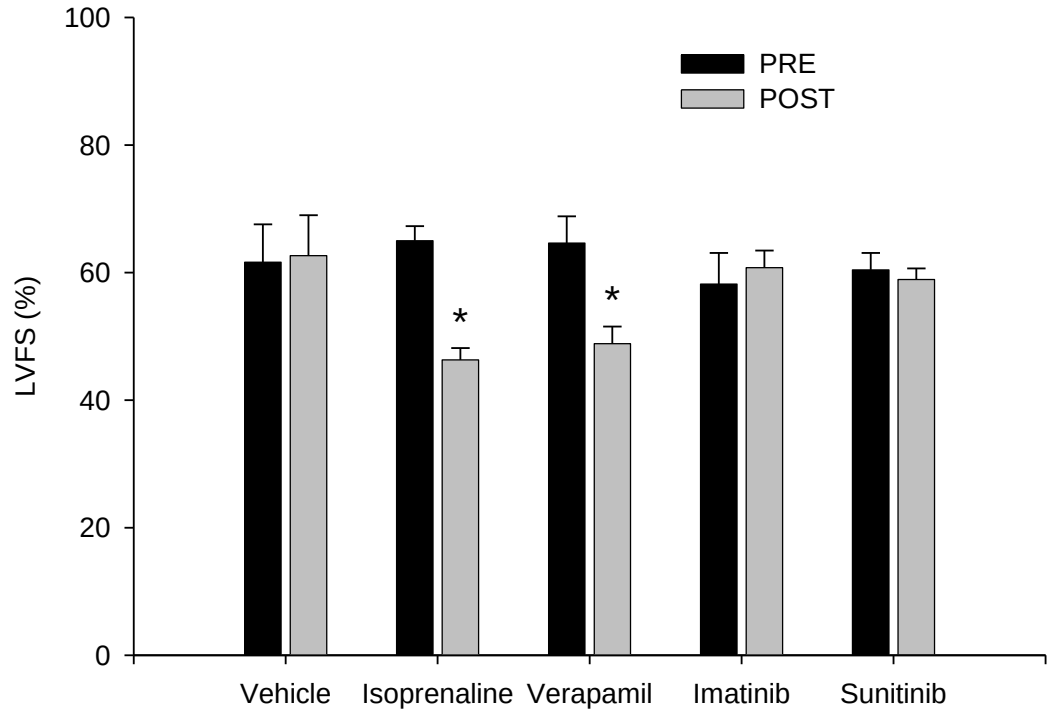

Figure 5.4 Left ventricular fractional shortening (FS) pre and post chronic *in vivo* drug administration. Data are presented as mean ± S.E.M values. Vehicle, verapamil, and sunitinib n = 6, isoprenaline n = 7, imatinib n = 5. * indicates P<0.05 compared to pre-drug value group, paired *t* test.

Table 5.1 Haemodynamic responses following chronic *in vivo* drug administration

	Heart rate (beats min^{-1})	**SBP (mmHg)**	**DBP (mmHg)**	**MABP (mmHg)**	**LVSP (mmHg)**	**LVEDP (mmHg)**	**$LVdP/dt_{max}$ (mmHg s^{-1})**	**QA interval (ms)**
Vehicle	288 ± 20	57 ± 3	36 ± 2	44 ± 3	56 ± 3	-3 ± 2	4809 ± 484	36 ± 1
Isoprenaline	300 ± 5	58 ± 2	37 ± 2	46 ± 1	64 ± 4	4 ± 3*	4779 ± 169	37 ± 2
Verapamil	264 ± 14	42 ± 3*	24 ± 3*	31 ± 3*	46 ± 2	-6 ± 1	3176 ± 436*	39 ± 3
Imatinib	318 ± 17	55 ± 3	28 ± 3	37 ± 3	48 ± 2	-6 ± 1	4938 ± 574	30 ± 1
Sunitinib	283 ± 4	53 ± 3	29 ± 1	38 ± 2	62 ± 6	-2 ± 1	4548 ± 156	35 ± 1

DBP, diastolic blood pressure; MABP, mean arterial blood pressure; $LVdP/dt_{max}$, left ventricular dP/dt_{max}; LVEDP, left ventricular end-diastolic blood pressure; LVSP, left ventricular systolic blood pressure; SBP, systolic blood pressure. Data are presented as mean ± S.E.M. Vehicle, verapamil, and sunitinib n = 6, isoprenaline n = 7, imatinib n = 5. * indicates $P<0.05$ compared to vehicle group, one way ANOVA plus Dunnett's test.

following imatinib administration came close to significance (P = 0.083).

5.3.3 Plasma drug levels

For each drug, except isoprenaline, total plasma concentrations were measured. PPB data was then determined allowing free drug concentrations to be calculated (Table 5.2). The total concentration of imatinib was higher than that of both verapamil and sunitinib. This was then followed by verapamil which was approximately 10-fold lower, then sunitinib which was approximately 100-fold lower. PPB values were as described in Section 2.3.5 with verapamil and sunitinib being fairly similar, but imatinib being much more highly bound. This led to the free concentration of verapamil being higher than the free concentration of imatinib. The free concentration of sunitinib was very low.

5.3.4 Effects of chronic *in vivo* drug administration on CaMKII expression and activity

Following chronic administration of isoprenaline, verapamil, imatinib, sunitinib, or vehicle *in vivo,* LV homogenates were prepared and CaMKIIδ expression and CaMKII activity were assessed.

Across all treatment groups CaMKIIδ expression was significantly increased compared to the vehicle group (Figure 5.5). Verapamil caused the biggest increase (96%), followed by imatinib (62%) whilst sunitinib and isoprenaline increased CaMKIIδ expression by a similar extent (23 and 22%, respectively).

Assessment of CaMKII activity by immunoblotting for the autophosphorylated form of CaMKII (pThr286-CaMKII) showed no significant effects in any treatment group compared to vehicle (Figure 5.6). However, assessment of CaMKII activity by the radioactive assay showed a significant increase in CaMKII activity in all groups (Figure 5.7). The biggest increase was in the sunitinib group (110%), followed by isoprenaline (78%), verapamil (70%) and imatinib (50%). Similarly, immunoblotting for pSer2815-RyR as a marker of CaMKII activity also indicated increased CaMKII activity across all treatment groups compared to vehicle (Figure 5.8). Again the biggest increase was following sunitinib treatment (123%), but this time it was followed by imatinib (61%) then isoprenaline and verapamil which were similarly affected showing increases in pSer2815-RyR expression of 16 and 12%, respectively.

Table 5.2 Drug concentrations measured in blood plasma following chronic *in vivo* drug administration

Drug	Dose given (mg kg^{-1} day^{-1})	Total plasma concentration (μM)	PPB (% free)	Calculated free concentration (μM)
Verapamil	10	0.157 ± 0.021	19.44	0.030 ± 0.004
Imatinib	100	1.359 ± 0.381	0.37	0.005 ± 0.002
Sunitinib	20	0.009 ± 0.002	13.40	0.001 ± 0.000

PPB, plasma protein binding. Data are presented as mean ± S.E.M. Verapamil and sunitinib n = 6, imatinib n = 5.

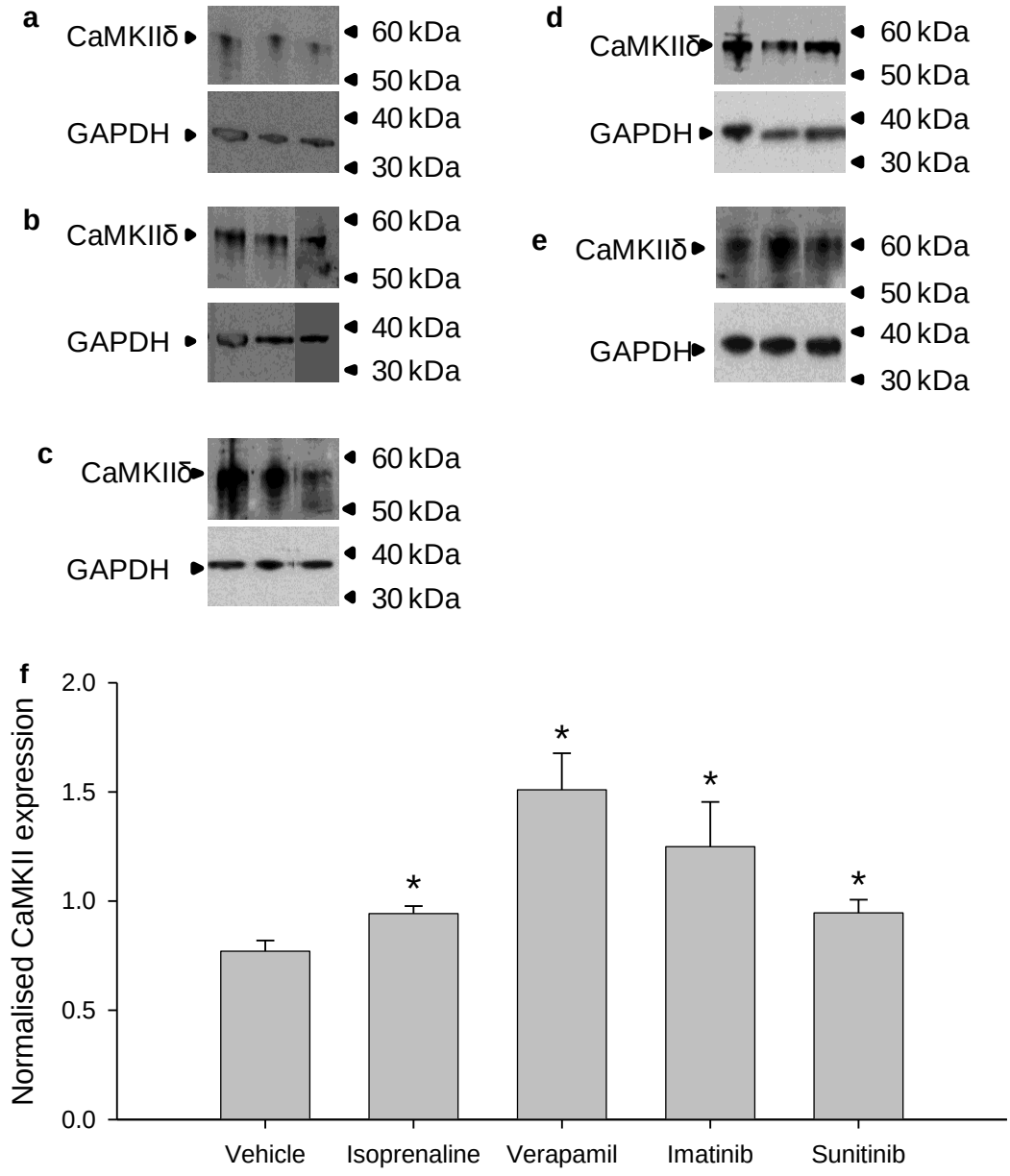

Figure 5.5 CaMKIIδ expression following chronic *in vivo* drug administration. Representative blots in triplicate following administration of **a)** vehicle, **b)** isoprenaline, **c)** verapamil, **d)** imatinib, **e)** sunitinib. Pooled data for each treatment are shown in **f)**. Data are presented as mean ± S.E.M values. Vehicle, verapamil, and sunitinib n = 6, isoprenaline n = 7, imatinib n = 5. * indicates $P<0.05$ compared to vehicle group, Kruskal-Wallis test.

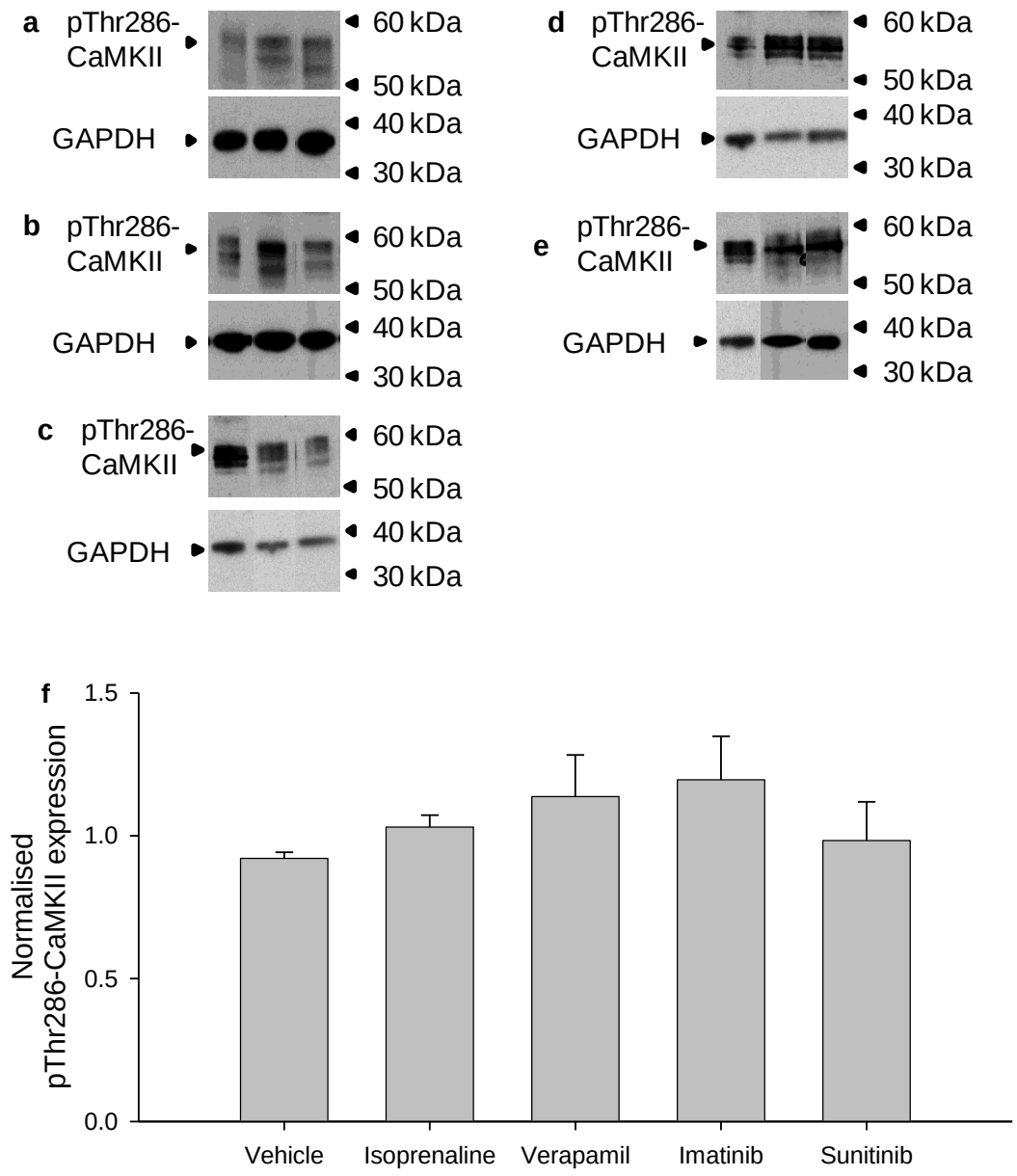

Figure 5.6 CaMKII activity assessed via the pThr286-CaMKII expression following chronic *in vivo* drug administration. Representative blots in triplicate following administration of **a)** vehicle, **b)** isoprenaline, **c)** verapamil, **d)** imatinib, **e)** sunitinib. Pooled data for each treatment are shown in **f)**. Data are presented as mean ± S.E.M values. Vehicle, verapamil, and sunitinib n = 6, isoprenaline n = 7, imatinib n = 5. There were no significant differences in any treatment group compared to vehicle, Kruskal-Wallis test.

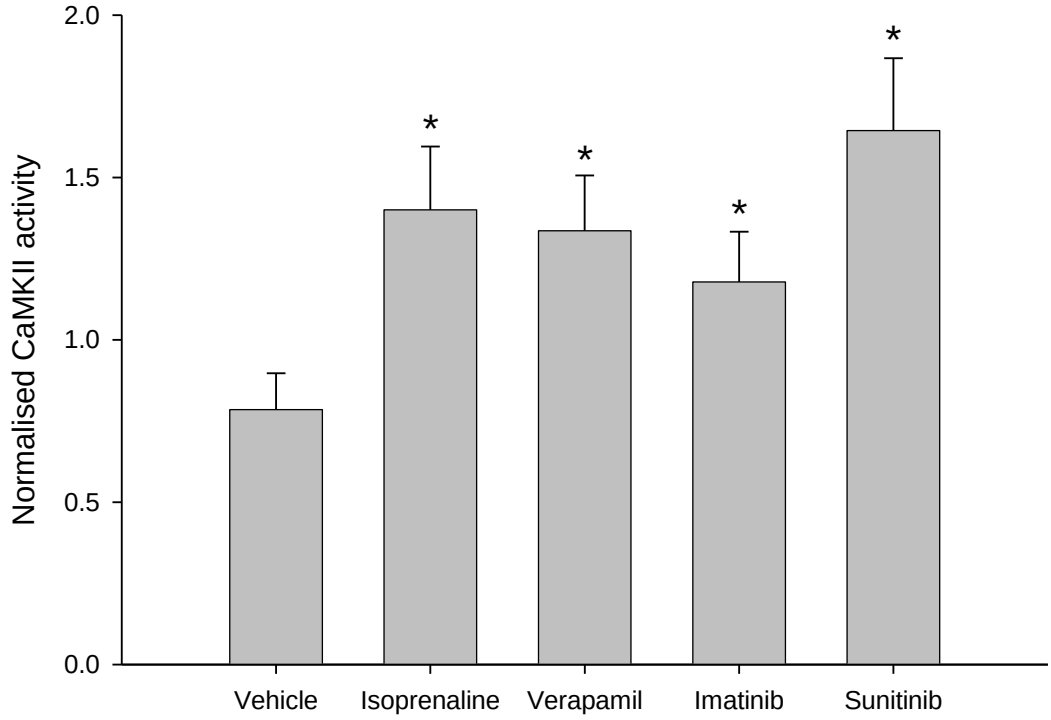

Figure 5.7 CaMKII activity assessed via the radioactive assay following chronic *in vivo* drug administration. Data are presented as mean ± S.E.M values. Vehicle, verapamil, and sunitinib n = 6, isoprenaline n = 7, imatinib n = 5. * indicates $P<0.05$ compared to vehicle group, Kruskal-Wallis test.

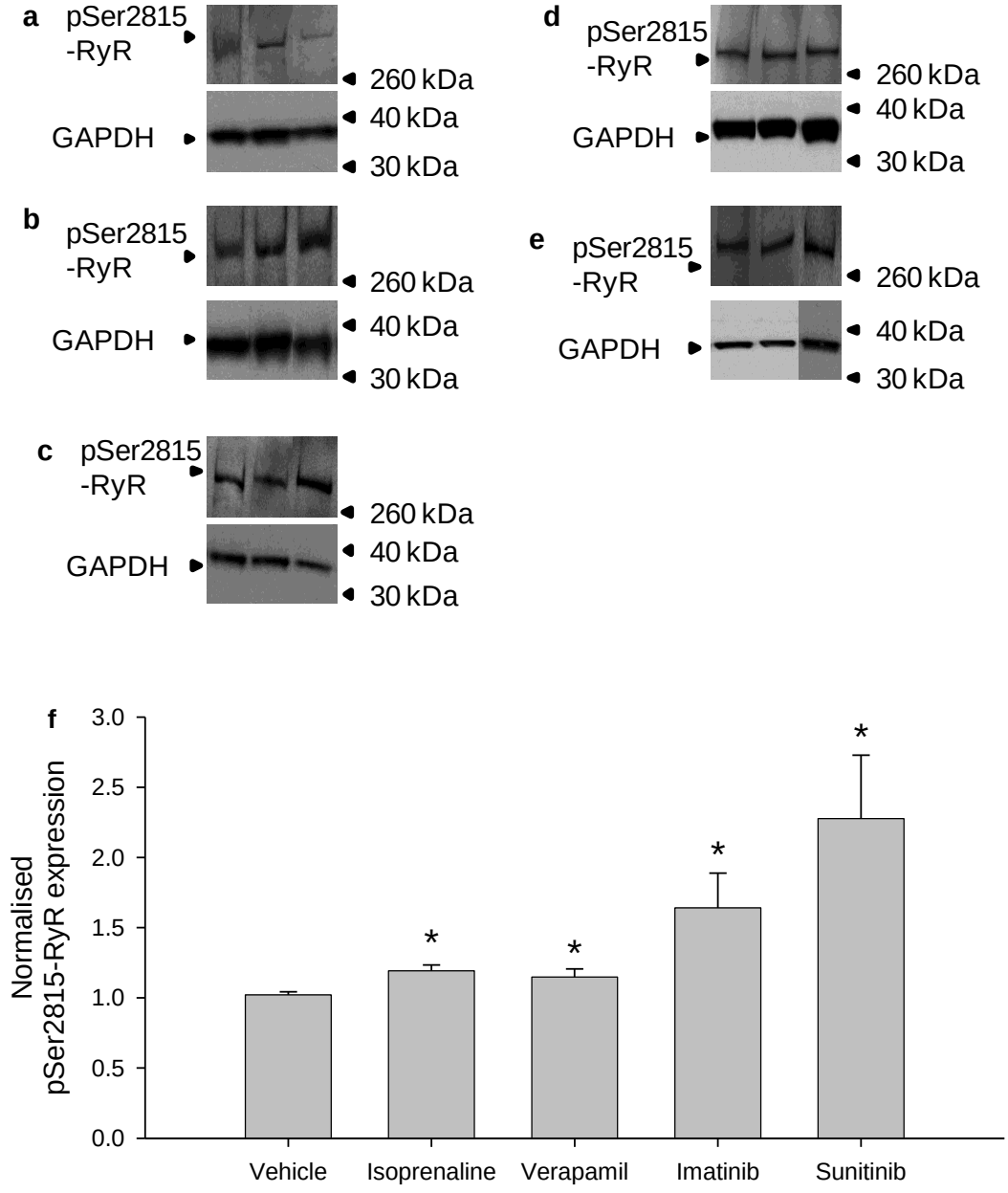

Figure 5.8 CaMKII activity assessed via pSer2815-RyR expression following chronic *in vivo* drug administration. Representative blots in triplicate following administration of **a)** vehicle, **b)** isoprenaline, **c)** verapamil, **d)** imatinib, **e)** sunitinib. Pooled data for each treatment are shown in **f)**. Data are presented as mean ± S.E.M values. Vehicle, verapamil, and sunitinib n = 6, isoprenaline n = 7, imatinib n = 5. * indicates $P<0.05$ compared to vehicle group, Kruskal-Wallis test.

5.3.5 Assessment of cardiac damage

As a marker of cardiac damage plasma cardiac troponin I levels were measured for each drug treatment (Table 5.3). The only drug to significantly alter cardiac troponin I levels was verapamil which significantly increased the concentration of cardiac troponin I.

As a second assessment of cardiac damage, ventricular samples were histologically assessed for gross morphological changes. Across all treatment groups there were no gross changes to either the ventricular volume or ventricular muscle and no histological changes were observed in the myocardium or vasculature.

Guinea pigs were weighed before and after drug treatments and the heart was weighed immediately after removal following the final haemodynamic assessment. These measurements along with the actual body weight gain, the body weight gain as a percentage of pre-drug body weight, and the heart:body weight ratio are shown in Table 5.4. All treatment groups were significantly lighter than the vehicle group before treatments. There were no significant differences in actual body weight gain or body weight gain as a percentage of pre-drug body weight compared to vehicle group. There were also no significant differences in heart:body weight ratios compared to vehicle group.

Table 5.3 Cardiac troponin I concentrations measured in blood plasma following chronic *in vivo* administration

Drug	**Cardiac troponin I (ng mL^{-1})**
Vehicle	1.42 ± 0.47
Isoprenaline	1.80 ± 0.37
Verapamil	9.16 ± 4.76*
Imatinib	2.24 ± 0.54
Sunitinib	3.56 ± 1.13

Data are presented as mean ± S.E.M. Vehicle, verapamil, and sunitinib n = 6, isoprenaline and imatinib n = 5. * indicates $P<0.05$ compared to vehicle group, Kruskal-Wallis test.

Table 5.4 Guinea pig weights pre and post chronic *in vivo* drug administration

Drug group	Pre-drug body weight (g)	Post-drug body weight (g)	Weight gain (g)	Weight gain (%)	Heart weight (g)	Heart:body weight ratio (x1000)
Vehicle	540 ± 17	581 ± 16	41 ± 1	7.53 ± 0.42	1.92 ± 0.07	3.31 ± 0.12
Isoprenaline	468 ± 24*	511 ± 34	43 ± 11	8.97 ± 1.98	1.49 ± 0.09	2.91 ± 0.04
Verapamil	447 ± 8*	476 ± 9	29 ± 7	6.52 ± 1.61	1.54 ± 0.05	3.25 ± 0.11
Imatinib	463 ± 13*	486 ± 26	23 ± 14	4.76 ± 2.92	1.56 ± 0.05	3.20 ± 0.11
Sunitinib	459 ± 15*	511 ± 26	52 ± 19	11.25 ± 4.09	1.64 ± 0.10	3.25 ± 0.25

Data are presented as mean ± S.E.M. Vehicle, verapamil, and sunitinib n = 6, isoprenaline and imatinib n = 5. * indicates $P<0.05$ compared to all other groups, one way ANOVA plus Tukey's test. There were no significant differences in weight gain (g) or weight gain as a percentage of pre-drug body weight compared to vehicle group, one way ANOVA, plus Dunnett's test. There were no significant differences in heart:body weight ratios, one way ANOVA, plus Dunnett's test.

5.4 Discussion

5.4.1 Main findings

This work demonstrates that chronic *in vivo* administration of both isoprenaline and verapamil for 6 days decreased cardiac contractility whilst imatinib and sunitinib had no effects over this time period. Following *in vivo* drug administration CaMKIIδ expression was increased across all treatment groups. Assessment of CaMKII activity by immunoblotting for pThr286-CaMKII showed no significant effects on CaMKII activity. However, using both the radioactive assay and immunoblotting for pSer2815-RyR, CaMKII activity was found to be increased by all drug treatments.

5.4.1.1 Optimisation of echocardiography

Echocardiography was employed as an additional measure of cardiac contractility as $LVdP/dt_{max}$ and the QA interval can be affected by factors other than contractility, as shown in Chapter 4. As echocardiography assessment is a non-invasive procedure it was possible to easily obtain pre- and post-drug measurements, allowing direct comparisons of drug effects within each animal.

Although echocardiography is non-invasive, animals need to be kept still for good quality images to be obtained and accurate measurements to be made. In some cases conscious animals are restrained by use of a sling, however, this requires training of animals to familiarise them with the procedure. Alternatively anaesthesia is used to immobilise the animal. As the first echocardiography assessment on day 0 was a recovery procedure, pentobarbital anaesthesia was unsuitable. Furthermore, under pentobarbital anaesthesia guinea pigs need to be artificially ventilated and cannulation of the trachea may interfere with image quality during echocardiography. Therefore, for echocardiography assessment guinea pigs were anaesthetised using a combination of Hypnorm® and Hypnovel® which allowed guinea pigs to breathe spontaneously. The Hypnorm® and Hypnovel® mix was tested in Chapter 2 at a dose of 8 mL kg^{-1}, however, these guinea pigs were not allowed to recover from anaesthesia. When this dose was tested in a recovery procedure the guinea pig took several hours to recover. In addition, whilst anaesthetised, spontaneous respiration was erratic and oxygen supplements were required frequently. On reducing the dose of Hypnorm/Hypnovel to 6 mL kg^{-1} guinea pigs recovered more quickly (within a couple of hours) and spontaneous

respiration was much improved. Another problem encountered with previous Hypnorm/Hypnovel experiments was a slow decline in heart rate from about 15 min becoming significantly decreased at 45 min (Figure 2.5). Although heart rate was not assessed during echocardiography, measurements were generally completed in around 15 to 30 min, i.e. before heart rate declined significantly. In addition the lower dose may also have prevented this from occurring although this was not assessed.

Prior to experiments in drug-treated animals, the procedure and measurements for echocardiography were determined. The guinea pig and transducer were positioned to give the highest quality images and be comfortable for the operator. Baseline measurements of LVDD, LVSD and FS were highly consistent with low errors associated with the mean values. On consulting previous studies that used echocardiography to measured these parameters in guinea pig, a very wide range of values were found (Ramírez-Gil *et al.*, 1998; Wang *et al.*, 1999; Ennis *et al.*, 2002; Bodi *et al.*, 2005; Cetin *et al.*, 2005; Micheletti *et al.*, 2007; Sharma *et al.*, 2007). The measurements made in the present study tended to fall close to the lower end of these ranges for LVDD and LVSD and, correspondingly, the upper end for FS. LVDD was very close to the values reported by Wang *et al.* (1999) and Cetin *et al.* (2005). However, LVSD tended to be slightly lower than previously reported values resulting in a slightly higher FS.

5.4.1.2 Assessment of cardiac contractility and haemodynamics following chronic in vivo drug administration

Drug effects on cardiac contractility and haemodynamics were assessed as in Chapter 2 using $LVdP/dt_{max}$ and the QA interval as indices of contractility. In addition, echocardiography was also employed providing pre- and post-drug measurements in each animal.

Isoprenaline

Chronic isoprenaline administration caused LVDD and LVSD to increase indicating an enlargement of the LV (Figure 5.2 and Figure 5.3). Importantly, the increase in LVSD was greater than the increase in LVDD leading to an overall decrease in FS (Figure 5.4). Therefore, isoprenaline had a negative inotropic effect when cardiac contractility was assessed via echocardiography.

Isoprenaline, as explained in Section 2.4.1.1, is a non-selective β-adrenoceptor agonist. Numerous studies have shown that chronic stimulation of the β_1-adrenoceptor is detrimental to cardiac function causing hypertrophy, heart failure and even death (Kudej *et al.*, 1997; Kitagawa *et al.*, 2007; Takeshita *et al.*, 2008). The majority of these studies have been performed in rats and mice and the doses of isoprenaline and duration of treatment vary greatly between studies. The guinea pig is less commonly used and previous studies (Maisel *et al.*, 1987) have used higher doses of isoprenaline and longer durations of treatment (3.5 mg^{-1} kg^{-1} day for 14 days) than used here. The cited study (Maisel *et al.*, 1987) reported a decrease in β-adrenoceptor number and AC activity, and β-adrenoceptor sequestration along with an increase in LV:body weight ratio and hypertrophy. The functional effects in the current study (i.e. the decrease in fractional shortening) were fairly modest and histological analysis did not identify any hypertrophic effects. This may be due to the lower dose and duration of isoprenaline administered.

It should be noted that $LVdP/dt_{max}$ and the QA interval were not significantly altered in the isoprenaline group compared to the vehicle group suggesting no significant changes in contractility (Table 5.1). This could indicate that echocardiography is a more sensitive measure of contractility, however, as described in Chapter 4 changes in heart rate and cardiac loading could influence both $LVdP/dt_{max}$ and the QA interval. Although no significant changes in heart rate or arterial blood pressure were found, isoprenaline did increase LVEDP significantly. This change in preload could oppose the effects of direct changes in contractility on $LVdP/dt_{max}$ and the QA interval resulting in no change in both indices overall.

As was the case in the acute study, plasma concentrations of isoprenaline could not be determined due to difficulties establishing a suitable method. See Section 2.4.1.4 for full details.

Verapamil

Chronic verapamil administration caused LVSD to increase with no change in LVDD leading to an overall decrease in FS (Figure 5.2, Figure 5.3 and Figure 5.4). This decrease in contractility indicated by echocardiography was also shown by a decrease in $LVdP/dt_{max}$ although the effects on this parameter may have been augmented by the decreases in blood pressure that also occurred (Table 5.1). Either way, these findings are in line with the mechanism of action of verapamil and

expected effects on cardiac contractility. Bosnjak *et al.* (1991) chronically treated rabbits with verapamil (2 mg kg^{-1} day^{-1}, 28 days) and reported a significantly lower force of contraction and a depressed contractile response to epinephrine in papillary muscles isolated from *in vivo* treated animals. Interestingly, they found these effects despite plasma samples containing no detectable amounts of verapamil. In the present study, the plasma concentrations of verapamil (Table 5.2) were quite low compared to the reported therapeutic concentrations (0.18 to 0.88 μM; Opie & Gersh, 2009) with the total concentration (0.157 ± 0.021) being only slightly lower than the lower end of this range, but free concentrations (0.030 ± 0.004) being approximately 6-fold lower. The decreases in contractility were relatively modest which may be explained by the low plasma concentrations of verapamil or alternatively by the shorter duration of drug administration used in the current study compared to Bosnjak *et al.* (1991).

Cardiotoxic drugs (imatinib and sunitinib)

Kerkelä *et al.* (2006) were the first to report adverse cardiac effects of imatinib presenting data from ten patients who developed severe congestive heart failure whilst being treated with imatinib and showing that imatinib-treated mice developed LV contractile dysfunction. Interestingly, this report came after imatinib gained FDA approval. The cardiotoxicity of imatinib was not predicted by the preclinical studies performed and summarised in the FDA pharmacology review (FDA, 2001). Adverse cardiac effects had also not been recognised in large clinical trials (O'Brien *et al.*, 2003; Druker *et al.*, 2006; Kantarjian *et al.*, 2006). Unsurprisingly, therefore, the severity of cardiotoxicity associated with imatinib cardiotoxicity was debatable and the study by Kerkelä *et al.*, (2006) came under much scrutiny with several letters in response to the study (Atallah *et al.*, 2007*b*; Gambacorti-Passerini *et al.*, 2007; Hatfield *et al.*, 2007; Rosti *et al.*, 2007) and subsequent reports (Perik *et al.*, 2007; Verweij *et al.*, 2007; Atallah *et al.*, 2007*a*) questioning the presence and clinical significance of adverse cardiac effects. It is now generally accepted that imatinib-induced cardiotoxicity is a rare complication of treatment, however, the risk may be increased in patients with other conditions predisposing to heart failure (e.g. hypertension, coronary artery disease or diabetes) or patients with previous exposure to one or more cardiotoxic drugs (Hatfield *et al.*, 2007; Distler & Distler, 2007; Atallah *et al.*, 2007*a*; Ribeiro *et al.*, 2008).

Unlike imatinib, preclinical evaluation of sunitinib provided an extensive profile of adverse cardiovascular effects (FDA, 2006) which translated into clinical cardiotoxicity in some patients (Pfizer, 2006). Sunitinib is generally regarded as posing a greater cardiotoxic risk than imatinib (Cheng & Force, 2010) and several studies have shown a decline in LV ejection fraction to below normal (Pfizer, 2006; Motzer *et al.*, 2007; Chu *et al.*, 2007; Telli *et al.*, 2008). However, similar to imatinib, factors such as previous cardiovascular disease or anthracycline therapy predispose to LV dysfunction with sunitinib treatment (Chu *et al.*, 2007; Telli *et al.*, 2008).

In the present study chronic administration of neither imatinib nor sunitinib had any significant effects on haemodynamics or cardiac contractility assessed via echocardiography (Figure 5.2, Figure 5.3 and Figure 5.4), $LVdP/dt_{max}$ and the QA interval (Table 5.1). Larger group sizes may have increased the chance of finding rare cardiotoxic effects, but the guinea pigs used here were healthy with no co-morbidities which may predispose to such effects. Another likely explanation for the absence of cardiac effects here is related to the dose and duration of treatment. Although imatinib and sunitinib were each administered over 6 days in this study, this is still far short of the weeks/months of treatment given to patients. In addition, other *in vivo* animal studies investigating cardiotoxicity have also been performed over longer durations (Kerkelä *et al.*, 2006; Chu *et al.*, 2007; Kerkelä *et al.*, 2009; Wolf *et al.*, 2010).

Plasma concentrations of imatinib measured in these experiments indicate total concentrations (1.359 ± 0.381 µM) to be approximately 3.5-fold lower than clinically relevant concentrations (5 µM) and free concentrations (0.005 ± 0.002 µM) to be 1000-fold lower. Sunitinib plasma concentrations also fell well below clinical exposures (0.03 µM) with total concentrations (0.009 ± 0.002 µM) being approximately 3-fold lower and free concentrations (0.001 ± 0.000 µM) being 30-fold lower. Such low exposures are therefore likely to account for the lack of (adverse) cardiac effects.

The dose and duration of administration of imatinib and sunitinib were limited by the poor solubility of these agents. As imatinib and sunitinib are of poor solubility, minipumps with the largest available reservoir (which contains the drug solution during delivery to the animal) were used to prepare these drugs at the highest possible solution strength and thus deliver the highest dose. The dosing period was

also limited by the model of minipump used which, due to the high rate of delivery required to meet the desired daily dose, could only deliver drugs for a period of one week. To dose for longer, minipumps would need to have been removed after one week and replaced with new minipumps filled with fresh drug solutions. The repeated anaesthesia required to do this and the reopening of a healed/healing wound both presented significant animal welfare issues.

Following removal of the heart and collection of blood samples at the end of the haemodynamic assessments, guinea pigs were euthanased and minipumps were removed from animals and checked for damage or blockages. It was noted that minipumps containing imatinib often appeared partially blocked and on opening the reservoir inside the minipump, it appeared that some of the drug had come out of solution. Therefore, it is likely that imatinib-treated guinea pigs did not receive the full dose of imatinib and this may explain the greater variability in plasma concentrations of imatinib. The total plasma concentrations of sunitinib were disproportionately lower than that of imatinib compared to the intended delivery doses. Although precipitation of sunitinib solutions inside minipumps and animals was not apparent, this could have potentially been an issue as sunitinib is a similar large molecule to imatinib. Alternatively, the difference could be due to potentially different pharmacokinetic profiles of imatinib and sunitinib in terms of metabolism and clearance.

5.4.1.3 Effects of chronic in vivo drug administration on CaMKII expression and activity

Following chronic *in vivo* drug treatments LV tissue was rapidly removed as before and CaMKIIδ expression and CaMKII activity were assessed using the methods detailed in Chapter 3. Additionally in this Chapter, immunoblotting for RyR phosphorylated at the CaMKII specific site (Ser2815) was employed as a third method to assess CaMKII activity.

Isoprenaline

As described in Section 3.4.1.2 isoprenaline has been shown in several reports to increase CaMKII expression and activity via PKA-dependent and PKA-independent mechanisms. Previous work has demonstrated that chronic stimulation of β_1-adrenoceptors (such as that seen following chronic isoprenaline treatment) leads to Ca^{2+} handling disturbances (Nakayama *et al.*, 2007) and is associated with

development of heart failure. Both CaMKII expression and activity have previously been shown to be increased in animal models of heart failure (Maier *et al.*, 2003; Zhang *et al.*, 2003) and in human heart failure (Hoch *et al.*, 1999; Kirchhefer *et al.*, 1999). Therefore, some of the detrimental effects of chronic β_1-adrenoceptor stimulation may be the result of CaMKII activation. In this study, chronic isoprenaline treatment caused a decline in LV function and a parallel increase in CaMKIIδ expression (Figure 5.5) and CaMKII activity (Figure 5.7) which is consistent with this suggestion. It has been demonstrated in previously published work that, increased activity of CaMKII results in increased phosphorylation of RyR (Currie *et al.*, 2004). Hyperphosphorylation of RyR can lead to diastolic Ca^{2+} leak from the SR (Maier *et al.*, 2003; Kohlhaas *et al.*, 2006) and contributes to the decline in cardiac contractility. Interestingly, results in the current study also show evidence for increased pSer2815-RyR following chronic isoprenaline treatment (Figure 5.8). This serves as a further marker for increased CaMKII activity and strengthens the evidence that increased CaMKII activation is associated with a decline in LV function.

Verapamil

As explained previously, by blocking Ca^{2+} entry into cardiomyocytes, theoretically verapamil should result in a decrease in CaMKII activity and this was apparent following acute verapamil treatment (Figure 3.13). However, chronic verapamil administration caused CaMKIIδ expression (Figure 5.5) and CaMKII activity (Figure 5.7 and Figure 5.8) to increase. Although this was initially surprising, similar effects of chronic verapamil treatment have been reported elsewhere. Zhou (2010) recently showed that chronic verapamil treatment (15 mg kg^{-1} day^{-1}) caused several biochemical and functional changes to EC-coupling proteins resulting in altered cardiac function. Of particular relevance to the findings here is the overexpression of CaMKII and hyperphosphorylation of RyR. Interestingly, Zhou (2010) also reported that these changes occurred in the absence of cardiac hypertrophy or fibrosis following chronic verapamil treatment. Although, plasma cardiac troponin I was significantly increased (Table 5.3) in the current study perhaps indicating cardiac damage, histological analysis revealed no morphological abnormalities. Thus, alterations at the biochemical level may evoke adverse effects on cardiac function without structural deficits.

Cardiotoxic drugs (imatinib and sunitinib)

Despite CaMKII being highlighted in reports reviewing drug-induced cardiotoxicity (Stummann *et al.*, 2009; Force & Kolaja, 2011), no studies have investigated the effects of imatinib or sunitinib on cardiac contractility and CaMKII expression and/or activity. The results here demonstrate that following chronic administration of imatinib or sunitinib, both CaMKIIδ expression (Figure 5.5) and CaMKII activity (Figure 5.7 and Figure 5.8) were significantly increased.

It seems unlikely that imatinib and sunitinib are directly targeting CaMKII as these drugs were designed as multiple kinase *inhibitors* rather than kinase *activators*. It is therefore more likely that these drugs affect other signalling molecules up or down stream of CaMKII which subsequently increase CaMKIIδ expression and CaMKII activity.

A potential link lies in the fact that CaMKII can be activated by oxidation (Erickson *et al.*, 2008). Erickson *et al.* (2008) initially showed that hydrogen peroxide, a powerful ROS, caused purified CaMKIIδ to become constitutively active in the presence of Ca^{2+}/CaM and independently of Thr286 autophosphorylation. Protein chemistry revealed that oxidation of Met281/282 in the autoregulatory domain could activate CaMKII. This was then followed by using an oxidation-specific antibody which showed that oxidation of Met281/282 occurs *in vivo* in mice hearts following angiotensin II treatment (which increases the generation of ROS).

Mitochondria are an important source of ROS within most mammalian cells, including cardiomyocytes, and this underlies oxidative damage in many pathologies (Murphy, 2009). Mitochondrial perturbation and toxicity have been identified as a "common theme" in drug-induced cardiotoxicity (Mellor *et al.*, 2011). Both imatinib and sunitinib have been linked to mitochondrial injury and abnormalities in mice, rat and humans (Kerkelä *et al.*, 2006, 2009; Chu *et al.*, 2007). More recently, sunitinib has been reported to increase the generation of reactive oxygen species *in vitro* (Zhaung *et al.*, 2011; Rainer *et al.*, 2012). Taken together these findings suggest a potential indirect route of CaMKII activation by oxidation resulting from imatinib and sunitinib effects on mitochondria and generation of ROS.

The alterations in CaMKIIδ expression and CaMKII activity following imatinib and sunitinib treatments could be an early indication of cellular cardiotoxicity that

precedes compromised cardiac function at the whole animal level. However, further studies are required to investigate this and the underlying mechanisms.

5.4.1.4 Correlation of changes in cardiac contractility and CaMKIIδ expression and/or CaMKII activity

All drug treatments increased CaMKIIδ expression and CaMKII activity, however, not all drug treatments altered cardiac contractility. In the case of isoprenaline and verapamil the increases in CaMKIIδ expression and CaMKII activity were associated with a decline in contractility. However, with the increases in CaMKIIδ expression and CaMKII activity following imatinib and sunitinib administration no alterations in contractility were seen.

It is likely that the increase in CaMKII expression and activity following isoprenaline and verapamil was not the primary cause of the effects on contractility which more likely resulted from additive effects, e.g. increases in PKA expression/activity which have also been also associated with a decline in LV function (Marks *et al.*, 2002). In the case of imatinib and sunitinib, however, perhaps these particular pathways were not activated and the increase in CaMKII expression and activity alone was not sufficient to alter contractility. This may also explain why patients with pre-existing cardiac disease, where CaMKII/PKA may already be increased, experienced a higher incidence of cardiotoxicity with these drugs.

5.4.2 Limitations

Minipumps were chosen for drug administration in this study as, in theory, this provides a much more consistent drug delivery than oral dosing (via food/water) particularly for drugs with different half lives. This method also tends to be less stressful to guinea pigs (which are easily stressed) than repeated injections or individual oral dosing (by gavage). In addition, guinea pigs were anaesthetised for echocardiography assessment so implanting the minipump at this time was convenient and better for animal welfare.

As explained earlier the largest available size of minipumps was used due to the poor solubility of imatinib and sunitinib. Minipumps were 5.1 cm in length and 1.4 cm in diameter and apparently suitable for subcutaneous implantation in animals weighing at least 150 g. At implantation of minipumps guinea pigs weighed at least 420 g. The minipumps are generally marketed for use in rats and mice and

although advised that they were suitable for guinea pigs, in some animals the minipump appeared to cause slight skin abrasion. This may be due to guinea pigs having much less subcutaneous space than rats. Although this did not warrant early termination of these guinea pigs, this size of minipump is perhaps too large and in future, particularly for longer durations of use, a smaller minipump should be used if possible.

5.4.3 Conclusions

The work presented in this Chapter has shown that chronic administration of both isoprenaline (0.372 mg kg^{-1} day^{-1}) and verapamil (10 mg kg^{-1} day^{-1}) decreased cardiac contractility and this was associated with increased CaMKIIδ expression and CaMKII activity. In the case of chronic imatinib and sunitinib treatment, although cardiac contractility was not altered significantly, CaMKIIδ expression and CaMKII activity were increased. CaMKIIδ expression and CaMKII activity were, therefore, increased following all chronic treatments, however, further investigation is required to define the subcellular mechanisms responsible for these changes. The circumstances under which increased CaMKII expression and activity translates to compromised contractile performance also require more detailed investigation.

CHAPTER 6 DISCUSSION

Recently several drugs in development or on the market have been found to have cardiotoxic effects. These effects include LV dysfunction, decreased contractility and heart failure (Force & Kerkelä, 2008; Cheng & Force, 2010; Force & Kolaja, 2011). There is a clear need to assess and identify these risks early in the drug development process. However, drug-induced effects on cardiac contractility have not been tested in routine safety pharmacological studies. Furthermore, the mechanisms underlying these cardiotoxicities remain largely unclear. It is known that the effects are commonly associated with drugs inhibiting the activity of protein kinases. Examples include the anti-cancer agents, imatinib and sunitinib, designed to target the aberrant activity of protein kinases involved in tumour progression. These drugs have both been implicated in causing LV dysfunction in patients and in animal studies (Kerkelä *et al.*, 2006; Chu *et al.*, 2007; Force & Kerkelä, 2008). Understanding how these adverse reactions occur is crucial to preventing these issues in future drug development.

CaMKIIδ has a pivotal role in regulating cardiac contractility via phosphorylation of key Ca^{2+} handling proteins in cardiomyocytes (Witcher *et al.*, 1991; Bassani *et al.*, 1995; Hain *et al.*, 1995; Karczewski *et al.*, 1997; Maier & Bers, 2007). Importantly, CaMKIIδ is also a recognised molecular switch triggering abnormal Ca^{2+} handling and contractile dysfunction in cardiomyopathy (Hoch *et al.*, 1999; Currie & Smith, 1999; Boknık *et al.*, 2001; Colomer, 2002; Mishra *et al.*, 2003; Zhang *et al.*, 2003; Erickson & Anderson, 2008). It is therefore also possible that CaMKIIδ may be an important intracellular target for drugs that alter cardiac performance. If so, CaMKIIδ could serve as a useful biochemical marker of *in vivo* changes in cardiac contractility and cardiac safety in drug development.

6.1 Main findings

The work presented in this thesis used an integrative approach to investigate drug effects on cardiac contractility and concomitant changes in CaMKIIδ expression and/or CaMKII activity. Firstly, in Chapter 2, an anaesthetised guinea pig model to assess haemodynamics and cardiac contractility via two indices of contractility - $LVdP/dt_{max}$ and the QA interval - was developed. This model was then used to assess the effects of known inotropes, isoprenaline, ouabain and verapamil, and the cardiotoxic agents, imatinib and sunitinib. Isoprenaline and ouabain produced positive inotropic effects whilst verapamil, imatinib and sunitinib had negative

inotropic effects. In addition, the responses of $LVdP/dt_{max}$ and the QA interval following isoprenaline, ouabain and verapamil correlated well. In Chapter 3, methods were successfully established to measure CaMKIIδ expression and CaMKII activity in LV tissue from guinea pig. These methods were then employed to assess CaMKIIδ expression and CaMKII activity in LV tissue from acute *in vivo* drug-treated animals from the previous Chapter. CaMKIIδ protein expression was similar across all treatment groups. CaMKII autophosphorylation was not altered in any treatment group when pThr286-CaMKII protein expression was assessed and CaMKII activity, assessed by a radioactive assay, was not significantly altered throughout groups although verapamil and sunitinib treatments tended to decrease CaMKII activity. $LVdP/dt_{max}$ and the QA interval were further explored in Chapter 4 by investigating the effects of changes in blood pressure and heart rate on $LVdP/dt_{max}$ and the QA interval. Both indices were positively altered by increases in blood pressure (induced by phenylephrine) and negatively altered by decreases in blood pressure (induced by sodium nitroprusside). In addition, $LVdP/dt_{max}$ was increased as heart rate increased from 160 to 220-249 beats min^{-1} at which point $LVdP/dt_{max}$ peaked and gradually fell at higher heart rates. Also in this Chapter, the assessment of drug-induced effects on cardiac contractility by PV loop measurement was investigated. Whilst positive and negative inotropic effects were detected following isoprenaline and verapamil administration, respectively, the technique did present several issues which must be addressed before the system can be used reliably. Chapter 5 brought together the methods established in earlier Chapters to investigate the effects of chronic *in vivo* drug administration (6 days) on cardiac contractility and CaMKIIδ expression and CaMKII activity. Chronic administration of both isoprenaline (0.372 mg kg^{-1} day^{-1}) and verapamil (10 mg kg^{-1} day^{-1}) decreased cardiac contractility and this was associated with increased CaMKIIδ expression and CaMKII activity. Chronic imatinib (100 mg kg^{-1} day^{-1}) and sunitinib (20 mg kg^{-1} day^{-1}) treatments, did not alter cardiac contractility significantly. However, CaMKIIδ expression and CaMKII activity were increased.

6.2 Methods to assess drug-induced effects on cardiac contractility in guinea pig

In Chapter 2 methods were developed to assess changes in contractility in the guinea pig via $LVdP/dt_{max}$ and the QA interval. Both indices responded to known inotropes as would be expected: the positive inotropes, isoprenaline and ouabain,

caused increases in $LVdP/dt_{max}$ with corresponding decreases in the QA interval, whilst the negative inotrope, verapamil, caused decreases in $LVdP/dt_{max}$ with corresponding increases in the QA interval (Figure 2.11 and Figure 2.13). These reciprocal responses of $LVdP/dt_{max}$ and the QA interval were well correlated showing a strong inverse relationship (Figure 2.14). In Chapter 4, however, a much larger guinea pig data set revealed that $LVdP/dt_{max}$ and the QA interval do not always respond reciprocally. The influence of concurrent changes in heart rate and blood pressure may be responsible for this as both indices were altered by changes in blood pressure (Figure 4.3), and $LVdP/dt_{max}$ was also altered by changes in heart rate (Figure 4.5). These inherent flaws of $LVdP/dt_{max}$ and the QA interval have been recognised by others (Wallace *et al.*, 1963; Cambridge & Whiting, 1986; Hamlin & Del Rio, 2010; Johnson *et al.*, 2012).

Measurement of LV PV loops is claimed to be the "gold standard" for estimating cardiac contractility providing load- and rate-independent indices of cardiac contractility. However, as conveyed in the description of the development and initial assessment of PV loops in Chapter 5, the technique is challenging and time-consuming - as is the analysis and interpretation of the data. Indeed this technique offers a plethora of information regarding cardiac function through several measures, not only related to contraction, but also relaxation and compliance of the heart (which were not assessed here). However, many of these parameters cannot be assessed continuously throughout drug infusions due to the need to perform an IVCO to obtain them.

This need not only limits the quantity of information that can be collected, but may also interfere with drug effects. The performance of the IVCO may affect catheter position either by the operator accidently knocking the catheter during the manoeuvre or due to the consequent physiological changes in pressure and volume. The frequency of IVCOs or the number of times this can be done in one animal were not assessed here, but may prove detrimental to the animal if performed too often - especially as mechanical ventilation must be ceased during this period. Furthermore, the laparotomy required to locate the IVC also poses a threat to the health of the animal as the risks of surgical trauma and potential blood loss are increased.

The PV catheter is extremely sensitive to position. Obtaining good quality baseline signals and PV loops could take some time and even then the stability of recordings could be an issue. Depending on the effects of test drugs, the catheter may also be disturbed part way through the assessment resulting in distorted signals and PV loops (as was the case for initial isoprenaline experiments in Chapter 4). If this happens, it may be possible to quickly reposition the catheter and regain signal and loop quality, however, subsequent data collection would not be directly comparable to previous data in this animal as every time the catheter position is altered, baseline values need to be reprocessed. The catheter is also extremely sensitive to electrical noise and PV recordings were impossible when ECG leads were attached to animals.

In comparison to PV loops, both LVdP/dt_{max} and the QA interval provided a far less cumbersome approach to assessing cardiac contractility. The experimental protocol used in Chapter 2 (but which was impossible in Chapter 4), provided much more information about drug effects over time and at different doses. In addition, simultaneous recording of ECGs was possible. Although this data has not been presented in this thesis, because it is focused on cardiac contractility, the effects of the various anaesthetics on ECG intervals have been published (Mooney *et al.*, 2012). Surgical procedures were less invasive and guinea pigs remained stable under maintenance anaesthesia for up to 5 hours. LVdP/dt_{max} and the QA interval therefore provided a much simpler, quicker and more informative assessment of cardiac contractility which is particularly appealing for safety pharmacology screens of potential drug candidates.

However, care must be taken in the interpretation of LVdP/dt_{max} and QA interval data where concurrent changes in heart rate and/or blood pressure also occur. If these indices of cardiac contractility respond reciprocally and all other parameters remain stable or somehow change in directions that may counterbalance each another, then it may be concluded that the test drug is directly affecting cardiac contractility. However, if, for example, the test drug caused a reduction in LVdP/dt_{max} and a decrease in arterial blood pressure then it should not be assumed that this drug is a negative inotrope. A full review of all cardiovascular parameters would be required before any conclusions could be drawn.

The work presented in Chapter 4 showed LVdP/dt_{max} was significantly increased at mean arterial blood pressures ≥80 ± 8 mmHg and significantly decreased at mean arterial blood pressures ≤39 ± 3 mmHg. The QA interval was significantly increased at mean arterial blood pressures ≥74 ± 5 mmHg and significantly decreased at mean arterial blood pressures ≤39 ± 3 mmHg. In the case of heart rate, peak LVdP/dt_{max} values occurred at 220-249 beats min^{-1}. Baseline heart rates tended to be around 245 to 265 beats min^{-1} in the anaesthetised guinea pigs tested in these experiments and therefore quite close to peak LVdP/dt_{max} values. Increases in heart rate from baseline may then be expected to decrease LVdP/dt_{max} whilst decreases in heart rate may initially increase or maintain LVdP/dt_{max} but then decrease this index at heart rates lower that 220 beats min^{-1}. These data provide threshold values for arterial blood pressure or heart rate that might be expected to cause changes in LVdP/dt_{max} or the QA interval in the anaesthetised guinea pig.

Of course in safety pharmacology assessments, significant and unintended drug-induced effects on heart rate and/or blood pressure would be undesirable, so the influence of these parameters on indices of contractility may not be of concern. However, if it was suspected that changes in LVdP/dt_{max} and/or the QA interval were confounded by concurrent heart rate and blood pressure effects, the initial assessment could be followed by additional tests. At this point PV loops could be measured if a suitable protocol and quality of signals could be achieved. Alternatively, the isolated Langendorff-perfused heart could provide a "load free" assessment although the influence of heart rate may remain an issue.

In Chapter 5 echocardiography was employed as an additional measure of cardiac contractility. Only short axis views of the LV were assessed as the resolution of long axis images (obtained by pivoting the transducer 90º) was poor. In addition to the measurements presented, short axis views can also provide measurements of the area of the LV and M-mode recordings allow the thickness of the anterior and posterior wall and interventricular septum to be measured (Zhou *et al.*, 2004). If good quality long axis images are obtained similar measures can be made as well as that of LV length (Zhou *et al.*, 2004). Doppler imaging can also be used in conjunction with echocardiography providing measures of the velocity of blood flow through the heart chambers (Coatney, 2001).

Echocardiography therefore has the potential to provide a wealth of structural, functional and haemodynamic information on the heart. The major advantage of this technique is that it is non-invasive and can be performed very quickly once the operator is proficient in obtaining good quality images. In the study in Chapter 5 animals were anaesthetised to keep them still during the echocardiography procedure. However, it is possible to obtain recordings from conscious animals. Larger animals can be trained to lie in a position suitable to perform echocardiography. Alternatively, apparatus, such as a sling, has been employed to restrain animals. This may be particularly feasible for guinea pigs which tend to be more docile than other small animals such as rats, however, animals would need to be habituated to these procedures before the study began. In chronic drug studies another major benefit of echocardiography is that it allows assessment of cardiac contractility at more than one time point as demonstrated in Chapter 5. Overall, echocardiography offers a quick, simple and very informative assessment of cardiac contractility.

6.3 Methods to assess drug effects on CaMKII activity in guinea pig

Following both acute and chronic *in vivo* drug administration, LV tissue was taken to assess the effects of drugs on CaMKIIδ expression and CaMKII activity. CaMKII activity in drug-treated tissues was assessed initially by immunoblotting for pThr286-CaMKII - the autophosphorylated and activated form of CaMKII. In untreated tissue with increasing total protein load, bands of increasing intensity, corresponding to pThr286-CaMKII, were detected indicating a basal level of active CaMKII in the LV tissue (Figure 3.6c). Acute *in vivo* drug treatments had no significant effects on basal pThr286-CaMKII expression (Figure 3.12). Due to the lack of published studies assessing CaMKII in guinea pig it was unclear if a change in CaMKII activity should have been expected following acute *in vivo* drug treatments. Differences in antibody sensitivity between different species can be an issue for detection and subsequent quantification of proteins. The reliability of the pThr286-CaMKII antibody in guinea pig had at times been problematic in the current study and the optimisation of signals proved more difficult in this species than in mouse and rabbit (Anthony, 2008; Martin, 2011). Therefore, a second measure of CaMKII activity was required. A radioactive assay measuring CaMKII activity by incorporation of phosphate into a CaMKII peptide substrate was used. This assay also showed detectable levels of

CaMKII activity in untreated LV tissue (Figure 3.8). In testing acute drug-treated tissues via this method, although no significant changes in CaMKII were found, the difference in mean values between treatment groups and the apparent changes in activity were far greater using the radioactive assay than pThr286-CaMKII expression (Figure 3.13). This indicated that the radioactive assay could be a more sensitive measure of CaMKII activity in the guinea pig than the antibody based technique.

In Chapter 5, following chronic *in vivo* drug treatments, CaMKII activity was assessed again using the pThr286-CaMKII antibody and the radioactive assay. As before, immunoblotting for pThr286-CaMKII showed no significant changes in CaMKII activity across treatment groups (Figure 5.6). In contrast, the radioactive assay showed substantial increases in CaMKII activity in all treatment groups, particularly the sunitinib group (Figure 5.7). To clarify this discrepancy in results, a third measure of CaMKII activity was required.

RyR is a target of CaMKII, known to be specifically phosphorylated by CaMKII at Ser2815. Immunoblotting using an antibody against pSer2815-RyR is a commonly used measure of CaMKII activity (Grimm & Brown, 2010). Using this technique, significant increases in CaMKII activity were found across all treatment groups (Figure 5.8). In comparison to the radioactive assay, similar percentage increases compared to vehicle were found in imatinib (pSer2815-RyR = 50%; radioactive assay = 61%) and sunitinib (pSer2815-RyR = 110%; radioactive assay = 123%) treatment groups. However, the percentage increases following isoprenaline (pSer2815-RyR = 16%; radioactive assay = 78%) and verapamil (pSer2815-RyR = 22%; radioactive assay = 70%) administration were somewhat lower in pSer2815-RyR assessment than the radioactive assay.

Importantly, the changes in CaMKII activity reflected by the radioactive assay represent global changes in CaMKII activity throughout the LV tissue. This includes the activity of all isoforms of CaMKII expressed in the heart (δ, γ and β) and their variants, e.g. CaMKIIδ_C localised to the cytosol and CaMKIIδ_B localised to the nucleus. In contrast, the changes in CaMKII activity assessed via pSer2815-RyR reflect only the activity of CaMKII associated with RyR. These results, therefore, represent a localised change in CaMKII activity at the SR where CaMKIIδ has been shown to be functionally coupled and associated with RyR_2 (Currie *et al.*, 2004).

Therefore, the profiles of CaMKII activity measured via the radioactive assay and pSer2815-RyR are not directly comparable as each method represents CaMKII activity in different subcellular compartments and localised pools.

CaMKII in different subcellular locations may be affected by drug treatments in different ways. In addition, the ratio of the other isoforms of CaMKII in the heart is not known although they are low (Colbran, 2004), but again drug treatments may well alter the expression and/or activity of these isoforms and to differing extents depending on the particular isoform.

6.4 Acute vs chronic effects of isoprenaline on cardiac contractility and CaMKII

In both acute and chronic studies isoprenaline was used as a positive control for both cardiac contractility and CaMKII activation. Following acute isoprenaline administration contractility was significantly increased, but there was no significant change in CaMKIIδ expression or CaMKII activity. In contrast, following chronic isoprenaline administration contractility was significantly decreased, and CaMKIIδ expression and CaMKII activity were both significantly increased.

Most experimental evidence disproves a role of CaMKII in acute β-adrenoceptor modulation of contractility. The acute effects of isoprenaline on contractility correlated with cAMP elevation and increased PKA activation whereas no correlation was found with CaMKII activation (Grimm & Brown, 2010). This is consistent with the effects observed following acute isoprenaline administration in Chapter 2.

However, pathophysiological conditions appear to change inotropic regulation. Chronic β-adrenoceptor stimulation (such as that seen following chronic isoprenaline treatment) caused a shift from PKA to CaMKII regulation of myocyte contractility (Wang *et al.*, 2004). Accordingly, excessive sympathetic nervous system activity and thus chronic β-adrenoceptor stimulation are observed in heart failure. Furthermore, both CaMKII expression and activity have been shown to be increased in animal models of heart failure (Maier *et al.*, 2003; Zhang *et al.*, 2003) and in human heart failure (Hoch *et al.*, 1999; Kirchhefer *et al.*, 1999). These data therefore suggest that CaMKII activity is particularly prominent under pathophysiological conditions where cardiac contractility is compromised and this

may explain the difference in CaMKII and contractility effects seen following chronic compared to acute isoprenaline administration in the present study.

6.5 Future work

The guinea pig model developed in Chapter 2 provides a sensitive and robust assessment of cardiac contractility via $LVdP/dt_{max}$ and the QA interval. However, if concurrent changes in heart rate and/or blood pressure confound the interpretation of these data, PV loop assessment may be desired. However, before the PV loop technique can be used reliably, there are several issues that must be addressed: i) the stability and reproducibility of recordings over time needs to be more thoroughly assessed; ii) the limits of PV loop quality with increases/decreases in LVP need to be determined, iii) the sensitivity of the system should be further tested using other positive and negative inotropes; iv) a suitable dosing protocol needs to be investigated (although this may need to be individually tailored to the effects of each drug); v) the usefulness of other outputs related to relaxation and compliance could be assessed if desired.

With regards to the mechanisms of cardiotoxicity related to kinase inhibitors, the work presented in this thesis, implicates, for the first time, a potential role of CaMKII evidenced by increases in CaMKIIδ expression and CaMKII activity following chronic administration of both imatinib and sunitinib.

The biochemical changes in CaMKII following imatinib and sunitinib treatment were not accompanied by a negative effect on cardiac contractility. This may be related to the dose or duration of drug administration used in the present study. Kerkelä *et al.* (2006) reported ultrastructural changes, mitochondrial abnormalities and changes in cardiomyocyte signalling in the absence of contractile dysfunction following 3 weeks of 50 mg kg^{-1} day imatinib treatment. However, increasing the dose and duration to 6 weeks of 200 mg kg^{-1} day caused mice to develop significant contractile dysfunction within 4 weeks (Kerkelä *et al.*, 2006). In a later publication from the same group, mice treated with 25 mg kg^{-1} day sunitinib for 5 weeks also developed mitochondrial abnormalities, but no adverse effects were observed on several echocardiography parameters (Chu *et al.*, 2007). No further dosing regimes were tested in mice, however, similar mitochondrial abnormalities and biochemical changes were subsequently reported in a patient who developed sunitinib-induced heart failure (Kerkelä *et al.*, 2009).

In the current study, it is therefore likely that if the dose and duration of imatinib and sunitinib treatments were increased, contractile dysfunction may have manifest. It is essential that a detrimental effect on contractility is observed to substantiate a link to CaMKII. It is also important that the increases in CaMKII are at least sustained, if not enhanced, if an effect on contractility occurs with greater doses. If this is the case, it may also be interesting to then block CaMKII activity (e.g. via the inhibitory peptide, AIP) or use a transgenic CaMKIIδ knockout mouse model whilst administering imatinib or sunitinib and determine if contractile defects still occur. Although, it is likely that CaMKII is solely responsible for the adverse effects of these agents. To further substantiate a link between CaMKII and cardiotoxicity associated with kinase inhibitors, more of these agents could be tested. For example, lapatinib and dasatinib have also been associated with decreased contractility and heart failure (Mellor *et al.*, 2011).

Following a thoroughly established link, the consequence of the increases in CaMKIIδ and CaMKII activity should be assessed. As mentioned in Section 1.3.2, CaMKII co-localises with and phosphorylates many key proteins involved in cardiac Ca^{2+} handling including LTCC (Dzhura *et al.*, 2000), SERCA (Narayanan & Xu, 1997), PLB (Wegener *et al.*, 1989) and RyR (Currie *et al.*, 2004). In the work presented in Chapter 5, imatinib and sunitinib treatments significantly increased phosphorylation of RyR at the CaMKII specific site (Ser2815). CaMKII mediated hyperphosphorylation of RyR has been shown to occur in heart failure and may underlie diastolic Ca^{2+} leak from the SR which depletes SR Ca^{2+} stores and thus the [Ca^{2+}] available for release during cardiac contractility (Currie *et al.*, 2011). However, increased CaMKII-mediated phosphorylation of other targets may impact Ca^{2+} entry to the myocyte (LTCC), and Ca^{2+} reuptake into the SR following contraction (SERCA and PLB). Such effects may also contribute to contractile dysfunction.

Of great importance is determining the mechanism by which imatinib and sunitinib caused increased CaMKIIδ expression and CaMKII activity. As mentioned in Section 5.4.1.3 it is unlikely that these drugs are directly targeting CaMKII and more likely that they are affecting other signalling molecules up or downstream of CaMKII which subsequently increase CaMKIIδ expression and CaMKII activity. There is great potential for cross-talk between various cell signalling pathways which makes speculative assessment of a potential mechanism difficult. However, one promising

link may be oxidation and activation of CaMKII by ROS. This hypothesis could initially be tested by using an oxidation-specific antibody to assess oxidised CaMKII levels in drug-treated and vehicle samples.

Pre-existing cardiovascular disease has been identified as a significant risk factor for drug-induced cardiotoxicity (Hatfield *et al.*, 2007; Telli *et al.*, 2008). Therefore, the use of healthy animals to investigate such risks may be questioned. The use of animal models of cardiac disease may yield more fruitful results in the quest to delineate the underlying mechanisms of cardiotoxicity.

Of course the relevance of animal studies and translation to the clinic may always be questioned. To combat this, LV biopsy samples from patients treated with imatinib or sunitinib could be assessed to determine CaMKIIδ expression and CaMKII activity levels. These could then be compared to CaMKII levels in samples either from non-treated patients or patients that have not experienced contractile dysfunction during treatment to determine if the increases in CaMKIIδ expression and CaMKII activity found in animal studies translate to patients.

6.6 Conclusions

The work presented in this thesis indicates that the guinea pig is a suitable species for the integrated assessment of cardiac contractility and CaMKII. Acute drug studies using this model showed positive and negative effects on contractility which were not associated with significant changes in CaMKIIδ expression or CaMKII activity. Subsequent chronic drug treatments in guinea pig caused significant increases in CaMKIIδ expression and CaMKII activity. In some cases these were associated with negative effects on contractility, however, in other cases no significant effects were detected. The difference in acute versus chronic treatments is consistent with previous suggestions that activation of CaMKII signalling is more prominent in chronic rather than acute stimulation scenarios. Furthermore, alterations in CaMKIIδ expression and CaMKII activity could be an early indication of cellular cardiotoxicity that precedes compromised cardiac function at the whole animal level. However, the circumstances under which increased CaMKII expression and activity translate to compromised contractile performance require more detailed investigation.

REFERENCES

Adeyemi O, Roberts S, Harris J, West H, Shome S & Dewhurst M (2009). QA interval as an indirect measure of cardiac contractility in the conscious telemeterised rat: model optimisation and evaluation. *Journal of Pharmacological and Toxicological Methods* **60,** 159–166.

Akera T, Yamamoto S, Chubb J, Mcnish R & Brody TM (1979). Biochemical basis for the low sensitivity of the rat heart to digitalis. *Naunyn-Schmiedeberg's Archives of Pharmacology* **308,** 81–88.

Anderson ME (2005). Calmodulin kinase signaling in heart: an intriguing candidate target for therapy of myocardial dysfunction and arrhythmias. *Pharmacology & Therapeutics* **106,** 39–55.

Anderson ME (2007). Multiple downstream proarrhythmic targets for calmodulin kinase II: Moving beyond an ion channel-centric focus. *Cardiovascular Research* **73,** 657–666.

von Anrep G (1912). On the part played by the suprarenals in the normal vascular reactions of the body. *Journal of Physiology* **45,** 307–317.

Anthony D (2008). *CaMKIIβ interaction with the RyR_2 complex in normal and failing rabbit hearts* (thesis). University of Strathclyde.

Anthony D, Beattie J, Paul A & Currie S (2007). Interaction of calcium/calmodulin dependent protein kinase II δC with sorcin indirectly modulates ryanodine receptor function in cardiac myocytes. *Journal of Molecular and Cellular Cardiology* **43,** 492–503.

Atallah E, Durand J-B, Kantarjian H & Cortes J (2007*a*). Congestive heart failure is a rare event in patients receiving imatinib therapy. *Blood* **110,** 1233–1237.

Atallah E, Kantarjian H & Cortes J (2007*b*). In reply to Cardiotoxicity of the cancer therapeutic agent imatinib mesylate. *Nature Medicine* **13,** 14–16.

Baan J & van der Velde E (1988). Sensitivity of left ventricular end-systolic pressure-volume relation to type of loading intervention in dogs. *Circulation Research* **62,** 1247–1258.

Baan J, van der Velde ET, de Bruin HG, Smeenk GJ, Koops J, van Dijk AD, Temmerman D, Senden J & Buis B (1984). Continuous measurement of left ventricular volume in animals and humans by conductance catheter. *Circulation* **70,** 812–823.

Barnes CS & Coker SJ (1995). Failure of nitric oxide donors to alter arrhythmias induced by acute myocardial ischaemia or reperfusion in anaesthetized rats. *British Journal of Pharmacology* **114,** 349–356.

Bassani R, Mattiazzi A & Bers D (1995). CaMKII is responsible for activity-dependent acceleration of relaxation in rat ventricular. *American Journal of Physiology* **268,** H703–H712.

Batey J, Lightbown I, Lambert J, Edwards G & Coker S (1997). Comparison of the acute cardiotoxicity of the antimalarial drug halofantrine *in vitro* and *in vivo* in anaesthetized guinea-pigs. *British Journal of Pharmacology* **122,** 563–569.

Beattie I, Smith A, Weston DJ, White P, Szwandt S & Sealey L (2012). Evaluation of laser diode thermal desorption (LDTD) coupled with tandem mass spectrometry (MS/MS) for support of *in vitro* drug discovery assays: increasing scope, robustness and throughput of the LDTD technique for use with chemically diverse compound lib. *Journal of Pharmaceutical and Biomedical Analysis* **59,** 18–28.

Beek OG (1982). A small animal model for monitoring inotropic responses to cardiotonic agents. *Journal of Pharmacological Methods* **7,** 321–329.

Bello CL, Mulay M, Huang X, Patyna S, Dinolfo M, Levine S, Van Vugt A, Toh M, Baum C & Rosen L (2009). Electrocardiographic characterization of the QTc interval in patients with advanced solid tumors: pharmacokinetic- pharmacodynamic evaluation of sunitinib. *Clinical Cancer Research* **15,** 7045–7052.

Berg J, Tymoczko J & Stryer L (2002). *Biochemistry*, 5th edn. W.H. Freeman and Company, New York, NY.

Bers DM (2002). Cardiac excitation-contraction coupling. *Nature* **415,** 198–205.

Bhargava P (2009). VEGF kinase inhibitors: how do they cause hypertension? *American Journal of Physiology: Regulatory, Integrative and Comparative Physiology* **297,** R1–R5.

Bodi I, Mikala G, Koch SE, Akhter SA & Schwartz A (2005). The L-type calcium channel in the heart : the beat goes on. *The Journal of Clinical Investigation* **115,** 3306–3317.

Boknık P, Heinroth-Hoffmann I, Kirchhefer U, Knapp J, Linck B, Hartmut L, Muller T, Schmitz W, Brodde O & Neumann J (2001). Enhanced protein phosphorylation in hypertensive hypertrophy. *Cardiovascular Research* **51,** 717–728.

Bosnjak ZJ, Marijic J, Roerig DL, Stowe DF, Murthy VS & Kampine JP (1991). Chronic verapamil treatment depresses automaticity and contractility in isolated cardiac tissues. *Anesthesia and Analgesia* **72,** 462–468.

Boswell-Smith V, Spina D & Page CP (2006). Phosphodiesterase inhibitors. *British Journal of Pharmacology* **147,** S252–7.

Braun AP & Schulman H (1995). The multifunctional calcium/calmodulin dependent protein kinase: From form to function. *Annual Review of Physiology* **57,** 417–445.

Brodde OE & Michel MC (1999). Adrenergic and muscarinic receptors in the human heart. *Pharmacological Reviews* **51,** 651–690.

Brown J, Del Re D & Sussman M (2006). The Rac and Rho hall of fame: A decade of hypertrophic signaling hits. *Circulation Research* **98,** 730–742.

Brown JN, Thorne PR & Nuttall AL (1989). Blood pressure and other physiological responses in awake and anesthetized guinea pigs. *Laboratory Animal Science* **39,** 142–148.

Brunton LL, Chabner BA & Knollmann BC (2011). *Goodman & Gilman's The Pharmacological Basis of Therapeutics*, 12th edn. The McGraw-Hill Companies, New York.

Buchanan KC, Burge RR & Ruble GR (1998). Evaluation of injectable anesthetics for major surgical procedures in guinea pigs. *Contemporary Topics in Laboratory Animal Science / American Association for Laboratory Animal Science* **37,** 58–63.

Burger H, van Tol H, Boersma AWM, Brok M, Wiemer E a C, Stoter G & Nooter K (2004). Imatinib mesylate (STI571) is a substrate for the breast cancer resistance protein (BCRP)/ABCG2 drug pump. *Blood* **104,** 2940–2942.

Burkhoff D, Mirsky I & Suga H (2005). Assessment of systolic and diastolic ventricular properties via pressure-volume analysis: a guide for clinical, translational, and basic researchers. *American Journal of Physiology: Heart Circulatory Physiology* **289,** H501–12.

Burkhoff D, Suigiura S, Yue D & Sagawa K (1987). Contractility-dependent curvilinearity of end-systolic pressure-volume relations. *American Journal of Physiology* **252,** H1218–1227.

Busch AE, Malloy K, Groh WJ, Varnum MD, Adelman JP & Maylie J (1994). The novel class III antiarrhythmics NE-10064 and NE-10133 inhibit IsK channels expressed in Xenopus oocytes and IKs in guinea pig cardiac myocytes. *Biochemical and Biophysical Research Communications* **202,** 265–270.

Calaghan SC & White E (1999). The role of calcium in the response of cardiac muscle to stretch. *Progress in Biophysics and Molecular Biology* **71,** 59–90.

Cambridge D & Whiting M (1986). Evaluation of the QA interval as an index of cardiac contractility in anaesthetised dogs: responses to changes in cardiac loading and heart rate. *Cardiovascular Research* **20,** 444–450.

Cetin N, Cetin E & Toker M (2005). Echocardiographic variables in healthy guineapigs anaesthetized with ketamine-xylazine. *Laboratory Animals* **39,** 100–106.

Champeroux P, Martel E, Vannier C, Blanc V, Leguennec JY, Fowler J & Richard S (2000). The preclinical assessment of the risk for QT interval prolongation. *Thérapie* **55,** 101–109.

Chen MH, Kerkelä R & Force T (2008). Mechanisms of cardiac dysfunction associated with tyrosine kinase inhibitor cancer therapeutics. *Circulation* **118,** 84–95.

Cheng H & Force T (2010). Molecular mechanisms of cardiovascular toxicity of targeted cancer therapeutics. *Circulation Research* **106,** 21–34.

Chess-Williams R, Williamson K & Broadley K (1990). Whether phenylephrine exerts inotropic effects through alpha- or beta-adrenoceptors depends upon the relative receptor populations. *Fundamentals in Clinical Pharmacology* **4,** 25–37.

Chu TF *et al.* (2007). Cardiotoxicity associated with tyrosine kinase inhibitor sunitinib. *Lancet* **370,** 2011–2019.

Clark JE, Kottam A, Motterlini R & Marber MS (2009). Measuring left ventricular function in the normal, infarcted and CORM-3-preconditioned mouse heart using complex admittance-derived pressure volume loops. *Journal of Pharmacological and Toxicological Methods* **59,** 94–99.

Coatney RW (2001). Ultrasound imaging: principles and applications in rodent research. *ILAR Journal* **42,** 233–247.

Cohen P (2001). The role of protein phosphorylation in human health and disease. The Sir Hans Krebs medal lecture. *European Journal of Biochemistry* **268,** 5001–5010.

Cohen P (2002). Protein kinases--the major drug targets of the twenty-first century? *Nature Reviews Drug Discovery* **1,** 309–315.

Coker S & Kane K (2009). Lack of preconditioning against ischemia-induced VF by isoflurane when used as the sole anaesthetic agent. *Proceedings of the British Pharmacological Society*.

Coker SJ & Ellis AM (1987). Ketanserin and ritanserin can reduce reperfusion-induced but not ischaemia-induced arrhythmias in anaesthetised rats. *Journal of Cardiovascular Pharmacology* **10,** 479–484.

Colbran R (2004). Targeting of calcium/calmodulin-dependent protein kinase II. *Biochemistry Journal* **378,** 1–16.

Colomer JM (2002). Pressure overload selectively up-regulates Ca^{2+}/calmodulin-dependent protein kinase II *in vivo*. *Molecular Endocrinology* **17,** 183–192.

Cunningham J (2002). *Textbook of Veterinary Physiology*, 3rd edn. Saunders, Philadelphia, PA.

Currie S (2009). Cardiac ryanodine receptor phosphorylation by Ca^{2+}/calmodulin dependent protein kinase II: keeping the balance right. *Frontiers in Bioscience* **14,** 5134–5156.

Currie S, Elliott EB, Smith GL & Loughrey CM (2011). Two candidates at the heart of dysfunction: The ryanodine receptor and calcium/calmodulin protein kinase II as potential targets for therapeutic intervention-An *in vivo* perspective. *Pharmacology & Therapeutics* **131,** 204–220.

Currie S, Loughrey CM, Craig M-A & Smith GL (2004). Calcium/calmodulin-dependent protein kinase IIδ associates with the ryanodine receptor complex and regulates channel function in rabbit heart. *The Biochemical Journal* **377,** 357–366.

Currie S, Quinn FR, Sayeed RA, Duncan AM, Kettlewell S & Smith GL (2005). Selective down-regulation of sub-endocardial ryanodine receptor expression in a rabbit model of left ventricular dysfunction. *Journal of Molecular and Cellular Cardiology* **39,** 309–317.

Currie S & Smith GL (1999). Enhanced phosphorylation of phospholamban and downregulation of sarco/endoplasmic reticulum Ca^{2+} ATPase type 2 (SERCA 2) in cardiac sarcoplasmic reticulum from rabbits with heart failure. *Cardiovascular Research* **41,** 135–146.

DeGeest H, Levy MN, Zieske H & Lipman RI (1965). Depression of ventricular contractility by stimulation of the vagus nerves. *Circulation Research* **17,** 222–235.

Dematteo RP, Ballman KV, Antonescu CR, Maki RG, Pisters PWT, Demetri GD, Blackstein ME, Blanke CD, von Mehren M, Brennan MF, Patel S, McCarter MD, Polikoff JA, Tan BR & Owzar K (2009). Adjuvant imatinib mesylate after resection of localised, primary gastrointestinal stromal tumour: a randomised, double-blind, placebo-controlled trial. *Lancet* **373,** 1097–1104.

Distler JHW & Distler O (2007). Cardiotoxicity of imatinib mesylate: an extremely rare phenomenon or a major side effect? *Annals of the Rheumatic Diseases* **66,** 836.

Drouin E, Lande G, Baro I & Escande D (2004). Anesthetized guinea-pig model reliably assess HERG-blocking drugs. Abstracts from the 3rd safety pharmacology society meeting. Noordwijk, The Netherlands, September 2003. *Journal of Pharmacological and Toxicological Methods* **49,** 222.

Druker B, Guilhot F, O'Brien S, Gathmann I, Kantarjian H & Gattermann N (2006). Five-year follow-up of patients receiving imatinib for chronic myeloid leukemia. *New England Journal of Medicine* **355,** 2408–2417.

Dzhura I, Wu Y, Colbran R, Balser J & Anderson M (2000). Calmodulin kinase determines calcium-dependent facilitation of L-type calcium channels. *Nature Cell Biology* **2,** 173–177.

Elliott WJ & Ram CVS (2011). Calcium channel blockers. *Journal of Clinical Hypertension* **13,** 687–689.

Endoh M (2004). Force-frequency relationship in intact mammalian ventricular myocardium: physiological and pathophysiological relevance. *European Journal of Pharmacology* **500,** 73–86.

Endoh M, Shimizu T & Yanagisawa T (1978). Characterization of adrenoceptors mediating positive inotropic responses in the ventricular myocardium of the dog. *British Journal of Pharmacology* **64,** 53–61.

Ennis IL, Li RA, Murphy AM, Marbán E & Nuss HB (2002). Dual gene therapy with SERCA1 and Kir2.1 abbreviates excitation without suppressing contractility. *The Journal of Clinical Investigation* **109,** 393–400.

Erickson JR & Anderson ME (2008). Molecular perspectives CaMKII and its role in cardiac arrhythmia. *Journal of Cardiovascular Electrophysiology* **19,** 1332–1336.

Erickson JR, He BJ, Grumbach IM & Anderson ME (2011). CaMKII in the cardiovascular system: sensing redox states. *Physiological Reviews* **91,** 889–915.

Erickson JR, Joiner MA, Guan X, Kutschke W, Yang J, Oddis CV, Bartlett RK, Lowe JS, O'Donnell SE, Aykin-Burns N, Zimmerman MC, Zimmerman K, Ham A-JL, Weiss RM, Spitz DR, Shea M a, Colbran RJ, Mohler PJ & Anderson ME (2008). A dynamic pathway for calcium-independent activation of CaMKII by methionine oxidation. *Cell* **133,** 462–474.

Eschenhagen T *et al.* (2011). Cardiovascular side effects of cancer therapies: a position statement from the Heart Failure Association of the European Society of Cardiology. *European Journal of Heart Failure* **13,** 1–10.

Estabragh ZR, Knight K, Watmough SJ, Lane S, Vinjamuri S, Hart G & Clark RE (2011). A prospective evaluation of cardiac function in patients with chronic myeloid leukaemia treated with imatinib. *Leukemia Research* **35,** 49–51.

Ewart L, Gallacher DJ, Gintant G, Guillon J-M, Leishman D, Levesque P, McMahon N, Mylecraine L, Sanders M, Suter W, Wallis R & Valentin J-P (2012). How do the top 12 pharmaceutical companies operate safety pharmacology? *Journal of Pharmacological and Toxicological Methods* **66,** 66–70.

Ewen A, Archer DP, Samanani N & Roth SH (1995). Hyperalgesia during sedation: effects of barbiturates and propofol in the rat. *Canadian Journal of Anaesthesia* **42,** 532–540.

FDA (2001). Gleevec® (Imatinib Mesylate) FDA NDA Pharm Review. Available at: http://www.accessdata.fda.gov/drugsatfda_docs/nda/2001/21335_Gleevec.cfm. [Accessed January 24, 2011].

FDA (2006). Sutent® (Sunitinib) FDA NDA Pharm Review. Available at: http://www.accessdata.fda.gov/drugsatfda_docs/nda/2006/021938_S000_Sutent_PharmR.pdf [Accessed January 24, 2011].

Fabiato A (1983). Calcium-induced release of calcium from the cardiac sarcoplasmic reticulum. *The American Journal of Physiology* **245,** C1–14.

Faivre S, Demetri G, Sargent W & Raymond E (2007). Molecular basis for sunitinib efficacy and future clinical development. *Nature Reviews Drug Discovery* **6,** 734–745.

Feldman M, Erikson J, Mao Y, Korcarz C, Lang R & Freeman G (2000). Validation of a mouse conductance system to determine LV volume: comparison to

echocardiography and crystals. *American Journal of Physiology: Heart and Circulation Physiology* **274,** H1698–H1707.

Feneley MP, Skelton TN, Kisslo KB, Davis JW, Bashore TM & Rankin JS (1992). Comparison of preload recruitable stroke work, end-systolic pressure-volume and dP/dtmax-end-diastolic volume relations as indexes of left ventricular contractile performance in patients undergoing routine cardiac catheterization. *Journal of the American College of Cardiology* **19,** 1522–1530.

Fernández A *et al.* (2007). An anticancer C-Kit kinase inhibitor is reengineered to make it more active and less cardiotoxic. *The Journal of Clinical Investigation* **117,** 4044–4054.

Ferrero P, Said M, Sánchez G, Vittone L, Valverde C, Donoso P, Mattiazzi A & Mundiña-Weilenmann C (2007). Ca^{2+}/calmodulin kinase II increases ryanodine binding and Ca^{2+}-induced sarcoplasmic reticulum Ca^{2+} release kinetics during [beta]-adrenergic stimulation. *Journal of Molecular and Cellular Cardiology* **43,** 281–291.

Field KJ & Lang CM (1988). Hazards of urethane (ethyl carbamate): a review of the literature. *Laboratory Animals* **22,** 255–262.

Fill M & Copello J a (2002). Ryanodine receptor calcium release channels. *Physiological Reviews* **82,** 893–922.

Fladmark K, Brustugun O, Mellgren G, Krakstad C, Boe R, Vintermyr O & Al E (2002). Ca^{2+}/calmodulin protein kinase II is required for microcystin-induced apoptosis. *Journal of Biological Chemistry* **277,** 2804–2811.

Foote K & Loughrey C (2010). A comparison of left ventricular pressure-volume measurements in adult rats using three different techniques. *Proceedings of the Physiological Society* **19,** PC22.

Force T & Kerkelä R (2008). Cardiotoxicity of the new cancer therapeutics--mechanisms of, and approaches to, the problem. *Drug Discovery Today* **13,** 778–784.

Force T & Kolaja KL (2011). Cardiotoxicity of kinase inhibitors: the prediction and translation of preclinical models to clinical outcomes. *Nature Reviews Drug Discovery* **10,** 111–126.

Force T, Kuida K, Namchuk M, Parang K & Kyriakis J (2004). Inhibitors of protein kinase signalling pathways: emerging therapies for cardiovascular disease. *Circulation* **109,** 1196–1205.

Fossa A, Wisialowski T & Wolfgang E (2004). Differential effect of HERG blocking agents on cardiac electrical alternans in the guinea pig. *European Journal of Pharmacology* **486,** 209–221.

Freeman G, Little W & O'Rourke R (1986). The effect of vasoactive agents on the left ventricular end-systolic pressure-volume relation in closed chest dogs. *Circulation* **74,** 1107–1113.

Friddle CJ, Koga T, Rubin EM & Bristow J (2000). Expression profiling reveals distinct sets of genes altered during induction and regression of cardiac hypertrophy.

Gambacorti-Passerini C, Tornaghi L, Franceschino A, Piazza R, Corneo G & Pogliani E (2007). In reply to Cardiotoxicity of the cancer therapeutic agent imatinib mesylate. *Nature Medicine* **13,** 13–14.

Georgakopoulos W, Mitzner C, Chen C, Byrne H, Millar J, Hare J & Kass D (1998). *In vivo* murine left ventricular pressure-volume relations by miniaturized conductance micromanometry. *American Journal of Physiology: Heart and Circulation Physiology* **274,** H1416–H1422.

Ginsburg KS & Bers DM (2004). Modulation of excitation-contraction coupling by isoproterenol in cardiomyocytes with controlled SR Ca^{2+} load and Ca^{2+} current trigger. *The Journal of Physiology* **556,** 463–480.

Glower DD, Spratt JA, Snow ND, Kabas JS, Davis JW, Olsen CO, Tyson GS, Sabiston DC & Rankin JS (1985). Linearity of the Frank-Starling relationship in the intact heart: the concept of preload recruitable stroke work. *Circulation* **71,** 994–1009.

Gonano LA, Sepúlveda M, Rico Y, Kaetzel M, Valverde CA, Dedman J, Mattiazzi M & Vila-Petroff M (2011). Calcium-calmodulin kinase II mediates digitalis-induced arrhythmias. *Circulation: Arrhythmias and Electrophysiology* **4,** 947–957.

Grimm M & Brown JH (2010). Beta-adrenergic receptor signaling in the heart: role of CaMKII. *Journal of Molecular and Cellular Cardiology* **48,** 322–330.

Grueter E, Colbran R & Anderson M (2007). CaMKII, an emerging molecular driver for calcium homeostasis, arrhythmias, and cardiac dysfunction. *Journal of Molecular Medicine* **85,** 5–14.

Hagemann D, Hoche B, Krause E & Karczewski P (1999). Developmental changes in isoform expression of Ca^{2+}/calmodulin-dependent protein kinase II delta-subunit in rat heart. *Journal of Cellular Biochemistry* **74,** 202–210.

Hain J, Onoue H, Mayrleitner M, Fleischer S & Schindler H (1995). Phosphorylation modulates the function of the calcium release channel of sarcoplasmic reticulum from cardiac muscle. *The Journal of Biological Chemistry* **270,** 2074–2081.

Hamlin RL, Kijtawornrat A, Keene BW & Hamlin DM (2003). QT and RR intervals in conscious and anesthetized guinea pigs with highly varying RR intervals and given QTc-lengthening test articles. *Toxicological Sciences* **76,** 437–442.

Hamlin RL & Del Rio C (2010). An approach to the assessment of drug-induced changes in non-electrophysiological properties of cardiovascular function. *Journal of Pharmacological and Toxicological Methods* **62,** 20–29.

Hamlin RL & Del Rio C (2012). dP/dt(max) - A measure of “baroinometry.” *Journal of Pharmacological and Toxicological Methods* **66,** 63–65.

Hammond T, Carlsson L, Davis A, Lynch W, Mackenzie I, Redfern W, Sullivan A & Camm A (2001). Methods of collecting and evaluating non-clinical cardiac electrophysiological data in the pharmaceutical industry: results of an international survey. *Cardiovascular Research* **49,** 741–750.

Hanson PI, Meyer T, Stryer L & Schulman H (1994). Dual role of calmodulin in autophosphorylation of multifunctional CaM kinase may underlie decoding of calcium signals. *Cell Press* **12,** 943–956.

Harden T (1983). Agonist-induced desensitization of the β-adrenergic adenylate cyclase. *Pharmacological Reviews* **35,** 5–32.

Harmer AR, Abi-Gerges N, Morton MJ, Pullen GF, Valentin JP & Pollard CE (2012). Validation of an *in vitro* contractility assay using canine ventricular myocytes. *Toxicology and Applied Pharmacology* **260,** 162–172.

Hata J, Williams M, Schroder J, Lima B, Key J, Blaxall B, Petrofski J, Jakoi A, Milano C & Koch W (2006). Mirror changes in the LVAD-supported failing human heart: Lower GRK2 associated with improved b-adrenergic signalling after mechanical unloading. *Journal of Cardiac Failure* **12,** 360–369.

Hatfield A, Owen S & Pilot P (2007). In reply to Cardiotoxicity of the cancer therapeutic agent imatinib mesylate. *Nature Medicine* **13,** 13–16.

Hauser DS, Stade M, Schmidt A & Hanauer G (2005). Cardiovascular parameters in anaesthetized guinea pigs: a safety pharmacology screening model. *Journal of Pharmacological and Toxicological Methods* **52,** 106–114.

Haverkamp W, Breithardt G, Camm A, Janse MJ, Rosen MR, Antzelevitch C, Escande D, Franz M, Malik M, Moss A & Shah R (2000). The potential for QT prolongation and proarrhythmia by non-antiarrhythmic drugs: clinical and regulatory implications. Report on a policy conference of the European Society of Cardiology. *European Heart Journal* **21,** 1216–1231.

Hayes JS (1982). A simple technique for determining contractility, intraventricular pressure, and heart rate in the anesthetized guinea pig. *Journal of Pharmacological Methods* **8,** 231–239.

Hoch B, Meyer R, Hetzer R, Krause E & Karczewski P (1999). Identification and expression of δ-isoforms of the multifunctional Ca^{2+}/calmodulin-dependent protein kinase in failing and nonfailing human myocardium. *Circulation Research* **84,** 713–721.

Hochhaus A, Druker B, Sawyers C, Guilhot F, Schiffer CA, Cortes J, Niederwieser DW, Gambacorti-Passerini C, Gambacorti C, Stone RM, Goldman J, Fischer T, O'Brien SG, Reiffers JJ, Mone M, Krahnke T, Talpaz M & Kantarjian HM (2008). Favorable long-term follow-up results over 6 years for response, survival, and safety with imatinib mesylate therapy in chronic-phase chronic myeloid leukemia after failure of interferon-alpha treatment. *Blood* **111,** 1039–1043.

Hoover DB, Ganote CE, Ferguson SM, Blakely RD & Parsons RL (2004). Localization of cholinergic innervation in guinea pig heart by immunohistochemistry for high-affinity choline transporters. *Cardiovascular Research* **62,** 112–121.

Houghton PJ, Germain GS, Harwood FC, Schuetz JD, Stewart CF, Buchdunger E & Traxler P (2004). Imatinib mesylate is a potent inhibitor of the ABCG2 (BCRP) transporter and reverses resistance to topotecan and SN-38 in vitro. *Cancer Research* **64,** 2333–2337.

Hudmon A & Schulman H (2002). Structure/function of the multifunctional Ca^{2+}/calmodulin-dependent protein kinase II. *Biochemistry Journal* **364,** 593–611.

Hughes D (1997). *Mechanistic studies on the effects of diazepam on chloroquine-induced cardiotoxicity* (thesis). University of Liverpool.

Huke S, Desantiago J, Kaetzel MA, Mishra S, Brown JH, Dedman JR & Bers DM (2011). SR-targeted CaMKII inhibition improves SR Ca^{2+} handling, but accelerates cardiac remodeling in mice overexpressing CaMKIIδC. *Journal of Molecular and Cellular Cardiology* **50,** 230–238.

ICH (2000). *Safety pharmacology studies for human pharmaceuticals S7A*.

ICH (2005). *The non-clinical evaluation of the potential for delayed ventricular repolarization (QT interval prolongation) by human pharmaceuticals S7B*.

Iaccarino G, Barbato E, Cipolletta E, De Amicis V, Margulies K, Leosco D & Al. E (2005). Elevated myocardial and lymphocyte GRK2 expression and activity in human heart failure. *European Heart Journal* **26,** 1752–1758.

Ikeda Y, Hoshijima M & Chien KR (2008). Toward biologically targeted therapy of calcium cycling defects in heart failure. *Physiology* **23,** 6–16.

Johnson DM, Geys R, Lissens J & Guns PJ (2012). Drug-induced effects on cardiovascular function in pentobarbital anaesthetized guinea-pigs: invasive LVP measurements versus the QA interval. *Journal of Pharmacological and Toxicological Methods* **66,** 152–159.

Kantarjian H, Talpaz M, O'Brien S, Jones D, Giles F, Garcia-Manero G & Al E (2006). Survival benefit with imatinib mesylate versus interferon-alpha-based regimens in newly diagnosed chronic-phase chronic myelogenous leukemia. *Blood* **108,** 1835–1840.

Karczewski P, Kuschel M, Baltas L, Bartel S & Krause E (1997). Site-specific phosphorylation of a phospholamban peptide by cyclic nucleotide- and Ca2+/calmodulin-dependent protein kinases of cardiac sarcoplasmic reticulum. *Basic Research in Cardiology* **92,** 37–43.

Kariv I, Cao H & Oldenburg KR (2001). Development of a high throughput equilibrium dialysis method. *Journal of Pharmaceutical Sciences* **90,** 580–587.

Kass D, Beyar R, Lankfor E, Heard M, Maughan W & Sagawa K (1989). Influence of contractile state on curvilinearity of in situ end-systolic pressure-volume relations. *Circulation* **79,** 167–178.

Kerkelä R, Grazette L, Yacobi R, Iliescu C, Patten R, Beahm C, Walters B, Shevtsov S, Pesant S, Clubb FJ, Rosenzweig A, Salomon RN, Van Etten RA, Alroy J, Durand J-B & Force T (2006). Cardiotoxicity of the cancer therapeutic agent imatinib mesylate. *Nature Medicine* **12,** 908–916.

Kerkelä R, Woulfe KC, Durand J, Vagnozzi R, Chu TF, Beahm C, Chen MH & Force T (2009). Sunitinib-induced cardiotoxicity is mediated by off-target inhibition of AMP-activated protein kinase. *Clinical Translational Science* **2,** 15–25.

Khoo M, Zhang R, Grueter C, Ni G, Painter C, Eren M & Al. E (2004). Calmodulin kinase inhibition improves cardiac function after myocardial infarction. *Journal of the American College Cardiology* **43,** 255A.

Kirchhefer U, Schmitz W, Scholz H & Neumann J (1999). Activity of cAMP-dependent protein kinase and Ca^{2+}-/dependent protein kinase in failing and nonfailing human hearts. *Cardiovascular Research* **42,** 254–261.

Kitagawa Y, Tamura Y, Shimizu J, Nakajima-Takenaka C, Taniguchi S, Uesato S & Takaki M (2007). Effects of a novel histone deacetylase inhibitor, N-(2-Aminophenyl) benzamide, on a reversible hypertrophy induced by isoproterenol in *in situ* rat hearts. *Journal of Pharmacological Sciences* **104,** 167–175.

Koga T, Shiraki Y & Sakai K (1989). Comparative effects of ouabain on isolated papillary muscle from tree shrews, guinea-pigs and rats. *The Journal of Pharmacy and Pharmacology* **41,** 212–213.

Kohlhaas M, Zhang T, Seidler T, Zibrova D, Dybkova N, Steen A, Wagner S, Chen L, Brown JH, Bers DM & Maier LS (2006). Increased sarcoplasmic reticulum calcium leak but unaltered contractility by acute CaMKII overexpression in isolated rabbit cardiac myocytes. *Circulation Research* **98,** 235–244.

Koomen JM, van Gilst WH, Schevers JA & Wilting J (1984). Biphasic positive inotropic actions of ouabain on rat, guinea-pig and cat heart: a mathematical description. *Basic Research in Cardiology* **79,** 102–109.

Krause D & Van Etten R (2005). Tyrosine kinases as targets for cancer therapy. *New England Journal of Medicine* **353,** 172–187.

Kronenberg MW, McCain RW, Boucek RJ, Grambow DW, Sagawa K & Friesinger GC (1989). Effects of methoxamine and phenylephrine on left ventricular contractility in rabbits. *Journal of the American College of Cardiology* **14,** 1350–1358.

Kudej RK, Iwase M, Uechi M, Vatner DE, Oka N, Ishikawa Y, Shannon RP, Bishop SP & Vatner SF (1997). Effects of chronic beta-adrenergic receptor stimulation in mice. *Journal of Molecular and Cellular Cardiology* **29,** 2735–2746.

Kumar R, Crouthamel M-C, Rominger DH, Gontarek RR, Tummino PJ, Levin RA & King AG (2009). Myelosuppression and kinase selectivity of multikinase angiogenesis inhibitors. *British Journal of Cancer* **101,** 1717–1723.

Kumar R, Singh V & Baker K (2007). Kinase inhibitors for cardiovascular disease. *Journal of Molecular and Cellular Cardiology* **42,** 1–11.

Kuschel M, Karczewski P, Hempel P, Schlegel WP, Krause EG & Bartel S (1999). Ser16 prevails over Thr17 phospholamban phosphorylation in the beta-adrenergic regulation of cardiac relaxation. *The American Journal of Physiology* **276,** H1625–33.

Lakatta EG (2004). Beyond Bowditch: The convergence of cardiac chronotropy and inotropy. *Cell Calcium* **35,** 629–642.

Laverty H, Benson C, Cartwright E, Cross M, Garland C, Hammond T & Al. E (2011). How can we improve our understanding of cardiovascular safety liabilities to develop safer medicines? *British Journal of Pharmacology* **163,** 675–693.

Levick J (2003). *An Introduction to Cardiovascular Physiology*, 4th edn. Edward Arnold Ltd, London, UK.

Librizzi L, Biella G, Cimino C & De Curtis M (1999). Arterial supply of limbic structures in the guinea pig. *The Journal of Comparative Neurology* **411,** 674–682.

Little W, Cheng C, Mumma M, Igarashi Y, Vinten-Johansen J & Johnston W (1989). Comparison of measures of left ventricular contractile performance derived from pressure-volume loops in conscious dogs. *Circulation* **80,** 1378–1387.

Little WC (1985). The left ventricular dP/dtmax-end-diastolic volume relation in closed-chest dogs. *Circulation Research* **56,** 808–815.

Mahler F, Ross J, O'Rourke RA & Covell JW (1975). Effects of changes in preload, afterload and inotropic state on ejection and isovolumic phase measures of contractility in the conscious dog. *The American Journal of Cardiology* **35,** 626–634.

Maier L & Bers D (2002). Calcium, Calmodulin, and Calcium-Calmodulin Kinase II: Heartbeat to Heartbeat and Beyond. *Journal of Molecular and Cellular Cardiology* **34,** 919–939.

Maier L, Zhang T, Chen L, DeSantiago J, Brown J & Bers D (2003). Transgenic CaMKIIδC overexpression uniquely alters cardiac myocyte Ca^{2+}- handling: reduced SR Ca2+ load and activated SR Ca^{2+} release. *Circulation Research* **92,** 904–911.

Maier LS & Bers DM (2007). Role of Ca^{2+}/calmodulin-dependent protein kinase (CaMK) in excitation-contraction coupling in the heart. *Cardiovascular Research* **73,** 631–640.

Maisel AS, Motulsky HJ & Insel PA (1987). Propranolol treatment externalizes beta-adrenergic receptors in guinea pig myocardium and prevents further externalization by ischemia. *Circulation Research* **60,** 108–112.

Majewska-Michalska E (1998). The vertebrobasilar arterial system in guinea pig as compared with dog and human. *Folia Morphologica* **57,** 121–131.

Manning G, Whyte D, Martinez R, Hunter T & Sudarsanam S (2002). The protein kinase complement of the human genome. *Science* **298,** 1912–1934.

Markert M, Trautmann T, Groß M, Ege A, Mayer K & Guth B (2012). Evaluation of a method to correct the contractility index LVdP/dt(max) for changes in heart rate. *Journal of Pharmacological and Toxicological Methods* **66,** 90–105.

Marks AR, Reiken S & Marx SO (2002). Progression of heart failure : Is protein kinase A hyperphosphorylation of the ryanodine receptor a contributing factor? *Circulation* **105,** 272–275.

Marks L, Borland S, Philp K, Ewart L, Lainée P, Skinner M, Kirk S & Valentin J-P (2012). The role of the anaesthetised guinea-pig in the preclinical cardiac safety evaluation of drug candidate compounds. *Toxicology and Applied Pharmacology* **263,** 171–183.

Martin T (2011). *The role of CaMKIIδ in modulation of NF-κB signalling in normal and hypertrophied mouse hearts* (thesis). University of Strathclyde.

Martini F (2004). *Fundamentals of Anatomy and Physiology*, 6th edn. Benjamin Cummings, San Francisco, CA.

Massion PB, Feron O, Dessy C & Balligand J-L (2003). Nitric oxide and cardiac function: ten years after, and continuing. *Circulation Research* **93,** 388–398.

Maughan W, Sunagawa K, Burkhoff D & Sagawa K (1984). Effect of arterial impedance changes on the end-systolic pressure-volume relation. *Circulation* **54,** 595–602.

McNeil I & Verma S (1973). Phenylephrine-induced increases in cardiac contractility, cyclic adenosine monophosphate and phosphorylase. *Journal of Pharmacology and Experimental Therapeutics* **187,** 296–299.

Mellor HR, Bell AR, Valentin J-P & Roberts RR (2011). Cardiotoxicity associated with targeting kinase pathways in cancer. *Toxicological Sciences* **120,** 14–32.

Michael G, Kane K a & Coker SJ (2008). Adrenaline reveals the torsadogenic effect of combined blockade of potassium channels in anaesthetized guinea pigs. *British Journal of Pharmacology* **154,** 1414–1426.

Micheletti R, Palazzo F, Barassi P, Giacalone G, Ferrandi M, Schiavone A, Moro B, Parodi O, Ferrari P & Bianchi G (2007). Istaroxime, a stimulator of sarcoplasmic reticulum calcium adenosine triphosphatase isoform 2a activity, as a novel therapeutic approach to heart failure. *The American Journal of Cardiology* **99,** 24A–32A.

Minematsu T, Ohtani H, Sato H & Iga T (1999*b*). Sustained QT prolongation induced by tacrolimus in guinea pigs. *Life Sciences* **65,** PL197–202.

Minematsu T, Ohtani H, Sato H & Iga T (1999*a*). Pharmacokinetic/pharmacodynamic analysis of tacrolimus-induced QT prolongation in guinea pigs. *Biological & Pharmaceutical Bulletin* **22,** 1341–1346.

Minkin P, Zhao M, Chen Z, Ouwerkerk J, Gelderblom H & Baker SD (2009). Quantification of sunitinib in human plasma by high-performance liquid chromatography-tandem mass spectrometry. *Journal of Chromatography B Analytical Technologies in the Biomedical and Life Sciences* **874,** 84–88.

Mishra S, Sabbah HN, Jain JC & Gupta RC (2003). Reduced Ca^{2+} -calmodulin-dependent protein kinase activity and expression in LV myocardium of dogs with heart failure. *American Journal of Physiology Heart Circulation Physiology* **284,** H876–H883.

Mooney L, Marks L, Philp KL, Skinner M, Coker SJ & Currie S (2012). Optimising conditions for studying the acute effects of drugs on indices of cardiac contractility and on haemodynamics in anaesthetized guinea pigs. *Journal of Pharmacological and Toxicological Methods* **66,** 43–51.

Moors J, Philp K, Harmer AR, Lainee P & Valentin J-P (2007). Incidence of cardiac contractility issues in safety pharmacology studies: Is the core battery sufficient? *Journal of Pharmacological and Toxicological Methods* **60,** 252.

Motzer R, Hutson T, Tomczak P, Michaelson M, Bukowski R, Rixe O, Oudard S, Negrier S, Szczylik C, Kim S & Al. E (2007). Sunitinib versus interferon alpha in metastatic renal-cell carcinoma. *New England Journal of Medicine* **356,** 115–124.

Murphy MP (2009). How mitochondria produce reactive oxygen species. *The Biochemical Journal* **417,** 1–13.

Métrich M, Lucas A, Gastineau M, Samuel J, Heymes C, Morel E & Lezoualc F (2008). Epac nediates β-adrenergic receptor induced cardiomyocyte hypertrophy. *Circulation Research* **102,** 959–965.

Nakai J, Imagawa T, Hakamat Y, Shigekawa M, Takeshima H & Numa S (1990). Primary structure and functional expression from cDNA of the cardiac ryanodine receptor/calcium release channel. *FEBS letters* **271,** 169–177.

Nakayama H, Chen X, Baines C, Klevitsky R, Zhang X, Zhang H & Al E (2007). Ca2+-and mitochondrial-dependent cardiomyocyte necrosis as a primary mediator of heart failure. *Journal of Clinical Investigation* **117,** 2431–2444.

Narayanan N & Xu A (1997). Phosphorylation and regulation of the Ca(2+)-pumping ATPase in cardiac sarcoplasmic reticulum by calcium/calmodulin-dependent protein kinase. *Basic Research in Cardiology* **92,** 25–35.

Netterwald J (2007). Who Likes Kinases? *Drug Discovery & Development Magazine* **10,** 18–22.

Nielsen J, Kristiansen S, Ringgaard S, Nielsen T, Flyvbjerg A, Redington A & Al. E (2007). Left ventricular volume measurement in mice by conductance catheter:

Evaluation and optimization of calibration. *American Journal of Physiology Heart Circulation Physiology* **293,** H534−H540.

Noma K, Oyama N & Liao J (2006). Physiological role of ROCKs in the cardiovascular system. *American Journal of Physiology Cell Physiology* **290,** C661–C668.

Norton K, Iacono G & Vezina M (2009). Assessment of the pharmacological effects of inotropic drugs on left ventricular pressure and contractility: an evaluation of the QA interval as an indirect indicator of cardiac inotropism. *Journal of Pharmacological and Toxicological Methods* **60,** 193–197.

Oestreich EA, Malik S, Goonasekera SA, Blaxall BC, Kelley GG, Dirksen RT & Smrcka AV (2009). Epac and phospholipase C elipson regulate Ca^{2+} release in the heart by activation of protein kinase C epsilon and calcium-calmodulin kinase II. *The Journal of Biological Chemistry* **284,** 1514–1522.

Oestreich EA, Wang H, Malik S, Kaproth-joslin KA, Blaxall BC, Kelley GG, Dirksen RT & Smrcka AV (2007). Epac-mediated activation of phospholipase C epsilon plays a critical role in β-adrenergic receptor-dependent enhancement of Ca^{2+} mobilization in cardiac myocytes. *The Journal of Biological Chemistry* **282,** 5488–5495.

Opie LH & Gersh BJ (2009). *Drugs for the Heart*, 7th edn. Saunders Elsevier, Philadelphia, PA.

Otsu K, Willard H, Khanna V, Zorzato F, Green N & MacLennan D (1990). Molecular cloning of cDNA encoding the Ca^{2+} release channel (ryanodine receptor) of rabbit cardiac muscle sarcoplasmic reticulum. *Journal of Biological Chemistry* **265,** 13472–13483.

O'Brien S, Guilhot F, Larson R, Gathmann I, Baccarani M, Cervantes F & Al E (2003). Imatinib compared with interferon and lowdose cytarabine for newly diagnosed chronic-phase chronic myeloid leukemia. *New England Journal of Medicine* **348,** 994–1004.

Pacher P, Nagayama T, Mukhopadhyay P, Bátkai S & Kass DA (2008). Measurement of cardiac function using pressure-volume conductance catheter technique in mice and rats. *Nature Protocols* **3,** 1422–1434.

Page E (1964). The actions of cardiac glycosides on heart muscle cells. *Circulation* **30,** 237–251.

Pandalai P, Bulcao C, Merrill W & Akhter S (2006). Restoration of myocardial beta-adrenergic receptor signaling after left ventricular assist device support. *Thoracic and Cardiovascular Surgery* **131,** 975–980.

Passier R, Zeng H, Frey N, Naya FJ, Nicol RL, McKinsey T, Overbeek P, Richardson J a, Grant SR & Olson EN (2000). CaM kinase signaling induces cardiac hypertrophy and activates the MEF2 transcription factor *in vivo*. *The Journal of Clinical Investigation* **105,** 1395–1406.

De Pauw M, Vilaine J & Heyndrickx G (2004). Role of force–frequency relation during AV-block, sinus node block and beta-adrenoceptor block in conscious animals. *Basic Research in Cardiology* **95,** 360–371.

Pereira L, Métrich M, Fernández-Velasco M, Lucas A, Leroy J, Perrier R, Morel E, Fischmeister R, Richard S, Bénitah J-P, Lezoualc'h F & Gómez AM (2007). The cAMP binding protein Epac modulates Ca2+ sparks by a Ca^{2+}/calmodulin kinase signalling pathway in rat cardiac myocytes. *The Journal of Physiology* **583,** 685–694.

Perik P, Rikhof B, de Jong F, Verweij J, Gietema J & van der Graaf W (2007). Results of plasma N-terminal pro B-type natriuretic peptide and cardiac troponin monitoring in GIST patients do not support the existence of imatinib-induced cardiotoxicity. *Annals of Oncology*.

Pfizer (2006). Sutent® (Sunitinib) Prescribing Information. Available at: www.sutent.com/GIST/gist_prescribing_information.aspx. [Accessed January 24, 2011].

Philp KL, Hussain M, Byrne NF, Diver MJ, Hart G & Coker SJ (2006). Greater antiarrhythmic activity of acute 17beta-estradiol in female than male anaesthetized rats: correlation with Ca^{2+} channel blockade. *British Journal of Pharmacology* **149,** 233–242.

Porterfield JE, Kottam ATG, Raghavan K, Escobedo D, Jenkins JT, Larson ER, Treviño RJ, Valvano JW, Pearce JA & Feldman MD (2009). Dynamic correction for parallel conductance, GP, and gain factor, alpha, in invasive murine left ventricular volume measurements. *Journal of Applied Physiology* **107,** 1693–1703.

Qian J-Y & Guo L (2009). Altered cardiomyocyte Ca^{2+} handling as a predictor of cardiotoxicity and arrhythmogenesis of drug candidates. *Journal of Pharmacological and Toxicological Methods* **60,** 233.

Qian J-Y & Guo L (2010). Altered cytosolic Ca^{2+} dynamics in cultured Guinea pig cardiomyocytes as an *in vitro* model to identify potential cardiotoxicants. *Toxicology In Vitro* **24,** 960–972.

Quinones MA, Gaasch WH & Alexander JK (1976). Influence of acute changes in preload, afterload, contractile state and heart rate on ejection and isovolumic indices of myocardial contractility in man. *Circulation* **53,** 293–302.

Raghavan K, Wei C, Kottam A, Altman D, Fernandez D, Reyes M & Al. E (2004). Design of instrumentation and data-acquisition system for complex admittance measurement. *Biomedical Sciences Instrumentation* **40,** 453−457.

Rainer PP, Doleschal B, Kirk JA, Sivakumaran V, Saad Z, Groschner K, Maechler H, Hoefler G, Bauernhofer T, Samonigg H, Hutterer G, Kass DA, Pieske B, von Lewinski D & Pichler M (2012). Sunitinib causes dose-dependent negative functional effects on myocardium and cardiomyocytes. *BJU International*; DOI: 10.1111/j.1464-410X.2012.11134.x.

Ramírez-Gil JF, Trouvé P, Mougenot N, Carayon A, Lechat P & Charlemagne D (1998). Modifications of myocardial Na^+,K^+-ATPase isoforms and Na^+/Ca^{2+} exchanger in aldosterone/salt-induced hypertension in guinea pigs. *Cardiovascular Research* **38,** 451–462.

Rang H, Dale M, Ritter J & Moore P (2003). *Pharmacology*, 5th edn. Churchill Livingstone, UK.

Repke K, Est M & Portius HJ (1965). On the cause of species differences in digitalis sensitivity. *Biochemical Pharmacology* **14,** 1785–1802.

Ribeiro AL, Marcolino MS, Bittencourt HNS, Barbosa MM, Nunes MDCP, Xavier VF & Clementino NCD (2008). An evaluation of the cardiotoxicity of imatinib mesylate. *Leukemia Research* **32,** 1809–1814.

Robertson D (2004). *Primer on the autonomic nervous system*, 2nd edn. Elsevier, San Diego, CA.

Rodriguez P, Bhogal M & J C (2003). Stoichiometric phosphorylation of cardiac ryanodine receptor on serine 2809 by calmodulin-dependent kinase II and protein kinase A. *Journal of Biological Chemistry* **278,** 38593–38600.

Rosti G, Martinelli G & Baccarani M (2007). In reply to Cardiotoxicity of the cancer therapeutic agent imatinib mesylate. *Nature Medicine* **13,** 15–16.

Sag CM, Köhler AC, Anderson ME, Backs J & Maier LS (2011). CaMKII-dependent SR Ca leak contributes to doxorubicin-induced impaired Ca handling in isolated cardiac myocytes. *Journal of Molecular and Cellular Cardiology* **51,** 749–759.

Sagawa K, Suga H, Shoukas A & Bakalar KM (1977). End-systolic pressure/volume ratio: a new index of ventricular contractility. *The American Journal of Cardiology* **40,** 748–753.

Said M, Mundina-Weilenmann C, Vittone L & Mattiazzi A (2002). The relative relevance of phosphorylation of the Thr 17 residue of phospholamban is different at different levels of β-adrenergic stimulation. *Plugers Archives - European Journal of Physiology* **444,** 801–809.

Salyers A, Rozek L & Bittner S (1988). Simultaneous determination of ventricular function and systemic hemodynamics in the conscious rat. *Journal of Pharmacological Methods* **19,** 267–274.

Sapia L, Palomeque J, Mattiazzi A & Petroff MV (2010). Na^+/K^+-ATPase inhibition by ouabain induces CaMKII-dependent apoptosis in adult rat cardiac myocytes. *Journal of Molecular and Cellular Cardiology* **49,** 459–468.

Schaub M, Hefti M & Zaugg M (2006). Integration of calcium with the signaling network in cardiac myocytes. *Journal of Molecular and Cellular Cardiology* **41,** 183–214.

Schramm M, Towart R, Kazda S, Thomas G & Franckowiak G (1985). Calcium agonism, a new mechanism for positive inotropy. Hemodynamic effects and mode of action of BAY K 8644. *Advances in Myocardiology* **6,** 59–70.

Schwenke DO & Cragg P a (2004). Comparison of the depressive effects of four anesthetic regimens on ventilatory and cardiovascular variables in the guinea pig. *Comparative Medicine* **54,** 77–85.

Scisense (2009). ADVantage^{TM} PV System manual 5.0.

Sebolt-Leopold J & English J (2006). Mechanisms of drug inhibition of signalling molecules. *Nature* **441,** 457–462.

Sharma AK, Dhingra S, Khaper N & Singal PK (2007). Activation of apoptotic processes during transition from hypertrophy to heart failure in guinea pigs. *American Journal of Physiology Heart and Circulatory Physiology* **293,** H1384–90.

Sherbenou D & Druker B (2007). Applying the discovery of the Philadelphia chromosome. *Journal of Clinical Investigation* **117,** 2067–2074.

Shibata S, Seriguchi DG, Iwadare S, Ishida Y & Shibata T (1980). The regional and species differences on the activation of myocardial alpha-adrenoceptors by phenylephrine and methoxamine. *General Pharmacology* **11,** 173–180.

Si J & Collins SJ (2008). Activated Ca^{2+}/calmodulin-dependent protein kinase IIγ is a critical regulator of myeloid leukemia cell proliferation. *Cancer research* **68,** 3733–3742.

Sproat TT & Lopez LM (1991). Around the beta-blockers, one more time. *DICP : The Annals of Pharmacotherapy* **25,** 962–971.

Srinivasan M, Edman C & Schulman H (1994). Alternative splicing introduces a nuclear localization signal that targets multifunctional CaM kinase to the nucleus. *Journal of Cellular Biology* **126,** 839–852.

St John Sutton MG, Plappert T & Rahmouni H (2009). Assessment of left ventricular systolic function by echocardiography. *Heart Failure Clinics* **5,** 177–190.

Stummann TC, Beilmann M, Duker G, Dumotier B, Fredriksson JM, Jones RL, Hasiwa M, Kang YJ, Mandenius C-F, Meyer T, Minotti G, Valentin YJ-P, Zünkler BJ & Bremer S (2009). Report and recommendations of the workshop of the European Centre for the Validation of Alternative Methods for Drug-Induced Cardiotoxicity. *Cardiovascular Toxicology* **9,** 107–125.

Sugden PH & Bogoyevitch MA (1995). Intracellular signalling through protein kinases in the heart. *Cardiovascular Research* **30,** 478–492.

Svendsen O, Kok L & Lauritzen B (2007). Nociception after intraperitoneal injection of a sodium pentobarbitone formulation with and without lidocaine in rats quantified by expression of neuronal c-fos in the spinal cord--a preliminary study. *Laboratory Animals* **41,** 197–203.

Takeshita D, Shimizu J, Kitagawa Y, Yamashita D, Tohne K, Nakajima-Takenaka C, Ito H & Takaki M (2008). Isoproterenol-induced hypertrophied rat hearts: Does short-term treatment correspond to long-term treatment? *Journal of Physiological Science* **58,** 179–188.

Telli M, Witteles R, Fisher G & Srinivas S (2008). Cardiotoxicity associated with the cancer therapeutic agent sunitinib malate. *Annals of Oncology* **19,** 1613–1618.

Testai L, Calderone V, Salvadori A, Breschi MC, Nieri P & Martinotti E (2004). QT prolongation in anaesthetized guinea-pigs: an experimental approach for preliminary screening of torsadogenicity of drugs and drug candidates. *Journal of Applied Toxicology* **24,** 217–222.

Thanopoulou E & Judson I (2012). The safety profile of imatinib in CML and GIST: long-term considerations. *Archives of Toxicology* **86,** 1–12.

Thomas G, Chung M & Cohen CJ (1985). A dihydropyridine (Bay k 8644) that enhances calcium currents in guinea pig and calf myocardial cells. A new type of positive inotropic agent. *Circulation Research* **56,** 87–96.

Tobimatsu T & Fujisawa H (1989). Tissue-specific expression of four types of rat calmodulin-dependent protein kinase II mRNAs. *Journal of Biological Chemistry* **260,** 17907–17912.

Toda N & West CT (1969). The action of ouabain on the function of the atrioventricular node in rabbits. *The Journal of Pharmacology and Experimental Therapeutics* **169,** 287–297.

Trent J, Patel S, Zhang J & Al. E (2010). Rare incidence of congestive heart failure in gastrointestinal stromal tumor and other sarcoma patients receiving imatinib mesylate. *Cancer* **116,** 184–192.

Ueyama Y, del Rio C & Hamlin RL (2011). Simultaneous assessment of ECG liabilities and load-independent myocardial function in vivo: Pressure-volume analysis in closed chest anesthetized guinea pigs. *Journal of Pharmacological and Toxicological Methods* **66,** 161.

Verkhivker G (2007). Exploring sequence-structure relationships in the tyrosine kinome space: functional classification of the binding specificity mechanisms for cancer therapeutics. *Bioinformatics* **23,** 1919–1926.

Verweij J, Casali P, Kotasek D, Le Cesne A, Reichard P, Judson I & Al. E (2007). Imatinib does not induce cardiac left ventricular failure in gastrointestinal stromal tumours patients: analysis of EORTC-ISG-AGITG study 62005. *European Journal of Cancer* **43,** 974–978.

Wallace AG, Skinner NS & Mitchell JH (1963). Hemodynamic determinants of the maximal rate of rise of left ventricular pressure. *The American Journal of Physiology* **205,** 30–36.

Wang W, Zhu W, Wang S, Yang D, Crow MT, Xiao R-P & Cheng H (2004). Sustained beta1-adrenergic stimulation modulates cardiac contractility by Ca2+/calmodulin kinase signaling pathway. *Circulation Research* **95,** 798–806.

Wang X, Li F & Gerdes AM (1999). Hypertrophy and Failure in Guinea Pigs: I. Regional Hemodynamics and Myocyte Remodeling. *Journal of Molecular and Cellular Cardiology* **317,** 307–317.

Wegener AD, Simmerman HK, Lindemann JP & Jones LR (1989). Phospholamban phosphorylation in intact ventricles. Phosphorylation of serine 16 and threonine 17 in response to beta-adrenergic stimulation. *The Journal of Biological Chemistry* **264,** 11468–11474.

Wehrens X, Lehnart S, Reiken S & Marks A (2004). Ca^{2+}/calmodulin dependent protein kinase II phosphorylation regulates the cardiac ryanodine receptor. *Circulation Research* **94,** e1–e70.

Weinhouse E, Kaplanski J, Danon A & Nudel DB (1989). Cardiac glycoside toxicity in small laboratory animals. *Life Sciences* **44,** 441–450.

Williams M, Hata J, Schroder J, Rampersaud E, Petrofski J, Jakoi A, Milano C & Koch W (2004). Targeted beta-adrenergic receptor kinase (betaARK1) inhibition by gene transfer in failing human hearts. *Circulation* **109,** 1590–1593.

Witcher DR, Kovacss RJ, Schulmans H, Cefali DC & Jones LR (1991). Unique phosphorylation site on the cardiac ryanodine receptor regulates calcium channel activity. *The Journal of Biological Chemistry* **266,** 11144–11152.

Wolf A, Couttet P, Dong M, Grenet O, Heron M, Junker U, Laengle U, Ledieu D, Marrer E, Nussher A, Persohn E, Pognan F, Rivière G-J, Roth DR, Trendelenburg C, Tsao J & Roman D (2010). Imatinib does not induce cardiotoxicity at clinically relevant concentrations in preclinical studies. *Leukemia Research* **34,** 1180–1188.

Wu Y, Colbran R & Anderson M (2001). Calmodulin kinase is a molecular switch for cardiac excitation-contraction coupling. *Proceedings of the National Academy of Sciences USA* **98,** 2877–2881.

Wu Y, Temple J, Zhang R, Dzhura I, Zhang W & Trimble R (2002). Calmodulin kinase II and arrhythmias in a mouse model of cardiac hypertrophy. *Circulation* **106,** 1288–1293.

Xenopoulos NP & Applegate RJ (1994). The effect of vagal stimulation on left ventricular systolic and diastolic performance. *The American Journal of Physiology* **266,** H2167–73.

Yamaguchi N & Meissner G (2007). Does Ca^{2+}/calmodulin-dependent protein kinase δC activate or inhibit the cardiac ryanodine receptor ion channel? *Circulation Research* **100,** 293–295.

Yang B, Beishchel D, Larson D, Kelley R, Shi J & Watson R (2001). Validation of conductance catheter system for quantification of murine pressure-volume loops. *Journal of Investigative Surgery* **14,** 341–355.

Yang Y, Zhu W-Z, Joiner M, Zhang R, Oddis CV, Hou Y, Yang J, Price EE, Gleaves L, Eren M, Ni G, Vaughan DE, Xiao R-P & Anderson ME (2006). Calmodulin kinase II inhibition protects against myocardial cell apoptosis in vivo. *American Journal of Physiology: Heart and Circulatory Physiology* **291,** H3065–3075.

Yao X, Anderson D, Ross S, Lang D, Desai B, Cooper D, Wheelan P, McIntyre M, Bergquist M, MacKenzie K, Becherer J & Hashim M (2008). Predicting QT prolongation in humans during early drug development using hERG inhibition and an anaesthetized guinea-pig model. *British Journal of Pharmacology* **154,** 1446–1456.

Yap YG & Camm AJ (2003). Drug induced QT prolongation and torsades de pointes. *Heart* **89,** 1363–1372.

Yoo B, Lemaire A, Mangmool S, Wolf MJ, Curcio A, Mao L & Rockman H a (2009). β_1-adrenergic receptors stimulate cardiac contractility and CaMKII activation in vivo and enhance cardiac dysfunction following myocardial infarction. *American Journal of Physiology Heart Circulation Physiology* **297,** H1377–86.

Zhang J, Yang P & Gray N (2009). Targeting cancer with small molecule kinase inhibitors. *Nature Reviews Cancer* **9,** 28–39.

Zhang T, Johnson E, Morissette M, Sah V, Gigena M, Belke D & Al E (2002). The cardiac-specific nuclear B isoform of Ca^{2+}/Calmodulin-dependent protein kinase II induces hypertrophy and dilated cardiomyopathy associated with increased protein phosphatase 2A activity. *Journal of Biological Chemistry* **277,** 1261–1267.

Zhang T, Maier LS, Dalton ND, Miyamoto S, Ross J, Bers DM & Brown JH (2003). The δ_C isoform of CaMKII is activated in cardiac hypertrophy and induces dilated cardiomyopathy and heart failure. *Circulation Research* **92,** 912–919.

Zhaung G, Shu-yan H, Chen Y, Jun G & Li P (2011). Mitochondrial reactive oxygen species in sunitinib induced cardiomyocytes apoptosis. *Chinese Journal of Pharmacology and Toxicology*.

Zhou J (2010). Cardiac adaptation to chronic blockade of voltage-gated L-type calcium channels in the sarcolemma. *Electronic Thesis and Dissertation Repository*. Available at: http://ir.lib.uwo.ca/etd/54.

Zhou Y-Q, Foster FS, Nieman BJ, Davidson L, Chen XJ & Henkelman RM (2004). Comprehensive transthoracic cardiac imaging in mice using ultrasound biomicroscopy with anatomical confirmation by magnetic resonance imaging. *Physiological Genomics* **18,** 232–244.

Zhu W, Wang S, Chakir K, Yang D, Zhang T, Brown JH, Devic E, Kobilka BK, Cheng H & Xiao R (2003). Linkage of β_1-adrenergic stimulation to apoptotic heart

cell death through protein kinase A–independent activation of Ca^{2+}/calmodulin kinase II. *Journal of Clinical Investigation* **111,** 617–625.

APPENDIX A – SUPPLIERS OF EQUIPMENT AND MATERIALS

Suppliers of Equipment and Materials – Strathclyde

MATERIALS AND EQUIPMENT	**SUPPLIER DETAILS**
3-way stopcock	Vygon, Cirencester, UK
25G 5/8” hypodermic needle	BD UK Ltd, Oxford, UK
23G 1” hypodermic needle	BD UK Ltd, Oxford, UK
21G 11/2” hypodermic needle	BD UK Ltd, Oxford, UK
AutoClip Kit 500: *500 clips, applier and remover*	Alzet®, DURECT Corporation, Cupertino, CA, USA
Cannulae: Venous – PP25 (internal diameter = 0.40 mm; external diameter = 0.80 mm); Arterial PP50 (internal diameter = 0.58 mm; external diameter = 0.96 mm) fine bore polythene tubing (non sterile)	SIMS, Portex, Hythe, Kent, UK
Centrifuge: Fisher Scientific AccuSpin MicroR	Fisher Scientific, Loughborough, UK
Data acquisition and analysis system: *Po-Ne-Mah P3 Plus*	Linton Instrumentation, Diss, Norfolk, UK
Densitometer: *GS-800*	Bio-Rad Laboratories Ltd., Hemel Hempstead, Hertfordshire, UK
ECG leads & needles	Made in-house
Electrophoresis gels: *10% Bis-tris, 7%*	Invitrogen, Inchinnan, Renfrewshire, UK

Tris-acetate gels (10 and 15 well)	
Electrophoresis system: *NuPAGE®*	Invitrogen, Inchinnan, Renfrewshire, UK
Filter paper: *Whatman17 Chr Size 46 x 57 cm*	Fisher Scientific, Loughborough, UK
Guinea pigs: *Male Dunkin-Hartley*	Harlan, Bicester, UK
Guinea pig food: *FD1 guinea pig diet*	www.sdsdiets.com
Infusion pump: Syringe infusion pump 22	Harvard Apparatus, Kent, UK
Mercury manometer	Yamasu, Japan
Microplate reader: *Model 680*	Bio-Rad Laboratories Ltd., Hemel Hempstead, Hertfordshire, UK
Millar Microtip® catheter: 2F and 3F	Linton Instrumentation, Diss, UK
Millar control box: *TC-510*	Linton Instrumentation, Diss, UK
Nitrocellulose membrane: *Whatman chromatography paper 17 Chr 460 mm x 570 mm sheet*	Fisher Scientific, Loughborough, UK
Osmotic minipumps: *2ML1*	Alzet®, DURECT Corporation, Cupertino, CA, USA
P81 Phosphocellulose squares	Merck Chemicals Ltd (Calbiochem), Nottingham, UK
Protein assay: *Coomassie Plus*	Pierce, Cramlington, Northumberland, UK
Pulse oximeter/capnograph: *Medair*	Kruuse UK Ltd, Sherburn in Elmet, UK

Lifesense™ Vet pulse oximeter/capnograph	
Quantity One software: *version 4.5.2*	Bio-Rad Laboratories Ltd., Hemel Hempstead, Hertfordshire, UK
Rats: *Male Sprague Dawley*	Biological Procedures Unit, University of Strathclyde, Glasgow, UK
Rat bedding: *Gold flakes (GR18)*	DBM Scotland Ltd, Grangemouth, UK
Rat cages: *RC2F*	North Kent Plastics, Rochester, Kent, UK
Rat food: *CRM (p) rat diet*	www.sdsdiets.com
Scintillation counter: *Liquid scintillation analyzer Tri-carb 1500*	Packard Instrument Company Inc, Downers Grove, Illinois, USA
SigmaPlot software	www.sigmaplot.com
Statistical analysis software: *StatsDirect*	www.statsdirect.com
Swabs (non-sterile gauze) 10 cm x 10 cm x 8 ply	Shermond Surgical Supply Ltd, Peachaven, UK
Syringes (1, 2, 5, 10 mL)	BD UK Ltd, Oxford, UK
Syringe infusion pumps: *Harvard Apparatus syringe infusion pump 22*	Harvard Apparatus, Kent, UK
Tracheal cannula	Made in-house
Tissue homogeniser: *Ultra Turrax*®	Fisher Scientific, Loughborough, UK
Ultrasound system: *HDI® 3000*	ASL Ultrasound, Bothwell, WA, USA

Ultrasound transducer: 13-MHz linear array transducer	ASL Ultrasound, Bothwell, WA, USA
Ventilation pump: *Scientific & Research Instruments Ltd, catalogue number 50-1718*	Edenbridge, Kent, UK
Western blot film: UltraCruz™ autoradiography film, Blue, 8x10	SantaCruz Biotechnology, Inc. Heidelberg, Germany

Suppliers of Equipment and Materials – AstraZeneca

MATERIALS AND EQUIPMENT	**SUPPLIER DETAILS**
3-way stopcock (Tro-Venoflow 3)	Troge Medical GMBH, Hamburg, Germany
25G 5/8” hypodermic needle (Tro-Can)	Troge Medical GMBH, Hamburg, Germany
23G 1” hypodermic needle	Troge Medical GMBH, Hamburg, Germany
ADVantage™ PV System Control Box	Scisense, London, ON, Canada
Blood gas analyser: *Gem Premier Blood Gas Analyser*	Instrumentation Laboratory, Warrington, UK
Centrifuge	Sanyo Micro Centaur MSE
Constant voltage isolated stimulator: *Model DS2A –Mk II*	Digitimer Ltd, Welwyn Garden City, Hertfordshire, UK
Data acquisition and analysis system:	Developed in-house

PharmLab on-line 5.0	
Data acquisition and analysis system: *NOTOCORD-hem version 4.2 Physiological Data Acquisition and Analysis System*	Notocord, Croissy-sur-Seine, France
ECG leads & needles	Made in-house
Guinea pigs: *Male Dunkin-Hartley*	Harlan, Bicester, UK
Guinea pig bedding: Aspen chip bedding and sizzle nest	www.datesand.com
Guinea pig food: Teklad global higher fibre guinea-pig diet 2041	Harlan, Bicester, UK
Homeothermic blanket control unit	Harvard apparatus
Pacing electrode	Made in-house
Polythene tubing (non-sterile)	SIMS, Portex, Hythe, Kent, UK
Pulse oximeter: *Medair PulseSense^{TM} VET*	Kruuse UK Ltd, Sherburn in Elmet, UK
Scisense pressure catheter: *1.6F FTS-1611B-0018*	Scisense, London, ON, Canada
Scisense pressure-volume catheter: *6mm catheter spacing*	Scisense, London, ON, Canada
Stimulator: *HSE Stimulator P*	Hugo Sachs Elektronic, Freiburg, Germany

Stimulating electrodes	Made in-house
Swabs (non-sterile gauze) 10 cm x 10 cm x 8 ply	Synergy Health Ltd, Healthcare Solutions, Matrix Park, Chorley, PR7 7NB, UK
Syringes (Primo Luer; 1, 2, 5, 10 mL)	CODAN Medial ApS, DK-4970, RØdby, Denmark
Syringe infusion pumps (KD scientific)	Linton Instrumentation, Diss, Norfolk
TnI assay kit: *Siemens ADVIA Centaur® CP Immunoassay System*	www.medical.siemens.com
Tracheal cannula	Made in-house
Ventilator: *TOPO^{TM} dual mode ventilator*	Kent Scientific, West Malling, UK
Ventilation pump	Ugo Basile, Biological Research Apparatus 21025, Comerio, VA, Italy

APPENDIX B – SUPPLIERS OF DRUGS

Suppliers and Storage Information -Strathclyde

Drugs & Materials	**Supplier**	**Storage**
"Abgent CaMKIIδ" primary antibody: *Rabbit anti-CaMKIIδ polyclonal antibody*	Abgent, Abington, Oxford, UK	-20°C
"Abgent CaMKIIδ-like" primary antibody: *Rabbit anti-CaMKIIδ-like polyclonal antibody*	Abgent, Abington, Oxford, UK	-20°C
Acetone	Sigma-Aldrich, Poole, Dorset, UK	Room temperature
"Anti-mouse 1" secondary antibody: *Sheep anti-mouse IgG-horseradish peroxidise liked species-specific whole antibody*	GE Healthcare, Bucks, UK	-20°C
"Anti-mouse 2" secondary antibody: *Peroxidase AffiniPure Donkey Anti-Mouse IgG (H+L)*	Jackson ImmunoResearch Laboratories Inc., Suffolk, UK	-80°C
"Anti-rabbit" secondary antibody: *Goat anti-rabbit IgG (whole molecule)-peroxidase conjugated*	Sigma-Aldrich, Poole, Dorset, UK	-20°C
Autocamtide-2	Sigma-Aldrich, Poole, Dorset, UK	-20°C
Ascorbic acid	Sigma, Poole, Dorset, UK	Room temperature

Autocamtide-2 related inhibitory peptide (AIP): *myristolated*	Merck Chemicals Ltd (Millipore), Nottingham, UK	-20°C
Adenosine-5'-trisphosphate (ATP)	Sigma-Aldrich, Poole, Dorset, UK	-20°C
β-glycerol phosphate	Sigma-Aldrich, Poole, Dorset, UK	Room temperature
"Bers CaMKII" primary antibody	Bers Laboratory, University of California Davies, CA, USA	-20°C
Bovine serum albumin (BSA): *Albumin from bovine serum minimum 98%*	Sigma-Aldrich, Poole, Dorset, UK	4°C
Bovine serum albumin (BSA) standards	Pierce, Cramlington, Northumberland, UK	4°C
Calcium chloride ($CaCl_2$)	VWR International, Lutterworth, Leicestershire, UK	Room temperature
Calmodulin	Merck Chemicals Ltd (Calbiochem), Nottingham, UK	-20°C
Calyculin A	Sigma-Aldrich, Poole, Dorset, UK	-20°C
Coumaric acid	GE Healthcare, Buckinghamshire, UK	-20°C

Creatine	Sigma-Aldrich, Poole, Dorset, UK	Room temperature
"Custom CaMKII" primary antibody: *Rabbit anti-CaMKII Polyclonal antibody*	Eurogentec, Seraing, Belgium	-80°C
Depilatory cream: Veet®	Pharmacist/Supermarkets	Room temperature
Dithiothreitol (DTT) / Cleland's' Reagent	Merck Chemicals Ltd (Calbiochem), Nottingham, UK	4°C
Electrophoresis running buffer: *NuPAGE® MOPS SDS running buffer (20x), NuPAGE® Tris-acetate SDS running buffer (20x)*	Invitrogen, Inchinnan, Renfrewshire, UK	4°C
Electrophoresis transfer buffer: *NuPAGE® transfer buffer (20x)*	Invitrogen, Inchinnan, Renfrewshire, UK *and* Made in-house	4°C
Enhanced chemiluminescence reagent (ECL)	Thermo Scientific, Runcorn, Cheshire, UK *and* Made in-house	4°C
Ethylene-diamine-tetraacetic acid (EDTA)	Sigma-Aldrich, Poole, Dorset, UK	Room temperature
Ethylene-glycol-tetraacetic acid (EGTA)	Sigma-Aldrich, Poole, Dorset, UK	Room temperature

Fentanyl citrate (50 µg mL^{-1})	Martindale Pharmaceuticals, Romford, Essex, UK	Room temperature
Euthatal® (sodium pentobarbital 200 mg mL^{-1})	Rhone, Metrieux, Harlow, Essex, UK	4°C
Fetal calf serum (FCS)	Invitrogen, Inchinnan, Renfrewshire, UK	-20°C
GAPDH primary antibody: Anti-GAPDH antibody, mouse monoclonal [6C5]	Abcam, Cambridge, UK	-20°C
Glycine	Sigma-Aldrich, Poole, Dorset, UK	Room temperature
Heparin sodium (mucous) 5000 units ml^{-1}	Leo Laboratories Ltd, Princes Risborough, Bucks, UK	4°C
4-(2-hydroxyethyl)-1-piperazineethanesulfonic acid (HEPES)	Sigma-Aldrich, Poole, Dorset, UK	Room temperature
Imatinib mesylate	LC Laboratories, Woburn, MA, USA *and* Sequoia Research Products Ltd, Pangbourne, UK	-20°C 4°C
Isoflurane	Veterinary wholesalers through the Biological	4°C

	Procedures Unit at the University of Strathclyde	
Isoprenaline HCl	Sigma, Poole, Dorset, UK	Room temperature
Luminol	GE Healthcare, Buckinghamshire, UK	-20°C
Magnesium chloride ($MgCl_2$)	Sigma-Aldrich, Poole, Dorset, UK	Room temperature
Methanol	Sigma-Aldrich, Poole, Dorset, UK	Room temperature
Molecular weight markers: *Novex® Sharp Prestained protein standards* OR *See Blue® Plus 2 Prestained Standards*	Invitrogen, Inchinnan, Renfrewshire, UK	-20°C
3-(N-morpholino) propanesulfonic acid(MOPS)	Sigma-Aldrich, Poole, Dorset, UK	Room temperature
Non-fat dry milk: *Marvel*	Most supermarkets	Room temperature
Ouabain octahydrate	Sigma, Poole, Dorset, UK	Room temperature
pThr286-CaMKII antibody: *Phospho-CaM Kinase II (Thr286), Mouse IgG1 mAb*	Thermo Scientific, Surrey, UK	-20°C
pSer2815-RyR antibody	Badrilla Ltd, Leeds, UK	-80°C
Phosphoric acid	Sigma-Aldrich, Poole, Dorset, UK	Room temperature
Potassium chloride (KCl)	Sigma-Aldrich, Poole,	Room temperature

	Dorset, UK	
Protease inhibitor cocktail: *set V, EDTA free*	Merck Chemicals Ltd (Calbiochem), Nottingham, UK	-20°C
Protein kinase A inhibitor peptide (PKI)	Merck Chemicals Ltd (Millipore), Nottingham, UK	-20°C
Protein kinase C inhibitor peptide	Merck Chemicals Ltd (Millipore), Nottingham, UK	-20°C
"R&D CaMKII" antibody: *Rabbit anti-CaMKIIδ-like polyclonal antibody*	R&D systems Abington, Oxford, UK	-20°C
Recombinant (human) CaMKIIδ	Merck Chemicals Ltd (Millipore), Nottingham, UK	-80°C
Sample loading buffer	Invitrogen, Inchinnan, Renfrewshire, UK	Room temperature
Scintillation fluid: Emulsifier-safe, High flash-point economy LSC-cocktail for aqueous samples	Packard Instrument Company Inc, Downers Grove, Illinois, USA	Room temperature
Sodium chloride (NaCl)	Sigma, Poole, Dorset, UK	Room temperature
Sodium pentobarbital	Sigma, Poole, Dorset, UK	Room temperature
Sodium phosphate (NaH_2PO_4)	Sigma-Aldrich, Poole, Dorset, UK	Room temperature

Sodium (Na) orthovanadate	Sigma-Aldrich, Poole, Dorset, UK	Room temperature
Sunitinib malate	Sequoia Research Products Ltd, Pangbourne, UK	4°C
Taurine	Sigma-Aldrich, Poole, Dorset, UK	Room temperature
Thimerosol	Sigma-Aldrich, Poole, Dorset, UK	4°C
Tris(hydroxymethyl)aminomethane (Tris) HCl: Trizma® HCl	Sigma-Aldrich, Poole, Dorset, UK	Room temperature
Triton X®	Sigma-Aldrich, Poole, Dorset, UK	Room temperature
Trizma® base	Sigma-Aldrich, Poole, Dorset, UK	Room temperature
Tween-20	Sigma-Aldrich, Poole, Dorset, UK	Room temperature
Ultrasound gel	Mount International Ultrasound Services Ltd, Gloucester, UK	Room temperature
Verapamil HCl	Sigma, Poole, Dorset, UK	Room temperature

Suppliers and Storage Information -AstraZeneca

Drugs & Materials	**Supplier**	**Storage**
Fentanyl citrate (50 µg mL^{-1})	Martindale Pharmaceuticals, Romford, Essex, UK	Room temperature
Euthatal® (pentobarbital sodium 200 mg mL^{-1})	Merial Animal Health Ltd, Harlow, Essex, UK	Room temperature
Heparin sodium (mucous) 5000 units mL^{-1}	LEO Laboratories Ltd, Princes Risborough, Bucks, UK	Room temperature
Hypnorm®	Vet Pharma, Chennai, India	Room temperature
Hypnovel®	Welwyn Garden City, UK	Room temperature
Phenylephrine	Sigma, Poole, Dorset, UK	4°C
Sodium nitroprusside	Sigma, Poole, Dorset, UK	4°C
Sodium pentobarbital	Sigma, Poole, Dorset, UK	Room temperature
Sunitinib malate	Sequoia Research Products Ltd, Pangbourne, UK	4°C

APPENDIX C – SCISENSE ADVANTAGE™ SYSTEM D METHOD

The details in this section are based on those in Scisense, 2009. The D method for volume calculation relies on the fact that the catheter based dipole field has two definable limits when measuring the admittance of any volume. The first defined point is that at which there is no blood in the LV and the catheter is surrounded by tissue only. The second limit is the point at which the catheter is surrounded by a volume of blood that exceeds the range of the field. At this point, there would be no tissue contribution to the measured admittance. Figure C1a illustrates these two points and the transition from one extreme to the other. Any given value of magnitude of admittance corresponds to a unique radius of the blood cylinder (i.e. the LV). The values of admittance measured by the catheter can be correlated to the measured LVP to define the end-systolic and end-diastolic values (Figure C1b). The corresponding radius can then be mathematically converted to blood volume.

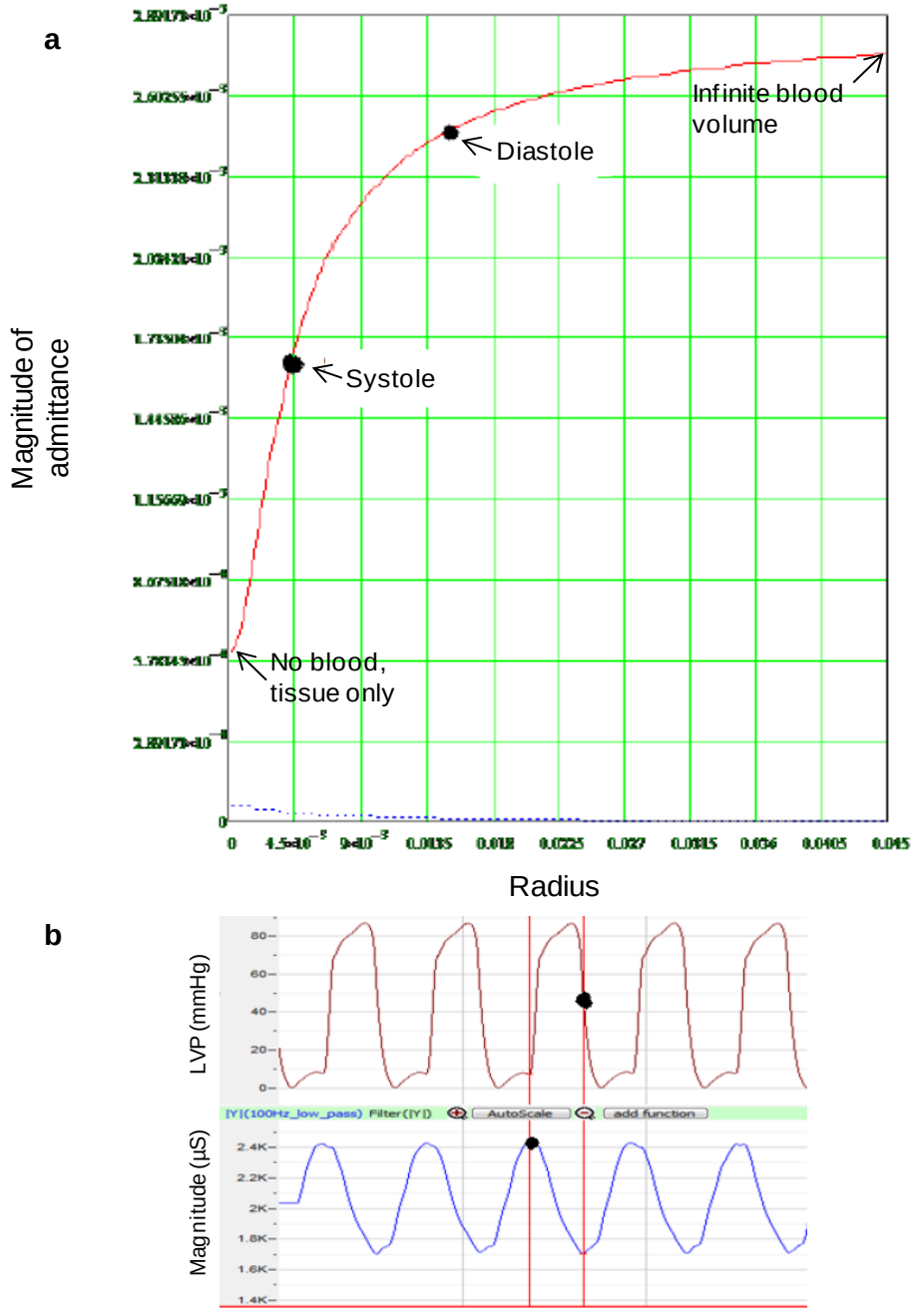

Figure C1 Scisense ADVantage™ system D method for volume calculation. **a)** Plot of magnitude of admittance vs radius of blood cylinder (i.e. the left ventricle). The plot has two unique points that indicate a condition of no blood and tissue only (bottom left) and an infinite volume of blood (top right). The mapped end-diastolic and end-systolic values for magnitude of admittance as determined in panel (b) are indicated. **b)** Magnitude of admittance values correlated to the left ventricular pressure (LVP) at end-diastole and end-systole of admittance (indicated by●).